

Two-component spinor techniques and Feynman rules for quantum field theory and supersymmetry

DRAFT version 1.15 April 4, 2008

HERBI K. DREINER¹, HOWARD E. HABER² AND STEPHEN P. MARTIN³

¹*Physikalisches Institut der Universität Bonn, Nußallee 12, 53115 Bonn, Germany*

²*Santa Cruz Institute for Particle Physics, University of California, Santa Cruz CA 95064*

³*Department of Physics, Northern Illinois University, DeKalb IL 60115 and
Fermi National Accelerator Laboratory, P.O. Box 500, Batavia IL 60510*

Abstract

We provide a complete set of Feynman rules for fermions using two-component spinor notation. These rules are suitable for practical calculations of cross-sections, decay rates, and radiative corrections in the Standard Model and its extensions, including supersymmetry. A unified treatment applies for massless Weyl fermions and massive Dirac and Majorana fermions. Numerous examples are given.

Contents

1	Introduction	3
2	Essential conventions and notations	6
3	Properties of fermion fields	14
3.1	A single two-component fermion field	14
3.2	Fermion mass diagonalization and external wave functions in a general theory . .	20
4	Feynman rules with two-component spinors	24
4.1	External fermion rules	24
4.2	Propagators	26
4.3	Fermion interactions with bosons	29
4.4	General structure and rules for Feynman graphs	33
4.5	Basic examples of writing down diagrams and amplitudes	34
4.6	Self-energy functions and pole masses for two-component fermions	42
5	Conventions for fermion and anti-fermion names and fields	49
6	Practical examples from the Standard Model and supersymmetry	54
6.1	Top quark decay: $t \rightarrow bW^+$	54
6.2	Z^0 vector boson decay: $Z^0 \rightarrow f\bar{f}$	55

6.3	Bhabha scattering: $e^-e^+ \rightarrow e^-e^+$	57
6.4	Polarized Muon Decay	59
6.5	Neutral Higgs boson decays $\phi^0 \rightarrow f\bar{f}$, for $\phi^0 = h^0, H^0, A^0$ in supersymmetry . . .	61
6.6	Sneutrino decay $\tilde{\nu}_e \rightarrow \tilde{C}_i^+ e^-$	63
6.7	Chargino Decay $\tilde{C}_i^+ \rightarrow \tilde{\nu}_e e^+$	64
6.8	Neutralino Decays $\tilde{N}_i \rightarrow \phi^0 \tilde{N}_j$, for $\phi^0 = h^0, H^0, A^0$	65
6.9	$\tilde{N}_i \rightarrow Z^0 \tilde{N}_j$	66
6.10	Selectron pair production in electron-electron collisions	67
6.10.1	$e^-e^- \rightarrow \tilde{e}_L^- \tilde{e}_R^-$	67
6.10.2	$e^-e^- \rightarrow \tilde{e}_R^- \tilde{e}_R^-$	69
6.10.3	$e^-e^- \rightarrow \tilde{e}_L^- \tilde{e}_L^-$	70
6.11	$e^-e^+ \rightarrow \tilde{\nu} \tilde{\nu}^*$	72
6.12	$e^-e^+ \rightarrow \tilde{N}_i \tilde{N}_j$	74
6.13	$e^-e^+ \rightarrow \tilde{C}_i^- \tilde{C}_j^+$	77
6.14	$u\bar{d} \rightarrow \tilde{C}_i^+ \tilde{N}_j$	80
6.15	$\tilde{N}_i \rightarrow \tilde{N}_j \tilde{N}_k \tilde{N}_\ell$	81
6.16	Three-body slepton decays $\tilde{\ell}_R^- \rightarrow \ell^- \tau^\pm \tilde{\tau}_1^\mp$ for $\ell = e, \mu$	84
6.17	Neutralino decay to photon and Goldstino: $\tilde{N}_i \rightarrow \gamma \tilde{G}$	86
6.18	Gluino pair production from gluon fusion: $gg \rightarrow \tilde{g}\tilde{g}$	88
6.19	R-parity violating stau decay: $\tilde{\tau}_R^+ \rightarrow e^+ \bar{\nu}_\mu$	92
6.20	R-parity violating neutralino decay: $\tilde{N}_i \rightarrow \mu^- u \bar{d}$	94
6.21	Top-quark condensation from a Nambu-Jona-Lasinio model gap equation	96
6.22	Electroweak vector boson self-energies from fermion loops	98
6.23	Self-energy and pole mass of the top quark	101
6.24	Self-energy and pole mass of the gluino	108
6.25	Triangle anomaly from chiral fermion loops	111
Appendix A: Two-component spinor identities in $d \neq 4$		115
Appendix B: Explicit forms for the two-component spinor wave functions		117
Appendix C: Path integral treatment of two-component fermion propagators		121
Appendix D: Matrix decompositions for fermion mass diagonalization		126
D.1	Singular Value Decomposition	126
D.2	Takagi Diagonalization	128
D.3	Relation between Takagi diagonalization and the singular value decomposition . .	130

Appendix E: Correspondence to four-component spinor notation	132
E.1 Dirac matrices and four-component spinors	132
E.2 Feynman rules for four-component fermions	137
E.3 Applications of four-component spinor Feynman rules	142
E.4 Self-energy functions and pole masses for four-component fermions	147
Appendix F: Covariant spin operators and the Bouchiat-Michel Formulae	149
F.1 The covariant spin operators for a spin-1/2 fermion	149
F.2 Two-component spinor wave function relations	150
F.3 Two-component Bouchiat-Michel formulae	152
F.4 Four-component Bouchiat-Michel formulae	155
Appendix G: The helicity amplitude technique	157
Appendix H: Standard Model fermion interaction vertices	159
Appendix I: MSSM Fermion Interaction Vertices	166
I.1 Higgs-fermion interaction vertices in the MSSM	166
I.2 Gauge interaction vertices for neutralinos and charginos	170
I.3 Higgs interactions with charginos and neutralinos	172
I.4 Chargino and neutralino interactions with fermions and sfermions	173
I.5 SUSY QCD Feynman Rules	179
Appendix J: Trilinear R-Parity Violating Fermion Interaction Vertices	181

1 Introduction

A crucial feature of the Standard Model of particle physics is the chiral nature of fermion quantum numbers and interactions. According to the modern understanding of the electroweak symmetry, the fundamental degrees of freedom for quarks and leptons are two-component Weyl-van der Waerden fermions, i.e. 2-component spinors under the Lorentz group, that transform as irreducible representations under the gauge group $SU(2)_L \times U(1)_Y$. **Furthermore, within the context of supersymmetric field theories, two-component spinors enter naturally, due to the spinor-nature of the symmetry generators themselves, as well as through the holomorphic nature of the superpotential.** Despite this, most pedagogical treatments and practical calculations in high-energy physics continue to use the four-component Dirac notation, which combines distinct irreducible representations of the symmetry groups. Parity-conserving theories such as QED and QCD are well-suited to the four-component fermion methods. There is also a certain perceived advantage to familiarity. However, as we progress to phenomena at and above the scale of

electroweak symmetry breaking, it seems increasingly natural to employ two-component fermion notation, in harmony with the irreducible transformation properties dictated by the physics.

One occasionally encounters the misconception that two-component fermion notations are somehow inherently ill-suited or unwieldy for practical use. Perhaps this is due in part to a lack of examples of calculations using two-component language in the pedagogical literature. In this paper, we seek to dispel this idea by presenting Feynman rules for fermions using two-component spinor notation, intended for practical calculations of cross-sections, decays, and radiative corrections. This formalism employs a unified framework that applies equally well to Dirac fermions like the Standard Model quarks and leptons, and to Majorana fermions such as the light neutrinos that appear in the seesaw extension of the Standard Model¹ or the neutralinos of the minimal supersymmetric extension of the Standard Model (MSSM) [47–49].

Spinors were introduced by E. Cartan in 1913 as projective representations of the rotation group [1]. They entered into physics via the Dirac equation in 1928 [3]. In the same year, H. Weyl discussed the representations of the Lorentz group, including the two-component spinor representations, in terms of stereographic projective coordinates [4]. The extension of the tensor calculus (or tensor analysis) to spinor calculus (spinor analysis) was given by B. L. van der Waerden [5], upon instigation of P. Ehrenfest. It is in this paper also that v. d. Waerden (not Weyl as often claimed in the literature) first introduces the notation of dotted and undotted indices for the irreducible $(\frac{1}{2}, 0)$ and $(0, \frac{1}{2})$ representations of the Lorentz group. Both Weyl and van der Waerden independently consider the decomposition of the Dirac equation into two coupled differential equations for two-component spinors. Early, more pedagogical discussions of two-component spinors are given in [6–8]. See also [9]. Ref. [6], is also the first English paper to employ the dotted and undotted index notation. Very nice early reviews on spinor techniques were written by Bade and Jehle in 1953 [10] and in German by Cap in 1954 [11].

Two component spinors have also been discussed in many non-supersymmetric textbooks, see for example [4, 12–31]. Among the early books, we would like to draw attention to [12], which has an extensive discussion and the appendix of [19]. Scheck [21] includes a short discussion of the field theory of two-component spinors, including the propagator. The most extensive field theoretic discussion is given by Ticciati [24]. This includes a complete set of Feynman rules for a Yukawa theory as well as three example calculations. recently, Srednicki [31] has written an introduction into quantum field theory with a discussion of two-component fermions, including their quantization.

[I have not checked the books [18, 26–28, 30] since they are not in our library.]

All text books on supersymmetry [32–45] include a discussion of two-component spinors on some level. This also typically includes a discussion of dotted and undotted indices as well

¹In the limit of zero mass, neutrinos can be described by either Majorana or Weyl fermions. Both are naturally described in the two-component fermion formalism.

as a collection of identities involving the sigma matrices. Particularly extensive and useful sets of identities can be found in [32, 37, 38, 42, 43]. Terning [43] also includes some field theoretic details.

[*This part is about the previous work on van der Waerden spinors in particle physics papers.*] The standard technique for computing scattering cross sections with initial and final state fermions involves squaring the amplitudes, summing over the spin states and then computing the traces of products of gamma matrices, or in the two-component case, over products of sigma matrices. We employ this latter technique throughout this paper. However, the computational effort rises with the square of the number of interfering diagrams. This typically becomes impractical with four or more particles in the final state. One approach to make such extensive calculations manageable, is the helicity amplitude technique. Here the scattering process is decomposed into the scattering of helicity eigenstates. Then the individual amplitudes are computed analytically in terms of Lorentz scalar invariants, i.e. a complex number, which can be readily computed. It is then a simple numerical task to sum the amplitudes and square them. This was first explored in refs [51–54], using four-component spinors, see also refs [55–59]. For spinor techniques in the helicity formalism see also [60]. The natural spinor formalism for the helicity amplitude techniques are in fact the 2-component Weyl-van der Waerden spinors, which we discuss in detail in this paper. They were implemented in the helicity amplitude technique in refs. [61–66]. Recently the two-component formalism has been implemented in a computer program for the numerical computation of amplitudes and cross sections for event generators multi-particle processes refs [133, 134]. In order to see how to apply our work to the case of multi-particle final states, we present in Appendix G the translation between our notation and that of the widely used Hagiwara and Zeppenfeld (HZ) formalism ref. [63]. It is then straightforward to implement amplitudes as computed here into a numerical cross section computation.

[*Something like this is still missing, I just sketched it.*] This report is outlined as follows. In Sect. 2, we present our conventions and notation. In Sect. 3 we derive the basic properties of the quantized two-component fermion fields. In Sect. 4 we derive the Feynman rules for two-component spinors and describe how to write down amplitudes in our formalism. In Sect. 5 we give our convention for fermion and anti-fermion names and fields. This is important for consistently writing down the amplitudes for a given physical process and also for comparing with previous 4-component computations. In Sect. 6 we then compute an extensive number of examples using our formalism. This is the central part of our paper.

2 Essential conventions and notations

We begin with a discussion of necessary conventions. The metric tensor is taken² to be:

$$g^{\mu\nu} = \text{diag}(+1, -1, -1, -1), \quad (2.1)$$

where $\mu, \nu, \rho \dots = 0, 1, 2, 3$ are spacetime vector indices. Contravariant four-vectors (e.g. positions and momenta) are defined with indices raised, and covariant four-vectors (e.g. derivatives) with lowered indices:

$$x^\mu = (t, \vec{x}), \quad (2.2)$$

$$p^\mu = (E, \vec{p}), \quad (2.3)$$

$$\partial_\mu \equiv \frac{\partial}{\partial x^\mu} = (\partial/\partial t, \vec{\nabla}), \quad (2.4)$$

in units with $c = 1$. The totally antisymmetric pseudo-tensor $\epsilon^{\mu\nu\rho\sigma}$ is defined such that

$$\epsilon^{0123} = -\epsilon_{0123} = +1. \quad (2.5)$$

The irreducible building blocks for spin-1/2 fermions are fields that transform either under the left-handed $(\frac{1}{2}, 0)$ or the right-handed $(0, \frac{1}{2})$ representation of the Lorentz group. Hermitian conjugation interchanges these two representations. A massive Majorana fermion field can be constructed from either representation; this is the spin-1/2 analog of a real scalar field. The Dirac field combines two equal mass two-component fields into a reducible representation of the form $(\frac{1}{2}, 0) \oplus (0, \frac{1}{2})$; this is the spin-1/2 analog of a complex scalar field. It is also possible to use four-component notation to describe Majorana fermions by imposing a reality condition on the spinor in order to reduce the number of degrees of freedom in half. However, in this paper, we shall focus primarily on two-component spinor notation for all fermions. In the following, $(\frac{1}{2}, 0)$ spinors carry undotted indices $\alpha, \beta, \dots = 1, 2$, and $(0, \frac{1}{2})$ spinors carry dotted indices $\dot{\alpha}, \dot{\beta}, \dots = 1, 2$.

We begin by briefly considering the representations of the Lorentz group. Under a Lorentz transformation, a contravariant four-vector x^μ transforms as

$$x^\mu \rightarrow x'^\mu = \Lambda^\mu{}_\nu x^\nu, \quad (2.6)$$

²The published version of this paper uses the $(+, -, -, -)$ metric. An otherwise identical version, using the $(-, +, +, +)$ metric favored by one of the authors, may be found at <http://zippy.physics.niu.edu/rules.html>. It can also be constructed by changing a single macro within the L^AT_EX source file, in an obvious way. You can tell which version you are presently reading from equation (2.1). In general, the relative minus sign needed to switch between one metric signature and the other is given by:

$$(-1)^{(N_\sigma + N_m + N_d)}$$

where N_σ is the total number of σ and $\bar{\sigma}$ matrices, N_m is the number of metric tensors appearing either explicitly or implicitly through contracted upper and lower indices, and N_d is the number of spacetime derivatives. This applies to any relativistically covariant term appearing additively in a valid equation.

where Λ satisfies $\Lambda^\mu{}_\nu g_{\mu\rho} \Lambda^\rho{}_\lambda = g_{\lambda\nu}$. It then follows that the transformation of the corresponding covariant four-vector $x_\mu \equiv g_{\mu\nu} x^\nu$ satisfies:

$$x_\nu = x'_\mu \Lambda^\mu{}_\nu. \quad (2.7)$$

The most general proper orthochronous Lorentz transformation (which is continuously connected to the identity), corresponding to a rotation by an angle θ about an axis $\hat{\mathbf{n}}$ [$\vec{\theta} \equiv \theta \hat{\mathbf{n}}$] and a boost vector $\vec{\zeta} \equiv \hat{\mathbf{v}} \tanh^{-1} \beta$ [where $\hat{\mathbf{v}} \equiv \vec{\mathbf{v}}/|\vec{\mathbf{v}}|$ and $\beta \equiv |\vec{\mathbf{v}}|$], is a 4×4 matrix given by:

$$\Lambda = \exp\left(-\frac{i}{2}\theta^{\rho\sigma} s_{\rho\sigma}\right) = \exp\left(-i\vec{\theta} \cdot \vec{s} - i\vec{\zeta} \cdot \vec{k}\right), \quad (2.8)$$

where $\theta^i \equiv \frac{1}{2}\epsilon^{ijk}\theta_{jk}$, $\zeta^i \equiv \theta^{i0} = -\theta^{0i}$, $s^i \equiv \frac{1}{2}\epsilon^{ijk}s_{jk}$, $k^i \equiv s^{0i} = -s^{i0}$ and

$$(s_{\rho\sigma})^\mu{}_\nu = i(g_\rho{}^\mu g_{\sigma\nu} - g_\sigma{}^\mu g_{\rho\nu}). \quad (2.9)$$

Here, the indices $i, j, k = 1, 2, 3$ and $\epsilon^{123} = +1$.

It follows from eqs. (2.8) and (2.9) that an infinitesimal orthochronous Lorentz transformation is given by $\Lambda^\mu{}_\nu \simeq \delta^\mu{}_\nu + \theta^\mu{}_\nu$ (after noting that $\theta^\mu{}_\nu = -\theta_\nu{}^\mu$). Moreover, the infinitesimal boost parameter is $\vec{\zeta} \equiv \hat{\mathbf{v}} \tanh^{-1} \beta \simeq \beta \hat{\mathbf{v}} \equiv \vec{\beta}$, since $\beta \ll 1$ for an infinitesimal boost. Hence, the actions of the infinitesimal boosts and rotations on the spacetime coordinates are

$$\text{Rotations:} \quad \begin{cases} \vec{x} \rightarrow \vec{x}' \simeq \vec{x} + (\vec{\theta} \times \vec{x}) \\ t \rightarrow t' \simeq t \end{cases} \quad (2.10)$$

$$\text{Boosts:} \quad \begin{cases} \vec{x} \rightarrow \vec{x}' \simeq \vec{x} + \vec{\beta}t \\ t \rightarrow t' \simeq t + \vec{\beta} \cdot \vec{x}, \end{cases} \quad (2.11)$$

with exactly analogous transformations for any contravariant four-vector.

With respect to the Lorentz transformation Λ , a general n -component field Φ transforms as $\Phi(x^\mu) \rightarrow M_R(\Lambda) \Phi'(x'^\mu)$, where $M_R(\Lambda)$ is a (finite) n -dimensional matrix representation, R , of the Lorentz group. Equivalently, the functional form of the transformed field Φ obeys

$$\Phi'(x^\mu) = M_R(\Lambda) \Phi([\Lambda^{-1}]^\mu{}_\nu x^\nu). \quad (2.12)$$

For proper orthochronous Lorentz transformations,

$$M_R = \exp\left(-\frac{i}{2}\theta_{\mu\nu} J^{\mu\nu}\right) \simeq I - i\vec{\theta} \cdot \vec{J} - i\vec{\zeta} \cdot \vec{K}, \quad (2.13)$$

where $\theta_{\mu\nu}$ parameterizes the Lorentz transformation Λ [eq. (2.8)], and $J^{\mu\nu}$ is a matrix-valued antisymmetric tensor corresponding to the representation R . For infinitesimal Lorentz transformations, we identify \vec{J} and \vec{K} as the generators of rotations parameterized by $\vec{\theta}$ and boosts parameterized by $\vec{\zeta}$, respectively. These three-vector generators are related to $J^{\mu\nu}$ by

$$J^i \equiv \frac{1}{2}\epsilon^{ijk} J_{jk}, \quad K^i \equiv J^{0i}. \quad (2.14)$$

Here we focus on the simplest non-trivial irreducible representations of the Lorentz algebra. These are the two-dimensional (inequivalent) representations: $(\frac{1}{2}, 0)$ and $(0, \frac{1}{2})$. In the $(\frac{1}{2}, 0)$ representation, $\vec{J} = \vec{\sigma}/2$ and $\vec{K} = -i\vec{\sigma}/2$ in eq. (2.13), where $\vec{\sigma}$ are the Pauli matrices. This yields

$$M_{(\frac{1}{2}, 0)} \equiv M \simeq I - i\vec{\theta} \cdot \vec{\sigma}/2 - \vec{\zeta} \cdot \vec{\sigma}/2. \quad (2.15)$$

By definition M carries undotted spinor indices, as indicated by M_α^β . A two-component $(\frac{1}{2}, 0)$ spinor is denoted by ψ_α and transforms as $\psi_\alpha \rightarrow M_\alpha^\beta \psi_\beta$, omitting the coordinate arguments of the fields, which are as in eq. (2.12). Note that in our conventions for the location of the spinor indices, one sums over a repeated index pair in which one index is lowered and one index is raised.

In the $(0, \frac{1}{2})$ representation, $\vec{J} = -\vec{\sigma}^*/2$ and $\vec{K} = -i\vec{\sigma}^*/2$ in eq. (2.13), so that its representation matrix is M^* , the complex conjugate of eq. (2.15). By definition, the indices carried by M^* are dotted, as indicated by $(M^*)_{\dot{\alpha}}^{\dot{\beta}}$. A two-component $(0, \frac{1}{2})$ spinor is denoted by $\bar{\psi}_{\dot{\alpha}}$ and transforms as $\bar{\psi}_{\dot{\alpha}} \rightarrow (M^*)_{\dot{\alpha}}^{\dot{\beta}} \bar{\psi}_{\dot{\beta}}$, again suppressing the coordinate arguments of the fields, which are as in eq. (2.12). The reason for distinguishing between the undotted and dotted spinor index types is that they cannot be directly contracted with each other to form a Lorentz invariant quantity.

It follows that the $(0, \frac{1}{2})$ and $(\frac{1}{2}, 0)$ representations can be related by complex conjugation. That is, if $\bar{\psi}_{\dot{\alpha}}$ is a $(0, \frac{1}{2})$ fermion, then $(\bar{\psi}_{\dot{\alpha}})^*$ transforms as a $(\frac{1}{2}, 0)$ fermion. This means that we can, and will, describe all fermion degrees of freedom using only fields defined as left-handed $(\frac{1}{2}, 0)$ fermions ψ_α , and their conjugates. We can combine spinors to make Lorentz tensors, so it is useful to regard $\bar{\psi}_{\dot{\alpha}}$ as a row vector, and ψ_α as a column vector, with:

$$\bar{\psi}_{\dot{\alpha}} \equiv (\psi_\alpha)^\dagger. \quad (2.16)$$

A check of the Lorentz transformation property of $\bar{\psi}_{\dot{\alpha}}$ then follows from $(\psi_\alpha)^\dagger \rightarrow (\psi_\beta)^\dagger (M^\dagger)^{\dot{\beta}}_{\dot{\alpha}}$, where $(M^\dagger)^{\dot{\beta}}_{\dot{\alpha}} = (M^*)_{\dot{\alpha}}^{\dot{\beta}}$ reflects the definition of the hermitian adjoint matrix as the complex conjugate transpose of the matrix. Again the coordinate arguments of the fields have been suppressed, and are as in eq. (2.12). We will use the dotted-index notation in association with the bar over the symbol as a synonym for hermitian conjugation, as above. [Many other references write ψ_α^\dagger to mean the same thing as eq. (2.16).]

There are two additional spin-1/2 irreducible representations of the Lorentz group, $(M^{-1})^\top$ and $(M^{-1})^\dagger$, but these are equivalent representations to the $(\frac{1}{2}, 0)$ and the $(0, \frac{1}{2})$ representations, respectively. The spinors that transform under these representations have raised spinor indices, *e.g.*, ψ^α and $\bar{\psi}^{\dot{\alpha}}$, respectively. The spinor indices are raised and lowered with the two-index antisymmetric symbol with components $\epsilon^{12} = -\epsilon^{21} = \epsilon_{21} = -\epsilon_{12} = 1$, and the same set of sign conventions for the corresponding dotted spinor indices. Thus

$$\psi_\alpha = \epsilon_{\alpha\beta} \psi^\beta, \quad \psi^\alpha = \epsilon^{\alpha\beta} \psi_\beta, \quad \bar{\psi}_{\dot{\alpha}} = \epsilon_{\dot{\alpha}\dot{\beta}} \bar{\psi}^{\dot{\beta}}, \quad \bar{\psi}^{\dot{\alpha}} = \epsilon^{\dot{\alpha}\dot{\beta}} \bar{\psi}_{\dot{\beta}}. \quad (2.17)$$

The ϵ symbol satisfies:³

$$\epsilon_{\alpha\beta}\epsilon^{\gamma\delta} = -\delta_{\alpha}^{\gamma}\delta_{\beta}^{\delta} + \delta_{\alpha}^{\delta}\delta_{\beta}^{\gamma}, \quad \epsilon_{\dot{\alpha}\dot{\beta}}\epsilon^{\dot{\gamma}\dot{\delta}} = -\delta_{\dot{\alpha}}^{\dot{\gamma}}\delta_{\dot{\beta}}^{\dot{\delta}} + \delta_{\dot{\alpha}}^{\dot{\delta}}\delta_{\dot{\beta}}^{\dot{\gamma}}, \quad (2.18)$$

from which it follows that:

$$\epsilon_{\alpha\beta}\epsilon^{\beta\gamma} = \epsilon^{\gamma\beta}\epsilon_{\beta\alpha} = \delta_{\alpha}^{\gamma}, \quad \epsilon_{\dot{\alpha}\dot{\beta}}\epsilon^{\dot{\beta}\dot{\gamma}} = \epsilon^{\dot{\gamma}\dot{\beta}}\epsilon_{\dot{\beta}\dot{\alpha}} = \delta_{\dot{\alpha}}^{\dot{\gamma}}. \quad (2.19)$$

$\epsilon^{\alpha\beta}$ ($\epsilon_{\alpha\beta}$) is also called the “spinor metric tensor” since it raises (lowers) spinor indices. It was first introduced in this context in [5], but see also [6, 7, 10, 50] for related early work.

To construct Lorentz invariant Lagrangians and observables, one needs to first combine products of spinors to make objects that transform as Lorentz tensors. In particular, Lorentz vectors are obtained by introducing the sigma matrices $\sigma_{\mu\alpha\dot{\beta}}$ and $\bar{\sigma}_{\mu}^{\dot{\alpha}\beta}$ defined by [4, 5, 7, 8]

$$\begin{aligned} \bar{\sigma}_0 = \sigma_0 &= \begin{pmatrix} 1 & 0 \\ 0 & 1 \end{pmatrix}, & \bar{\sigma}_1 = -\sigma_1 &= \begin{pmatrix} 0 & 1 \\ 1 & 0 \end{pmatrix}, \\ \bar{\sigma}_2 = -\sigma_2 &= \begin{pmatrix} 0 & -i \\ i & 0 \end{pmatrix}, & \bar{\sigma}_3 = -\sigma_3 &= \begin{pmatrix} 1 & 0 \\ 0 & -1 \end{pmatrix}. \end{aligned} \quad (2.20)$$

The σ -matrices above have been defined with a lower (covariant) index. We also define the corresponding quantities with upper (contravariant) indices:

$$\sigma^{\mu} = g^{\mu\nu}\sigma_{\nu} = (I_2; \vec{\sigma}), \quad \bar{\sigma}^{\mu} = g^{\mu\nu}\bar{\sigma}_{\nu} = (I_2; -\vec{\sigma}), \quad (2.21)$$

where I_2 is the 2×2 identity matrix. The relations between σ^{μ} and $\bar{\sigma}^{\mu}$ are

$$\sigma^{\mu}_{\alpha\dot{\alpha}} = \epsilon_{\alpha\beta}\epsilon_{\dot{\alpha}\dot{\beta}}\bar{\sigma}^{\mu\dot{\beta}\beta}, \quad \bar{\sigma}^{\mu\dot{\alpha}\alpha} = \epsilon^{\alpha\beta}\epsilon^{\dot{\alpha}\dot{\beta}}\sigma^{\mu}_{\beta\dot{\beta}}, \quad (2.22)$$

$$\epsilon^{\alpha\beta}\sigma^{\mu}_{\beta\dot{\alpha}} = \epsilon_{\dot{\alpha}\dot{\beta}}\bar{\sigma}^{\mu\dot{\beta}\alpha}, \quad \epsilon^{\dot{\alpha}\dot{\beta}}\sigma^{\mu}_{\alpha\dot{\beta}} = \epsilon_{\alpha\beta}\bar{\sigma}^{\mu\dot{\alpha}\beta}. \quad (2.23)$$

In general, just like tensors, we can have spinor objects with more than one spinor index: $S_{\alpha_1\alpha_2\ldots\alpha_n\dot{\beta}_1\dot{\beta}_2\ldots\dot{\beta}_n}$, where each α -index transforms separately according to $M_{\alpha'_i}^{\alpha_i}$ in eq. (2.15) and each $\dot{\beta}$ -index transforms according to $(M^*)_{\dot{\beta}'_i}^{\dot{\beta}_i}$. Using the above $\bar{\sigma}_{\mu}^{\dot{\beta}\alpha}$ there is a one-to-one correspondence between each bi-spinor $V_{\alpha\dot{\beta}}$ and a corresponding Lorentz four-vector V^{μ}

$$V^{\mu} \equiv \bar{\sigma}_{\mu}^{\dot{\beta}\alpha} V_{\alpha\dot{\beta}} \quad (2.24)$$

³Various subsets of the subsequent identities in this section involving commuting and non-commuting two-component spinors, as well as the ϵ and σ -matrices appear in many books, and papers, *e.g.* the books [8, 32–45], and the papers [61–66]

When constructing Lorentz tensors from fermion fields, the heights of spinor indices must be consistent in the sense that lowered indices must only be contracted with raised indices. As a convention, indices contracted like

$$\begin{matrix} \alpha \\ \alpha \end{matrix} \quad \text{and} \quad \begin{matrix} \dot{\alpha} \\ \dot{\alpha} \end{matrix}, \quad (2.25)$$

can be suppressed. In all spinor products given in this paper, contracted indices always have heights that conform to eq. (2.25). For example,

$$\xi\eta \equiv \xi^\alpha\eta_\alpha, \quad (2.26)$$

$$\bar{\xi}\bar{\eta} \equiv \bar{\xi}_{\dot{\alpha}}\bar{\eta}^{\dot{\alpha}}, \quad (2.27)$$

$$\bar{\xi}\bar{\sigma}^\mu\eta \equiv \bar{\xi}_{\dot{\alpha}}\bar{\sigma}^{\mu\dot{\alpha}\beta}\eta_\beta, \quad (2.28)$$

$$\xi\sigma^\mu\bar{\eta} \equiv \xi^\alpha\sigma^\mu_{\alpha\dot{\beta}}\bar{\eta}^{\dot{\beta}}. \quad (2.29)$$

As previously noted, it is convenient to regard η_α as a column vector and $\bar{\xi}_{\dot{\alpha}}$ as a row vector. Consequently, if we also regard ξ^α as a row vector and $\bar{\eta}^{\dot{\alpha}}$ as a column vector then all the spinor-index contracted products above have natural interpretations as products of matrices and vectors.

The behavior of the spinor products under hermitian conjugation (for quantum field operators) or complex conjugation (for classical fields) is as follows:

$$(\xi\eta)^\dagger = \bar{\eta}\bar{\xi}, \quad (2.30)$$

$$(\xi\sigma^\mu\bar{\eta})^\dagger = \eta\sigma^\mu\bar{\xi}, \quad (2.31)$$

$$(\bar{\xi}\bar{\sigma}^\mu\eta)^\dagger = \bar{\eta}\bar{\sigma}^\mu\xi, \quad (2.32)$$

$$(\xi\sigma^\mu\bar{\sigma}^\nu\eta)^\dagger = \bar{\eta}\bar{\sigma}^\nu\sigma^\mu\bar{\xi}. \quad (2.33)$$

More generally,

$$(\xi\Sigma\eta)^\dagger = \bar{\eta}\Sigma_r\bar{\xi}, \quad (2.34)$$

$$(\xi\Sigma\bar{\eta})^\dagger = \eta\Sigma_r\bar{\xi}, \quad (2.35)$$

where in each case Σ stands for any sequence of alternating σ and $\bar{\sigma}$ matrices, and Σ_r is obtained from Σ by reversing the order of all of the σ and $\bar{\sigma}$ matrices. Note that eqs. (2.30)–(2.35) are applicable both to anti-commuting and to commuting spinors.

The following identities can be used to systematically simplify expressions involving prod-

ucts of σ and $\bar{\sigma}$ matrices:

$$\sigma_{\alpha\dot{\alpha}}^{\mu}\bar{\sigma}_{\mu}^{\dot{\beta}\beta} = 2\delta_{\alpha}^{\beta}\delta_{\dot{\alpha}}^{\dot{\beta}}, \quad (2.36)$$

$$\sigma_{\alpha\dot{\alpha}}^{\mu}\sigma_{\mu\beta\dot{\beta}} = 2\epsilon_{\alpha\beta}\epsilon_{\dot{\alpha}\dot{\beta}}, \quad (2.37)$$

$$\bar{\sigma}^{\mu\dot{\alpha}\alpha}\bar{\sigma}_{\mu}^{\dot{\beta}\beta} = 2\epsilon^{\alpha\beta}\epsilon^{\dot{\alpha}\dot{\beta}}, \quad (2.38)$$

$$[\sigma^{\mu}\bar{\sigma}^{\nu} + \sigma^{\nu}\bar{\sigma}^{\mu}]_{\alpha}^{\beta} = 2g^{\mu\nu}\delta_{\alpha}^{\beta}, \quad (2.39)$$

$$[\bar{\sigma}^{\mu}\sigma^{\nu} + \bar{\sigma}^{\nu}\sigma^{\mu}]^{\dot{\alpha}}_{\dot{\beta}} = 2g^{\mu\nu}\delta_{\dot{\beta}}^{\dot{\alpha}}, \quad (2.40)$$

$$\sigma^{\mu}\bar{\sigma}^{\nu}\sigma^{\rho} = g^{\mu\nu}\sigma^{\rho} - g^{\mu\rho}\sigma^{\nu} + g^{\nu\rho}\sigma^{\mu} + i\epsilon^{\mu\nu\rho\kappa}\sigma_{\kappa}, \quad (2.41)$$

$$\bar{\sigma}^{\mu}\sigma^{\nu}\bar{\sigma}^{\rho} = g^{\mu\nu}\bar{\sigma}^{\rho} - g^{\mu\rho}\bar{\sigma}^{\nu} + g^{\nu\rho}\bar{\sigma}^{\mu} - i\epsilon^{\mu\nu\rho\kappa}\bar{\sigma}_{\kappa}. \quad (2.42)$$

Computations of cross sections and decay rates generally require traces of alternating products of σ and $\bar{\sigma}$ matrices (see for example [62]):

$$\text{Tr}[\sigma^{\mu}\bar{\sigma}^{\nu}] = \text{Tr}[\bar{\sigma}^{\mu}\sigma^{\nu}] = 2g^{\mu\nu}, \quad (2.43)$$

$$\text{Tr}[\sigma^{\mu}\bar{\sigma}^{\nu}\sigma^{\rho}\bar{\sigma}^{\kappa}] = 2(g^{\mu\nu}g^{\rho\kappa} - g^{\mu\rho}g^{\nu\kappa} + g^{\mu\kappa}g^{\nu\rho} + i\epsilon^{\mu\nu\rho\kappa}), \quad (2.44)$$

$$\text{Tr}[\bar{\sigma}^{\mu}\sigma^{\nu}\bar{\sigma}^{\rho}\sigma^{\kappa}] = 2(g^{\mu\nu}g^{\rho\kappa} - g^{\mu\rho}g^{\nu\kappa} + g^{\mu\kappa}g^{\nu\rho} - i\epsilon^{\mu\nu\rho\kappa}). \quad (2.45)$$

Traces involving a larger even number of σ and $\bar{\sigma}$ matrices can be systematically obtained from eqs. (2.43)–(2.45) by repeated use of eqs. (2.39) and (2.40) and the cyclic property of the trace. Traces involving an odd number of σ and $\bar{\sigma}$ matrices cannot arise, since there is no way to connect the spinor indices consistently.

In addition to manipulating expressions containing anticommuting fermion fields, we often must deal with products of *commuting* spinor wave functions that arise when evaluating the Feynman rules. In the following expressions we denote the generic spinor by z_i . In the various identities listed below, an extra minus sign arises when manipulating a product of anticommuting fermion fields. Thus, we employ the notation:

$$(-1)^A \equiv \begin{cases} +1, & \text{commuting spinors,} \\ -1, & \text{anticommuting spinors.} \end{cases} \quad (2.46)$$

The following identities hold for the z_i :

$$z_1 z_2 = -(-1)^A z_2 z_1 \quad (2.47)$$

$$\bar{z}_1 \bar{z}_2 = -(-1)^A \bar{z}_2 \bar{z}_1 \quad (2.48)$$

$$z_1 \sigma^{\mu} \bar{z}_2 = (-1)^A \bar{z}_2 \bar{\sigma}^{\mu} z_1 \quad (2.49)$$

$$z_1 \sigma^{\mu} \bar{\sigma}^{\nu} z_2 = -(-1)^A z_2 \sigma^{\nu} \bar{\sigma}^{\mu} z_1 \quad (2.50)$$

$$\bar{z}_1 \bar{\sigma}^{\mu} \sigma^{\nu} \bar{z}_2 = -(-1)^A \bar{z}_2 \bar{\sigma}^{\nu} \sigma^{\mu} \bar{z}_1 \quad (2.51)$$

$$\bar{z}_1 \bar{\sigma}^{\mu} \sigma^{\rho} \bar{\sigma}^{\nu} z_2 = (-1)^A z_2 \sigma^{\nu} \bar{\sigma}^{\rho} \sigma^{\mu} \bar{z}_1, \quad (2.52)$$

and so on.

Two-component spinor products can often be simplified by using Fierz identities. The antisymmetry of the suppressed two-component ϵ symbol [eq. (2.18)] implies the identities:

$$(z_1 z_2)(z_3 z_4) = -(z_1 z_3)(z_4 z_2) - (z_1 z_4)(z_2 z_3), \quad (2.53)$$

$$(\bar{z}_1 \bar{z}_2)(\bar{z}_3 \bar{z}_4) = -(\bar{z}_1 \bar{z}_3)(\bar{z}_4 \bar{z}_2) - (\bar{z}_1 \bar{z}_4)(\bar{z}_2 \bar{z}_3), \quad (2.54)$$

where we have used eqs. (2.47) and (2.48) to cancel out any residual factors of $(-1)^A$. Similarly, eq. (2.36) can be used to derive

$$(z_1 \sigma^\mu \bar{z}_2)(\bar{z}_3 \bar{\sigma}_\mu z_4) = -2(z_1 z_4)(\bar{z}_2 \bar{z}_3), \quad (2.55)$$

$$(\bar{z}_1 \bar{\sigma}^\mu z_2)(\bar{z}_3 \bar{\sigma}_\mu z_4) = 2(\bar{z}_1 \bar{z}_3)(z_4 z_2), \quad (2.56)$$

$$(z_1 \sigma^\mu \bar{z}_2)(z_3 \sigma_\mu \bar{z}_4) = 2(z_1 z_3)(\bar{z}_4 \bar{z}_2). \quad (2.57)$$

Eqs. (2.53)–(2.57) hold for both commuting and anticommuting spinors. Other Fierz identities for spinors can be constructed trivially from these by appropriate choices of z_1 , z_2 , z_3 , and z_4 .

From the sigma matrices, one can construct the antisymmetrized products:

$$(\sigma^{\mu\nu})_\alpha{}^\beta \equiv \frac{i}{4} \left(\sigma_{\alpha\dot{\gamma}}^\mu \bar{\sigma}^{\nu\dot{\gamma}\beta} - \sigma_{\alpha\dot{\gamma}}^\nu \bar{\sigma}^{\mu\dot{\gamma}\beta} \right), \quad (2.58)$$

$$(\bar{\sigma}^{\mu\nu})^{\dot{\alpha}}{}_{\dot{\beta}} \equiv \frac{i}{4} \left(\bar{\sigma}^{\mu\dot{\alpha}\gamma} \sigma_{\gamma\dot{\beta}}^\nu - \bar{\sigma}^{\nu\dot{\alpha}\gamma} \sigma_{\gamma\dot{\beta}}^\mu \right). \quad (2.59)$$

The matrices $\sigma^{\mu\nu}$ and $\bar{\sigma}^{\mu\nu}$ satisfy self-duality relations

$$\sigma^{\mu\nu} = -\frac{1}{2}i\epsilon^{\mu\nu\rho\kappa}\sigma_{\rho\kappa}, \quad \bar{\sigma}^{\mu\nu} = \frac{1}{2}i\epsilon^{\mu\nu\rho\kappa}\bar{\sigma}_{\rho\kappa}. \quad (2.60)$$

In addition, eq. (2.18) implies that

$$\epsilon_{\beta\rho}\epsilon^{\alpha\tau}\sigma^{\mu\nu}{}_\alpha{}^\beta = \sigma^{\mu\nu}{}_\rho{}^\tau, \quad \epsilon^{\dot{\beta}\dot{\rho}}\epsilon_{\dot{\alpha}\dot{\tau}}\bar{\sigma}^{\mu\nu}{}^{\dot{\alpha}}{}_{\dot{\beta}} = \bar{\sigma}^{\mu\nu}{}^{\dot{\rho}}{}_{\dot{\tau}}, \quad (2.61)$$

$$\epsilon^{\alpha\tau}\sigma^{\mu\nu}{}_\alpha{}^\beta = \epsilon^{\rho\beta}\sigma^{\mu\nu}{}_\rho{}^\tau, \quad \epsilon_{\dot{\alpha}\dot{\tau}}\bar{\sigma}^{\mu\nu}{}^{\dot{\alpha}}{}_{\dot{\beta}} = \epsilon_{\dot{\rho}\dot{\beta}}\bar{\sigma}^{\mu\nu}{}^{\dot{\rho}}{}_{\dot{\tau}}, \quad (2.62)$$

where we have used $\text{Tr}(\sigma^{\mu\nu}) = \text{Tr}(\bar{\sigma}^{\mu\nu}) = 0$.

The $\sigma^{\mu\nu}$ and $\bar{\sigma}^{\mu\nu}$ can be identified as the generators $J^{\mu\nu}$ [see eq. (2.13)] of the Lorentz group in the $(\frac{1}{2}, 0)$ and $(0, \frac{1}{2})$ representations, respectively. That is, for the $(\frac{1}{2}, 0)$ representation with a lowered undotted index (*e.g.* ψ_α), $J^{\mu\nu} = \sigma^{\mu\nu}$, while for the $(0, \frac{1}{2})$ representation with a raised dotted index (*e.g.* $\bar{\psi}^{\dot{\alpha}}$), $J^{\mu\nu} = \bar{\sigma}^{\mu\nu}$. In particular, the infinitesimal forms for the 4×4 Lorentz transformation matrix Λ and the corresponding matrices M and $(M^{-1})^\dagger$ that transform the $(\frac{1}{2}, 0)$ and $(0, \frac{1}{2})$ spinors, respectively, are given by:

$$M \simeq I_2 - \frac{i}{2}\theta_{\mu\nu}\sigma^{\mu\nu}, \quad (2.63)$$

$$(M^{-1})^\dagger \simeq I_2 - \frac{i}{2}\theta_{\mu\nu}\bar{\sigma}^{\mu\nu}, \quad (2.64)$$

$$\Lambda^\mu{}_\nu \simeq \delta^\mu{}_\nu + \frac{1}{2} \left(\theta_{\alpha\nu} g^{\alpha\mu} - \theta_{\nu\beta} g^{\beta\mu} \right). \quad (2.65)$$

The inverses of these quantities are obtained (to first order in θ) by replacing $\theta \rightarrow -\theta$ in the above formulae. Using these infinitesimal forms [with the assistance of eqs. (A.18)–(A.21)], one can establish the following two results:

$$M^\dagger \bar{\sigma}^\mu M = \Lambda^\mu{}_\nu \bar{\sigma}^\nu, \quad (2.66)$$

$$M^{-1} \sigma^\mu (M^{-1})^\dagger = \Lambda^\mu{}_\nu \sigma^\nu. \quad (2.67)$$

Eqs. (2.66) and (2.67) can be used to prove the covariance properties (with respect to Lorentz transformations) of the transformation law for the two-component undotted and dotted spinor fields, respectively.

As an example, consider a pure boost from the rest frame to a frame where $p^\mu = (E_{\mathbf{p}}, \vec{\mathbf{p}})$, which corresponds to $\theta_{ij} = 0$ and $\zeta^i = \theta^{i0} = -\theta^{0i}$. The matrices $M_\alpha{}^\beta$ and $[(M^{-1})^\dagger]_{\dot{\beta}}{}^{\dot{\alpha}}$ that govern the Lorentz transformations of spinor fields with a lowered undotted index and spinor fields with a raised dotted index, respectively, are given by:

$$\exp\left(-\frac{i}{2}\theta_{\mu\nu}J^{\mu\nu}\right) = \begin{cases} M = \exp\left(-\frac{1}{2}\vec{\zeta} \cdot \vec{\sigma}\right) = \sqrt{\frac{p \cdot \sigma}{m}}, & \text{for } (\tfrac{1}{2}, 0), \\ (M^{-1})^\dagger = \exp\left(\frac{1}{2}\vec{\zeta} \cdot \vec{\sigma}\right) = \sqrt{\frac{p \cdot \bar{\sigma}}{m}}, & \text{for } (0, \tfrac{1}{2}), \end{cases} \quad (2.68)$$

where⁴

$$\sqrt{p \cdot \sigma} \equiv \frac{E_{\mathbf{p}} + m - \vec{\sigma} \cdot \vec{\mathbf{p}}}{\sqrt{2(E_{\mathbf{p}} + m)}}, \quad (2.69)$$

$$\sqrt{p \cdot \bar{\sigma}} \equiv \frac{E_{\mathbf{p}} + m + \vec{\sigma} \cdot \vec{\mathbf{p}}}{\sqrt{2(E_{\mathbf{p}} + m)}}. \quad (2.70)$$

These matrix square roots are defined under the assumption that $p^0 = E_{\mathbf{p}} \equiv (|\vec{\mathbf{p}}|^2 + m^2)^{1/2}$, and are chosen to be the unique hermitian matrices with non-negative eigenvalues whose squares are equal to $p \cdot \sigma$ and $p \cdot \bar{\sigma}$, respectively.

Consider an arbitrary four-vector S^μ [defined in a reference frame where $p^\mu = (E; \vec{\mathbf{p}})$], whose rest frame value is S_R^μ , i.e.

$$S^\mu = \Lambda^\mu{}_\nu S_R^\nu, \quad \text{with} \quad \Lambda = \begin{pmatrix} E/m & p^j/m \\ p^i/m & \delta_{ij} + \frac{p^i p^j}{m(E + m)} \end{pmatrix}. \quad (2.71)$$

Then, using eqs. (2.7), (2.67) and (2.68), it follows that:

$$\sqrt{p \cdot \sigma} S \cdot \bar{\sigma} \sqrt{p \cdot \sigma} = m S_R \cdot \bar{\sigma}, \quad (2.72)$$

$$\sqrt{p \cdot \bar{\sigma}} S \cdot \sigma \sqrt{p \cdot \bar{\sigma}} = m S_R \cdot \sigma. \quad (2.73)$$

⁴One can check the validity of eqs. (2.69) and (2.70) by squaring both sides of the respective equations.

The generalization of the spinor results of this section to $d \neq 4$, useful for dimensional continuation regularization schemes, is discussed in Appendix A. In particular, the Fierz identities of eqs. (2.36)–(2.37) and eqs. (2.55)–(2.57) and the identities (2.41), (2.42), (2.44) and (2.45) involving the 4-dimensional ϵ tensor are not valid unless μ is a Lorentz vector index in exactly 4 dimensions. In $d \neq 4$ dimensions, as used for loop amplitudes in dimensional regularization and dimensional reduction schemes, the necessary modifications are given in Appendix A. We also direct the reader's attention to Appendix E, which gives a detailed correspondence between two-component spinor and four-component spinor notations.

3 Properties of fermion fields

3.1 A single two-component fermion field

We begin by describing the properties of a free neutral massive anti-commuting spin-1/2 field, denoted $\xi_\alpha(x)$, which transforms as $(\frac{1}{2}, 0)$ under the Lorentz group. The field ξ_α therefore describes a Majorana fermion. The free-field Lagrangian density is [5–7]:

$$\mathcal{L} = i\bar{\xi}\bar{\sigma}^\mu\partial_\mu\xi - \frac{1}{2}m(\xi\xi + \bar{\xi}\bar{\xi}). \quad (3.1)$$

On-shell, ξ satisfies the free-field Dirac equation [4, 5],

$$i\bar{\sigma}^{\mu\dot{\alpha}\beta}\partial_\mu\xi_\beta = m\bar{\xi}^{\dot{\alpha}}. \quad (3.2)$$

Consequently after quantization, ξ_α can be expanded in a Fourier series [46]:

$$\xi_\alpha(x) = \sum_s \int \frac{d^3\vec{p}}{(2\pi)^{3/2}(2E_{\vec{p}})^{1/2}} \left[x_\alpha(\vec{p}, s) a(\vec{p}, s) e^{-ip \cdot x} + y_\alpha(\vec{p}, s) a^\dagger(\vec{p}, s) e^{ip \cdot x} \right], \quad (3.3)$$

where $E_{\vec{p}} \equiv (|\vec{p}|^2 + m^2)^{1/2}$, and the creation and annihilation operators a^\dagger and a satisfy anti-commutation relations:

$$\{a(\vec{p}, s), a^\dagger(\vec{p}', s')\} = \delta^3(\vec{p} - \vec{p}') \delta_{ss'}, \quad (3.4)$$

and all other anticommutators vanish. It follows that

$$\bar{\xi}_{\dot{\alpha}}(x) \equiv (\xi_\alpha)^\dagger = \sum_s \int \frac{d^3\vec{p}}{(2\pi)^{3/2}(2E_{\vec{p}})^{1/2}} \left[\bar{x}_{\dot{\alpha}}(\vec{p}, s) a^\dagger(\vec{p}, s) e^{ip \cdot x} + \bar{y}_{\dot{\alpha}}(\vec{p}, s) a(\vec{p}, s) e^{-ip \cdot x} \right]. \quad (3.5)$$

We employ covariant normalization of the one particle states, i.e., we act with one creation operator on the vacuum with the following convention

$$|\vec{p}, s\rangle \equiv (2\pi)^{3/2}(2E_{\vec{p}})^{1/2} a^\dagger(\vec{p}, s) |0\rangle, \quad (3.6)$$

so that $\langle \vec{p}, s | \vec{p}', s' \rangle = (2\pi)^3 (2E_{\vec{p}}) \delta^3(\vec{p} - \vec{p}') \delta_{ss'}$. Therefore,

$$\langle 0 | \xi_\alpha(x) | \vec{p}, s \rangle = x_\alpha(\vec{p}, s) e^{-ip \cdot x}, \quad \langle 0 | \bar{\xi}_{\dot{\alpha}}(x) | \vec{p}, s \rangle = \bar{y}_{\dot{\alpha}}(\vec{p}, s) e^{-ip \cdot x}, \quad (3.7)$$

$$\langle \vec{p}, s | \xi_\alpha(x) | 0 \rangle = y_\alpha(\vec{p}, s) e^{ip \cdot x}, \quad \langle \vec{p}, s | \bar{\xi}_{\dot{\alpha}}(x) | 0 \rangle = \bar{x}_{\dot{\alpha}}(\vec{p}, s) e^{ip \cdot x}. \quad (3.8)$$

It should be emphasized that $\xi_\alpha(x)$ is an anticommuting spinor field, whereas x_α and y_α are *commuting* two-component spinor wave functions. The anticommuting properties of the fields are carried by the creation and annihilation operators.

Applying eq. (3.2) to eq. (3.3), we find that the x_α and y_α satisfy momentum space Dirac equations. These conditions can be written down in a number of equivalent ways:

$$(p \cdot \bar{\sigma})^{\dot{\alpha}\beta} x_\beta = m \bar{y}^{\dot{\alpha}} , \quad (p \cdot \sigma)_{\alpha\dot{\beta}} \bar{y}^{\dot{\beta}} = m x_\alpha , \quad (3.9)$$

$$(p \cdot \sigma)_{\alpha\dot{\beta}} \bar{x}^{\dot{\beta}} = -m y_\alpha , \quad (p \cdot \bar{\sigma})^{\dot{\alpha}\beta} y_\beta = -m \bar{x}^{\dot{\alpha}} , \quad (3.10)$$

$$x^\alpha (p \cdot \sigma)_{\alpha\dot{\beta}} = -m \bar{y}_{\dot{\beta}} , \quad \bar{y}_{\dot{\alpha}} (p \cdot \bar{\sigma})^{\dot{\alpha}\beta} = -m x^\beta , \quad (3.11)$$

$$\bar{x}_{\dot{\alpha}} (p \cdot \bar{\sigma})^{\dot{\alpha}\beta} = m y^\beta , \quad y^\alpha (p \cdot \sigma)_{\alpha\dot{\beta}} = m \bar{x}_{\dot{\beta}} . \quad (3.12)$$

Using the identities $[(p \cdot \sigma)(p \cdot \bar{\sigma})]_\alpha^\beta = p^2 \delta_\alpha^\beta$ and $[(p \cdot \bar{\sigma})(p \cdot \sigma)]_{\dot{\alpha}}^{\dot{\beta}} = p^2 \delta_{\dot{\alpha}}^{\dot{\beta}}$, one can quickly check that both x_α and y_α must satisfy the mass-shell condition, $p^2 = m^2$ (or equivalently, $p^0 = E_{\mathbf{p}}$). We will later see that eqs. (3.9)–(3.12) are often useful for simplifying matrix elements.

The quantum number s labels the spin or helicity of the spin-1/2 fermion. We shall consider two approaches for constructing the spin-1/2 states. In the first approach, we consider the particle in its rest frame and quantize the spin along a fixed axis specified by the unit vector $\hat{\mathbf{s}} \equiv (\sin \theta \cos \phi, \sin \theta \sin \phi, \cos \theta)$ with polar angle θ and azimuthal angle ϕ with respect to a fixed z -axis.⁵ The corresponding spin states will be called fixed-axis spin states. The relevant basis of two-component spinors χ_s are eigenstates of $\frac{1}{2} \vec{\sigma} \cdot \hat{\mathbf{s}}$, i.e.,

$$\frac{1}{2} \vec{\sigma} \cdot \hat{\mathbf{s}} \chi_s = s \chi_s , \quad s = \pm \frac{1}{2} . \quad (3.13)$$

Explicit forms for the two-component spinors χ_s and their properties are given in Appendix B.

The fixed-axis spin states described above are not very convenient for particles in relativistic motion. Moreover, these states cannot be employed for massless particles since no rest frame exists. Thus, a second approach is to consider helicity states and the corresponding basis of two-component helicity spinors χ_λ that are eigenstates of $\frac{1}{2} \vec{\sigma} \cdot \hat{\mathbf{p}}$, i.e.,

$$\frac{1}{2} \vec{\sigma} \cdot \hat{\mathbf{p}} \chi_\lambda = \lambda \chi_\lambda , \quad \lambda = \pm \frac{1}{2} . \quad (3.14)$$

Here $\hat{\mathbf{p}}$ is the unit vector in the direction of the three-momentum, with polar angle θ and azimuthal angle ϕ with respect to a fixed z -axis. That is, the two-component helicity spinors can be obtained from the fixed-axis spinors by replacing $\hat{\mathbf{s}}$ by $\hat{\mathbf{p}}$ and identifying θ and ϕ as the polar and azimuthal angles of $\hat{\mathbf{p}}$.

For fermions of mass $m \neq 0$, it is possible to define the spin four-vector S^μ , which is specified in the rest frame by $(0; \hat{\mathbf{s}})$. The unit three-vector $\hat{\mathbf{s}}$ corresponds to the axis of spin quantization

⁵In the literature, it is a common practice to choose $\hat{\mathbf{s}} = \hat{\mathbf{z}}$. However in order to be somewhat more general, we shall not assume this convention here.

in the case of fixed-axis spin states. In an arbitrary reference frame, the spin four-vector satisfies $S \cdot p = 0$ and $S \cdot S = -1$. After boosting from the rest frame to a frame in which $p^\mu = (E, \vec{p})$ [cf. eq. (2.71)], one finds:

$$S^\mu = \left(\frac{\vec{p} \cdot \hat{s}}{m}; \hat{s} + \frac{(\vec{p} \cdot \hat{s}) \vec{p}}{m(E + m)} \right). \quad (3.15)$$

If necessary, we shall write $S^\mu(\hat{s})$ to emphasize the dependence of S^μ on \hat{s} .

The spin four-vector for helicity states is defined by taking $\hat{s} = \hat{p}$. Eq. (3.15) then reduces to

$$S^\mu = \frac{1}{m} (|\vec{p}|; E\hat{p}). \quad (3.16)$$

In the non-relativistic limit, the spin four-vector for helicity states is $S^\mu \approx (0; \hat{p})$, as expected.⁶ In the high energy limit ($E \gg m$), $S^\mu = p^\mu/m + \mathcal{O}(m/E)$. For a massless fermion, the spin four-vector does not exist (as there is no rest frame). Nevertheless, one can obtain consistent results by working with massive helicity states and taking the $m \rightarrow 0$ limit at the end of the computation. In this case, one can simply use $S^\mu = p^\mu/m + \mathcal{O}(m/E)$; in practical computations the final result will be well-defined in the zero mass limit. In contrast, for massive fermions at rest, the helicity state does not exist without reference to some particular boost direction as noted in footnote 6.

Using eqs. (2.72) and (2.73), with $S_R^\mu = (0; \hat{s})$, the following two important formulae are obtained:

$$\sqrt{p \cdot \sigma} S \cdot \bar{\sigma} \sqrt{p \cdot \sigma} = m \vec{\sigma} \cdot \hat{s}, \quad (3.17)$$

$$\sqrt{p \cdot \bar{\sigma}} S \cdot \sigma \sqrt{p \cdot \bar{\sigma}} = -m \vec{\sigma} \cdot \hat{s}. \quad (3.18)$$

These results can also be derived directly by employing the explicit form for the spin vector S^μ [eq. (3.15)] and the results of eqs. (2.69) and (2.70).

The two-component spinor wave functions x and y can now be given explicitly in terms of the χ_s defined in eq. (B.6). First, we note that eq. (3.9) when evaluated in the rest frame yields $x_1 = \bar{y}^1$ and $x_2 = \bar{y}^2$. That is, as column vectors, $x_\alpha(\vec{p} = 0) = \bar{y}^\alpha(\vec{p} = 0)$ can be expressed in general as some linear combination of the χ_s ($s = \pm \frac{1}{2}$). Hence, we may choose $x_\alpha(\vec{p} = 0, s) = \bar{y}^\alpha(\vec{p} = 0, s) = \sqrt{m} \chi_s$, where the factor of \sqrt{m} reflects the standard relativistic normalization of the rest-frame spin states. These wave functions can be boosted to an arbitrary frame using eq. (2.68). The resulting undotted spinor wave functions are given by (see [62]) for related expressions

$$x_\alpha(\vec{p}, s) = \sqrt{p \cdot \sigma} \chi_s, \quad x^\alpha(\vec{p}, s) = -2s \chi_{-s}^\dagger \sqrt{p \cdot \bar{\sigma}}, \quad (3.19)$$

$$y_\alpha(\vec{p}, s) = 2s \sqrt{p \cdot \sigma} \chi_{-s}, \quad y^\alpha(\vec{p}, s) = \chi_s^\dagger \sqrt{p \cdot \bar{\sigma}}, \quad (3.20)$$

⁶Strictly speaking, \hat{p} is not defined in the rest frame. In practice, helicity states are defined in some moving frame with momentum \vec{p} . The rest frame is achieved by boosting in the direction of $-\vec{p}$.

and the dotted spinor wave functions are given by

$$\bar{x}^{\dot{\alpha}}(\vec{p}, s) = -2s\sqrt{p \cdot \bar{\sigma}} \chi_{-s}, \quad \bar{x}_{\dot{\alpha}}(\vec{p}, s) = \chi_s^{\dagger} \sqrt{p \cdot \sigma}, \quad (3.21)$$

$$\bar{y}^{\dot{\alpha}}(\vec{p}, s) = \sqrt{p \cdot \bar{\sigma}} \chi_s, \quad \bar{y}_{\dot{\alpha}}(\vec{p}, s) = 2s\chi_{-s}^{\dagger} \sqrt{p \cdot \sigma}, \quad (3.22)$$

where $\sqrt{p \cdot \sigma}$ and $\sqrt{p \cdot \bar{\sigma}}$ are defined in eqs. (2.69) and (2.70).

The phase choices in eqs. (3.19)–(3.22) are consistent with those employed for four-component spinor wave functions [see Appendix E]. We again emphasize that in eqs. (3.19)–(3.22), one may either choose χ_s to be an eigenstate of $\vec{\sigma} \cdot \hat{s}$, where the spin is measured in the rest frame along the quantization axis \hat{s} , or choose χ_s to be an eigenstate of $\vec{\sigma} \cdot \hat{p}$ (in this case we write $s = \lambda$), which yields the helicity spinor wave functions.

The following equations can now be derived:

$$(S \cdot \bar{\sigma})^{\dot{\alpha}\beta} x_{\beta}(\vec{p}, s) = 2s\bar{y}^{\dot{\alpha}}(\vec{p}, s), \quad (S \cdot \sigma)_{\alpha\dot{\beta}} \bar{y}^{\dot{\beta}}(\vec{p}, s) = -2sx_{\alpha}(\vec{p}, s), \quad (3.23)$$

$$(S \cdot \sigma)_{\alpha\dot{\beta}} \bar{x}^{\dot{\beta}}(\vec{p}, s) = -2sy_{\alpha}(\vec{p}, s), \quad (S \cdot \bar{\sigma})^{\dot{\alpha}\beta} y_{\beta}(\vec{p}, s) = 2s\bar{x}^{\dot{\alpha}}(\vec{p}, s), \quad (3.24)$$

$$x^{\alpha}(\vec{p}, s)(S \cdot \sigma)_{\alpha\dot{\beta}} = -2s\bar{y}_{\dot{\beta}}(\vec{p}, s), \quad \bar{y}_{\dot{\alpha}}(\vec{p}, s)(S \cdot \bar{\sigma})^{\dot{\alpha}\beta} = 2sx^{\beta}(\vec{p}, s), \quad (3.25)$$

$$\bar{x}_{\dot{\alpha}}(\vec{p}, s)(S \cdot \bar{\sigma})^{\dot{\alpha}\beta} = 2sy^{\beta}(\vec{p}, s), \quad y^{\alpha}(\vec{p}, s)(S \cdot \sigma)_{\alpha\dot{\beta}} = -2s\bar{x}_{\dot{\beta}}(\vec{p}, s). \quad (3.26)$$

For example, using eqs. (3.17) and (3.18) and the definitions above for $x_{\alpha}(\vec{p}, s)$ and $\bar{y}^{\dot{\alpha}}(\vec{p}, s)$, we find (suppressing spinor indices),

$$\sqrt{p \cdot \sigma} S \cdot \bar{\sigma} x(\vec{p}, s) = \sqrt{p \cdot \sigma} S \cdot \bar{\sigma} \sqrt{p \cdot \sigma} \chi_s = m \vec{\sigma} \cdot \hat{s} \chi_s = 2sm \chi_s. \quad (3.27)$$

Multiplying both sides of eq. (3.27) by $\sqrt{p \cdot \bar{\sigma}}$ and noting that $\sqrt{p \cdot \bar{\sigma}} \sqrt{p \cdot \sigma} = m$, we end up with

$$S \cdot \bar{\sigma} x(\vec{p}, s) = 2s\sqrt{p \cdot \bar{\sigma}} \chi_s = 2s\bar{y}(\vec{p}, s). \quad (3.28)$$

All the results of eqs. (3.23)–(3.26) can be derived in this manner.

The consistency of eqs. (3.23)–(3.26) can also be checked as follows. First, each of these equations yields

$$(S \cdot \sigma)_{\alpha\dot{\alpha}} (S \cdot \bar{\sigma})^{\dot{\alpha}\beta} = -\delta_{\alpha}^{\beta}, \quad (S \cdot \bar{\sigma})^{\dot{\alpha}\alpha} (S \cdot \sigma)_{\alpha\dot{\beta}} = -\delta_{\dot{\beta}}^{\dot{\alpha}}. \quad (3.29)$$

after noting that $4s^2 = 1$ (for $s = \pm \frac{1}{2}$). From eqs. (2.39) and (2.40) it follows that $S \cdot S = -1$, as required. Second, if one applies

$$(p \cdot \sigma S \cdot \bar{\sigma} + S \cdot \sigma p \cdot \bar{\sigma})_{\alpha}^{\beta} = 2p \cdot S \delta_{\alpha}^{\beta}, \quad (p \cdot \bar{\sigma} S \cdot \sigma + S \cdot \bar{\sigma} p \cdot \sigma)^{\dot{\alpha}}_{\dot{\beta}} = 2p \cdot S \delta_{\dot{\beta}}^{\dot{\alpha}}, \quad (3.30)$$

to eqs. (3.9)–(3.12) and eqs. (3.23)–(3.26), it follows that $p \cdot S = 0$.

It is useful to combine the results of eqs. (3.9)–(3.12) and eqs. (3.23)–(3.26) as follows:

$$(p^{\mu} - 2smS^{\mu}) \bar{\sigma}_{\mu}^{\dot{\alpha}\beta} x_{\beta}(\vec{p}, s) = 0, \quad (p_{\mu} - 2smS_{\mu}) \sigma_{\alpha\dot{\beta}}^{\mu} \bar{x}^{\dot{\beta}}(\vec{p}, s) = 0, \quad (3.31)$$

$$(p^{\mu} + 2smS^{\mu}) \bar{\sigma}_{\mu}^{\dot{\alpha}\beta} y_{\beta}(\vec{p}, s) = 0, \quad (p_{\mu} + 2smS_{\mu}) \sigma_{\alpha\dot{\beta}}^{\mu} \bar{y}^{\dot{\beta}}(\vec{p}, s) = 0, \quad (3.32)$$

$$x^{\alpha}(\vec{p}, s) \sigma_{\alpha\dot{\beta}}^{\mu} (p_{\mu} - 2smS_{\mu}) = 0, \quad \bar{x}_{\dot{\alpha}}(\vec{p}, s) \bar{\sigma}_{\mu}^{\dot{\alpha}\beta} (p^{\mu} - 2smS^{\mu}) = 0, \quad (3.33)$$

$$y^{\alpha}(\vec{p}, s) \sigma_{\alpha\dot{\beta}}^{\mu} (p_{\mu} + 2smS_{\mu}) = 0, \quad \bar{y}_{\dot{\alpha}}(\vec{p}, s) \bar{\sigma}_{\mu}^{\dot{\alpha}\beta} (p^{\mu} + 2smS^{\mu}) = 0. \quad (3.34)$$

Eqs. (3.23)–(3.26) and eqs. (3.31)–(3.34) also apply to the helicity wave functions $x(\vec{p}, \lambda)$ and $y(\vec{p}, \lambda)$ simply by replacing s with λ and $S^\mu(\hat{s})$ [eq. (3.15)] with $S^\mu(\hat{p})$ [eq. (3.16)].

The above results are applicable only for massive fermions (where the spin four-vector S^μ exists). We may treat the case of massless fermions directly by employing helicity spinors in eqs. (3.19)–(3.22). Putting $E = |\vec{p}|$ and $m = 0$, we easily obtain:

$$x_\alpha(\vec{p}, \lambda) = \sqrt{2E} \left(\frac{1}{2} - \lambda\right) \chi_\lambda, \quad x^\alpha(\vec{p}, \lambda) = \sqrt{2E} \left(\frac{1}{2} - \lambda\right) \chi_{-\lambda}^\dagger, \quad (3.35)$$

$$y_\alpha(\vec{p}, \lambda) = \sqrt{2E} \left(\frac{1}{2} + \lambda\right) \chi_{-\lambda}, \quad y^\alpha(\vec{p}, \lambda) = \sqrt{2E} \left(\frac{1}{2} + \lambda\right) \chi_\lambda^\dagger, \quad (3.36)$$

or equivalently

$$\bar{x}^{\dot{\alpha}}(\vec{p}, \lambda) = \sqrt{2E} \left(\frac{1}{2} - \lambda\right) \chi_{-\lambda}, \quad \bar{x}_{\dot{\alpha}}(\vec{p}, \lambda) = \sqrt{2E} \left(\frac{1}{2} - \lambda\right) \chi_\lambda^\dagger, \quad (3.37)$$

$$\bar{y}^{\dot{\alpha}}(\vec{p}, \lambda) = \sqrt{2E} \left(\frac{1}{2} + \lambda\right) \chi_\lambda, \quad \bar{y}_{\dot{\alpha}}(\vec{p}, \lambda) = \sqrt{2E} \left(\frac{1}{2} + \lambda\right) \chi_{-\lambda}^\dagger. \quad (3.38)$$

It follows that:

$$\left(\frac{1}{2} + \lambda\right) x(\vec{p}, \lambda) = 0, \quad \left(\frac{1}{2} + \lambda\right) \bar{x}(\vec{p}, \lambda) = 0, \quad (3.39)$$

$$\left(\frac{1}{2} - \lambda\right) y(\vec{p}, \lambda) = 0, \quad \left(\frac{1}{2} - \lambda\right) \bar{y}(\vec{p}, \lambda) = 0, \quad (3.40)$$

The significance of eqs. (3.39) and (3.40) is clear; for massless fermions, only one helicity component of x and y is non-zero. Applying this result to neutrinos, we find that massless neutrinos are left-handed ($\lambda = -1/2$), while anti-neutrinos are right-handed ($\lambda = +1/2$).

Eqs. (3.39) and (3.40) can also be derived by carefully taking the $m \rightarrow 0$ limit of eqs. (3.31) and (3.32) applied to the helicity wave functions $x(\vec{p}, \lambda)$ and $y(\vec{p}, \lambda)$ [i.e., replacing s with λ]. We then replace mS^μ with p^μ , which is the leading term in the limit of $E \gg m$. Using the results of eqs. (3.9) and (3.10) and dividing out by an overall factor of m (before finally taking the $m \rightarrow 0$ limit) reproduces eqs. (3.39) and (3.40).

Having defined explicit forms for the two-component spinor wave functions, we can now write down the spin projection matrices. Noting that $\frac{1}{2}(1 + 2s \vec{\sigma} \cdot \hat{s}) \chi_{s'} = \frac{1}{2}(1 + 4ss') \chi_{s'} = \delta_{ss'} \chi_{s'}$ (since $s, s' = \pm \frac{1}{2}$), one can write:

$$\chi_s \chi_s^\dagger = \frac{1}{2} (1 + 2s \vec{\sigma} \cdot \hat{s}) \sum_{s'} \chi_{s'} \chi_{s'}^\dagger. \quad (3.41)$$

Using the completeness relation given in eq. (B.8), and eq. (3.17) for $\vec{\sigma} \cdot \hat{s}$, it follows that

$$\chi_s \chi_s^\dagger = \frac{1}{2} \left(1 + \frac{2s}{m} \sqrt{p \cdot \sigma} S \cdot \bar{\sigma} \sqrt{p \cdot \sigma} \right), \quad (3.42)$$

Hence, with both spinor indices in the lowered position,

$$\begin{aligned}
x(\vec{p}, s)\bar{x}(\vec{p}, s) &= \sqrt{p \cdot \sigma} \chi_s \chi_s^\dagger \sqrt{p \cdot \sigma} \\
&= \frac{1}{2} \sqrt{p \cdot \sigma} \left[1 + \frac{2s}{m} \sqrt{p \cdot \sigma} S \cdot \bar{\sigma} \sqrt{p \cdot \sigma} \right] \sqrt{p \cdot \sigma} \\
&= \frac{1}{2} \left[p \cdot \sigma + \frac{2s}{m} p \cdot \sigma S \cdot \bar{\sigma} p \cdot \sigma \right] \\
&= \frac{1}{2} [p \cdot \sigma - 2sm S \cdot \sigma] .
\end{aligned} \tag{3.43}$$

In the final step above, we simplified the product of three dot-products by noting that $p \cdot S = 0$ implies that $S \cdot \bar{\sigma} p \cdot \sigma = -p \cdot \bar{\sigma} S \cdot \sigma$. The other spin projection formulae for massive fermions can be similarly derived. The complete set of such formulae is given below: (see also [62])

$$x_\alpha(\vec{p}, s)\bar{x}_{\dot{\beta}}(\vec{p}, s) = \frac{1}{2}(p_\mu - 2smS_\mu)\sigma_{\alpha\dot{\beta}}^\mu, \tag{3.44}$$

$$\bar{y}^{\dot{\alpha}}(\vec{p}, s)y^\beta(\vec{p}, s) = \frac{1}{2}(p^\mu + 2smS^\mu)\bar{\sigma}_\mu^{\dot{\alpha}\beta}, \tag{3.45}$$

$$x_\alpha(\vec{p}, s)y^\beta(\vec{p}, s) = \frac{1}{2} \left(m\delta_\alpha^\beta - 2s[S \cdot \sigma p \cdot \bar{\sigma}]_\alpha^\beta \right), \tag{3.46}$$

$$\bar{y}^{\dot{\alpha}}(\vec{p}, s)\bar{x}_{\dot{\beta}}(\vec{p}, s) = \frac{1}{2} \left(m\delta_{\dot{\alpha}}^{\dot{\beta}} + 2s[S \cdot \bar{\sigma} p \cdot \sigma]_{\dot{\alpha}}^{\dot{\beta}} \right), \tag{3.47}$$

or equivalently,

$$\bar{x}^{\dot{\alpha}}(\vec{p}, s)x^\beta(\vec{p}, s) = \frac{1}{2}(p^\mu - 2smS^\mu)\bar{\sigma}_\mu^{\dot{\alpha}\beta}, \tag{3.48}$$

$$y_\alpha(\vec{p}, s)\bar{y}_{\dot{\beta}}(\vec{p}, s) = \frac{1}{2}(p_\mu + 2smS_\mu)\sigma_{\alpha\dot{\beta}}^\mu, \tag{3.49}$$

$$y_\alpha(\vec{p}, s)x^\beta(\vec{p}, s) = -\frac{1}{2} \left(m\delta_\alpha^\beta + 2s[S \cdot \sigma p \cdot \bar{\sigma}]_\alpha^\beta \right), \tag{3.50}$$

$$\bar{x}^{\dot{\alpha}}(\vec{p}, s)\bar{y}_{\dot{\beta}}(\vec{p}, s) = -\frac{1}{2} \left(m\delta_{\dot{\alpha}}^{\dot{\beta}} - 2s[S \cdot \bar{\sigma} p \cdot \sigma]_{\dot{\alpha}}^{\dot{\beta}} \right). \tag{3.51}$$

For the case of massless spin-1/2 fermions, we must use helicity spinor wave functions. The corresponding massless projection operators can be obtained directly from the explicit forms for the two-component spinor wave functions given in eqs. (3.35)–(3.38):

$$x_\alpha(\vec{p}, \lambda)\bar{x}_{\dot{\beta}}(\vec{p}, \lambda) = (\tfrac{1}{2} - \lambda)p \cdot \sigma_{\alpha\dot{\beta}}, \quad \bar{x}^{\dot{\alpha}}(\vec{p}, \lambda)x^\beta(\vec{p}, \lambda) = (\tfrac{1}{2} - \lambda)p \cdot \bar{\sigma}^{\dot{\alpha}\beta}, \tag{3.52}$$

$$\bar{y}^{\dot{\alpha}}(\vec{p}, \lambda)y^\beta(\vec{p}, \lambda) = (\tfrac{1}{2} + \lambda)p \cdot \bar{\sigma}^{\dot{\alpha}\beta}, \quad y_\alpha(\vec{p}, \lambda)\bar{y}_{\dot{\beta}}(\vec{p}, \lambda) = (\tfrac{1}{2} + \lambda)p \cdot \sigma_{\alpha\dot{\beta}}, \tag{3.53}$$

$$x_\alpha(\vec{p}, \lambda)y^\beta(\vec{p}, \lambda) = 0, \quad y_\alpha(\vec{p}, \lambda)x^\beta(\vec{p}, \lambda) = 0, \tag{3.54}$$

$$\bar{y}^{\dot{\alpha}}(\vec{p}, \lambda)\bar{x}_{\dot{\beta}}(\vec{p}, \lambda) = 0, \quad \bar{x}^{\dot{\alpha}}(\vec{p}, \lambda)\bar{y}_{\dot{\beta}}(\vec{p}, \lambda) = 0. \tag{3.55}$$

As a check, one can verify that the above results follow from eqs. (3.44)–(3.51), by replacing s with λ , setting $mS^\mu = p^\mu$, and taking the $m \rightarrow 0$ limit at the end of the computation.

Having listed the projection operators for definite spin projection or helicity, we may now sum over spins to derive the spin-sum identities. These arise when computing squared matrix elements for unpolarized scattering and decay. There are only four basic identities, but for

convenience we list each of them with the two index height permutations that can occur in squared amplitudes by following the rules given in this paper. The results can be derived by inspection of the spin projection operators, since summing over $s = \pm \frac{1}{2}$ simply removes all terms linear in the spin four-vector S^μ .

$$\sum_s x_\alpha(\vec{p}, s) \bar{x}_{\dot{\beta}}(\vec{p}, s) = p \cdot \sigma_{\alpha\dot{\beta}}, \quad \sum_s \bar{x}^{\dot{\alpha}}(\vec{p}, s) x^\beta(\vec{p}, s) = p \cdot \bar{\sigma}^{\dot{\alpha}\beta}, \quad (3.56)$$

$$\sum_s \bar{y}^{\dot{\alpha}}(\vec{p}, s) y^\beta(\vec{p}, s) = p \cdot \bar{\sigma}^{\dot{\alpha}\beta}, \quad \sum_s y_\alpha(\vec{p}, s) \bar{y}_{\dot{\beta}}(\vec{p}, s) = p \cdot \sigma_{\alpha\dot{\beta}}, \quad (3.57)$$

$$\sum_s x_\alpha(\vec{p}, s) y^\beta(\vec{p}, s) = m \delta_\alpha^\beta, \quad \sum_s y_\alpha(\vec{p}, s) x^\beta(\vec{p}, s) = -m \delta_\alpha^\beta, \quad (3.58)$$

$$\sum_s \bar{y}^{\dot{\alpha}}(\vec{p}, s) \bar{x}_{\dot{\beta}}(\vec{p}, s) = m \delta_{\dot{\alpha}}^{\dot{\beta}}, \quad \sum_s \bar{x}^{\dot{\alpha}}(\vec{p}, s) \bar{y}_{\dot{\beta}}(\vec{p}, s) = -m \delta_{\dot{\alpha}}^{\dot{\beta}}. \quad (3.59)$$

These results are applicable both to spin-sums and helicity-sums, and hold for both massive and massless spin-1/2 fermions.

One can also work out generalizations of the massive and massive projection operators. These are products of two-component spinor wave functions, where the spin or helicity of each spinor may be different. These are the Bouchiat-Michel formulae [135], which are derived in Appendix F.

3.2 Fermion mass diagonalization and external wave functions in a general theory

Consider a collection of free anti-commuting two-component spin-1/2 fields, $\hat{\xi}_{\alpha i}(x)$, which transform as $(\frac{1}{2}, 0)$ fields under the Lorentz group. Here, α is the spinor index, and i labels the distinct fields of the collection. The free-field Lagrangian is given by (see for example [67] for a discussion of this Lagrangian)

$$\mathcal{L} = i \bar{\hat{\xi}}^i \bar{\sigma}^\mu \partial_\mu \hat{\xi}_i - \frac{1}{2} M^{ij} \hat{\xi}_i \hat{\xi}_j - \frac{1}{2} M_{ij} \bar{\hat{\xi}}^i \bar{\hat{\xi}}^j, \quad (3.60)$$

where

$$M_{ij} \equiv (M^{ij})^*. \quad (3.61)$$

Note that M^{ij} is a complex symmetric matrix, since the product of anticommuting two-component fields satisfies $\hat{\xi}_i \hat{\xi}_j = \hat{\xi}_j \hat{\xi}_i$ [with the spinor contraction rule according to eq. (2.25)].

In eq. (3.60), we have used the following convention concerning the “flavor” labels i and j . Each left-handed $(\frac{1}{2}, 0)$ fermion always has an index with the opposite height of the corresponding right-handed $(0, \frac{1}{2})$ fermion. Raised indices can only be contracted with lowered indices and vice versa. Flipping the heights of all flavor indices of an object corresponds to complex conjugation,

as in eq. (3.61).⁷

We can diagonalize the mass matrix and rewrite the Lagrangian in terms of mass eigenstates $\xi_{\alpha i}$, which have corresponding real non-negative masses m_i . To do this, we introduce a unitary matrix Ω

$$\hat{\xi}_i = \Omega_i^k \xi_k \quad (3.62)$$

and demand that $M^{ij} \Omega_i^k \Omega_j^\ell = m_k \delta^{k\ell}$ (no sum over k), where the m_k are real and non-negative. Equivalently, in matrix notation with suppressed indices,⁸

$$\Omega^\top M \Omega = \mathbf{m} = \text{diag}(m_1, m_2, \dots). \quad (3.63)$$

This is the so-called Takagi diagonalization [69, 70] of an arbitrary complex symmetric matrix, which is discussed in more detail in Appendix D. To compute the values of the diagonal elements of \mathbf{m} , note that

$$\Omega M^\dagger M \Omega^\dagger = \mathbf{m}^2. \quad (3.64)$$

Indeed $M^\dagger M$ is hermitian and thus it can be diagonalized by a unitary matrix. Hence, the elements of the diagonal matrix \mathbf{m} are the non-negative square roots of the corresponding eigenvalues of $M^\dagger M$. However, in cases where $M^\dagger M$ has degenerate eigenvalues, eq. (3.64) *cannot* be employed to determine the unitary matrix Ω that satisfies eq. (3.63). A more general technique for determining Ω that works in all cases is given in Appendix D.

In terms of the mass eigenstates,

$$\mathcal{L} = i \bar{\xi}^i \bar{\sigma}^\mu \partial_\mu \xi_i - \frac{1}{2} m_i (\xi_i \xi_i + \bar{\xi}^i \bar{\xi}^i). \quad (3.65)$$

Each $\xi_{\alpha i}$ can now be expanded in a Fourier series, exactly as in the previous subsection:

$$\xi_{\alpha i}(x) = \sum_s \int \frac{d^3 \vec{p}}{(2\pi)^{3/2} (2E_{i\vec{p}})^{1/2}} \left[x_{\alpha i}(\vec{p}, s) a_i(\vec{p}, s) e^{-ip \cdot x} + y_{\alpha i}(\vec{p}, s) a_i^\dagger(\vec{p}, s) e^{ip \cdot x} \right], \quad (3.66)$$

where $E_{i\vec{p}} \equiv (|\vec{p}|^2 + m_i^2)^{1/2}$, and the creation and annihilation operators, a_i^\dagger and a_i satisfy anticommutation relations:

$$\{a_i(\vec{p}, s), a_j^\dagger(\vec{p}', s')\} = \delta^3(\vec{p} - \vec{p}') \delta_{ss'} \delta_{ij}. \quad (3.67)$$

We employ covariant normalization of the one particle states, i.e., we act with one creation operator on the vacuum with the following convention

$$|\vec{p}, s\rangle \equiv (2\pi)^{3/2} (2E_{i\vec{p}})^{1/2} a_i^\dagger(\vec{p}, s) |0\rangle, \quad (3.68)$$

⁷In the case at hand, we have more specifically chosen all of the left-handed fermions to have lowered flavor indices, which implies that all of the right-handed fermions have raised flavor indices. However, in cases where a subset of left-handed fermions transform according to some representation R of a (global) symmetry whereas a different subset of left-handed fermions transform according to the conjugate representation R^* , it is often more convenient to employ a raised flavor index for the latter subset of left-handed fields.

⁸In general, the m_i are *not* the eigenvalues of M . Rather, they are the *singular values* of the matrix M , which are defined to be the positive square roots of the eigenvalues of $M^\dagger M$. See Appendix D for further details.

so that $\langle \vec{p} | \vec{p}' \rangle = (2\pi)^3 (2E_{\vec{p}}) \delta^3(\vec{p} - \vec{p}')$.

There is a useful modification to the mass diagonalization procedure above that is convenient when there are massive Dirac fermions carrying a conserved charge. The key observation is that one only needs a diagonal *squared*-mass matrix to ensure that the denominators of propagators are diagonal. If χ_α is a charged massive field, then there must be an associated independent two-component spinor field η_α of equal mass with the opposite charge. They appear in the free-field Lagrangian as [6]:

$$\mathcal{L} = i\bar{\chi}\bar{\sigma}^\mu\partial_\mu\chi + i\bar{\eta}\bar{\sigma}^\mu\partial_\mu\eta - m(\chi\eta + \bar{\chi}\bar{\eta}). \quad (3.69)$$

Together, χ and $\bar{\eta}$ constitute a single Dirac fermion. We can then write:

$$\chi_\alpha(x) = \sum_s \int \frac{d^3\vec{p}}{(2\pi)^{3/2}(2E_{\vec{p}})^{1/2}} \left[x_\alpha(\vec{p}, s) a(\vec{p}, s) e^{-ip \cdot x} + y_\alpha(\vec{p}, s) b^\dagger(\vec{p}, s) e^{ip \cdot x} \right], \quad (3.70)$$

$$\eta_\alpha(x) = \sum_s \int \frac{d^3\vec{p}}{(2\pi)^{3/2}(2E_{\vec{p}})^{1/2}} \left[x_\alpha(\vec{p}, s) b(\vec{p}, s) e^{-ip \cdot x} + y_\alpha(\vec{p}, s) a^\dagger(\vec{p}, s) e^{ip \cdot x} \right], \quad (3.71)$$

where $E_{\vec{p}} \equiv (|\vec{p}|^2 + m^2)^{1/2}$, the creation and annihilation operators, a^\dagger , b^\dagger , a and b satisfy anticommutation relations:

$$\{a(\vec{p}, s), a^\dagger(\vec{p}', s')\} = \{b(\vec{p}, s), b^\dagger(\vec{p}', s')\} = \delta^3(\vec{p} - \vec{p}') \delta_{s, s'}, \quad (3.72)$$

and all other anticommutators vanish. We now must distinguish between two types of one particle states, which we can call fermion (F) and anti-fermion (A):

$$|\vec{p}, s; F\rangle \equiv (2\pi)^{3/2} (2E_{\vec{p}})^{1/2} a^\dagger(\vec{p}, s) |0\rangle, \quad (3.73)$$

$$|\vec{p}, s; A\rangle \equiv (2\pi)^{3/2} (2E_{\vec{p}})^{1/2} b^\dagger(\vec{p}, s) |0\rangle. \quad (3.74)$$

Note that both $\eta(x)$ and $\bar{\chi}(x)$ can create $|\vec{p}, s; F\rangle$ from the vacuum, while $\bar{\eta}(x)$ and $\chi(x)$ can create $|\vec{p}, s; A\rangle$. The one-particle wave functions are given by:

$$\langle 0 | \chi_\alpha(x) | \vec{p}, s; F \rangle = x_\alpha(\vec{p}, s) e^{-ip \cdot x}, \quad \langle 0 | \bar{\eta}_{\dot{\alpha}}(x) | \vec{p}, s; F \rangle = \bar{y}_{\dot{\alpha}}(\vec{p}, s) e^{-ip \cdot x}, \quad (3.75)$$

$$\langle F; \vec{p}, s | \eta_\alpha(x) | 0 \rangle = y_\alpha(\vec{p}, s) e^{ip \cdot x}, \quad \langle F; \vec{p}, s | \bar{\chi}_{\dot{\alpha}}(x) | 0 \rangle = \bar{x}_{\dot{\alpha}}(\vec{p}, s) e^{ip \cdot x}, \quad (3.76)$$

$$\langle 0 | \eta_\alpha(x) | \vec{p}, s; A \rangle = x_\alpha(\vec{p}, s) e^{-ip \cdot x}, \quad \langle 0 | \bar{\chi}_{\dot{\alpha}}(x) | \vec{p}, s; A \rangle = \bar{y}_{\dot{\alpha}}(\vec{p}, s) e^{-ip \cdot x}, \quad (3.77)$$

$$\langle A; \vec{p}, s | \chi_\alpha(x) | 0 \rangle = y_\alpha(\vec{p}, s) e^{ip \cdot x}, \quad \langle A; \vec{p}, s | \bar{\eta}_{\dot{\alpha}}(x) | 0 \rangle = \bar{x}_{\dot{\alpha}}(\vec{p}, s) e^{ip \cdot x}, \quad (3.78)$$

and the eight other single-particle matrix elements vanish.

More generally, consider a collection of such free anti-commuting charged massive spin-1/2 fields, which can be represented by pairs of two-component fields $\hat{\chi}_{\alpha i}(x)$, $\hat{\eta}_{\dot{\alpha}}^i(x)$. These fields transform in (possibly reducible) representations of the unbroken symmetry group that

are complex conjugates of each other. (This is the reason for the difference in the flavor index height i .) The free-field Lagrangian is given by

$$\mathcal{L} = i\bar{\chi}^i \bar{\sigma}^\mu \partial_\mu \hat{\chi}_i + i\bar{\eta}^i \bar{\sigma}^\mu \partial_\mu \hat{\eta}^i - M^i_j \hat{\chi}_i \hat{\eta}^j - M_i^j \bar{\chi}^i \bar{\eta}^j, \quad (3.79)$$

where M^i_j is an arbitrary complex matrix, and $M_i^j \equiv (M^i_j)^*$ as before. We diagonalize the mass matrix by introducing eigenstates χ_i and η^i and unitary matrices L and R ,

$$\hat{\chi}_i = L_i^k \chi_k, \quad \hat{\eta}^i = R^i_k \eta^k, \quad (3.80)$$

and demand that $M^i_j L_i^k R^j_\ell = m_k \delta_\ell^k$ (no sum over k). In matrix form, this is written as (see footnote 8):

$$L^\top M R = \mathbf{M} = \text{diag}(M_1, M_2, \dots), \quad (3.81)$$

with the m_i real and non-negative. The singular-value decomposition of linear algebra, discussed more fully in Appendix D, states that for any complex matrix M , unitary matrices L and R exist such that eq. (3.81) is satisfied. It follows that:⁹

$$L^\top (M M^\dagger) L^* = R^\dagger (M^\dagger M) R = \mathbf{M}^2. \quad (3.82)$$

That is, since $M M^\dagger$ and $M^\dagger M$ are both hermitian (with the same real non-negative eigenvalues), they can be diagonalized by unitary matrices. The diagonal elements of \mathbf{M} are therefore the non-negative square roots of the corresponding eigenvalues of $M M^\dagger$ (or $M^\dagger M$).

Thus, in terms of the mass eigenstates,

$$\mathcal{L} = i\bar{\chi}^i \bar{\sigma}^\mu \partial_\mu \chi_i + i\bar{\eta}^i \bar{\sigma}^\mu \partial_\mu \eta^i - m_i (\chi_i \eta^i + \bar{\chi}^i \bar{\eta}_i). \quad (3.83)$$

The mass matrix now consists of 2×2 blocks $\begin{pmatrix} 0 & m_i \\ m_i & 0 \end{pmatrix}$ along the diagonal. More importantly, the squared-mass matrix is diagonal with doubly degenerate entries m_i^2 that will appear in the denominators of the propagators of the theory. It describes a collection of Dirac fermions.¹⁰

Therefore, the result of the mass diagonalization procedure in a general theory always consists of a collection of Majorana fermions as in equation (3.65), plus a collection of Dirac fermions as in equation (3.83). This is the basis of the Feynman rules to be presented in the next section.

For completeness, we review the squared-mass matrix diagonalization procedure for scalar fields. First, consider a collection of free commuting real spin-0 fields, $\hat{\varphi}_i(x)$, where the flavor

⁹Consistency of notation requires that $(M^\dagger)^i_j = M_j^i = (M^j_i)^*$ [and likewise $(M^\dagger)_i^j = M_i^j = (M_j^i)^*$]. This permits the multiplication of $M M^\dagger$ and $M^\dagger M$ in a $U(N)$ -covariant fashion.

¹⁰Of course, one could always choose instead to treat the Dirac fermions in a basis with a fully diagonalized mass matrix, as in equation (3.65), by defining $\xi_{2i-1} = (\chi_i + \eta^i)/\sqrt{2}$ and $\xi_{2i} = i(\chi_i - \eta^i)/\sqrt{2}$. These fermion fields do not carry well-defined charges, and are analogous to writing a charged scalar field ϕ and its oppositely-charged conjugate ϕ^* in terms of their real and imaginary parts. However, it is rarely, if ever, convenient to do so; practical calculations only require that the squared-mass matrix is diagonal, and it is of course more pleasant to employ fields that carry well-defined charges.

index i again labels the distinct scalar fields of the collection. The free-field Lagrangian is given by

$$\mathcal{L} = \frac{1}{2} \partial_\mu \hat{\varphi}_i \partial^\mu \hat{\varphi}_i - \frac{1}{2} M_{ij}^2 \hat{\varphi}_i \hat{\varphi}_j, \quad (3.84)$$

where M_{ij}^2 is a real symmetric matrix. We diagonalize the scalar squared-mass matrix by introducing mass-eigenstates φ_i and the orthogonal matrix Q such that $\hat{\varphi}_i = Q_{ij} \varphi_j$, with $M_{ij}^2 Q_{ik} Q_{j\ell} = m_k^2 \delta_{k\ell}$ (no sum over k). In matrix form, the latter reads

$$Q^\top M^2 Q = \mathbf{m}^2 = \text{diag}(m_1^2, m_2^2, \dots). \quad (3.85)$$

This is the standard diagonalization problem for a real symmetric matrix. The eigenvalues m_k^2 are real.¹¹

Second, consider a collection of free commuting complex spin-0 fields, $\hat{\Phi}_i(x)$. For complex fields, we follow the convention for flavor indices enunciated below eq. (3.61) [*e.g.*, $\hat{\Phi}^i = (\hat{\Phi}_i)^*$]. The free-field Lagrangian is given by

$$\mathcal{L} = \partial_\mu \hat{\Phi}^i \partial^\mu \hat{\Phi}_i - (M^2)^i_j \hat{\Phi}_i \hat{\Phi}^j, \quad (3.86)$$

where $(M^2)^i_j$ is an hermitian matrix [which satisfies $(M^2)^i_j = (M^2)_j^i$ (see footnote 9)].

We diagonalize the scalar squared-mass matrix by introducing mass-eigenstates Φ_i and the unitary matrix W such that $\hat{\Phi}_i = W_i^k \Phi_k$ (and $\hat{\Phi}^i = W^i_k \Phi^k$), with $(M^2)^i_j W_i^k W^j_\ell = M_k^2 \delta_\ell^k$ (no sum over k). In matrix form, the latter reads

$$W^\dagger M^2 W = \mathbf{M}^2 = \text{diag}(M_1^2, M_2^2, \dots). \quad (3.87)$$

This is the standard diagonalization problem for an hermitian matrix. The eigenvalues m_k^2 are real (see footnote 11).

4 Feynman rules with two-component spinors

In order to systematically perform perturbative calculations using two-component spinors, we here present the basic Feynman rules. The Feynman rules for some specific models are given in the Appendices E, F and G. Two-component Feynman rules have also been discussed in [24, 64–66]

4.1 External fermion rules

Let us consider a general theory, for which we may assume that the mass matrix for fermions has been diagonalized as discussed in the previous section. The rules for assigning two-component external state spinors are then as follows.¹²

¹¹Negative eigenvalues of M^2 imply that the naive vacuum is unstable. One should shift the scalar fields by their vacuum expectation values and check that the resulting scalar squared-matrix possesses only non-negative eigenvalues.

¹²We will often suppress the momentum and spin arguments of the spinor wave functions.

- For an initial-state left-handed $(\frac{1}{2}, 0)$ fermion: x .
- For an initial-state right-handed $(0, \frac{1}{2})$ fermion: \bar{y} .
- For a final-state left-handed $(\frac{1}{2}, 0)$ fermion: \bar{x} .
- For a final-state right-handed $(0, \frac{1}{2})$ fermion: y .

Note that, in general, the two-component external state fermion wave functions are distinguished by their Lorentz group transformation properties, rather than by their particle or antiparticle status as in four-component Feynman rules. This helps to explain why two-component notation is especially convenient for (i) theories with Majorana particles, in which there is no fundamental distinction between particles and antiparticles, and (ii) theories like the Standard Model and MSSM in which the left and right-handed fermions transform under different representations of the gauge group and (iii) problems with polarized particle beams. These rules are summarized in the mnemonic diagram of Figure 1.

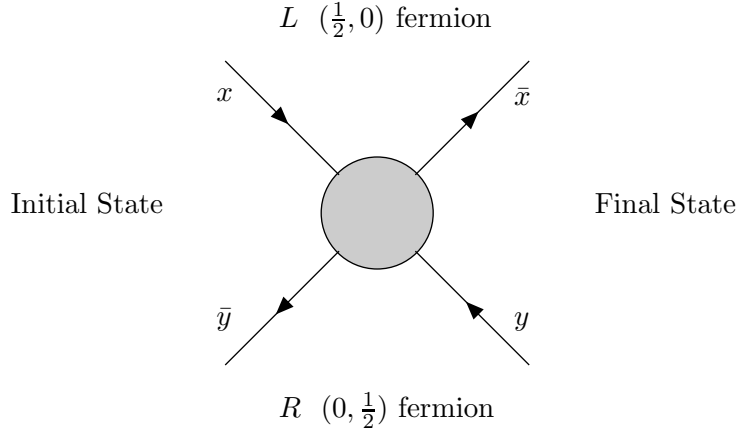


Figure 1: The external wave-function spinors should be assigned as indicated here, for initial-state and final-state left-handed $(\frac{1}{2}, 0)$ and right-handed $(0, \frac{1}{2})$ fermions.

In contrast to four-component Feynman rules, the direction of the arrows do *not* correspond to the flow of charge or fermion number. These rules simply correspond to the formulae for the one-particle wave functions given in eqs. (3.7) and (3.8) [with the convention that $|\vec{p}, s\rangle$ is an initial-state fermion and $\langle \vec{p}, s|$ is a final-state fermion]. In particular, the arrows indicate the spinor index structure, with fields of undotted indices flowing *into* any vertex and fields of dotted indices flowing *out* of any vertex.

The rules above apply to any mass eigenstate two-component fermion external wave functions. It is noteworthy that the same rules apply for the two-component fermions governed by the Lagrangians of eq. (3.65) [Majorana] and eq. (3.83) [Dirac].

4.2 Propagators

Next we turn to the subject of fermion propagators for two-component fermions. A derivation of the two-component fermion propagators using path integral techniques is given in Appendix C. Here, we will follow the more elementary approach typically given in an initial textbook treatment of quantum field theory.

Fermion propagators are the Fourier transforms of the free-field vacuum expectation values of time-ordered products of two fermion fields. They are obtained by inserting the free-field expansion of the two-component fermion field and evaluating the spin sums using the formulas given in eqs. (3.56) and (3.59). For the case of a single neutral two-component fermion field ξ of mass m [see eqs. (3.65)-(3.68)] [24, 46, 64–66, 68],

$$\langle 0 | T \xi_\alpha(x) \bar{\xi}_\beta(y) | 0 \rangle_{\text{FT}} = \frac{i}{p^2 - m^2 + i\epsilon} \sum_s x_\alpha(\vec{p}, s) \bar{x}_\beta(\vec{p}, s) = \frac{i}{p^2 - m^2 + i\epsilon} p \cdot \sigma_{\alpha\dot{\beta}}, \quad (4.1)$$

$$\langle 0 | T \bar{\xi}^{\dot{\alpha}}(x) \xi^\beta(y) | 0 \rangle_{\text{FT}} = \frac{i}{p^2 - m^2 + i\epsilon} \sum_s \bar{y}^{\dot{\alpha}}(\vec{p}, s) y^\beta(\vec{p}, s) = \frac{i}{p^2 - m^2 + i\epsilon} p \cdot \bar{\sigma}^{\dot{\alpha}\beta}, \quad (4.2)$$

$$\langle 0 | T \bar{\xi}^{\dot{\alpha}}(x) \bar{\xi}_\beta(y) | 0 \rangle_{\text{FT}} = \frac{i}{p^2 - m^2 + i\epsilon} \sum_s \bar{y}^{\dot{\alpha}}(\vec{p}, s) \bar{x}_\beta(\vec{p}, s) = \frac{i}{p^2 - m^2 + i\epsilon} m \delta^{\dot{\alpha}}_{\dot{\beta}}, \quad (4.3)$$

$$\langle 0 | T \xi_\alpha(x) \xi^\beta(y) | 0 \rangle_{\text{FT}} = \frac{i}{p^2 - m^2 + i\epsilon} \sum_s x_\alpha(\vec{p}, s) y^\beta(\vec{p}, s) = \frac{i}{p^2 - m^2 + i\epsilon} m \delta_\alpha^\beta, \quad (4.4)$$

where FT indicates the Fourier transform from position to momentum space.¹³ These results have an obvious diagrammatic representation, as shown in Fig. 2.

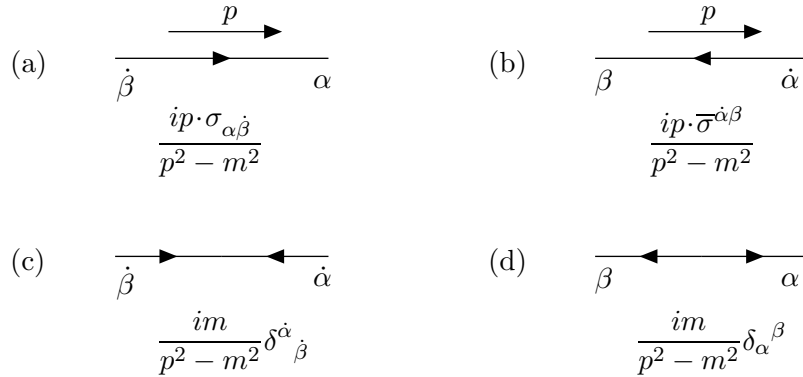


Figure 2: Feynman rules for propagator lines of a neutral two-component fermion with mass m . (The $+i\epsilon$ terms in the denominators have been omitted here and from now on, for simplicity.)

¹³The Fourier transform of a translationally invariant function $f(x, y) \equiv f(x - y)$ is given by

$$f(x, y) = \int \frac{d^4 p}{(2\pi)^4} \hat{f}(p) e^{-ip \cdot (x - y)}.$$

In the notation of the text above, $f(x, y)_{\text{FT}} \equiv \hat{f}(p)$.

$$\begin{array}{ccc}
\begin{array}{c} \xrightarrow{p} \\ \dot{\beta} \quad \quad \alpha \end{array} & \frac{ip \cdot \sigma_{\alpha\dot{\beta}}}{p^2 - m^2} & \text{or} \quad \frac{-ip \cdot \bar{\sigma}^{\dot{\beta}\alpha}}{p^2 - m^2}
\end{array}$$

Figure 3: This rule summarizes the results of both figs. 2(a) and (b) for a neutral two-component fermion with mass m .

Note that the direction of the momentum flow p^μ here is determined by the creation operator that appears in the evaluation of the free-field propagator. Arrows on fermion lines always run away from dotted indices at a vertex and toward undotted indices at a vertex.

There are clearly two types of fermion propagators. The first type preserves the direction of arrows, so it has one dotted and one undotted index. For this type of propagator, it is convenient to establish a convention where p^μ in the diagram is defined to be the momentum flowing in the direction of the arrow on the fermion propagator. With this convention, the two rules above for propagators of the first type can be summarized by one rule, as shown in Fig. 3. Here the choice of the σ or the $\bar{\sigma}$ version of the rule is uniquely determined by the height of the indices on the vertex to which the propagator is connected.¹⁴ These heights should always be chosen so that they are contracted as in eq. (2.25). It should be noted that in diagrams (a) and (b) of Fig. 2 as drawn, the indices on the σ and $\bar{\sigma}$ read from right to left. This means that the most efficient way to use the propagator rules of diagrams (a) and (b) [or equivalently, the propagator rule of Fig. 3] in a Feynman diagram computation is to traverse the propagator lines in the direction antiparallel [parallel] to the arrowed line segment for the σ [$\bar{\sigma}$] version of the rule.

The second type of propagator shown in diagrams (c) and (d) of Fig. 2 does not preserve the direction of arrows, and corresponds to an odd number of mass insertions. The indices on $\delta^{\dot{\alpha}}_{\dot{\beta}}$ and δ_{α}^{β} are staggered as shown to indicate that $\dot{\alpha}$ or α are to be contracted with an expression to the left, while $\dot{\beta}$ or β are to be contracted with an expression to the right, in accord with eq. (2.25).¹⁵

Starting with massless fermion propagators, one can derive the massive fermion propagators by employing mass insertions as interaction vertices, as shown in Fig. 4. By summing up an infinite chain of such mass insertions between massless fermion propagators, one can reproduce the massive fermion propagators of both types.

It is convenient to treat separately the case of charged massive fermions. Consider a charged Dirac fermion of mass m , which is described by a pair of two-component fields χ and η [eq. (3.69)]. Using the free field expansions given by eqs. (3.70) and (3.71), and the appropriate spin-sums

¹⁴The second form of the rule in Fig. 3 arises when one flips diagram (b) of Fig. 2 around by a 180° rotation (about an axis perpendicular to the plane of the diagram), and then relabels $p \rightarrow -p$, $\dot{\alpha} \rightarrow \dot{\beta}$ and $\beta \rightarrow \alpha$.

¹⁵As in Fig. 3, alternative versions of the rules corresponding to diagrams (c) and (d) of Fig. 2 can be given for which the indices on the Kronicker deltas are staggered as $\delta^{\dot{\beta}}_{\dot{\alpha}}$ and δ_{β}^{α} . These versions correspond to flipping the two respective diagrams by 180° and relabeling the indices $\dot{\alpha} \rightarrow \dot{\beta}$ and $\beta \rightarrow \alpha$.



Figure 4: Fermion mass insertions (indicated by the crosses) can be treated as a type of interaction vertex, using the Feynman rules shown here.

[eqs. (3.56)–(3.59)], the two-component free-field propagators are obtained:

$$\langle 0 | T \chi_{\alpha}(x) \bar{\chi}_{\dot{\beta}}(y) | 0 \rangle_{\text{FT}} = \langle 0 | T \eta_{\alpha}(x) \bar{\eta}_{\dot{\beta}}(y) | 0 \rangle_{\text{FT}} = \frac{i}{p^2 - m^2} p \cdot \sigma_{\alpha \dot{\beta}}, \quad (4.5)$$

$$\langle 0 | T \bar{\chi}^{\dot{\alpha}}(x) \chi^{\beta}(y) | 0 \rangle_{\text{FT}} = \langle 0 | T \bar{\eta}^{\dot{\alpha}}(x) \eta^{\beta}(y) | 0 \rangle_{\text{FT}} = \frac{i}{p^2 - m^2} p \cdot \bar{\sigma}^{\dot{\alpha} \beta}, \quad (4.6)$$

$$\langle 0 | T \chi_{\alpha}(x) \eta^{\beta}(y) | 0 \rangle_{\text{FT}} = \langle 0 | T \eta_{\alpha}(x) \chi^{\beta}(y) | 0 \rangle_{\text{FT}} = \frac{i}{p^2 - m^2} m \delta_{\alpha}^{\beta}, \quad (4.7)$$

$$\langle 0 | T \bar{\chi}^{\dot{\alpha}}(x) \bar{\eta}_{\dot{\beta}}(y) | 0 \rangle_{\text{FT}} = \langle 0 | T \bar{\eta}^{\dot{\alpha}}(x) \bar{\chi}_{\dot{\beta}}(y) | 0 \rangle_{\text{FT}} = \frac{i}{p^2 - m^2} m \delta_{\dot{\beta}}^{\dot{\alpha}}. \quad (4.8)$$

For all other combinations of fermion bilinears, the corresponding two-point functions vanish. These results again have a simple diagrammatic representation, as shown in Fig. 5.

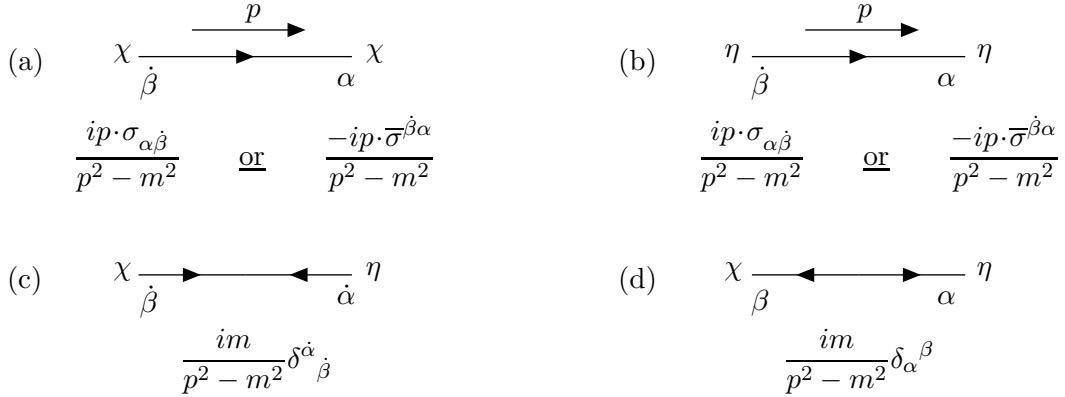
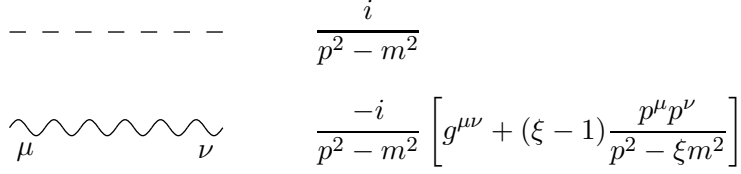


Figure 5: Feynman rules for propagator lines of a pair of charged two-component fermions with a Dirac mass m . As in Fig. 3, the direction of the momentum is taken to flow from the dotted to the undotted index in diagrams (a) and (b).

Note that for Dirac fermions, the propagators with opposing arrows (proportional to a mass) necessarily change the identity (χ or η) of the two-component fermion, while the single-arrow propagators are diagonal in the fields. In processes involving such a charged fermion, one must of course distinguish between the χ and η fields.

For completeness, we provide the propagators for scalar and vector bosons in Fig. 6.



$$\begin{array}{cc}
\text{---} & \frac{i}{p^2 - m^2} \\
\text{~~~~~} & \\
\text{~~~~~} & \frac{-i}{p^2 - m^2} \left[g^{\mu\nu} + (\xi - 1) \frac{p^\mu p^\nu}{p^2 - \xi m^2} \right]
\end{array}$$

Figure 6: The Feynman rules for propagators of scalar bosons, and vector bosons in R_ξ gauge, carrying momentum p^μ in each case. Here $\xi = 1$ is Feynman gauge, and $\xi = 0$ is Landau gauge.

4.3 Fermion interactions with bosons

We next discuss the interaction vertices for fermions with bosons. Renormalizable Lorentz-invariant interactions involving fermions must consist of bilinears in the fermion fields, which transform as a Lorentz scalar or vector, coupled to the appropriate bosonic scalar or vector field to make an overall Lorentz scalar quantity.

Let us write all of the two-component left-handed fermions of the theory as $\hat{\psi}_j$, where j runs over all of the gauge group representation and flavor degrees of freedom. The most general set of interactions with the scalars of the theory $\hat{\phi}_I$ are then given by:

$$\mathcal{L}_{\text{int}} = -\frac{1}{2}\hat{Y}^{Ijk}\hat{\phi}_I\hat{\psi}_j\hat{\psi}_k - \frac{1}{2}\hat{Y}_{Ijk}\hat{\phi}^I\bar{\hat{\psi}}^j\bar{\hat{\psi}}^k, \quad (4.9)$$

where $\hat{Y}_{Ijk} = (\hat{Y}^{Ijk})^*$ and $\hat{\phi}^I = (\hat{\phi}_I)^*$. We have suppressed the spinor indices here; the product of two component spinors is always performed according to the index convention indicated in eq. (2.25). The flavor index I runs over a collection of real scalar fields $\hat{\phi}_i$ and pairs of complex scalar fields $\hat{\Phi}_j$ and $(\hat{\Phi}_j)^*$.¹⁶ The Yukawa couplings \hat{Y}^{Ijk} are symmetric under interchange of j and k . The hatted fields are the so-called interaction-eigenstate fields.

However, in general the mass-eigenstates can be different, as discussed in subsection 3.2. The computation of matrix elements for physical processes is more conveniently done in terms of the propagating mass-eigenstate fields. In general, the interaction-eigenstate $(\frac{1}{2}, 0)$ -fermion fields $\hat{\psi}_i$ consist of Majorana fermions $\hat{\xi}_i$, and Dirac fermion pairs $\hat{\chi}_i$ and $\hat{\eta}^i$ after mass terms (both explicit and coming from spontaneous symmetry breaking) are taken into account. The mass-eigenstate basis ψ is related to the interaction-eigenstate basis $\hat{\psi}$ by a unitary rotation U_i^j on the flavor indices. In matrix form:

$$\hat{\psi} \equiv \begin{pmatrix} \hat{\xi} \\ \hat{\chi} \\ \hat{\eta} \end{pmatrix} = U\psi \equiv \begin{pmatrix} \Omega & 0 & 0 \\ 0 & L & 0 \\ 0 & 0 & R \end{pmatrix} \begin{pmatrix} \xi \\ \chi \\ \eta \end{pmatrix}, \quad (4.10)$$

where Ω , L , and R are constructed as described previously in Section 3.2 [see eqs. (3.63) and (3.81)]. Likewise, the interaction-eigenstate scalar fields $\hat{\phi}_I$ generally consist of real scalar fields

¹⁶For example, in a theory with one complex scalar field $\hat{\Phi}$, we would take $\hat{\phi}_1 = \hat{\Phi}$ and $\hat{\phi}_2 = \hat{\Phi}^*$.

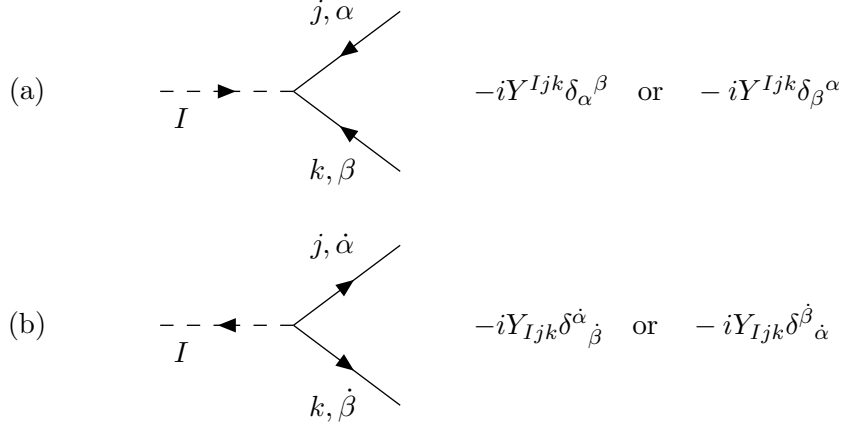


Figure 7: Feynman rules for Yukawa couplings of scalars to two-component fermions in a general field theory. The choice of which rule to use depends on how the vertex connects to the rest of the amplitude. When indices are suppressed, the spinor index part is always just proportional to the identity matrix.

$\hat{\varphi}_i$ and complex scalar fields $\hat{\Phi}_i$. The mass eigenstate basis ϕ is related to the interaction eigenstate basis $\hat{\phi}$ by a unitary rotation V_I^J on the flavor indices. In matrix form:

$$\hat{\phi} \equiv \begin{pmatrix} \hat{\varphi} \\ \hat{\Phi} \end{pmatrix} = V \phi \equiv \begin{pmatrix} Q & 0 \\ 0 & W \end{pmatrix} \begin{pmatrix} \varphi \\ \Phi \end{pmatrix}, \quad (4.11)$$

where Q and W are constructed according to eqs. (3.85) and (3.87).

Thus, we may rewrite eq. (4.9) in terms of mass-eigenstate fields:

$$\mathcal{L}_{\text{int}} = -\frac{1}{2} Y^{Ijk} \phi_I \psi_j \psi_k - \frac{1}{2} Y_{Ijk} \phi^I \bar{\psi}^j \bar{\psi}^k, \quad (4.12)$$

where

$$Y^{Ijk} = V_L^I U_m^j U_n^k \hat{Y}^{Lmn}. \quad (4.13)$$

The corresponding Feynman rules are shown in Fig. 7. Note that if the scalar ϕ_I is complex, then one can associate an arrow with the flow of analyticity,¹⁷ which would point into the vertex in (a) and would point out of the vertex in (b).

The renormalizable interactions of vector bosons with fermions and scalars arise from gauge interactions. These interaction terms of the Lagrangian derive from the respective kinetic energy terms of the fermions and scalars when the derivative is promoted to the covariant derivative:

$$(D_\mu)_i^j \equiv \delta_i^j \partial_\mu + i g_a A_\mu^a (\mathbf{T}^a)_i^j, \quad (4.14)$$

where the index a labels the (real or complex) vector bosons A_a^μ and is summed over. The index

¹⁷As in the case of the fermions, the arrow on the dashed line representing the scalar field does *not* represent the flow of a conserved charge. It simply keeps track of the height of the scalar flavor index entering or leaving a given vertex.

a runs over the adjoint representation of the gauge group,¹⁸ and the $(\mathbf{T}^a)_i^j$ are hermitian representation matrices¹⁹ of the Lie algebra of the gauge group acting on the left-handed fermions. There is a separate coupling g_a for each simple group or U(1) factor of the gauge group G .²⁰

In the gauge-interaction basis for the left-handed two-component fermions the corresponding interaction Lagrangian is given by

$$\mathcal{L}_{\text{int}} = -g_a A_a^\mu \bar{\psi}^i \bar{\sigma}_\mu (\mathbf{T}^a)_i^j \hat{\psi}_j. \quad (4.15)$$

In the case of spontaneously broken gauge theories, one must diagonalize the vector boson squared mass matrix. The form of eq. (4.15) still applies where A_μ^a are gauge boson fields of definite mass, although in this case for a fixed value of a , $g_a \mathbf{T}^a$ [which multiplies A_μ^a in eq. (4.15)] is some linear combination of the original $g_a \mathbf{T}^a$ of the unbroken theory.²¹ Henceforth, we assume that the A_μ^a are the gauge boson mass-eigenstate fields.

To obtain the desired Feynman rule, we must rewrite eq. (4.15) in terms of mass-eigenstate fermion fields. The resulting interaction Lagrangian takes the form

$$\mathcal{L}_{\text{int}} = -A_\mu^a \bar{\psi}^i \bar{\sigma}_\mu (G^a)_i^j \psi_j, \quad (4.17)$$

where

$$(G^a)_i^j = g_a U^k{}_i (\mathbf{T}^a)_k{}^m U_m{}^j, \quad (4.18)$$

or in matrix form, $G^a = g_a U^\dagger \mathbf{T}^a U$ (no sum over a). Note that G^a is an hermitian matrix. The corresponding Feynman rule is shown in Fig. 8.

The above treatment of gauge interactions of (two-component) fermions is general, but it is useful to consider separately the special case of gauge interactions of charged Dirac fermions. Consider pairs of left-handed $(\frac{1}{2}, 0)$ interaction-eigenstate fermions $\hat{\chi}_i$ and $\hat{\eta}^i$ that transform as conjugate representations of the gauge group (hence the difference in the flavor index heights). The fermion mass matrix couples χ and η type fields as in eq. (3.79). The Lagrangian for the gauge interactions of Dirac fermions can be written in the form:

$$\mathcal{L}_{\text{int}} = -g_a A_a^\mu \bar{\chi}^i \bar{\sigma}_\mu (\mathbf{T}^a)_i^j \hat{\chi}_j + g_a A_a^\mu \bar{\eta}_i \bar{\sigma}_\mu (\mathbf{T}^a)_j^i \hat{\eta}^j, \quad (4.19)$$

¹⁸Since the adjoint representation is a real representation, the height of the adjoint index a is not significant. The choice of a subscript or superscript adjoint index is based solely on typographical considerations.

¹⁹For a $U(1)$ gauge group, the \mathbf{T}^a are replaced by real numbers corresponding to the U(1) charges of the left-handed $(\frac{1}{2}, 0)$ fermions.

²⁰That is, the generators T^a separate out into distinct classes, each of which is associated with a simple group or one of the U(1) factors contained in the direct product that defines G . In particular, $g_a = g_b$ if T^a and T^b are in the same class. If G is simple, then $g_a = g$ for all a .

²¹For example, in the electroweak Standard Model, $G = \text{SU}(2) \times \text{U}(1)$ and $\mathbf{T}^a = (\frac{1}{2}\tau^a, \frac{1}{2}Y)$, where the τ^a are the usual Pauli matrices. Then, after diagonalizing the gauge boson squared-mass matrix, one finds:

$$\frac{1}{2}gW_\mu^a\tau^a + \frac{1}{2}g'B_\mu Y = \frac{g}{2\sqrt{2}}(W_\mu^+\tau^+ + W_\mu^-\tau^-) + \frac{g}{2\cos\theta_W}(\tau^3 + 2Q\sin^2\theta_W)Z_\mu + eQA_\mu, \quad (4.16)$$

where $\tau^\pm \equiv \tau^1 \pm i\tau^2$, $Q = \frac{1}{2}(\tau^3 + Y)$, and $e = g\sin\theta_W = g'\cos\theta_W$. Here $\{W_\mu^a, B_\mu\}$ are the gauge fields of the unbroken theory and W^\pm , Z and A are the gauge boson mass-eigenstates of the broken theory.

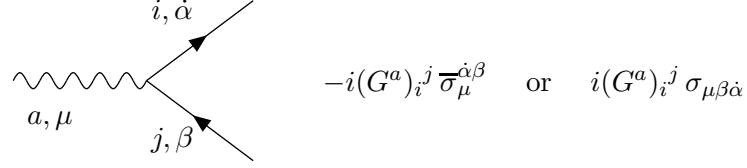


Figure 8: The Feynman rules for two-component fermion interactions with vector bosons. The choice of which rule to use depends on how the vertex connects to the rest of the amplitude. G^a is defined in eq. (4.18).

where the A_μ^a are gauge boson mass-eigenstate fields. Here we have used the fact that if $(\mathbf{T}^a)_i^j$ are the representation matrices for the $\hat{\chi}_i$, then the $\hat{\eta}_i$ transform in the complex conjugate representation with generator matrices $-(\mathbf{T}^a)^* = -(\mathbf{T}^a)^\top$, where we have used the hermiticity of the generator matrices. Again we rewrite eq. (4.19) in terms of mass-eigenstate fermion fields. The resulting interaction Lagrangian is given by:

$$\mathcal{L}_{\text{int}} = -A_\mu^a \bar{\chi}^i \bar{\sigma}_\mu (G_L^a)_i^j \chi_j + A_\mu^a \bar{\eta}_i \bar{\sigma}_\mu (G_R^a)_j^i \eta^j, \quad (4.20)$$

where

$$(G_L^a)_i^j = g_a L^k{}_i (\mathbf{T}^a)_k{}^m L_m{}^j, \quad (4.21)$$

$$(G_R^a)_j^i = g_a R^m{}_j (\mathbf{T}^a)_m{}^k R_k{}^i. \quad (4.22)$$

In matrix form, eqs. (4.21) and (4.22) read: $G_L^a = g_a L^\dagger \mathbf{T}^a L$ and $G_R^a = g_a R^\dagger \mathbf{T}^a R$ (no sum over a); G_L^a and G_R^a are hermitian matrices. The corresponding Feynman rules for the gauge interactions of Dirac fermions are shown in Fig. 9.

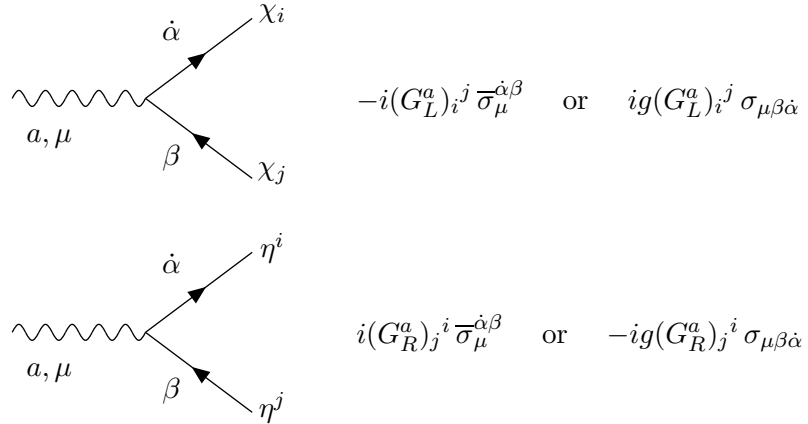


Figure 9: The Feynman rules for two-component fermion interactions with vector bosons, in the case that χ_i and η^i form a Dirac fermion. The matrices G_L^a and G_R^a are related to the group generators for the representation carried by the χ_i according to eqs. (4.21) and (4.22). The two-component field labels conform to the conventions of Section 5.

In Figs. 7–9, two versions are given for each of the boson-fermion-fermion Feynman rules. The correct version to use depends in a unique way on the heights of indices used to connect

each fermion line to the rest of the diagram. For example, the way of writing the vector-fermion-fermion interaction rule depends on whether we used $\bar{\psi}^i \bar{\sigma}^\mu \psi_j$, or its equivalent form $-\psi_j \sigma^\mu \bar{\psi}^i$, from eq. (4.15). Note the different heights of the undotted and dotted spinor indices that adorn σ^μ and $\bar{\sigma}^\mu$. The choice of which rule to use is thus dictated by the height of the indices on the lines that connect to the vertex. These heights should always be chosen so that they are contracted as in eq. (2.25). Similarly, for the scalar-fermion-fermion vertices, one should choose the rule which correctly matches the indices with the rest of the diagram. However, when all spinor indices are suppressed, the scalar-fermion-fermion rules will have an identical appearance for both cases, since they are just proportional to the identity matrix on the 2×2 spinor space.)

These above comments will be clarified by examples in Section 4.5. Numerous examples and applications of the results of this subsection can be found in Appendices D and E.

4.4 General structure and rules for Feynman graphs

When computing an amplitude for a given process, all possible diagrams should be drawn that conform with the rules given above for external wavefunctions, propagators, and interactions. Starting from any external wave function spinor, or from any vertex on a fermion loop, factors corresponding to each propagator and vertex should be written down from left to right, following the line until it ends at another external state wave function or at the original point on the fermion loop. If one starts a fermion line at an x or y external state spinor, it should have a raised undotted index in accord with eq. (2.25). Or, if one starts with an \bar{x} or \bar{y} , it should have a lowered dotted spinor index. Then, all spinor indices should always be contracted as in eq. (2.25). If one ends with an x or y external state spinor, it will have a lowered undotted index, while if one ends with an \bar{x} or \bar{y} spinor, it will have a raised dotted index. For arrow-preserving fermion propagators and gauge vertices, the preceding determines whether the σ or $\bar{\sigma}$ rule should be used. With only a little practice, one can write down amplitudes immediately with all spinor indices suppressed.

Symmetry factors for identical particles are implemented in the usual way. Fermi-Dirac statistics are implemented by the following rules:

- Each closed fermion loop gets a factor of -1 .
- A relative minus sign is imposed between terms contributing to a given amplitude whenever the ordering of external state spinors (written left-to-right) differs by an odd permutation.

Amplitudes generated according to these rules will contain objects of the form:

$$a = z_1 \Sigma z_2 \tag{4.23}$$

where z_1 and z_2 are each commuting external spinor wave functions x , \bar{x} , y , or \bar{y} , and Σ is a

sequence of alternating σ and $\bar{\sigma}$ matrices. The complex conjugate of this quantity is given by

$$a^* = \bar{z}_2 \Sigma_r \bar{z}_1 \quad (4.24)$$

where Σ_r is obtained from Σ by reversing the order of all the σ and $\bar{\sigma}$ matrices, and using the same rule for suppressed spinor indices. (Notice that this rule for taking complex conjugates has the same form as for anticommuting spinors.) We emphasize that in principle, it does not matter in what direction a diagram is traversed while applying the rules. However, for each diagram one must include a sign that depends on the ordering of the external fermions. This sign can be fixed by first choosing some canonical ordering of the external fermions. Then for any graph that contributes to the process of interest, the corresponding sign is positive (negative) if the ordering of external fermions is an even (odd) permutation with respect to the canonical ordering. If one chooses a different canonical ordering, then the resulting amplitude changes by an overall sign (is unchanged) if this ordering is an odd (even) permutation of the original canonical ordering.²² This is consistent with the fact that the amplitude is only defined up to an overall sign, which is not physically observable.

Note that different graphs contributing to the same process will often have different external state wave function spinors, with different arrow directions, for the same external fermion. Furthermore, there are no arbitrary choices to be made for arrow directions, as there are in some four-component Feynman rules for Majorana fermions. Instead, one must add together *all* Feynman graphs that obey the rules.

4.5 Basic examples of writing down diagrams and amplitudes

A few simple examples will help clarify these rules. (A larger number of examples, drawn from practical calculations, are given in section 6.) Let us first consider a theory with a single, uncharged, massive $(\frac{1}{2}, 0)$ fermion ξ , and a real scalar ϕ , with interaction

$$\mathcal{L}_{\text{int}} = -\frac{1}{2} (\lambda \xi \xi + \lambda^* \bar{\xi} \bar{\xi}) \phi. \quad (4.25)$$

Consider the decay $\phi \rightarrow \xi(\vec{p}_1, s_1) \xi(\vec{p}_2, s_2)$, where by ξ we mean the one particle state given by eq. (3.6). Two diagrams contribute to this process, as shown in Figure 10.

The matrix element is then given by

$$\begin{aligned} i\mathcal{M} &= y(\vec{p}_1, s_1)^\alpha (-i\lambda \delta_\alpha^\beta) y(\vec{p}_2, s_2)_\beta + \bar{x}(\vec{p}_1, s_1)_{\dot{\alpha}} (-i\lambda^* \delta_{\dot{\beta}}^{\dot{\alpha}}) \bar{x}(\vec{p}_2, s_2)^{\dot{\beta}} \\ &= -i\lambda y(\vec{p}_1, s_1) y(\vec{p}_2, s_2) - i\lambda^* \bar{x}(\vec{p}_1, s_1) \bar{x}(\vec{p}_2, s_2). \end{aligned} \quad (4.26)$$

²²For a process with exactly two external fermions, it is convenient to apply the Feynman rules by starting from the same fermion external state in all diagrams. That way, all terms in the amplitude have the same canonical ordering of fermions and there are no additional minus signs between diagrams. However, if there are four or more external fermions, it may happen that there is no way to choose the same ordering of external state spinors for all graphs when the amplitude is written down. Then the relative signs between different graphs must be chosen according to the relative sign of the permutation of the corresponding external fermion spinors. This guarantees that the total amplitude is antisymmetric under the interchange of any pair of external fermions.



Figure 10: The two tree-level Feynman diagrams contributing to the decay of a scalar into a Majorana fermion pair.

The second line could be written down directly by recalling that the sum over suppressed spinor indices is taken according to eq. (2.25). Note that if we reverse the ordering for the external fermions, the overall sign of the amplitude changes sign. This is easily checked, since for the commuting spinor wave functions (x and y), the spinor products in eq. (4.26) change sign when the order is reversed [see eqs. (2.47) and (2.48)]. This overall sign is not significant and depends on the order used in constructing the two particle state. One could even make the choice of starting the first diagram from fermion 1, and the second diagram from fermion 2:

$$i\mathcal{M} = -i\lambda y(\vec{p}_1, s_1)y(\vec{p}_2, s_2) - (-1)i\lambda^* \bar{x}(\vec{p}_2, s_2)\bar{x}(\vec{p}_1, s_1). \quad (4.27)$$

Here the first term establishes the canonical ordering of fermions (12), and the contribution from the second diagram therefore includes the relative minus sign in parentheses. Indeed, eqs. (4.26) and (4.27) are equal. The computation of the total decay rate is straightforward. Of course, one must multiply the integral over the total phase space by 1/2 to account for the identical particles.

Consider next the decay of a massive neutral vector A_μ into a Majorana fermion pair $A_\mu \rightarrow \xi(\vec{p}_1, s_1)\xi(\vec{p}_2, s_2)$, following from the interaction

$$\mathcal{L}_{\text{int}} = -GA^\mu \bar{\xi} \bar{\sigma}_\mu \xi, \quad (4.28)$$

where G is a real coupling parameter. The two diagrams shown in Figure 11 contribute.

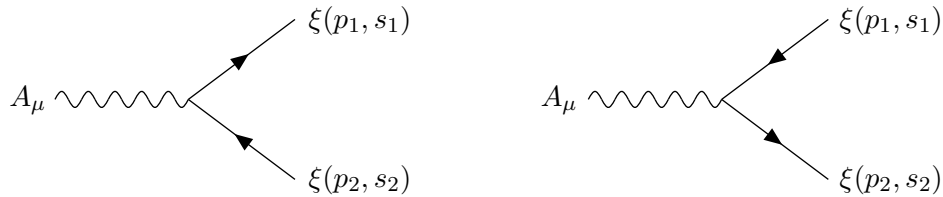


Figure 11: The two tree-level Feynman diagrams contributing to the decay of a massive vector boson A_μ into a pair of Majorana fermions ξ .

We start from the fermion with momentum p_1 and spin vector s_1 and end at the fermion with momentum p_2 and spin vector s_2 , using the rules of Fig. 8. The resulting amplitude for

the decay is

$$i\mathcal{M} = \varepsilon^\mu [-iG\bar{x}(\vec{p}_1, s_1)\bar{\sigma}_\mu y(\vec{p}_2, s_2) + iGy(\vec{p}_1, s_1)\sigma_\mu\bar{x}(\vec{p}_2, s_2)] \quad (4.29)$$

where ε^μ is the vector boson polarization vector. We have used the $\bar{\sigma}$ -version of the vector-fermion-fermion rule [see Fig. 8] for the first diagram of Fig. 11 and the σ -version for the second diagram of Fig. 11, as dictated by the implicit spinor indices, which we have suppressed. However, we could have chosen to evaluate the second diagram of Fig. 11 using the $\bar{\sigma}$ -version of the vector-fermion-fermion rule by starting from the fermion with momentum p_2 . In that case, the factor $+iGy(\vec{p}_1, s_1)\sigma_\mu\bar{x}(\vec{p}_2, s_2)$ in eq. (4.29) is replaced by

$$(-1)[-iG\bar{x}(\vec{p}_2, s_2)\bar{\sigma}_\mu y(\vec{p}_1, s_1)]. \quad (4.30)$$

In eq. (4.30), the factor of $-iG$ arises from the use of the $\bar{\sigma}$ -version of the vector-fermion-fermion rule, and the overall factor of -1 appears because the order of the fermion wave functions has been reversed; i.e. (21) is an odd permutation of (12). This is in accord with the ordering rule stated at the end of Section 4.4. Thus, the resulting amplitude for the decay of the vector boson into the pair of Majorana fermions now takes the form:

$$i\mathcal{M} = \varepsilon^\mu [-iG\bar{x}(\vec{p}_1, s_1)\bar{\sigma}_\mu y(\vec{p}_2, s_2) + iG\bar{x}(\vec{p}_2, s_2)\bar{\sigma}_\mu y(\vec{p}_1, s_1)] . \quad (4.31)$$

By using $y\sigma^\mu\bar{x} = \bar{x}\bar{\sigma}^\mu y$, which follows from eq. (2.49) with commuting spinors, one sees that eqs. (4.29) and (4.31) are identical. The form given in eq. (4.31) explicitly exhibits the fact that the amplitude is antisymmetric under the interchange of the two external identical fermions. Again, the absolute sign of the total amplitude is not significant and depends on the choice of ordering of the outgoing states.

Next, we consider the decay of a massive neutral vector boson into a charged fermion-antifermion pair. Suppose that we identify χ and η as left-handed fields with charges $Q = 1$ and $Q = -1$, respectively. The corresponding interaction is given by:

$$\mathcal{L}_{\text{int}} = -A^\mu [G_L \bar{\chi} \bar{\sigma}_\mu \chi - G_R \bar{\eta} \bar{\sigma}_\mu \eta]. \quad (4.32)$$

There are two contributing graphs, as shown in Figure 12.

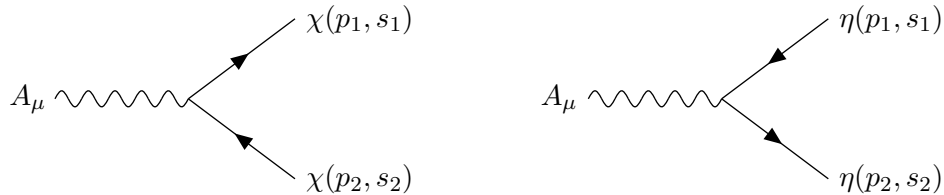


Figure 12: The two tree-level Feynman diagrams contributing to the decay of a massive neutral vector boson A_μ into a Dirac fermion-antifermion pair.

To evaluate the amplitude, we start from the charge $Q = +1$ fermion (with momentum p_1 and spin vector s_1), and end at the charge $Q = -1$ fermion (with momentum p_2 and spin

vector s_2). In particular, for the final state fermion lines, the outgoing χ with arrow pointing outward from the vertex and the outgoing η with arrow pointing inward to the vertex both correspond to outgoing $Q = +1$ states. The amplitude for the decay is

$$\begin{aligned} i\mathcal{M} &= \varepsilon^\mu [-iG_L \bar{x}(\vec{p}_1, s_1) \bar{\sigma}_\mu y(\vec{p}_2, s_2) - iG_R y(\vec{p}_1, s_1) \sigma_\mu \bar{x}(\vec{p}_2, s_2)] \\ &= \varepsilon^\mu [-iG_L \bar{x}(\vec{p}_1, s_1) \bar{\sigma}_\mu y(\vec{p}_2, s_2) - iG_R \bar{x}(\vec{p}_2, s_2) \bar{\sigma}_\mu y(\vec{p}_1, s_1)] . \end{aligned} \quad (4.33)$$

As in the case of the decay to a pair of Majorana fermions, we have exhibited two forms for the amplitude in eq. (4.33) that depend on whether the $\bar{\sigma}$ -version or the σ -version of the Feynman rule has been employed. Of course, the resulting amplitude is the same in each method (up to an overall sign of the total amplitude which is not determined).

The next level of complexity consists of diagrams that involve fermion propagators. For our first example of this type, consider the tree-level matrix element for the scattering of a neutral scalar and a two-component neutral massive fermion ($\phi\xi \rightarrow \phi\xi$), with the interaction Lagrangian given above in eq. (4.25). Using the corresponding Feynman rules, there are eight contributing diagrams. Four are depicted in Fig. 13; there are another four diagrams (not shown) where the initial and final state scalars are crossed (i.e., the initial state scalar is attached to the same vertex as the final state fermion).

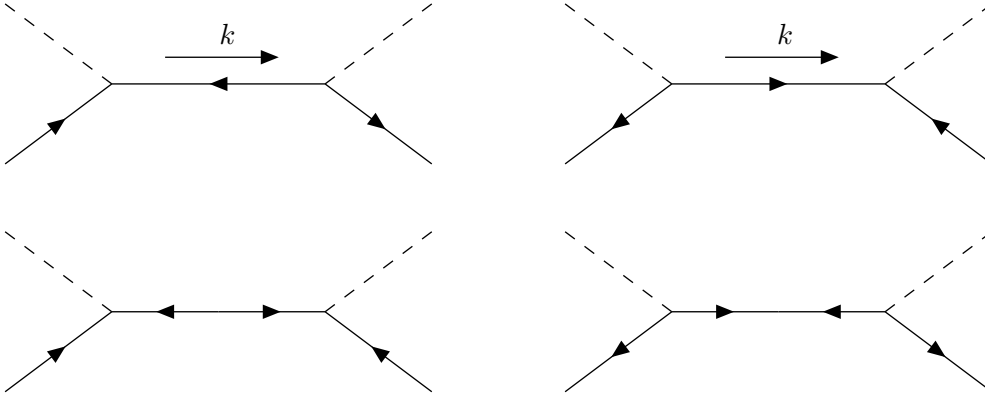


Figure 13: Tree-level Feynman diagrams contributing to the elastic scattering of a neutral scalar and a neutral two-component fermion. There are four more diagrams, obtained from these by crossing the initial and final scalar lines.

We shall write down the amplitudes for the four diagrams shown, starting with the final state fermion line and moving toward the initial state fermion line. Then,

$$\begin{aligned} i\mathcal{M} &= \frac{-i}{k^2 - m_\xi^2} \left\{ |\lambda|^2 [\bar{x}(\vec{p}_2, s_2) \bar{\sigma} \cdot k x(\vec{p}_1, s_1) + y(\vec{p}_2, s_2) \sigma \cdot k \bar{y}(\vec{p}_1, s_1)] \right. \\ &\quad \left. + m_\xi [\lambda^2 y(\vec{p}_2, s_2) x(\vec{p}_1, s_1) + (\lambda^*)^2 \bar{x}(\vec{p}_2, s_2) \bar{y}(\vec{p}_1, s_1)] \right\} + (\text{crossed}) . \end{aligned} \quad (4.34)$$

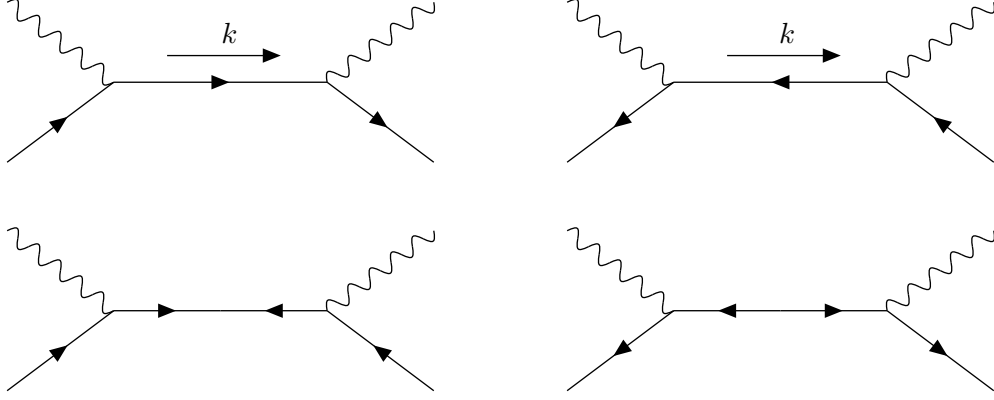


Figure 14: Tree-level Feynman diagrams contributing to the elastic scattering of a neutral vector boson and a neutral two-component fermion. There are four more diagrams, obtained from these by crossing the initial and final scalar lines.

where k^μ is the sum of the two incoming (or outgoing) four-momenta, (p_1, s_1) are the momentum and spin four-vectors of the incoming fermion, and (p_2, s_2) are those of the outgoing fermion. (We will not write down the “crossed” terms, which have the the initial and final scalars interchanged.) Note that we could have evaluated the diagrams above by starting with the initial vertex and moving toward the final vertex. It is easy to check that the resulting amplitude is the negative of the one obtained in eq. (4.34); the overall sign change simply corresponds to swapping the order of the two fermions and has no physical consequence. The overall minus sign is a consequence of eqs. (2.47)–(2.49) and the minus sign difference between the two ways of evaluating the propagator that preserves the arrow direction.

Next, we compute the tree-level matrix element for the scattering of a vector boson and a neutral massive two-component fermion ξ with the interaction Lagrangian of eq. (4.28). Again there are eight diagrams: the four diagrams depicted in Fig. 14 plus another four (not shown) where the initial and final state vector bosons are crossed. Starting with the final state fermion line and moving toward the initial state, we obtain

$$i\mathcal{M} = \frac{-iG^2}{k^2 - m_\xi^2} \left\{ \bar{x}(\vec{p}_2, s_2) \bar{\sigma} \cdot \varepsilon_2^* \sigma \cdot k \bar{\sigma} \cdot \varepsilon_1 x(\vec{p}_1, s_1) + y(\vec{p}_2, s_2) \sigma \cdot \varepsilon_2^* \bar{\sigma} \cdot k \sigma \cdot \varepsilon_1 \bar{y}(\vec{p}_1, s_1) \right. \\ \left. - m_\xi [y(\vec{p}_2, s_2) \sigma \cdot \varepsilon_2^* \bar{\sigma} \cdot \varepsilon_1 x(\vec{p}_1, s_1) + \bar{x}(\vec{p}_2, s_2) \bar{\sigma} \cdot \varepsilon_2^* \sigma \cdot \varepsilon_1 \bar{y}(\vec{p}_1, s_1)] \right\} + (\text{crossed}), \quad (4.35)$$

where ε_1 and ε_2 are the initial and final vector boson polarization four-vectors, respectively. As before, k^μ is the sum of the two incoming (or outgoing) four-momenta, and (p_1, s_1) are the momentum and spin four-vectors of the incoming fermion, and (p_2, s_2) are those of the outgoing fermion. (We again omit the “crossed” terms, which have the the initial and final vector bosons interchanged.) If one evaluates the diagrams above by starting with the initial vertex and moving toward the final vertex, the resulting amplitude is the negative of the one obtained in eq. (4.35),

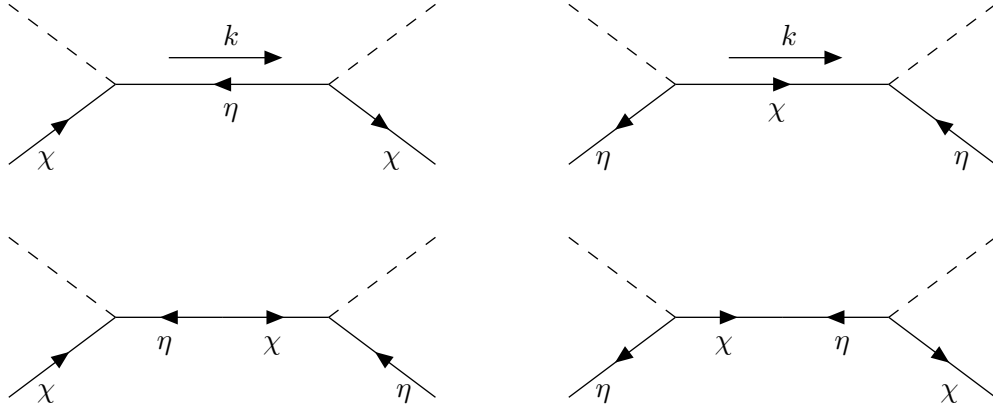


Figure 15: Tree-level Feynman diagrams contributing to the elastic scattering of a neutral scalar and a charged fermion. There are four more diagrams, obtained from these by crossing the initial and final scalar lines.

as expected.

As our next example, we consider the scattering of a charged Dirac fermion with a neutral scalar. The left-handed fields χ and η have opposite charges $Q = +1$ and -1 respectively, and interact with the scalar ϕ according to

$$\mathcal{L}_{\text{int}} = -\phi[\kappa\chi\eta + \kappa^*\bar{\chi}\bar{\eta}], \quad (4.36)$$

where κ is a coupling parameter. Then, for the elastic scattering of a $Q = +1$ fermion and a scalar, the diagrams of Fig. 15 contribute at tree-level plus another four diagrams (not shown) where the initial and final state scalars are crossed. Now, these diagrams match precisely those of Fig. 13. Thus, applying the Feynman rules yields the same matrix element, eq. (4.34), previously obtained for the scattering of a neutral scalar and neutral two-component fermion, with the replacement of λ with κ .

Consider next the scattering of a charged Dirac fermion and a charged scalar, where both the scalar and fermion have the same absolute value of the charge. As above, we denote the charged $Q = \pm 1$ fermion by the pair of two-component fermions χ and η and the (intermediate state) neutral two-component fermion by ξ . The charged $Q = \pm 1$ scalar is represented by the scalar field ϕ and its complex conjugate. The interaction Lagrangian takes the form:

$$\mathcal{L}_{\text{int}} = -\phi^*[\kappa_1\chi\xi + \kappa_2^*\bar{\eta}\bar{\xi}] - \phi[\kappa_1^*\bar{\chi}\bar{\xi} + \kappa_2\eta\xi]. \quad (4.37)$$

Consider the scattering of an initial boson-fermion state into its charge-conjugated final state via the exchange of a neutral fermion. The relevant diagrams are shown in Fig. 16 plus the corresponding diagrams with the initial and final scalars crossed. We define the four-momentum k to be the sum of the two initial state four-momenta as shown in Fig. 16. The derivation of

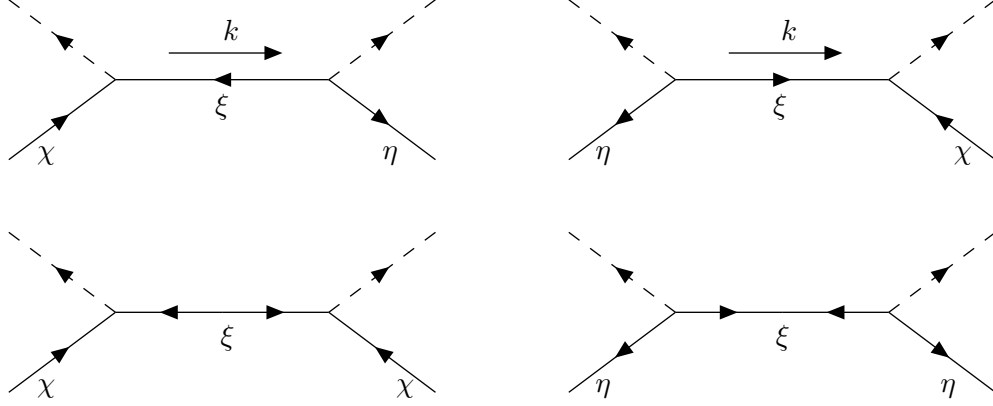


Figure 16: Tree-level Feynman diagrams contributing to the scattering of an initial charged scalar and a charged fermion into its charge-conjugated final state. The unlabeled intermediate state is a neutral fermion. There are four more diagrams, obtained from these by crossing the initial and final scalar lines.

the amplitude is similar to the ones given previously, and we end up with

$$i\mathcal{M} = \frac{-i}{k^2 - m_\xi^2} \left\{ \kappa_1 \kappa_2^* [\bar{x}(\vec{p}_2, s_2) \bar{\sigma} \cdot k x(\vec{p}_1, s_1) + y(\vec{p}_2, s_2) \sigma \cdot k \bar{y}(\vec{p}_1, s_1)] \right. \\ \left. + m_\xi [\kappa_1^2 y(\vec{p}_2, s_2) x(\vec{p}_1, s_1) + (\kappa_2^*)^2 \bar{x}(\vec{p}_2, s_2) \bar{y}(\vec{p}_1, s_1)] \right\} + (\text{crossed}). \quad (4.38)$$

The scattering of a charged fermion and a neutral spin-1 vector boson can be similarly treated. For example, consider the amplitude for the elastic scattering of a charged fermion and a neutral vector boson. Again taking the interactions as given in eq. (4.32), the relevant diagrams are those shown in Fig. 17, plus four diagrams (not shown) obtained from these by crossing the initial and final state vectors.

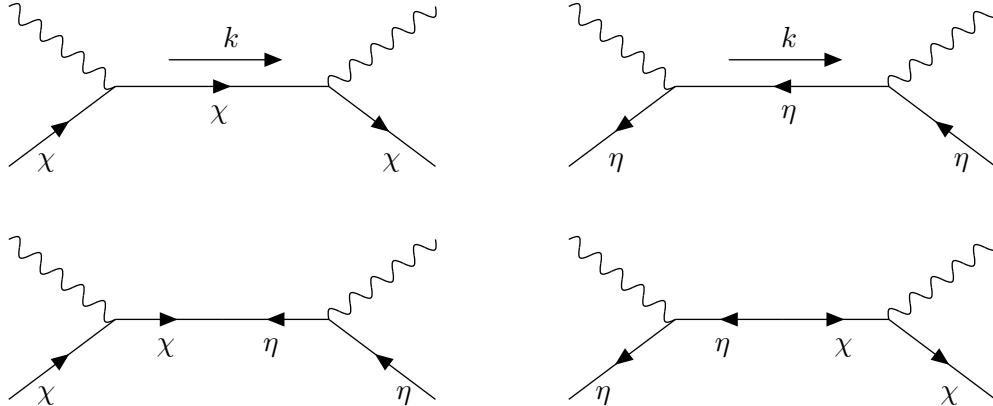


Figure 17: Tree-level Feynman diagrams contributing to the elastic scattering of a neutral vector boson and a charged Dirac fermion. There are four more diagrams, obtained from these by crossing the initial and final vector lines.

Applying the Feynman rules following from eq. (4.28) as before, one obtains the following matrix element

$$i\mathcal{M} = \frac{-i}{k^2 - m_\xi^2} \left\{ G_L^2 \bar{x}(\vec{p}_2, s_2) \bar{\sigma} \cdot \varepsilon_2^* \sigma \cdot k \bar{\sigma} \cdot \varepsilon_1 x(\vec{p}_1, s_1) + G_R^2 y(\vec{p}_2, s_2) \sigma \cdot \varepsilon_2^* \bar{\sigma} \cdot k \sigma \cdot \varepsilon_1 \bar{y}(\vec{p}_1, s_1) \right. \\ \left. - m G_L G_R [y(\vec{p}_2, s_2) \sigma \cdot \varepsilon_2^* \bar{\sigma} \cdot \varepsilon_1 x(\vec{p}_1, s_1) + \bar{x}(\vec{p}_2, s_2) \bar{\sigma} \cdot \varepsilon_2^* \sigma \cdot \varepsilon_1 \bar{y}(\vec{p}_1, s_1)] \right\} + (\text{crossed}) \quad (4.39)$$

and the assignments of momenta and spins are as before.

The computation of the amplitude for the scattering of a charged fermion and a charged vector boson is straightforward and will not be given explicitly here.

Finally, let us work out an example with four external-state fermions. Consider the case of elastic scattering of two identical Majorana fermions due to scalar exchange, governed by the interaction of eq. (4.25). The diagrams for scattering initial fermions labeled 1, 2 into final state fermions labeled 3, 4 are shown in Fig. 18. The resulting matrix element is:

$$i\mathcal{M} = \frac{-i}{s - m_\phi^2} \left\{ \lambda^2 (x_1 x_2) (y_3 y_4) + (\lambda^*)^2 (\bar{y}_1 \bar{y}_2) (\bar{x}_3 \bar{x}_4) + |\lambda|^2 [(x_1 x_2) (\bar{x}_3 \bar{x}_4) + (\bar{y}_1 \bar{y}_2) (y_3 y_4)] \right\} \\ + (-1) \frac{-i}{t - m_\phi^2} \left\{ \lambda^2 (y_3 x_1) (y_4 x_2) + (\lambda^*)^2 (\bar{x}_3 \bar{y}_1) (\bar{x}_4 \bar{y}_2) + |\lambda|^2 [(\bar{x}_3 \bar{y}_1) (y_4 x_2) + (y_3 x_1) (\bar{x}_4 \bar{y}_2)] \right\} \\ + \frac{-i}{u - m_\phi^2} \left\{ \lambda^2 (y_4 x_1) (y_3 x_2) + (\lambda^*)^2 (\bar{x}_4 \bar{y}_1) (\bar{x}_3 \bar{y}_2) + |\lambda|^2 [(\bar{x}_4 \bar{y}_1) (y_3 x_2) + (y_4 x_1) (\bar{x}_3 \bar{y}_2)] \right\}, \quad (4.40)$$

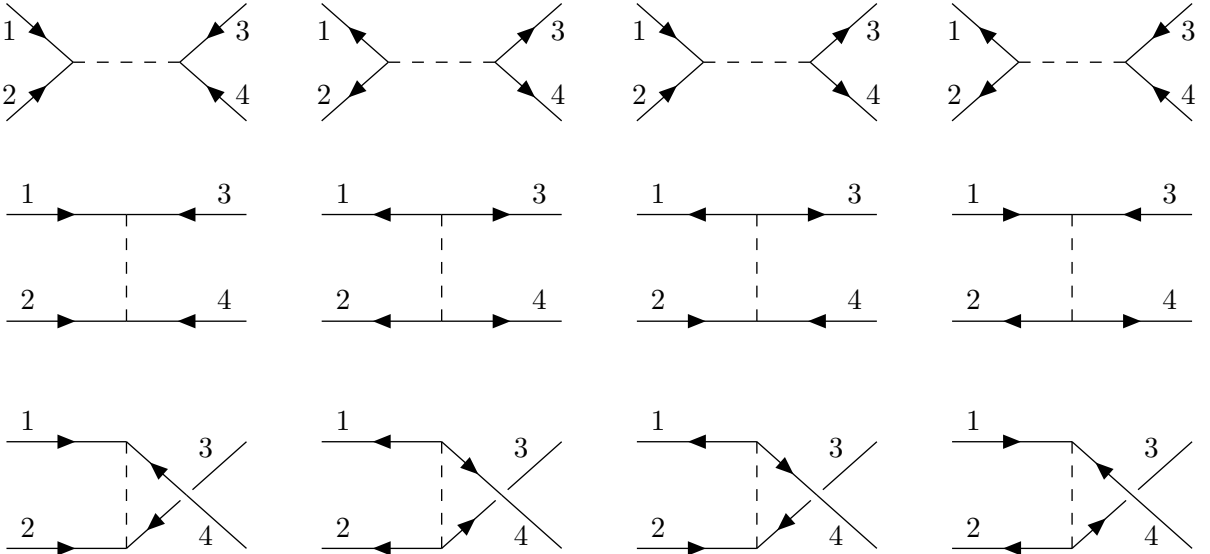


Figure 18: Tree-level Feynman diagrams contributing to the elastic scattering of identical neutral Majorana fermions via scalar exchange in the s -channel (top row), t -channel (middle row), and u -channel (bottom row).

where $x_i \equiv x(\vec{p}_i, s_i)$, $y_i \equiv y(\vec{p}_i, s_i)$, m_ϕ is the mass of the exchanged scalar, $s = (p_1 + p_2)^2$, $t = (p_1 - p_3)^2$ and $u = (p_1 - p_4)^2$. The relative minus sign (in parentheses) between the t -channel diagram and the s and u -channel diagrams is obtained by observing that 3142 is an odd permutation and 4132 is an even permutation of 1234.²³

Eq. (4.40) can be factorized with respect to the scalar line:

$$\begin{aligned} i\mathcal{M} = & \frac{-i}{s - m_\phi^2} (\lambda x_1 x_2 + \lambda^* \bar{y}_1 \bar{y}_2) (\lambda y_3 y_4 + \lambda^* \bar{x}_3 \bar{x}_4) + \frac{i}{t - m_\phi^2} (\lambda y_3 x_1 + \lambda^* \bar{x}_3 \bar{y}_1) (\lambda y_4 x_2 + \lambda^* \bar{x}_4 \bar{y}_2) \\ & + \frac{-i}{u - m_\phi^2} (\lambda y_4 x_1 + \lambda^* \bar{x}_4 \bar{y}_1) (\lambda y_3 x_2 + \lambda^* \bar{x}_3 \bar{y}_2). \end{aligned} \quad (4.41)$$

This is a common feature of Feynman graphs with a virtual boson. This example also illustrates the typical feature that, compared to the four-component formalism, two-component fermion Feynman rules yield more diagrams, although the contribution of each of the diagrams is simpler.

4.6 Self-energy functions and pole masses for two-component fermions

In this section, we discuss the self-energy functions for fermions in two-component notation, taking into account the possibilities of loop-induced mixing and absorptive parts corresponding to decays to intermediate states. This formalism is useful in the computation of loop-corrected physical pole masses.

Consider a theory with left-handed fermion degrees of freedom $\hat{\psi}_i$ labeled by an index $i = 1, 2, \dots, N$. Associated with each $\hat{\psi}_i$ is a right-handed fermion $\hat{\bar{\psi}}^i$, where the flavor labels are treated as described below eq. (3.61). The theory is assumed to contain arbitrary interactions, which we will not need to refer to explicitly. As discussed in Section 3.2, we diagonalize the fermion mass matrix and identify the fermion mass-eigenstates ψ_i as indicated in eq. (4.10). In general, the mass-eigenstates consist of neutral Majorana fermions ξ_k ($k = 1, \dots, N - 2n$) and Dirac fermion pairs χ_ℓ and η_ℓ ($\ell = 1, \dots, n$).²⁴ With respect to this basis, the symmetric $N \times N$ tree-level fermion mass matrix, \mathbf{m}^{ij} , is made up of diagonal elements m_k and 2×2 blocks $\begin{pmatrix} 0 & m_\ell \\ m_\ell & 0 \end{pmatrix}$ along the diagonal, where the m_k and m_ℓ are real and non-negative. Since \mathbf{m}^{ij} is real, the height of the flavor indices is not significant. Nevertheless, it is useful to define $\bar{\mathbf{m}}_{ij} \equiv \mathbf{m}^{ij}$ in order to maintain the convention that two repeated flavor indices are summed when one index is raised and the other is lowered.²⁵ Note that $\bar{\mathbf{m}}_{ik} \mathbf{m}^{kj} = \mathbf{m}^{ik} \bar{\mathbf{m}}_{kj} = m_i^2 \delta_i^j$ is a diagonal matrix.

The full, loop-corrected Feynman propagators with four-momentum p^μ are defined by the Fourier transforms of vacuum expectation values of time-ordered products of bilinears of the

²³Note that we would have obtained the same sign for the u -channel diagram had we crossed the initial state fermion lines instead of the final state fermion lines.

²⁴In order to have a unified description, we shall take the flavor index of all left-handed fields (including η_k) in the lowered position in this subsection, in contrast to the convention adopted in subsections 3.2 and 4.3.

²⁵We will soon be suppressing the indices, so the reason for the bar on $\bar{\mathbf{m}}_{ij}$ is merely to distinguish the lowered-index mass matrix.

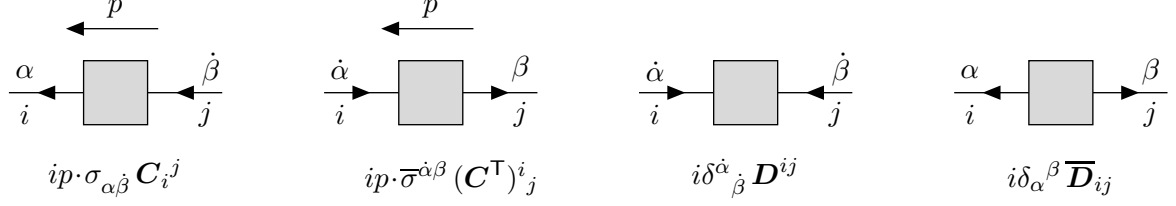


Figure 19: The full, loop-corrected propagators for two-component fermions are associated with functions $\mathbf{C}(p^2)_{i\dot{j}}$ [and its matrix transpose], $\mathbf{D}(p^2)^{ij}$, and $\bar{\mathbf{D}}(p^2)_{ij}$, as shown. The shaded boxes represent the sum of all connected Feynman diagrams, with external legs included. The four-momentum p flows from right to left.

fully interacting two-component fermion fields [cf. footnotefnft]. Following eqs. (4.1)–(4.4), we define:

$$\langle 0 | T \psi_{\alpha i}(x) \bar{\psi}_{\dot{\beta}}^j(y) | 0 \rangle_{\text{FT}} = ip \cdot \sigma_{\alpha\dot{\beta}} \mathbf{C}_i^{\dot{j}}(p^2), \quad (4.42)$$

$$\langle 0 | T \bar{\psi}^{\dot{\alpha} i}(x) \psi_j^\beta(y) | 0 \rangle_{\text{FT}} = ip \cdot \bar{\sigma}^{\dot{\alpha}\beta} (\mathbf{C}^\top)^i_j(p^2), \quad (4.43)$$

$$\langle 0 | T \bar{\psi}^{\dot{\alpha} i}(x) \bar{\psi}_{\dot{\beta}}^j(y) | 0 \rangle_{\text{FT}} = i\delta_{\alpha}^{\dot{\beta}} \mathbf{D}^{ij}(p^2), \quad (4.44)$$

$$\langle 0 | T \psi_{\alpha i}(x) \psi_j^\beta(y) | 0 \rangle_{\text{FT}} = i\delta_{\alpha}^{\beta} \bar{\mathbf{D}}_{ij}(p^2), \quad (4.45)$$

where

$$(\mathbf{C}^\top)^i_j \equiv \mathbf{C}_j^i. \quad (4.46)$$

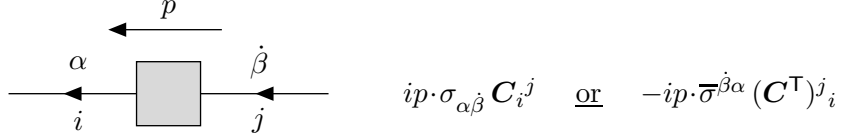
One can derive eq. (4.43) from eq. (4.42) by first writing

$$\bar{\psi}^{\dot{\alpha} i}(x) \psi_j^\beta(y) = -\epsilon^{\beta\alpha} \epsilon^{\dot{\alpha}\dot{\beta}} \psi_{\alpha j}(y) \bar{\psi}_{\dot{\beta}}^i(x), \quad (4.47)$$

where the minus sign arises due to the anticommutativity of the fields, and then using eq. (2.22); the interchange of x and y (after FT) simply changes p^μ to $-p^\mu$.

In general, \mathbf{D} and $\bar{\mathbf{D}}$ are complex symmetric matrices, and $\bar{\mathbf{D}} = \mathbf{D}^*$. The matrix \mathbf{C} satisfies the hermiticity condition $[\mathbf{C}^\top]^* = \mathbf{C}$. Here, we have introduced the star symbol to mean that a quantity Q^* is obtained from Q by taking the complex conjugate of all Lagrangian parameters appearing in its calculation, but not taking the complex conjugates of Euclideanized loop integral functions, whose imaginary (absorptive) parts correspond to fermion decay widths to multi-particle intermediate states. That is, the dispersive part of \mathbf{C} is hermitian and the absorptive part of \mathbf{C} is anti-hermitian.

The diagrammatic representations of the full propagators are displayed in Fig. 19, where $\mathbf{C}_i^{\dot{j}}$, \mathbf{D}^{ij} , and $\bar{\mathbf{D}}_{ij}$ defined above are each $N \times N$ matrix functions. Note that the second diagram of Fig. 19, when flipped by 180° about the vertical axis, is equivalent to the first diagram of Fig. 19 (with $p \rightarrow -p$, $\alpha \rightarrow \beta$, $\dot{\beta} \rightarrow \dot{\alpha}$ and $i \leftrightarrow j$). In analogy with Fig. 3, one could replace the first two diagrammatic rules of Fig. 19 with a single rule:



where we have used eq. (4.46) to rewrite the second version of the rule in terms of \mathbf{C}^\top . Indeed, by using the second version of the above rule and flipping the corresponding diagram by 180° as described above, one reproduces the rule of the second diagram of Fig. 19.

In what follows, we prefer to keep the first two rules of Fig. 19 as separate entities. This will permit us to conveniently assemble the four diagrams of Fig. 19 into a 2×2 block matrix of two-component propagators [*c.f.* eq. (E.58)]. In addition, by choosing the momentum flow in the two-component propagators from right to left, the left-to-right orderings of the spinor labels of the diagrams coincide with the ordering of spinor indices that occurs in the corresponding algebraic representations. Thus, we can multiply diagrams together and interpret them as the product of the respective algebraic quantities taken from left to right in the normal fashion.

Starting at tree-level and comparing with Fig. 2, the full propagator functions are given by:

$$\mathbf{C}_i^j = \delta_i^j / (p^2 - m_i^2) + \dots \quad (4.48)$$

$$\mathbf{D}^{ij} = \mathbf{m}^{ij} / (p^2 - m_i^2) + \dots \quad (4.49)$$

$$\overline{\mathbf{D}}_{ij} = \overline{\mathbf{m}}_{ij} / (p^2 - m_i^2) + \dots, \quad (4.50)$$

with no sum on i in each case. They are functions of the external momentum invariant p^2 and of the masses and couplings of the theory. Inserting the leading terms [eqs. (4.48)–(4.50)] into Fig. 19 and organizing the result in a 2×2 block matrix of two-component propagators reproduces the usual four-component fermion tree-level propagator given in eq. (E.58).

The computation of the full propagators can be organized, as usual in quantum field theory, in terms of one-particle irreducible (1PI) self-energy functions. These are formally defined to be the sum of all Feynman diagrams (excluding the tree-level) that contribute to the 1PI two-point Green function. Diagrammatically, the 1PI self-energy functions are defined in Fig. 20.

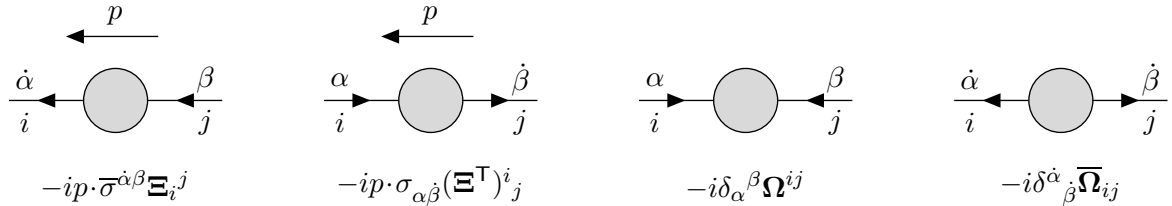


Figure 20: The self-energy functions for two-component fermions are associated with functions $\Xi(p^2)_i^j$ [and its matrix transpose], $\Omega(p^2)^{ij}$, and $\overline{\Omega}(p^2)_{ij}$, as shown. The shaded circles represent the sum of all one-particle irreducible, connected Feynman diagrams, and the external legs are amputated. The four-momentum p flows from right to left.

As in the case of the full loop-corrected propagators, $[\Xi^\top]^\star = \Xi$ and $\bar{\Omega} = \Omega^\star$, where the star symbol was defined in the paragraph following eq. (4.47), and $(\Xi^\top)^i_j \equiv \Xi_j^i$.

We illustrate the computation of the full propagator by considering first the following diagrammatic identity (with momentum p flowing from right to left):

$$\begin{aligned}
\frac{\alpha}{i} \leftarrow \boxed{} \leftarrow \frac{\dot{\beta}}{j} &= \frac{\alpha}{i} \leftarrow \frac{\dot{\beta}}{j} \\
&+ \frac{\alpha}{i} \leftarrow \frac{\dot{\gamma}}{k} \bigcirc \frac{\delta}{\ell} \leftarrow \boxed{} \leftarrow \frac{\dot{\beta}}{j} + \frac{\alpha}{i} \leftarrow \frac{\dot{\gamma}}{k} \bigcirc \frac{\dot{\delta}}{\ell} \leftarrow \boxed{} \leftarrow \frac{\dot{\beta}}{j} \\
&+ \frac{\alpha}{i} \leftarrow \frac{\gamma}{k} \bigcirc \frac{\delta}{\ell} \leftarrow \boxed{} \leftarrow \frac{\dot{\beta}}{j} + \frac{\alpha}{i} \leftarrow \frac{\gamma}{k} \bigcirc \frac{\dot{\delta}}{\ell} \leftarrow \boxed{} \leftarrow \frac{\dot{\beta}}{j}
\end{aligned} \tag{4.51}$$

Similar diagrammatic identities can be constructed for the three other full loop-corrected propagators of Fig. 19. The resulting four equations can be neatly summarized by the following matrix diagrammatic identity:

$$\begin{pmatrix} \leftarrow \boxed{} \rightarrow & \leftarrow \boxed{} \leftarrow \\ \rightarrow \boxed{} \rightarrow & \rightarrow \boxed{} \leftarrow \end{pmatrix} = \begin{pmatrix} \leftrightarrow & \leftarrow \\ \rightarrow & \leftrightarrow \end{pmatrix} \left[\begin{pmatrix} 1 & 0 \\ 0 & 1 \end{pmatrix} + \begin{pmatrix} \rightarrow \bigcirc \leftarrow & \rightarrow \bigcirc \rightarrow \\ \leftarrow \bigcirc \leftarrow & \leftarrow \bigcirc \rightarrow \end{pmatrix} \begin{pmatrix} \leftarrow \boxed{} \rightarrow & \leftarrow \boxed{} \leftarrow \\ \rightarrow \boxed{} \rightarrow & \rightarrow \boxed{} \leftarrow \end{pmatrix} \right] \tag{4.52}$$

We have chosen the labeling and momentum flow in Figs. 19 and 20 such that the spinor and flavor labels of the diagrams appear in the appropriate left-to-right order to permit the interpretation of eq. (4.52) as a matrix equation. The algebraic representation of eq. (4.52) can be written as $F = T + TSF$, where F is the matrix of full loop-corrected propagators, T is the matrix of tree-level propagators and S is the matrix of self-energy functions. Multiplying²⁶ on the left by T^{-1} and on the right by F^{-1} yields $T^{-1} = F^{-1} + S$. Thus, $F = [T^{-1} - S]^{-1}$. In pictures:

$$\begin{pmatrix} \leftarrow \boxed{} \rightarrow & \leftarrow \boxed{} \leftarrow \\ \rightarrow \boxed{} \rightarrow & \rightarrow \boxed{} \leftarrow \end{pmatrix} = \left[\begin{pmatrix} \leftrightarrow & \leftarrow \\ \rightarrow & \leftrightarrow \end{pmatrix}^{-1} - \begin{pmatrix} \rightarrow \bigcirc \leftarrow & \rightarrow \bigcirc \rightarrow \\ \leftarrow \bigcirc \leftarrow & \leftarrow \bigcirc \rightarrow \end{pmatrix} \right]^{-1}. \tag{4.53}$$

²⁶Alternatively, one can solve eq. (4.52) by iteration. This yields:

$$F = T + TS(T + TS(T + TS(\dots))) = T + TST + TSTST + \dots = T[1 + ST + (ST)^2 + \dots] = T[1 - ST]^{-1},$$

where in the last step, we have summed the geometric series. Taking the inverse of $F = T[1 - ST]^{-1}$, multiplying out the resulting expression and then taking the inverse of both sides yields eq. (4.53).

We evaluate the tree-level propagator matrix and its inverse using eqs. (4.48)–(4.50), keeping in mind that the direction of momentum flow is from right to left:

$$\begin{pmatrix} \overleftrightarrow{\quad} & \overleftarrow{\quad} \\ \overrightarrow{\quad} & \overleftrightarrow{\quad} \end{pmatrix} = \frac{1}{p^2 - m_i^2} \begin{pmatrix} i\overline{\mathbf{m}}_{ij} \delta_\alpha^\beta & ip \cdot \sigma_{\alpha\dot{\beta}} \delta_i^j \\ ip \cdot \overline{\sigma}^{\dot{\alpha}\beta} \delta_i^j & i\mathbf{m}^{ij} \delta_{\dot{\beta}}^\alpha \end{pmatrix}, \quad (4.54)$$

$$\begin{pmatrix} \overleftrightarrow{\quad} & \overleftarrow{\quad} \\ \overrightarrow{\quad} & \overleftrightarrow{\quad} \end{pmatrix}^{-1} = \begin{pmatrix} i\mathbf{m}^{ij} \delta_\alpha^\beta & -ip \cdot \sigma_{\alpha\dot{\beta}} \delta_i^j \\ -ip \cdot \overline{\sigma}^{\dot{\alpha}\beta} \delta_i^j & i\overline{\mathbf{m}}_{ij} \delta_{\dot{\beta}}^\alpha \end{pmatrix}, \quad (4.55)$$

where we follow the index structure defined in Figs. 19 and 20. Inserting eq. (4.55) into eq. (4.53), one obtains a $4N \times 4N$ matrix equation for the full propagator functions:

$$\begin{pmatrix} i\overline{\mathbf{D}} & ip \cdot \sigma \mathbf{C} \\ ip \cdot \overline{\sigma} \mathbf{C}^\top & i\mathbf{D} \end{pmatrix} = \begin{pmatrix} i(\mathbf{m} + \boldsymbol{\Omega}) & -ip \cdot \sigma (\mathbf{1} - \boldsymbol{\Xi}^\top) \\ -ip \cdot \overline{\sigma} (\mathbf{1} - \boldsymbol{\Xi}) & i(\overline{\mathbf{m}} + \overline{\boldsymbol{\Omega}}) \end{pmatrix}^{-1}, \quad (4.56)$$

where $\mathbf{1}$ is the $N \times N$ identity matrix. The right hand side of eq. (4.56) can be evaluated by employing the following identity for the inverse of a block-partitioned matrix [71]:

$$\begin{pmatrix} P & Q \\ R & S \end{pmatrix}^{-1} = \begin{pmatrix} (P - QS^{-1}R)^{-1} & (R - SQ^{-1}P)^{-1} \\ (Q - PR^{-1}S)^{-1} & (S - RP^{-1}Q)^{-1} \end{pmatrix}, \quad (4.57)$$

under the assumption that all inverses appearing in eq. (4.57) exist. Applying this result to eq. (4.56), we obtain

$$\mathbf{C}^{-1} = p^2(\mathbf{1} - \boldsymbol{\Xi}) - (\overline{\mathbf{m}} + \overline{\boldsymbol{\Omega}})(\mathbf{1} - \boldsymbol{\Xi}^\top)^{-1}(\mathbf{m} + \boldsymbol{\Omega}), \quad (4.58)$$

$$\mathbf{D}^{-1} = p^2(\mathbf{1} - \boldsymbol{\Xi})(\mathbf{m} + \boldsymbol{\Omega})^{-1}(\mathbf{1} - \boldsymbol{\Xi}^\top) - (\overline{\mathbf{m}} + \overline{\boldsymbol{\Omega}}), \quad (4.59)$$

$$\overline{\mathbf{D}}^{-1} = p^2(\mathbf{1} - \boldsymbol{\Xi}^\top)(\overline{\mathbf{m}} + \overline{\boldsymbol{\Omega}})^{-1}(\mathbf{1} - \boldsymbol{\Xi}) - (\mathbf{m} + \boldsymbol{\Omega}). \quad (4.60)$$

Note that eq. (4.60) is consistent with eq. (4.59) as $\boldsymbol{\Xi}^\star = \boldsymbol{\Xi}^\top$.

The pole mass can be found most easily by considering the rest frame of the (off-shell) fermion, in which the space components of p^μ vanish. This reduces the spinor-index dependence to a triviality. Setting $p^\mu = (\sqrt{s}; \mathbf{0})$, we search for values of s where the inverse of the full propagator has a zero eigenvalue. This is equivalent to setting the determinant of the inverse of the full propagator to zero. Here we shall use the well-known formula for the determinant of a block-partitioned matrix [71]:

$$\det \begin{pmatrix} P & Q \\ R & S \end{pmatrix} = \det P \det (S - RP^{-1}Q). \quad (4.61)$$

The end result is that the poles of the full propagator (which are in general complex),

$$s_{\text{pole},j} \equiv M_j^2 - i\Gamma_j M_j, \quad (4.62)$$

are formally the solutions to the non-linear equation²⁷

$$\det [s\mathbf{1} - (\mathbf{1} - \mathbf{\Xi}^\top)^{-1}(\mathbf{m} + \mathbf{\Omega})(\mathbf{1} - \mathbf{\Xi})^{-1}(\overline{\mathbf{m}} + \overline{\mathbf{\Omega}})] = 0, \quad (4.63)$$

with $s \equiv p^2$.

Some care is required in using eq. (4.63), since the pole squared mass always has a *non-positive* imaginary part, while the loop integrals used to find the self-energy functions are complex functions of a real variable s that is given an infinitesimal *positive* imaginary part. Therefore, eq. (4.63) should be solved iteratively by first expanding the self-energy function matrices $\mathbf{\Xi}$, $\mathbf{\Omega}$ and $\overline{\mathbf{\Omega}}$ in a series in s about either $m_j^2 + i\epsilon$ or $M_j^2 + i\epsilon$. The complex pole mass quantities $s_{\text{pole},j}$ are renormalization-group and gauge invariant physical observables. Examples are given in subsections 6.23 and 6.24.

The results of this section can be applied to an arbitrary collection of fermions (both Majorana or Dirac). However, it is convenient to treat separately the case where all fermions are Dirac fermions (consisting of pairs of two-component fields χ_i and η_i). As discussed in Section 3.2, the Dirac fermion mass-eigenstates are defined in eq. (3.80) and are determined by the singular value decomposition of the Dirac fermion mass matrix. With respect to the mass basis, we denote the diagonal Dirac fermion mass matrix by \mathbf{M}^{ij} . The elements of this matrix are real and non-negative. Nevertheless, it will be convenient as before to define $\overline{\mathbf{M}}_{ij} \equiv \mathbf{M}^{ij}$ to maintain covariance when manipulating tensors with flavor indices.

At tree-level, there are four propagators for each pair of χ and η fields as shown in Fig. 5. The corresponding full, loop-corrected propagators are shown in Fig. 21.

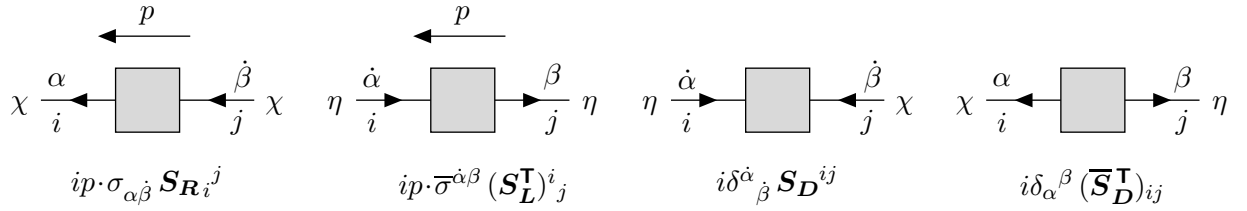


Figure 21: The full, loop-corrected propagators for Dirac fermions, represented by pairs of two-component (oppositely charged) fermion fields χ_i and η_i , are associated with functions $S_R(p^2)_{i,j}$, $S_L^\top(p^2)^{i,j}$, $S_D(p^2)^{ij}$, and $\bar{S}_D^\top(p^2)_{ij}$, as shown. The shaded boxes represent the sum of all connected Feynman diagrams, with external legs included. The four-momentum p and the charge of χ flow from right to left.

The naming and sign conventions employed for the full, loop-corrected Dirac fermion propagator functions in Fig. 21 derives from the corresponding functions used in the more traditional four-component treatment presented in Appendix E [c.f. eq. (E.79)].

²⁷The determinant of the inverse of the full propagator [the inverse of eq. (4.56)] is equal to eq. (4.63) multiplied by $\det [-(\mathbf{1} - \mathbf{\Xi})(\mathbf{1} - \mathbf{\Xi}^\top)]$. We assume that the latter does not vanish. This must be true perturbatively since the eigenvalues of $\mathbf{\Xi}$ are one-loop (or higher) quantities, which one assumes cannot be as large as 1.

In general, the complex matrices \mathbf{S}_R and \mathbf{S}_L satisfy hermiticity conditions $[\mathbf{S}_R^\mathbf{T}]^* = \mathbf{S}_R$ and $[\mathbf{S}_L^\mathbf{T}]^* = \mathbf{S}_L$, whereas the complex matrices \mathbf{S}_D and $\bar{\mathbf{S}}_D$ are related by $\bar{\mathbf{S}}_D = \mathbf{S}_D^*$, where the star symbol is defined in the paragraph below eq. (4.47). In contrast to the general case treated earlier, \mathbf{S}_R and \mathbf{S}_L are unrelated and \mathbf{S}_D is a complex matrix (not necessarily symmetric).

Instead of working in a χ - η basis for the two-component Dirac fermion fields, one can Takagi-digonalize the fermion mass matrix. In the new ψ -basis, the loop-corrected propagators of Fig. 19 are applicable. It is easy to check that the number of independent functions is the same in both methods for treating Dirac fermions. In particular, the loop-corrected propagator functions in the ψ -basis are given in terms of the corresponding functions in the χ - η basis by:²⁸

$$\mathbf{C} = \begin{pmatrix} \mathbf{S}_R & 0 \\ 0 & \mathbf{S}_L \end{pmatrix}, \quad \mathbf{D} = \begin{pmatrix} 0 & \mathbf{S}_D^\mathbf{T} \\ \mathbf{S}_D & 0 \end{pmatrix}, \quad \bar{\mathbf{D}} = \begin{pmatrix} 0 & \bar{\mathbf{S}}_D^\mathbf{T} \\ \bar{\mathbf{S}}_D & 0 \end{pmatrix}. \quad (4.64)$$

We similarly introduce the 1PI self-energy matrix functions for the Dirac fermions in the χ - η basis, where the corresponding self-energy functions are defined in Fig. 22.

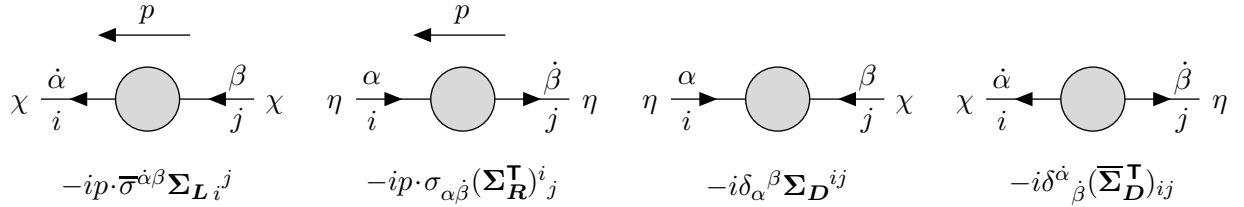


Figure 22: The self-energy functions for two-component Dirac fermions, represented by pairs of two-component (oppositely charged) fermion fields χ_i and η_i , are associated with functions $\Sigma_L(p^2)_{ij}$, $\Sigma_R^\mathbf{T}(p^2)^i_j$, $\Sigma_D(p^2)^{ij}$, and $\bar{\Sigma}_D^\mathbf{T}(p^2)_{ij}$, as shown. The shaded circles represent the sum of all one-particle irreducible, connected Feynman diagrams, and the external legs are amputated. The four-momentum p flows from right to left.

As before, the naming and sign conventions employed for the Dirac fermion self-energy functions above derives from the corresponding functions used in the more traditional four-component treatment of Appendix E [*c.f.* eq. (E.80)].

Once again, the complex matrices Σ_L and Σ_R satisfy hermiticity conditions $[\Sigma_L^\mathbf{T}]^* = \Sigma_L$ and $[\Sigma_R^\mathbf{T}]^* = \Sigma_R$, whereas the complex matrices Σ_D and $\bar{\Sigma}_D$ are related by $\bar{\Sigma}_D = \Sigma_D^*$, where the star symbol is defined in the paragraph below eq. (4.47). Likewise, Σ_L and Σ_R are unrelated and Σ_D is a complex matrix (not necessarily symmetric). The self-energy functions in the ψ -basis are given in terms of the corresponding functions in the χ - η basis by:²⁸

$$\Xi = \begin{pmatrix} \Sigma_L & 0 \\ 0 & \Sigma_R \end{pmatrix}, \quad \Omega = \begin{pmatrix} 0 & \Sigma_D^\mathbf{T} \\ \Sigma_D & 0 \end{pmatrix}, \quad \bar{\Omega} = \begin{pmatrix} 0 & \bar{\Sigma}_D^\mathbf{T} \\ \bar{\Sigma}_D & 0 \end{pmatrix}. \quad (4.65)$$

²⁸The simple forms of \mathbf{C} in eq. (4.64) and Ξ in eq. (4.65) motivate our definitions of \mathbf{S}_L and Σ_R with the transpose as indicated in Figs. 21 and 22, respectively.

In the case of Dirac fermions fields, eq. (4.53) still holds in the χ - η basis, which yields:

$$\begin{pmatrix} i\bar{\mathbf{S}}_D^T & ip \cdot \sigma \mathbf{S}_R \\ ip \cdot \bar{\sigma} \mathbf{S}_L^T & i\mathbf{S}_D \end{pmatrix} = \begin{pmatrix} i(\mathbf{M} + \boldsymbol{\Sigma}_D) & -ip \cdot \sigma (\mathbf{1} - \boldsymbol{\Sigma}_R^T) \\ -ip \cdot \bar{\sigma} (\mathbf{1} - \boldsymbol{\Sigma}_L) & i(\bar{\mathbf{M}} + \bar{\boldsymbol{\Sigma}}_D^T) \end{pmatrix}^{-1}, \quad (4.66)$$

Using eq. (4.57), it follows that:

$$\mathbf{S}_L^{-1} = p^2(\mathbf{1} - \boldsymbol{\Sigma}_R) - (\bar{\mathbf{M}} + \bar{\boldsymbol{\Sigma}}_D)(\mathbf{1} - \boldsymbol{\Sigma}_L^T)^{-1}(\mathbf{M} + \boldsymbol{\Sigma}_D^T), \quad (4.67)$$

$$\mathbf{S}_R^{-1} = p^2(\mathbf{1} - \boldsymbol{\Sigma}_L) - (\bar{\mathbf{M}} + \bar{\boldsymbol{\Sigma}}_D^T)(\mathbf{1} - \boldsymbol{\Sigma}_R^T)^{-1}(\mathbf{M} + \boldsymbol{\Sigma}_D), \quad (4.68)$$

$$\mathbf{S}_D^{-1} = p^2(\mathbf{1} - \boldsymbol{\Sigma}_L)(\mathbf{M} + \boldsymbol{\Sigma}_D)^{-1}(\mathbf{1} - \boldsymbol{\Sigma}_R^T) - (\bar{\mathbf{M}} + \bar{\boldsymbol{\Sigma}}_D^T), \quad (4.69)$$

$$\bar{\mathbf{S}}_D^{-1} = p^2(\mathbf{1} - \boldsymbol{\Sigma}_L^T)(\bar{\mathbf{M}} + \bar{\boldsymbol{\Sigma}}_D)^{-1}(\mathbf{1} - \boldsymbol{\Sigma}_R) - (\mathbf{M} + \boldsymbol{\Sigma}_D^T). \quad (4.70)$$

Note that eq. (4.70) is consistent with eq. (4.69) as $\boldsymbol{\Sigma}_{L,R}^* = \boldsymbol{\Sigma}_{L,R}^T$.

The pole mass is now easily computed using the technique previously outlined. In particular, eq. (4.63) is replaced by:

$$\det [s\mathbf{1} - (\mathbf{1} - \boldsymbol{\Sigma}_R^T)^{-1}(\mathbf{M} + \boldsymbol{\Sigma}_D)(\mathbf{1} - \boldsymbol{\Sigma}_L)^{-1}(\bar{\mathbf{M}} + \bar{\boldsymbol{\Sigma}}_D^T)] = 0, \quad (4.71)$$

which determines the complex pole squared masses s_{pole} of the corresponding Dirac fermions. Again, the self-energy functions should be expanded in a series in s about a point with an infinitesimal positive imaginary part.

Finally, we examine the special case of a parity-conserving vectorlike theory of Dirac fermions (such as QED or QCD). In this case, the following relations hold among the loop-corrected propagator functions and self-energy functions, respectively:²⁹

$$\mathbf{S}_{Ri}{}^j = (\mathbf{S}_L^T)^i{}_j, \quad \mathbf{S}_D{}^{ij} = (\bar{\mathbf{S}}_D^T)_{ij}, \quad (4.72)$$

$$\boldsymbol{\Sigma}_{Li}{}^j = (\boldsymbol{\Sigma}_R^T)^i{}_j, \quad \boldsymbol{\Sigma}_D{}^{ij} = (\bar{\boldsymbol{\Sigma}}_D^T)_{ij}. \quad (4.73)$$

By imposing eq. (4.73) on eqs. (4.67)–(4.70) and recalling that $\bar{\mathbf{M}}_{ij} = \mathbf{M}^{ij}$, it is straightforward to verify that eq. (4.72) is satisfied.

5 Conventions for fermion and anti-fermion names and fields

In this section, we discuss conventions for labeling Feynman diagrams that contain two-component fermion fields of the Standard Model (SM) and its minimal supersymmetric extension (MSSM).

In the case of Majorana fermions, there is a one-to-one correspondence between the particle names and the unbarred $(\frac{1}{2}, 0)$ [left-handed] fields. In contrast, for Dirac fermions there are always two distinct two-component fields that correspond to each particle name. This is illustrated in Table 1, which lists the SM and MSSM fermion particle names together with the

²⁹These relations are derived using four-component spinor methods in Appendix E [cf. eqs. (E.87) and (E.88)].

Table 1: Fermion and anti-fermion names and two-component fields in the Standard Model and the MSSM. In the listing of two-component fields, the first is an unbarred $(\frac{1}{2}, 0)$ [left-handed] field and the second is a barred $(0, \frac{1}{2})$ [right-handed] field. (In this table, neutrinos are considered to be exactly massless and the left-handed antineutrino ν^c is absent from the spectrum).

Fermion name	Two-component fields
ℓ^- (lepton)	$\ell, \bar{\ell}^c$
ℓ^+ (anti-lepton)	$\ell^c, \bar{\ell}$
ν (neutrino)	$\nu, -$
$\bar{\nu}$ (antineutrino)	$-, \bar{\nu}$
q (quark)	q, \bar{q}^c
\bar{q} (anti-quark)	q^c, \bar{q}
f (quark or lepton)	f, \bar{f}^c
\bar{f} (anti-quark or anti-lepton)	f^c, \bar{f}
\tilde{N}_i (neutralino)	$\chi_i^0, \overline{\chi_i^0}$
\tilde{C}_i^+ (chargino)	$\chi_i^+, \overline{\chi_i^-}$
\tilde{C}_i^- (anti-chargino)	$\chi_i^-, \overline{\chi_i^+}$
\tilde{g} (gluino)	$\tilde{g}, \tilde{\bar{g}}$

corresponding two-component fields. For each particle, we list the two-component field with the same quantum numbers, i.e., the field that contains a creation operator for that one-particle state when acting to the right on the vacuum state $|0\rangle$.

There is an option of labeling fermion lines in Feynman diagrams by particle names or by field names; each choice has advantages and disadvantages.³⁰ In all of the examples that follow, we have chosen to eliminate the possibility of ambiguity as follows. We always label fermion lines with two-component fields (rather than particle names), and adopt the following conventions:

- In the Feynman rules for interaction vertices, the external lines are always labeled by the unbarred $(\frac{1}{2}, 0)$ [left-handed] field, regardless of whether the corresponding arrow is pointed in or out of the vertex. Two-component fermion lines with arrows pointing away from the vertex correspond to dotted indices, and two-component fermion lines with arrows pointing toward the vertex always correspond to undotted indices. This also applies to Feynman diagrams where the initial state and the final state roles are ambiguous (such as self-energy diagrams).

³⁰Unfortunately, the notation for fermion names can be ambiguous because some of the symbols used also appear as names for one of the two-component fermion fields. In practice, it should be clear from the context which set of names are being employed.

- Internal fermion lines in Feynman diagrams are also always labeled by the unbarred $(\frac{1}{2}, 0)$ [left-handed] field(s). Internal fermion lines containing a propagator with opposing arrows can carry two labels (see *e.g.* Fig. 15).

- Initial-state external fermion lines (which always have physical four-momenta pointing into the vertex) in Feynman diagrams are labeled by the corresponding unbarred $(\frac{1}{2}, 0)$ [left-handed] field if the arrow is into the vertex, and by the barred $(0, \frac{1}{2})$ [right-handed] field if the arrow is away from the vertex.

- Final-state external fermion lines in complete Feynman diagrams (which always have physical four-momenta pointing out of the vertex) are labeled by the corresponding barred $(0, \frac{1}{2})$ [right-handed] field if the arrow is into the vertex, and by the unbarred $(\frac{1}{2}, 0)$ [left-handed] field if the arrow is away from the vertex.

In particular, the field labels used for external fermion lines always correspond to the same conserved quantities (charges, lepton numbers, baryon numbers) as the corresponding physical particle. As an example, for either initial or final states, the two-component fields e and \bar{e}^c both represent the negatively charged electron, conventionally denoted by e^- , whereas both e^c and \bar{e} represent the positively charged positron, conventionally denoted by e^+ (as indicated in Table 1). The rules for using these states as external particles are summarized in Fig. 23.

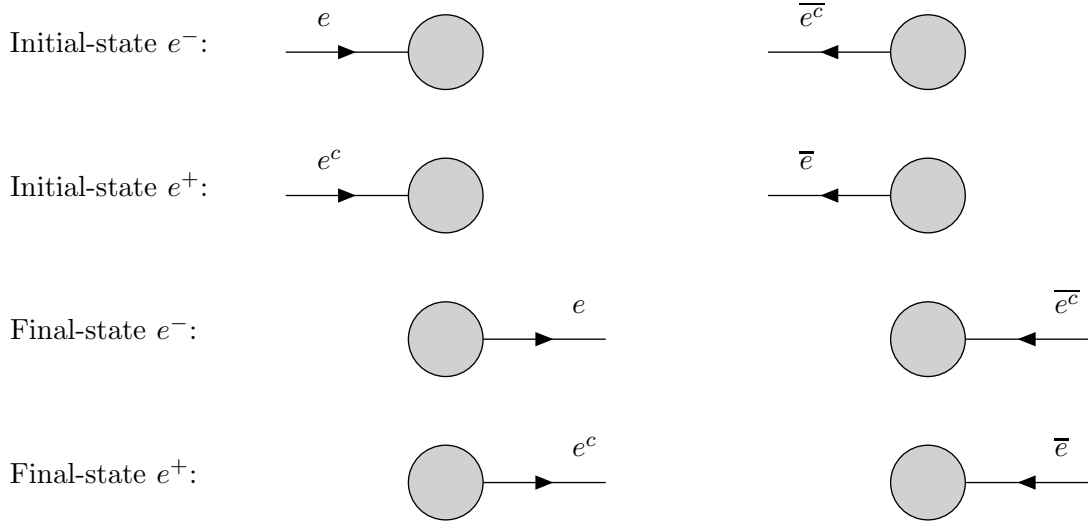


Figure 23: The two-component field labeling conventions for external fermion lines in a Feynman diagram for a physical process. The top row corresponds to an initial-state electron, the second row to an initial-state positron, the third row to a final-state electron, and the fourth row to a final-state positron. The labels above each line are the two-component field names. The corresponding conventions for a massless neutrino are obtained by deleting the diagrams with e^c or \bar{e}^c , and of course changing e and \bar{e} to ν and $\bar{\nu}$.

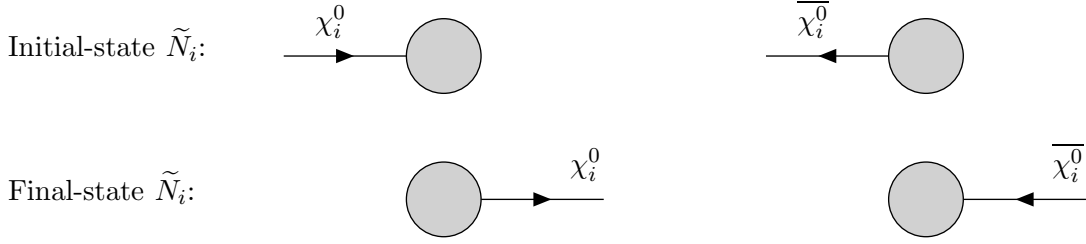


Figure 24: The two-component field labeling conventions for external neutralino lines in a Feynman diagram for a physical process. The top row corresponds to an initial-state neutralino, and the second row to a final-state neutralino. The labels above each line are the two-component field names. (The neutralino is its own antiparticle.)

The applicaiton of our naming conventions to processes involving Majorana fermions is completely straightforward. For example, the conventions for employing the neutralino states as external particles are summarized in Fig. 24.

As a simple example, consider Bhabha scattering ($e^-e^+ \rightarrow e^-e^+$) [72]. We require the the two-component Feynman rules for the QED coupling of electrons and positrons to the photon, which are exhibited in Fig. 25. Consider the s -channel tree-level Feynman diagrams that contribute to the invariant amplitude for $e^-e^+ \rightarrow e^-e^+$. If we were to label the external fermion lines according to the corresponding particle names (which does *not* conform to the conventions introduced above), the result is shown in Fig. 26. One can find the identity of the external two-component fermion fields by carefully observing the direction of the arrow of each

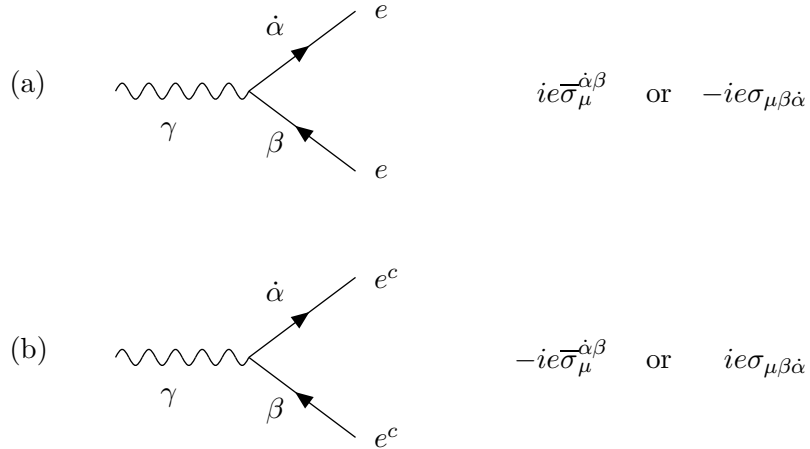


Figure 25: The two-component Feynman rules for the QED vertex. Following the conventions outlined in this Section, we label these rules with the $(\frac{1}{2}, 0)$ [left-handed] fields e and e^c , which comprise the Dirac electron. Note that $e > 0$ and $Q_e = -1$ [cf. Fig. 67].

fermion line. For contrast, the same diagrams, relabeled with two-component fields following the conventions established in this section (*c.f.* Fig. 23), are shown in Fig. 27. An explicit computation of the invariant amplitude is given in Section 6.3.

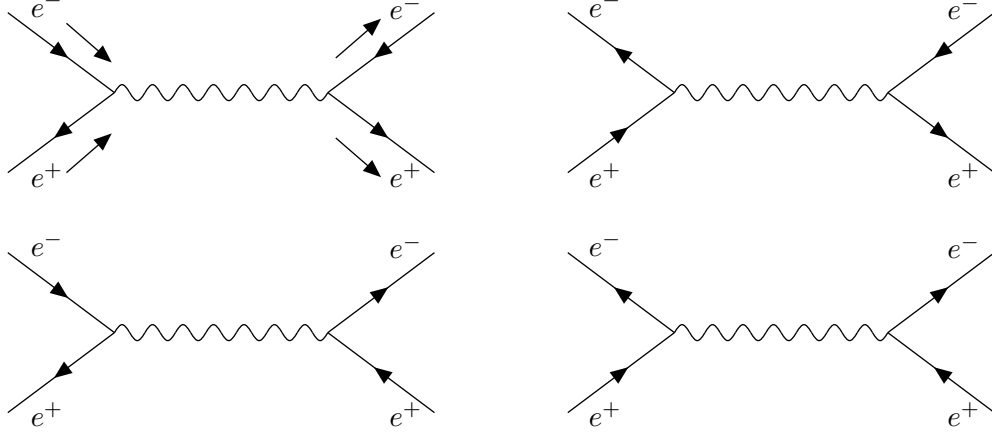


Figure 26: Tree-level s -channel Feynman diagrams for $e^-e^+ \rightarrow e^-e^+$, with the external lines labeled according to the particle names. The initial state is on the left, and the final state is on the right. Thus, the physical momentum flow of the external particles, as well as the flow of the labeled charges, are indicated by the arrows adjacent to the corresponding fermion lines in the upper left diagram.

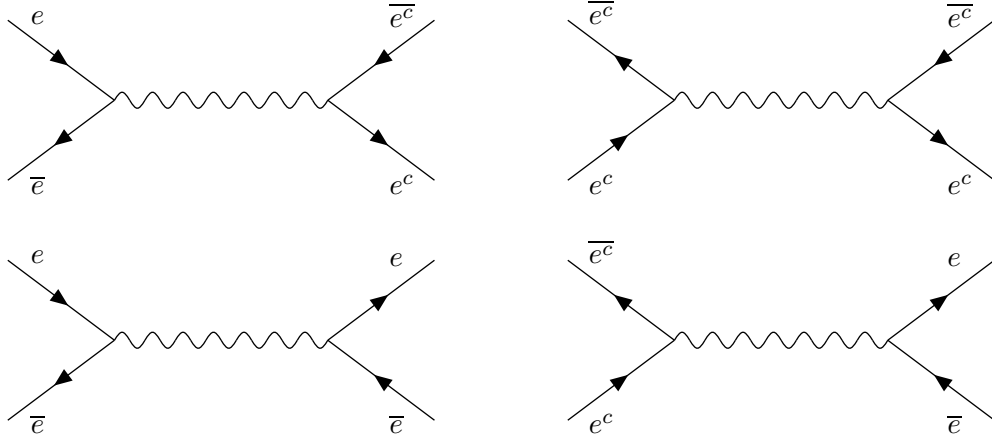


Figure 27: Tree-level s -channel Feynman diagrams for $e^+e^- \rightarrow e^+e^-$. These diagrams are the same as in Fig. 26, but with the external lines relabeled by the two-component fermion fields according to our conventions.

6 Practical examples from the Standard Model and supersymmetry

In this section we will present some examples to illustrate the use of the rules presented in this paper. These examples are chosen from the Standard Model [73] and the MSSM [47–49], in order to provide an unambiguous point of reference. In all cases, the fermion lines in Feynman diagrams are labeled by two-component field names, rather than the particle names, as explained in Section 5.

6.1 Top quark decay: $t \rightarrow bW^+$

We begin by calculating the decay width of a top quark into a bottom quark and W^+ vector boson. For simplicity, we treat this as a one-generation problem and ignore Cabibbo-Kobayashi-Maskawa (CKM) [74] mixing among the three quark generations [see eq. (H.7) and the surrounding text]. Let the four-momenta and helicities of these particle be (p_t, λ_t) , (k_b, λ_b) and (k_W, λ_W) , respectively. Then $p_t^2 = m_t^2$, $k_b^2 = m_b^2$ and $k_W^2 = m_W^2$ and

$$2p_t \cdot k_W = m_t^2 - m_b^2 + m_W^2, \quad (6.1)$$

$$2p_t \cdot k_b = m_t^2 + m_b^2 - m_W^2, \quad (6.2)$$

$$2k_W \cdot k_b = m_t^2 - m_b^2 - m_W^2. \quad (6.3)$$

Because only left-handed top quarks couple to the W boson, the only Feynman diagram for $t \rightarrow bW^+$ is the one shown in Fig. 28. The corresponding amplitude can be read off of the Feynman rule of Fig. 67 in Appendix H. Here the initial-state top quark is a two-component field t going into the vertex and the final-state bottom quark is created by a two-component field \bar{b} . Therefore the amplitude is given by:

$$i\mathcal{M} = -i\frac{g}{\sqrt{2}}\varepsilon_\mu^* \bar{x}_b \bar{\sigma}^\mu x_t, \quad (6.4)$$

where $\varepsilon_\mu^* \equiv \varepsilon_\mu^*(k_W, \lambda_W)$ is the polarization vector of the W^+ , and $\bar{x}_b \equiv \bar{x}(\vec{k}_b, \lambda_b)$ and $x_t \equiv x(\vec{p}_t, \lambda_t)$ are the external-state wavefunction factors for the bottom and top quark. Squaring this amplitude yields:

$$|\mathcal{M}|^2 = \frac{g^2}{2} \varepsilon_\mu^* \varepsilon_\nu (\bar{x}_b \bar{\sigma}^\mu x_t) (\bar{x}_t \bar{\sigma}^\nu x_b), \quad (6.5)$$

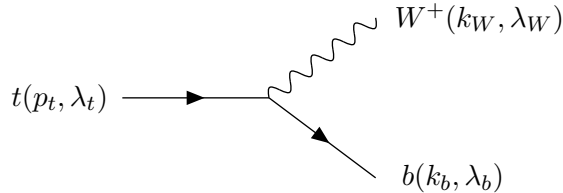


Figure 28: The Feynman diagram for $t \rightarrow bW^+$ at tree level.

where we have used equation (2.32). Next, we can average over the top quark spin polarizations using eq. (3.56):

$$\frac{1}{2} \sum_{\lambda_t} |\mathcal{M}|^2 = \frac{g^2}{4} \varepsilon_\mu^* \varepsilon_\nu \bar{x}_b \bar{\sigma}^\mu p_t \cdot \sigma \bar{\sigma}^\nu x_b. \quad (6.6)$$

Summing over the bottom quark spin polarizations in the same way yields a trace over spinor indices:

$$\frac{1}{2} \sum_{\lambda_t, \lambda_b} |\mathcal{M}|^2 = \frac{g^2}{4} \varepsilon_\mu^* \varepsilon_\nu \text{Tr}[\bar{\sigma}^\mu p_t \cdot \sigma \bar{\sigma}^\nu k_b \cdot \sigma] = \frac{g^2}{2} \varepsilon_\mu^* \varepsilon_\nu (p_t^\mu k_b^\nu + k_b^\mu p_t^\nu - g^{\mu\nu} p_t \cdot k_b), \quad (6.7)$$

where we have used eq. (2.45). Finally we can sum over the W^+ polarizations according to:

$$\sum_{\lambda_W} \varepsilon_\mu^* \varepsilon_\nu = -g_{\mu\nu} + (k_W)_\mu (k_W)_\nu / m_W^2. \quad (6.8)$$

The result is:

$$\frac{1}{2} \sum_{\text{spins}} |\mathcal{M}|^2 = \frac{g^2}{2} [p_t \cdot k_b + 2(p_t \cdot k_W)(k_b \cdot k_W)/m_W^2]. \quad (6.9)$$

After performing the phase space integration, one obtains:

$$\Gamma(t \rightarrow bW^+) = \frac{1}{16\pi m_t^3} \lambda^{1/2}(m_t^2, m_W^2, m_b^2) \left(\frac{1}{2} \sum_{\text{spins}} |\mathcal{M}|^2 \right) \quad (6.10)$$

$$= \frac{g^2}{64\pi m_W^2 m_t^3} \lambda^{1/2}(m_t^2, m_W^2, m_b^2) [(m_t^2 + 2m_W^2)(m_t^2 - m_W^2) + m_b^2(m_W^2 - 2m_t^2) + m_b^4], \quad (6.11)$$

where

$$\lambda(x, y, z) \equiv x^2 + y^2 + z^2 - 2xy - 2xz - 2yz. \quad (6.12)$$

In the approximation $m_b \ll m_W, m_t$, one ends up with the well-known result [75]

$$\Gamma(t \rightarrow bW^+) = \frac{g^2 m_t}{64\pi} \left(2 + \frac{m_t^2}{m_W^2} \right) \left(1 - \frac{m_W^2}{m_t^2} \right)^2, \quad (6.13)$$

which exhibits the Nambu-Goldstone enhancement factor (m_t^2/m_W^2) for the longitudinal W contribution compared to the two transverse W contributions [75].

6.2 Z^0 vector boson decay: $Z^0 \rightarrow f \bar{f}$

Consider the partial decay width of the Z^0 boson into Standard Model fermion-antifermion final states. There are two Feynman diagrams (as in the generic example of Fig. 12), shown in Fig. 29. In the first diagram, the fermion particle f in the final state is created by a two-component field f in the Feynman rule, and the anti-fermion particle \bar{f} by a two-component field \bar{f} . In the second diagram, the fermion particle f in the final state is created by a two-component field

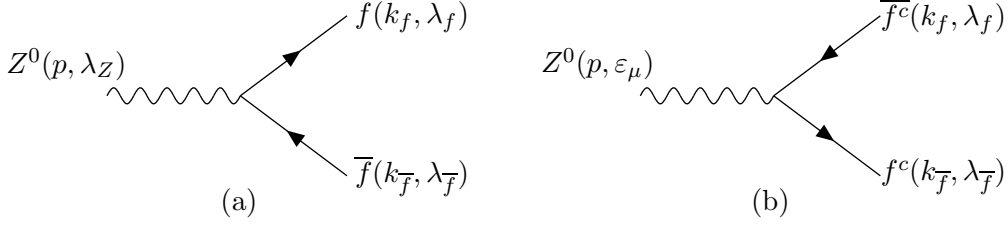


Figure 29: The Feynman diagrams for Z^0 decay into a fermion-antifermion pair. Fermion lines are labeled according to the two-component fermion field labeling convention (see Section 5).

f^c , and the anti-fermion particle \bar{f} by a two-component field \bar{f}^c . Let us call the initial Z^0 four-momentum and helicity (p, λ_Z) and the final state fermion (f) and anti-fermion (\bar{f}) momentum and helicities (k_f, λ_f) and $(k_{\bar{f}}, \lambda_{\bar{f}})$, respectively. Then, $k_f^2 = k_{\bar{f}}^2 = m_f^2$ and $p^2 = m_Z^2$, and

$$k_f \cdot k_{\bar{f}} = \frac{1}{2} m_Z^2 - m_f^2, \quad (6.14)$$

$$p \cdot k_f = p \cdot k_{\bar{f}} = \frac{1}{2} m_Z^2. \quad (6.15)$$

According to the rules of Fig. 67, the matrix elements for the two Feynman graphs are:

$$i\mathcal{M}_a = -i \frac{g}{c_W} (T_3^f - Q_f s_W^2) \varepsilon_\mu \bar{x}_f \bar{\sigma}^\mu y_{\bar{f}}, \quad (6.16)$$

$$i\mathcal{M}_b = ig Q_f \frac{s_W^2}{c_W} \varepsilon_\mu y_f \sigma^\mu \bar{x}_{\bar{f}}, \quad (6.17)$$

where $x_i \equiv x(\vec{k}_i, \lambda_i)$ and $y_i \equiv y(\vec{k}_i, \lambda_i)$, for $i = f, \bar{f}$, and $\varepsilon_\mu \equiv \varepsilon_\mu(p, \lambda_Z)$.

Using the Bouchiat-Michel formulae developed in Appendix F, one can explicitly evaluate \mathcal{M}_a and \mathcal{M}_b as a function of the final state fermion helicities. The result of this computation is given in eqs. (F.64) and (F.65). If the final state helicities are not measured, then it is simpler to square the amplitude and sum over the final state spins.

It is convenient to define:

$$a_f \equiv T_3^f - Q_f s_W^2; \quad b_f \equiv -Q_f s_W^2. \quad (6.18)$$

Then the squared matrix element for the decay is, using eqs. (2.31) and (2.32),

$$|\mathcal{M}|^2 = \frac{g^2}{c_W^2} \varepsilon_\mu \varepsilon_\nu^* \left(a_f \bar{x}_f \bar{\sigma}^\mu y_{\bar{f}} + b_f y_f \sigma^\mu \bar{x}_{\bar{f}} \right) \left(a_f \bar{y}_{\bar{f}} \bar{\sigma}^\nu x_f + b_f x_{\bar{f}} \sigma^\nu \bar{y}_f \right). \quad (6.19)$$

Summing over the anti-fermion helicity using eqs. (3.56)–(3.59) gives:

$$\begin{aligned} \sum_{\lambda_{\bar{f}}} |\mathcal{M}|^2 = & \frac{g^2}{c_W^2} \varepsilon_\mu \varepsilon_\nu^* \left(a_f^2 \bar{x}_f \bar{\sigma}^\mu k_{\bar{f}} \cdot \sigma \bar{\sigma}^\nu x_f + b_f^2 y_f \sigma^\mu k_{\bar{f}} \cdot \bar{\sigma} \sigma^\nu \bar{y}_f \right. \\ & \left. - m_f a_f b_f \bar{x}_f \bar{\sigma}^\mu \sigma^\nu \bar{y}_f - m_f a_f b_f y_f \sigma^\mu \bar{\sigma}^\nu x_f \right). \end{aligned} \quad (6.20)$$

Next, we sum over the fermion helicity:

$$\sum_{\lambda_f, \lambda_{\bar{f}}} |\mathcal{M}|^2 = \frac{g^2}{c_W^2} \varepsilon_\mu \varepsilon_\nu^* \left(a_f^2 \text{Tr}[\bar{\sigma}^\mu k_{\bar{f}} \cdot \sigma \bar{\sigma}^\nu k_f \cdot \sigma] + b_f^2 \text{Tr}[\sigma^\mu k_{\bar{f}} \cdot \bar{\sigma} \sigma^\nu k_f \cdot \bar{\sigma}] \right. \\ \left. - m_f^2 a_f b_f \text{Tr}[\bar{\sigma}^\mu \sigma^\nu] - m_f^2 a_f b_f \text{Tr}[\sigma^\mu \bar{\sigma}^\nu] \right). \quad (6.21)$$

Averaging over the Z^0 polarization using

$$\frac{1}{3} \sum_{\lambda_Z} \varepsilon_\mu \varepsilon_\nu^* = \frac{1}{3} (-g_{\mu\nu} + p_\mu p_\nu / m_Z^2) \quad (6.22)$$

and applying eqs. (2.43)–(2.45), one gets:

$$\frac{1}{3} \sum_{\text{spins}} |\mathcal{M}|^2 = \frac{g^2}{3c_W^2} \left[(a_f^2 + b_f^2) \left(2k_f \cdot k_{\bar{f}} + 4k_f \cdot p k_{\bar{f}} \cdot p / m_Z^2 \right) + 12a_f b_f m_f^2 \right] \quad (6.23)$$

$$= \frac{2g^2}{3c_W^2} \left[(a_f^2 + b_f^2)(m_Z^2 - m_f^2) + 6a_f b_f m_f^2 \right], \quad (6.24)$$

where we have used eqs. (6.14) and (6.15). After the standard phase-space integration, we obtain the well-known result for the partial width of the Z^0 :

$$\Gamma(Z^0 \rightarrow f \bar{f}) = \frac{N_c^f}{16\pi m_Z} \left(1 - \frac{4m_f^2}{m_Z^2} \right)^{1/2} \left(\frac{1}{3} \sum_{\text{spins}} |\mathcal{M}|^2 \right) \quad (6.25)$$

$$= \frac{N_c^f g^2 m_Z}{24\pi c_W^2} \left(1 - \frac{4m_f^2}{m_Z^2} \right)^{1/2} \left[(a_f^2 + b_f^2) \left(1 - \frac{m_f^2}{m_Z^2} \right) + 6a_f b_f \frac{m_f^2}{m_Z^2} \right]. \quad (6.26)$$

Here we have also included a factor of N_c^f (equal to 1 for leptons and 3 for quarks) for the sum over colors. (Since the Z^0 is a color singlet, the color factor is simply equal to the dimension of the color representation of the outgoing fermions.)

6.3 Bhabha scattering: $e^- e^+ \rightarrow e^- e^+$

In our next example, we consider the computation of Bhabha scattering in QED (that is, we consider photon exchange but neglect Z^0 -exchange) [72]. **Bhabha scattering has also been computed using two-component spinors in [62].** We denote the initial state electron and positron momenta and helicities by (p_1, λ_1) and (p_2, λ_2) and the final state electron and positron momenta and helicities by (p_3, λ_3) and (p_4, λ_4) , respectively. Neglecting the electron mass, we have in terms of the usual Mandelstam variables s, t, u :

$$p_1 \cdot p_2 = p_3 \cdot p_4 \equiv \frac{1}{2}s, \quad (6.27)$$

$$p_1 \cdot p_3 = p_2 \cdot p_4 \equiv -\frac{1}{2}t, \quad (6.28)$$

$$p_1 \cdot p_4 = p_2 \cdot p_3 \equiv -\frac{1}{2}u, \quad (6.29)$$

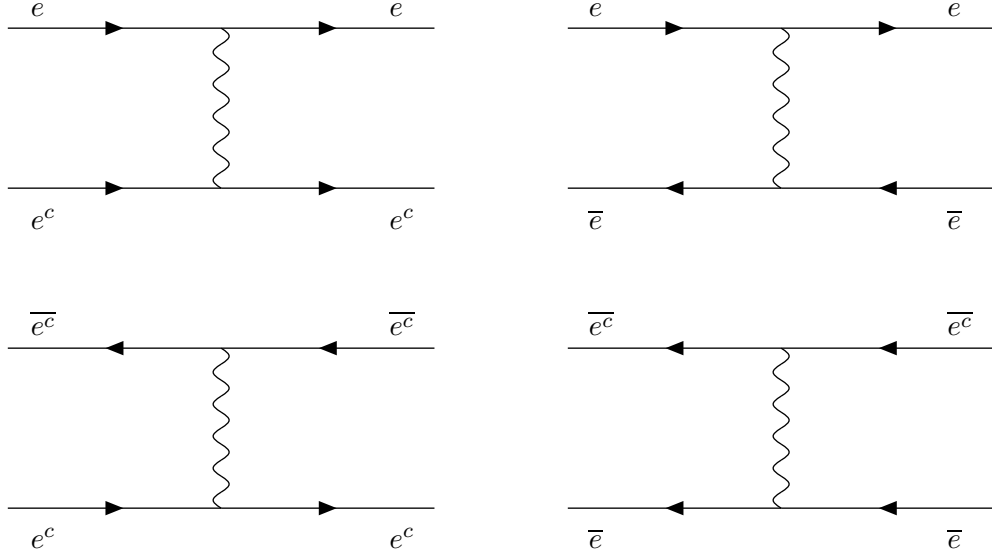


Figure 30: Tree-level t -channel Feynman diagrams for $e^-e^+ \rightarrow e^-e^+$, with the external lines labeled according to the two-component field names. The momentum flow of the external particles is from left to right.

and $p_i^2 = 0$ for $i = 1, \dots, 4$. There are eight distinct Feynman diagrams. First, there are four s -channel diagrams, as shown in Fig. 27 with amplitudes that follow from the Feynman rules of Fig. 25 (more generally, see Fig. 67 in Appendix H):

$$i\mathcal{M}_s = \left(\frac{-ig^{\mu\nu}}{s} \right) \left[(-ie x_1 \sigma_\mu \bar{y}_2)(ie y_3 \sigma_\nu \bar{x}_4) + (-ie \bar{y}_1 \bar{\sigma}_\mu x_2)(ie y_3 \sigma_\nu \bar{x}_4) \right. \\ \left. + (-ie x_1 \sigma_\mu \bar{y}_2)(ie \bar{x}_3 \bar{\sigma}_\nu y_4) + (-ie \bar{y}_1 \bar{\sigma}_\mu x_2)(ie \bar{x}_3 \bar{\sigma}_\nu y_4) \right], \quad (6.30)$$

where $x_i \equiv x(\vec{p}_i, \lambda_i)$ and $y_i \equiv y(\vec{p}_i, \lambda_i)$, for $i = 1, 4$. The photon propagator in Feynman gauge is $-ig^{\mu\nu}/(p_1 + p_2)^2 = -ig^{\mu\nu}/s$. Here, we have chosen to follow the fermion lines in the order 1, 2, 3, 4. This dictates in each term the use of either the $\bar{\sigma}$ or σ forms of the Feynman rules of Fig. 25. One can group the terms of eq. (6.30) together more compactly:

$$i\mathcal{M}_s = e^2 \left(\frac{-ig^{\mu\nu}}{s} \right) (x_1 \sigma_\mu \bar{y}_2 + \bar{y}_1 \bar{\sigma}_\mu x_2) (y_3 \sigma_\nu \bar{x}_4 + \bar{x}_3 \bar{\sigma}_\nu y_4). \quad (6.31)$$

There are also four t -channel diagrams, as shown in Fig. 30. The corresponding amplitudes for these four diagrams can be written:

$$i\mathcal{M}_t = (-1)e^2 \left(\frac{-ig^{\mu\nu}}{t} \right) (x_1 \sigma_\mu \bar{x}_3 + \bar{y}_1 \bar{\sigma}_\mu y_3) (x_2 \sigma_\nu \bar{x}_4 + \bar{y}_2 \bar{\sigma}_\nu y_4). \quad (6.32)$$

Here, the overall factor of (-1) comes from Fermi-Dirac statistics, since the external fermion wave functions are written in an odd permutation $(1, 3, 2, 4)$ of the original order $(1, 2, 3, 4)$ established by the first term in eq. (6.30).

Fierzing each term using eqs. (2.55)–(2.57), and using eqs. (2.47) and (2.48), the total

amplitude can be written as:

$$\begin{aligned}\mathcal{M} = \mathcal{M}_s + \mathcal{M}_t = 2e^2 & \left[\frac{1}{s}(x_1 y_3)(\bar{y}_2 \bar{x}_4) + \frac{1}{s}(\bar{y}_1 \bar{x}_3)(x_2 y_4) + \left(\frac{1}{s} + \frac{1}{t}\right)(\bar{y}_1 \bar{x}_4)(x_2 y_3) \right. \\ & \left. + \left(\frac{1}{s} + \frac{1}{t}\right)(x_1 y_4)(\bar{y}_2 \bar{x}_3) - \frac{1}{t}(x_1 x_2)(\bar{x}_3 \bar{x}_4) - \frac{1}{t}(\bar{y}_1 \bar{y}_2)(y_3 y_4) \right].\end{aligned}\quad (6.33)$$

Squaring this amplitude and summing over spins, all of the cross-terms will vanish in the $m_e \rightarrow 0$ limit. This is because each cross term will have an x or an \bar{x} for some electron or positron combined with a y or a \bar{y} for the same particle, and the corresponding spin sum is proportional to m_e [see eqs. (3.58) and (3.59)]. Hence, summing over final state spins and averaging over initial state spins, the end result contains only the sum of the squares of the six terms in eq. (6.33):

$$\begin{aligned}\frac{1}{4} \sum_{\text{spins}} |\mathcal{M}|^2 = e^4 \sum_{\lambda_1, \lambda_2, \lambda_3, \lambda_4} & \left\{ \frac{1}{s^2} [(x_1 y_3)(\bar{y}_3 \bar{x}_1)(\bar{y}_2 \bar{x}_4)(x_4 y_2) + (\bar{y}_1 \bar{x}_3)(x_3 y_1)(x_2 y_4)(\bar{y}_4 \bar{x}_2)] \right. \\ & + \left(\frac{1}{s} + \frac{1}{t}\right)^2 [(\bar{y}_1 \bar{x}_4)(x_4 y_1)(x_2 y_3)(\bar{y}_3 \bar{x}_2) + (x_1 y_4)(\bar{y}_4 \bar{x}_1)(\bar{y}_2 \bar{x}_3)(x_3 y_2)] \\ & \left. + \frac{1}{t^2} [(x_1 x_2)(\bar{x}_2 \bar{x}_1)(\bar{x}_3 \bar{x}_4)(x_4 x_3) + (\bar{y}_1 \bar{y}_2)(y_2 y_1)(y_3 y_4)(\bar{y}_4 \bar{y}_3)] \right\}.\end{aligned}\quad (6.34)$$

Here we have used eq. (2.30) to get the complex square of the fermion bilinears. Performing these spin sums using eqs. (3.56) and (3.57) and using the trace identities eq. (A.3):

$$\begin{aligned}\frac{1}{4} \sum_{\text{spins}} |\mathcal{M}|^2 &= 8e^4 \left[\frac{p_2 \cdot p_4 p_1 \cdot p_3}{s^2} + \frac{p_1 \cdot p_2 p_3 \cdot p_4}{t^2} + \left(\frac{1}{s} + \frac{1}{t}\right)^2 p_1 \cdot p_4 p_2 \cdot p_3 \right] \\ &= 2e^4 \left[\frac{t^2}{s^2} + \frac{s^2}{t^2} + \left(\frac{u}{s} + \frac{u}{t}\right)^2 \right].\end{aligned}\quad (6.35)$$

Thus, the differential cross section for Bhabha scattering is given by:

$$\frac{d\sigma}{dt} = \frac{1}{16\pi s^2} \left(\frac{1}{4} \sum_{\text{spins}} |\mathcal{M}|^2 \right) = \frac{2\pi\alpha^2}{s^2} \left[\frac{t^2}{s^2} + \frac{s^2}{t^2} + \left(\frac{u}{s} + \frac{u}{t}\right)^2 \right].\quad (6.36)$$

This agrees with the result of, for example, problem 5.2 of ref. [76].

6.4 Polarized Muon Decay

So far we have only treated cases where the initial state fermion spins are averaged and the final state spins are summed. In the case of the polarized decay of a particle or polarized scattering we must project out the appropriate polarization of the particles in the spin sums. This is achieved by replacing the spin sums given in eqs. (3.56)-(3.59) by the corresponding polarized spin projections eqs. (3.31)-(3.34). As an example, we consider the decay of a polarized muon. Polarized muon decay has also been computed using two-component spinors in [62], however with an effective four-fermion interaction.

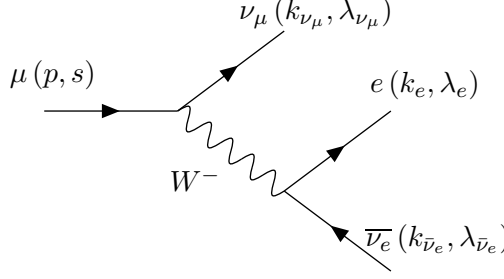


Figure 31: Feynman diagram for electroweak muon decay.

In Fig. 31, we show the single leading order Feynman diagram for muon decay, including the definition of the momenta. We denote the mass of the muon by m_μ , and neglect the electron mass. We shall assume the muon is polarized with a (contravariant) spin four-vector³¹

$$s^\rho = (0; 0, 0, 1), \quad (6.37)$$

along the z -axis in the muon rest frame. The amplitude is then given by

$$i\mathcal{M} = \left(\frac{-ig}{\sqrt{2}} \right)^2 (\bar{x}_{\nu_\mu} \bar{\sigma}_\rho x_\mu) (\bar{x}_e \bar{\sigma}_\tau y_{\bar{\nu}_e}) \left(\frac{-ig^{\rho\tau}}{D_W} \right), \quad (6.38)$$

where $D_W = (p - k_{\nu_\mu})^2 - M_W^2$ is the denominator of the W -boson propagator. Here $x_\mu \equiv x(\vec{p}, s)$ for the spin-polarized initial state muon, and $\bar{x}_{\nu_\mu} \equiv \bar{x}(\vec{k}_{\nu_\mu}, \lambda_{\nu_\mu})$, $\bar{x}_e \equiv \bar{x}(\vec{k}_e, \lambda_e)$, and $y_{\bar{\nu}_e} \equiv y(\vec{k}_{\bar{\nu}_e}, \lambda_{\bar{\nu}_e})$. Squaring the amplitude using eq. (2.32), we obtain

$$|\mathcal{M}|^2 = \frac{g^4}{4D_W^2} (\bar{x}_{\nu_\mu} \bar{\sigma}^\rho x_\mu) (\bar{x}_\mu \bar{\sigma}^\tau x_{\nu_\mu}) (\bar{x}_e \bar{\sigma}_\rho y_{\bar{\nu}_e}) (\bar{y}_{\bar{\nu}_e} \bar{\sigma}_\tau x_e) \quad (6.39)$$

Summing over the neutrino and electron spins using eqs. (3.56)-(3.57), and using eq. (3.44) for the muon spin yields:

$$\sum_{\lambda_{\nu_\mu} \lambda_e \lambda_{\bar{\nu}_e}} |\mathcal{M}|^2 = \frac{g^4}{8D_W^2} \text{Tr}[k_{\nu_\mu} \cdot \sigma \bar{\sigma}^\rho (p \cdot \sigma - m_\mu s \cdot \sigma) \bar{\sigma}^\tau] \text{Tr}[k_e \cdot \sigma \bar{\sigma}_\rho k_{\bar{\nu}_e} \cdot \sigma \bar{\sigma}_\tau], \quad (6.40)$$

$$= \frac{2g^4}{D_W^2} k_e \cdot k_{\nu_\mu} k_{\bar{\nu}_e} \cdot (p - m_\mu s). \quad (6.41)$$

To obtain the second line we have used the trace identity eq. (2.44) twice; note that the resulting terms linear in the antisymmetric tensor do not contribute, but the term quadratic in the antisymmetric tensor does.

The differential decay amplitude is now given by

$$d\Gamma = \frac{1}{2m_\mu} |\mathcal{M}|^2 \frac{d^3 \vec{k}_e}{(2\pi)^3 2E_e} \frac{d^3 \vec{k}_{\bar{\nu}_e}}{(2\pi)^3 2E_{\bar{\nu}_e}} \frac{d^3 \vec{k}_{\nu_\mu}}{(2\pi)^3 2E_{\nu_\mu}} (2\pi)^4 \delta^4(p - k_e - k_{\bar{\nu}_e} - k_{\nu_\mu}), \quad (6.42)$$

³¹Throughout this subsection μ and ν are particle labels and not Lorentz vector indices. Instead we use ρ, τ .

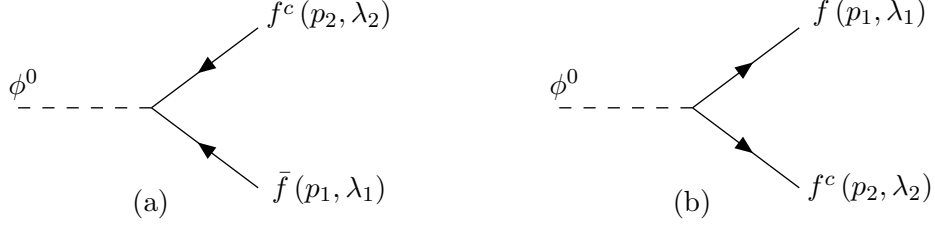


Figure 32: The Feynman diagrams for the decays $\phi^0 \rightarrow f\bar{f}$, where $\phi^0 = h^0, H^0, A^0$ are the neutral Higgs scalar bosons of minimal supersymmetry, and f is a Standard Model quark or lepton, and \bar{f} is the corresponding antiparticle. We have labeled the external fermions according to the two-component field names.

where E_i , $i = e, \bar{\nu}_e, \nu_\mu$ are the energies of the final state particles in the muon rest frame. In the following we shall neglect both the electron mass and the momentum in the W -propagator compared to the W -boson mass, so $D_W \rightarrow -M_W^2$. We can now use the following identity to integrate over the neutrino momenta [77]

$$\int \frac{d^3\vec{k}_{\bar{\nu}_e}}{(2\pi)^3 2E_{\bar{\nu}_e}} \frac{d^3\vec{k}_{\nu_\mu}}{(2\pi)^3 2E_{\nu_\mu}} (2\pi)^4 \delta^4(q - k_{\bar{\nu}_e} - k_{\nu_\mu}) k_{\bar{\nu}_e}^\rho k_{\nu_\mu}^\tau = \frac{1}{96\pi} (q^2 g^{\rho\tau} + 2q^\rho q^\tau), \quad (6.43)$$

where $q = p - k_e$. It follows that

$$d\Gamma = \frac{g^4}{1536\pi^4 m_\mu M_W^4} [q^2 k_e \cdot (p - m_\mu s) + 2q \cdot k_e q \cdot (p - m_\mu s)] \frac{d^3\vec{k}_e}{E_e} \quad (6.44)$$

In the muon rest frame $k_e = E_e(1; \cos\phi \sin\theta, \sin\phi \sin\theta, \cos\theta)$, so that $q^2 = m_\mu^2 - 2E_e m_\mu$ and $k_e \cdot (p - m_\mu s) = m_\mu E_e(1 + \cos\theta)$ and $q \cdot k_e = m_\mu E_e$ and $q \cdot (p - m_\mu s) = m_\mu(m_\mu - E_e - E_e \cos\theta)$. Noting that the maximum energy of the electron is $m_\mu/2$ (when the neutrino and antineutrino both recoil in the opposite direction), we obtain

$$\frac{d\Gamma}{d(\cos\theta)} = \frac{g^4 m_\mu^2}{768\pi^3 M_W^4} \int_0^{m_\mu/2} dE_e E_e^2 \left[3 - \frac{4E_e}{m_\mu} + \left(1 - \frac{4E_e}{m_\mu} \right) \cos\theta \right] \quad (6.45)$$

$$= \frac{g^4 m_\mu^5}{12288\pi^3 M_W^4} \left(1 - \frac{1}{3} \cos\theta \right) \quad (6.46)$$

in agreement with ref. [77].

6.5 Neutral Higgs boson decays $\phi^0 \rightarrow f\bar{f}$, for $\phi^0 = h^0, H^0, A^0$ in supersymmetry

In this subsection, we consider the decays of the neutral Higgs scalar bosons $\phi^0 = h^0, H^0$, and A^0 of minimal supersymmetry into Standard Model fermion-antifermion pairs. The relevant tree-level Feynman diagrams are shown in Fig. 32. The final state fermion is assigned four-momentum p_1 and polarization λ_1 , and the antifermion is assigned four-momentum p_2 and polarization λ_2 . We will first work out the case that f is a charge $-1/3$ quark or a charged lepton, and later

note the simple change needed for charge $+2/3$ quarks. Then the Feynman rules of Figure 70 of Appendix I tell us that the resulting amplitudes are:

$$i\mathcal{M}_a = \frac{i}{\sqrt{2}} Y_f k_{d\phi^0}^* y_1 y_2, \quad (6.47)$$

$$i\mathcal{M}_b = \frac{i}{\sqrt{2}} Y_f k_{d\phi^0} \bar{x}_1 \bar{x}_2. \quad (6.48)$$

Here Y_f is the Yukawa coupling of the fermion, $k_{d\phi^0}$ is the Higgs mixing parameter from eq. (I.6), and the external wave functions are denoted $x_1 \equiv x(\vec{p}_1, \lambda_1)$, $y_1 \equiv y(\vec{p}_1, \lambda_1)$ for the fermion and $x_2 \equiv x(\vec{p}_2, \lambda_2)$, $y_2 \equiv y(\vec{p}_2, \lambda_2)$ for the antifermion. Squaring the total amplitude $i\mathcal{M} = i\mathcal{M}_a + i\mathcal{M}_b$ using eq. (2.30) results in:

$$|\mathcal{M}|^2 = \frac{1}{2} |Y_f|^2 \left[|k_{d\phi^0}|^2 (y_1 y_2 \bar{y}_2 \bar{y}_1 + \bar{x}_1 \bar{x}_2 x_2 x_1) + (k_{d\phi^0})^2 \bar{x}_1 \bar{x}_2 \bar{y}_2 \bar{y}_1 + (k_{d\phi^0}^*)^2 y_1 y_2 x_2 x_1 \right]. \quad (6.49)$$

Summing over the final-state antifermion spin using eqs. (3.56)-(3.59) gives:

$$\sum_{\lambda_2} |\mathcal{M}|^2 = \frac{1}{2} |Y_f|^2 \left[|k_{d\phi^0}|^2 (y_1 p_2 \cdot \sigma \bar{y}_1 + \bar{x}_1 p_2 \cdot \bar{\sigma} x_1) - (k_{d\phi^0})^2 m_f \bar{x}_1 \bar{y}_1 - (k_{d\phi^0}^*)^2 m_f y_1 x_1 \right]. \quad (6.50)$$

Summing over the fermion spins in the same way yields:

$$\sum_{\lambda_1, \lambda_2} |\mathcal{M}|^2 = \frac{1}{2} |Y_f|^2 \left\{ |k_{d\phi^0}|^2 (\text{Tr}[p_2 \cdot \sigma p_1 \cdot \bar{\sigma}] + \text{Tr}[p_2 \cdot \bar{\sigma} p_1 \cdot \sigma]) - 2(k_{d\phi^0})^2 m_f^2 - 2(k_{d\phi^0}^*)^2 m_f^2 \right\} \quad (6.51)$$

$$= |Y_f|^2 \left\{ 2|k_{d\phi^0}|^2 p_1 \cdot p_2 - 2\text{Re}[(k_{d\phi^0})^2] m_f^2 \right\} \quad (6.52)$$

$$= |Y_f|^2 \left\{ |k_{d\phi^0}|^2 (m_{\phi^0}^2 - 2m_f^2) - 2\text{Re}[(k_{d\phi^0})^2] m_f^2 \right\}, \quad (6.53)$$

where we have used the trace identity eq. (2.43) to obtain the second equality. The corresponding expression for charge $+2/3$ quarks can be obtained by simply replacing $k_{d\phi^0}$ with $k_{u\phi^0}$. The total decay rates now follow from integration over phase space [78]

$$\Gamma(\phi^0 \rightarrow f\bar{f}) = \frac{N_c^f}{16\pi m_{\phi^0}} \left(1 - 4m_f^2/m_{\phi^0}^2\right)^{1/2} \sum_{\lambda_1, \lambda_2} |\mathcal{M}|^2. \quad (6.54)$$

The factor of $N_c^f = 3$ for quarks and 1 for leptons comes from the sum over colors.

Results for special cases are obtained by putting in the relevant values for the couplings and the mixing parameters including eqs. (I.5) and (I.6). In particular, for the CP-even Higgs bosons h^0 and H^0 , $k_{d\phi^0}$ and $k_{u\phi^0}$ are real, so one obtains:

$$\Gamma(h^0 \rightarrow b\bar{b}) = \frac{3}{16\pi} Y_b^2 \sin^2 \alpha m_{h^0} (1 - 4m_b^2/m_{h^0}^2)^{3/2}, \quad (6.55)$$

$$\Gamma(h^0 \rightarrow c\bar{c}) = \frac{3}{16\pi} Y_c^2 \cos^2 \alpha m_{h^0} (1 - 4m_c^2/m_{h^0}^2)^{3/2}, \quad (6.56)$$

$$\Gamma(h^0 \rightarrow \tau^+ \tau^-) = \frac{1}{16\pi} Y_\tau^2 \sin^2 \alpha m_{h^0} (1 - 4m_\tau^2/m_{h^0}^2)^{3/2}, \quad (6.57)$$

$$\Gamma(H^0 \rightarrow t\bar{t}) = \frac{3}{16\pi} Y_t^2 \sin^2 \alpha m_{H^0} (1 - 4m_t^2/m_{H^0}^2)^{3/2}, \quad (6.58)$$

$$\Gamma(H^0 \rightarrow b\bar{b}) = \frac{3}{16\pi} Y_b^2 \cos^2 \alpha m_{H^0} (1 - 4m_b^2/m_{H^0}^2)^{3/2}, \quad (6.59)$$

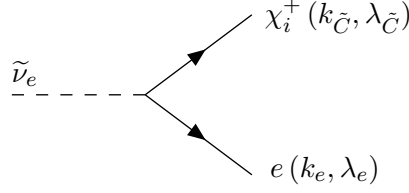


Figure 33: The Feynman diagram for $\tilde{\nu}_e \rightarrow \tilde{C}_i^+ e^-$ in the MSSM.

etc., which check with the expressions in Appendix B of ref. [79]. For the pseudo-scalar Higgs boson A^0 , the mixing parameters $k_{uA^0} = i \cos \beta_0$ and $k_{dA^0} = i \sin \beta_0$ are purely imaginary, so

$$\Gamma(A^0 \rightarrow t\bar{t}) = \frac{3}{16\pi} Y_t^2 \cos^2 \beta_0 m_{A^0} (1 - 4m_t^2/m_{A^0}^2)^{1/2}, \quad (6.60)$$

$$\Gamma(A^0 \rightarrow b\bar{b}) = \frac{3}{16\pi} Y_b^2 \sin^2 \beta_0 m_{A^0} (1 - 4m_b^2/m_{A^0}^2)^{1/2}, \quad (6.61)$$

$$\Gamma(A^0 \rightarrow \tau^+ \tau^-) = \frac{1}{16\pi} Y_\tau^2 \sin^2 \beta_0 m_{A^0} (1 - 4m_\tau^2/m_{A^0}^2)^{1/2}. \quad (6.62)$$

Note that the differing kinematic factors for the pseudo-scalar decays came about because of the different relative sign between the two Feynman diagrams. For example, in the case of $h^0 \rightarrow b\bar{b}$, the matrix element is

$$i\mathcal{M} = \frac{i}{\sqrt{2}} Y_b \sin \alpha (y_1 y_2 + \bar{x}_1 \bar{x}_2), \quad (6.63)$$

while for $A^0 \rightarrow b\bar{b}$, it is

$$i\mathcal{M} = \frac{1}{\sqrt{2}} Y_b \sin \beta_0 (y_1 y_2 - \bar{x}_1 \bar{x}_2). \quad (6.64)$$

The differing sign follows from the imaginary pseudo-scalar Lagrangian coupling, which is complex conjugated in the second diagram.

6.6 Sneutrino decay $\tilde{\nu}_e \rightarrow \tilde{C}_i^+ e^-$

Next we consider the process of sneutrino decay $\tilde{\nu}_e \rightarrow \tilde{C}_i^+ e^-$ in minimal supersymmetry. Because only the left-handed electron can couple to the chargino and sneutrino (with the excellent approximation that the electron Yukawa coupling is 0), there is just one Feynman diagram, shown in Fig. 33. The external wave functions of the electron and chargino are denoted as $x_e \equiv x(\vec{k}_e, \lambda_e)$, and $x_{\tilde{C}} \equiv x(\vec{k}_{\tilde{C}}, \lambda_{\tilde{C}})$, respectively. From the corresponding Feynman rule given in Fig. 75 of Appendix I, the amplitude is:

$$i\mathcal{M} = -igV_{i1} \bar{x}_{\tilde{C}} \bar{x}_e, \quad (6.65)$$

where V_{ij} is one of the two matrices used to diagonalize the chargino masses [*cf.* eq. (I.21)]. Squaring this using eq. (2.30) yields:

$$|\mathcal{M}|^2 = g^2 |V_{i1}|^2 (\bar{x}_{\tilde{C}} \bar{x}_e)(x_e x_{\tilde{C}}). \quad (6.66)$$

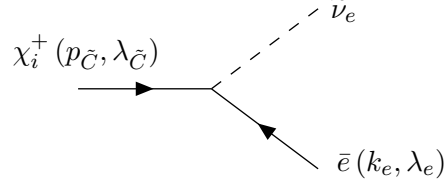


Figure 34: The Feynman diagram for $\tilde{C}_i^+ \rightarrow \tilde{\nu}_e e^+$ in the MSSM.

Now summing over the electron and chargino spin polarizations using eq. (3.56) yields

$$\sum_{\lambda_e, \lambda_{\tilde{C}}} |\mathcal{M}|^2 = g^2 |V_{i1}|^2 \text{Tr}[k_e \cdot \bar{\sigma} k_{\tilde{C}} \cdot \sigma] = 2g^2 |V_{i1}|^2 k_e \cdot k_{\tilde{C}} = g^2 |V_{i1}|^2 (m_{\tilde{\nu}_e}^2 - m_{\tilde{C}_i}^2), \quad (6.67)$$

where we have used $2k_e \cdot k_{\tilde{C}} = m_{\tilde{\nu}_e}^2 - m_{\tilde{C}_i}^2$, neglecting the electron mass. Therefore, after integrating over phase space in the standard way, the decay width is:

$$\Gamma(\tilde{\nu}_e \rightarrow \tilde{C}_i^+ e^-) = \frac{1}{16\pi m_{\tilde{\nu}_e}} \left(1 - \frac{m_{\tilde{C}_i}^2}{m_{\tilde{\nu}_e}^2}\right) \left[\sum_{\lambda_e, \lambda_{\tilde{C}}} |\mathcal{M}|^2 \right] = \frac{g^2}{16\pi} |V_{i1}|^2 m_{\tilde{\nu}_e} \left(1 - \frac{m_{\tilde{C}_i}^2}{m_{\tilde{\nu}_e}^2}\right)^2, \quad (6.68)$$

which agrees with ref. [80] and eq. (3.8) in ref. [48].

6.7 Chargino Decay $\tilde{C}_i^+ \rightarrow \tilde{\nu}_e e^+$

Here again, there is just one Feynman diagram (neglecting the electron mass in the Yukawa coupling) shown in Fig. 34. The external wave functions for the chargino and the positron are denoted by $x_{\tilde{C}} \equiv x(\vec{p}_{\tilde{C}}, \lambda_{\tilde{C}})$ and $y_e \equiv y(\vec{k}_e, \lambda_e)$, respectively. The fermion momenta and helicities are denoted as in Fig. 34. As in the previous example, the amplitude can be directly determined using the Feynman rule given in Fig. 75 in Appendix I:

$$\mathcal{M} = -igV_{i1}^* x_{\tilde{C}} y_e. \quad (6.69)$$

Squaring this using eq. (2.30) yields:

$$|\mathcal{M}|^2 = g^2 |V_{i1}|^2 (x_{\tilde{C}} y_e) (\bar{y}_e \bar{x}_{\tilde{C}}). \quad (6.70)$$

Summing over the electron helicity and averaging over the chargino helicity using eqs. (3.56) and (3.57) we obtain:

$$\frac{1}{2} \sum_{\lambda_e, \lambda_{\tilde{C}}} |\mathcal{M}|^2 = \frac{1}{2} g^2 |V_{i1}|^2 \text{Tr}[k_e \cdot \sigma p_{\tilde{C}} \cdot \bar{\sigma}] = g^2 |V_{i1}|^2 k_e \cdot p_{\tilde{C}} = \frac{g^2}{2} |V_{i1}|^2 (m_{\tilde{C}_i}^2 - m_{\tilde{\nu}_e}^2). \quad (6.71)$$

So the decay width is, neglecting the electron mass:

$$\Gamma(\tilde{C}_i^+ \rightarrow \tilde{\nu}_e e^+) = \frac{1}{16\pi m_{\tilde{C}_i}} \left(1 - \frac{m_{\tilde{\nu}_e}^2}{m_{\tilde{C}_i}^2}\right) \left(\frac{1}{2} \sum_{\lambda_e, \lambda_{\tilde{C}}} |\mathcal{M}|^2 \right) = \frac{g^2}{32\pi} |V_{i1}|^2 m_{\tilde{C}_i} \left(1 - \frac{m_{\tilde{\nu}_e}^2}{m_{\tilde{C}_i}^2}\right)^2, \quad (6.72)$$

which agrees with ref. [80].

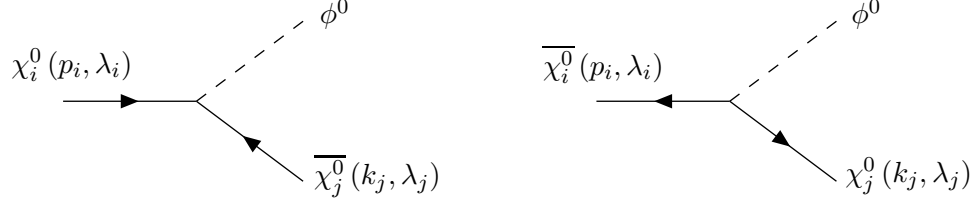


Figure 35: The Feynman diagrams for $\tilde{N}_i \rightarrow \tilde{N}_j \phi^0$ in the MSSM.

6.8 Neutralino Decays $\tilde{N}_i \rightarrow \phi^0 \tilde{N}_j$, for $\phi^0 = h^0, H^0, A^0$

Next we consider the decay of a neutralino to a lighter neutralino and neutral Higgs scalar boson $\phi^0 = h^0, H^0$, or A^0 . The two tree-level Feynman graphs are shown in Fig. 35, where we have also labeled the momenta and helicities. We denote the masses for the neutralinos and the Higgs boson as $m_{\tilde{N}_i}$, $m_{\tilde{N}_j}$, and m_{ϕ^0} . Using the Feynman rules of Fig. 74, the amplitudes are respectively given by

$$i\mathcal{M}_1 = -iY x_i y_j, \quad (6.73)$$

$$i\mathcal{M}_2 = -iY^* \bar{y}_i \bar{x}_j, \quad (6.74)$$

where the coupling $Y \equiv Y^{\phi^0 \chi_i^0 \chi_j^0}$ is defined in eq. (I.25), and the external wave functions are $x_i \equiv x(\vec{p}_i, \lambda_i)$, $\bar{y}_i \equiv \bar{y}(\vec{p}_i, \lambda_i)$, $y_j \equiv y(\vec{k}_j, \lambda_j)$, and $\bar{x}_j \equiv \bar{x}(\vec{k}_j, \lambda_j)$.

Taking the square of the total matrix element using eq. (2.30) gives:

$$|\mathcal{M}|^2 = |Y|^2 (x_i y_j \bar{y}_j \bar{x}_i + \bar{y}_i \bar{x}_j x_j y_i) + Y^2 x_i y_j x_j y_i + Y^{*2} \bar{y}_i \bar{x}_j \bar{y}_j \bar{x}_i. \quad (6.75)$$

Now summing over the final-state neutralino spins using eqs. (3.56)-(3.59) yields

$$\sum_{\lambda_j} |\mathcal{M}|^2 = |Y|^2 (x_i k_j \cdot \sigma \bar{x}_i + \bar{y}_i k_j \cdot \bar{\sigma} y_i) - Y^2 m_{\tilde{N}_j} x_i y_i - Y^{*2} m_{\tilde{N}_j} \bar{y}_i \bar{x}_i. \quad (6.76)$$

Averaging over the initial-state neutralino spins in the same way gives

$$\frac{1}{2} \sum_{\lambda_i, \lambda_j} |\mathcal{M}|^2 = \frac{1}{2} |Y|^2 (\text{Tr}[k_j \cdot \sigma p_i \cdot \bar{\sigma}] + \text{Tr}[k_j \cdot \bar{\sigma} p_i \cdot \sigma]) + \text{Re}[Y^2] m_{\tilde{N}_i} m_{\tilde{N}_j} \text{Tr}[1] \quad (6.77)$$

$$= 2|Y|^2 p_i \cdot k_j + 2\text{Re}[Y^2] m_{\tilde{N}_i} m_{\tilde{N}_j} \quad (6.78)$$

$$= |Y|^2 (m_{\tilde{N}_i}^2 + m_{\tilde{N}_j}^2 - m_{\phi^0}^2) + 2\text{Re}[Y^2] m_{\tilde{N}_i} m_{\tilde{N}_j}, \quad (6.79)$$

where we have used eq. (2.43) to obtain the second equality. The total decay rate is therefore

$$\Gamma(\tilde{N}_i \rightarrow \phi^0 \tilde{N}_j) = \frac{1}{16\pi m_{\tilde{N}_i}^3} \lambda^{1/2}(m_{\tilde{N}_i}^2, m_{\phi^0}^2, m_{\tilde{N}_j}^2) \left(\frac{1}{2} \sum_{\lambda_i, \lambda_j} |\mathcal{M}|^2 \right) \quad (6.80)$$

$$= \frac{m_{\tilde{N}_i}}{16\pi} \lambda^{1/2}(1, r_\phi, r_j) \left[|Y^{\phi^0 \chi_i^0 \chi_j^0}|^2 (1 + r_j - r_\phi) + 2\text{Re}[(Y^{\phi^0 \chi_i^0 \chi_j^0})^2] \sqrt{r_j} \right], \quad (6.81)$$

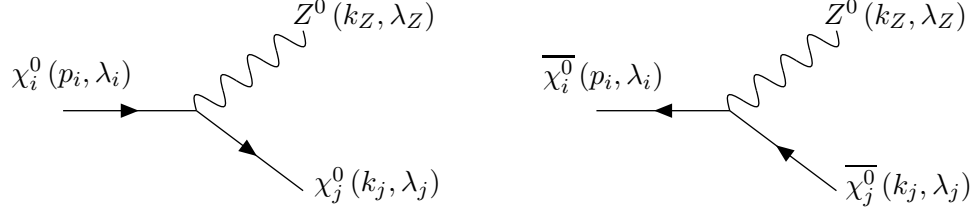


Figure 36: The Feynman diagrams for $\tilde{N}_i \rightarrow \tilde{N}_j Z^0$ in the MSSM.

where $r_j \equiv m_{\tilde{N}_j}^2/m_{\tilde{N}_i}^2$ and $r_\phi \equiv m_{\phi^0}^2/m_{\tilde{N}_i}^2$. The results for $\phi^0 = h^0, H^0, A^0$ can now be obtained by using eqs. (I.5) and (I.6) in eq. (I.25). In comparing eq. (6.81) with the original calculation in [81], it is helpful to employ eqs. (4.51) and (4.53) of [82]. The results agree.

6.9 $\tilde{N}_i \rightarrow Z^0 \tilde{N}_j$

For this two-body decay there are two tree-level Feynman diagrams, shown in Fig. 36 with the definitions of the helicities and the momenta. The two amplitudes are given by³²

$$i\mathcal{M}_1 = -i \frac{g}{c_W} \mathcal{O}_{ji}^{\prime\prime L} x_i \sigma^\mu \bar{x}_j \varepsilon_\mu^* \quad (6.82)$$

$$i\mathcal{M}_2 = i \frac{g}{c_W} \mathcal{O}_{ij}^{\prime\prime L} \bar{y}_i \bar{\sigma}^\mu y_j \varepsilon_\mu^* \quad (6.83)$$

where the external wave functions are $x_i = x(\vec{p}_i, \lambda_i)$, $\bar{y}_i = \bar{y}(\vec{p}_i, \lambda_i)$, $\bar{x}_j = \bar{x}(\vec{k}_j, \lambda_j)$, $y_j = y(\vec{k}_j, \lambda_j)$, and $\varepsilon_\mu^* = \varepsilon_\mu^*(\vec{k}_Z, \lambda_Z)$. Noting that $\mathcal{O}_{ji}^{\prime\prime L} = \mathcal{O}_{ij}^{\prime\prime L*}$ [see eq. (I.20)], and applying eqs. (2.31) and (2.32), we find that the matrix element squared is:

$$|\mathcal{M}|^2 = \frac{g^2}{c_W^2} \varepsilon_\mu^* \varepsilon_\nu \left[|\mathcal{O}_{ij}^{\prime\prime L}|^2 (x_i \sigma^\mu \bar{x}_j x_j \sigma^\nu \bar{x}_i + \bar{y}_i \bar{\sigma}^\mu y_j \bar{y}_j \bar{\sigma}^\nu y_i) \right. \quad (6.84)$$

$$\left. - (\mathcal{O}_{ij}^{\prime\prime L})^2 \bar{y}_i \bar{\sigma}^\mu y_j x_j \sigma^\nu \bar{x}_i - (\mathcal{O}_{ij}^{\prime\prime L*})^2 x_i \sigma^\mu \bar{x}_j \bar{y}_j \bar{\sigma}^\nu y_i \right] \quad (6.85)$$

Now summing over the final-state neutralino spin using eqs. (3.56)-(3.59) yields:

$$\sum_{\lambda_j} |\mathcal{M}|^2 = \frac{g^2}{c_W^2} \varepsilon_\mu^* \varepsilon_\nu \left[|\mathcal{O}_{ij}^{\prime\prime L}|^2 (x_i \sigma^\mu k_j \cdot \bar{\sigma} \sigma^\nu \bar{x}_i + \bar{y}_i \bar{\sigma}^\mu k_j \cdot \sigma \bar{\sigma}^\nu y_i) \right. \quad (6.86)$$

$$\left. + (\mathcal{O}_{ij}^{\prime\prime L})^2 m_{\tilde{N}_j} \bar{y}_i \bar{\sigma}^\mu \sigma^\nu \bar{x}_i + (\mathcal{O}_{ij}^{\prime\prime L*})^2 m_{\tilde{N}_j} x_i \sigma^\mu \bar{\sigma}^\nu y_i \right]. \quad (6.87)$$

Averaging over the initial-state neutralino spins in the same way gives

$$\frac{1}{2} \sum_{\lambda_i, \lambda_j} |\mathcal{M}|^2 = \frac{g^2}{2c_W^2} \varepsilon_\mu^* \varepsilon_\nu \left[|\mathcal{O}_{ij}^{\prime\prime L}|^2 \left(\text{Tr}[\sigma^\mu k_j \cdot \bar{\sigma} \sigma^\nu p_i \cdot \bar{\sigma}] + \text{Tr}[\bar{\sigma}^\mu k_j \cdot \sigma \bar{\sigma}^\nu p_i \cdot \sigma] \right) \right. \quad (6.88)$$

$$\left. - (\mathcal{O}_{ij}^{\prime\prime L})^2 m_{\tilde{N}_i} m_{\tilde{N}_j} \text{Tr}[\bar{\sigma}^\mu \sigma^\nu] - (\mathcal{O}_{ij}^{\prime\prime L*})^2 m_{\tilde{N}_i} m_{\tilde{N}_j} \text{Tr}[\sigma^\mu \bar{\sigma}^\nu] \right] \quad (6.89)$$

$$= \frac{2g^2}{c_W^2} \varepsilon_\mu^* \varepsilon_\nu \left\{ |\mathcal{O}_{ij}^{\prime\prime L}|^2 \left(k_j^\mu p_i^\nu + p_i^\mu k_j^\nu - p_i \cdot k_j g^{\mu\nu} \right) - \text{Re} \left[(\mathcal{O}_{ij}^{\prime\prime L})^2 \right] m_{\tilde{N}_i} m_{\tilde{N}_j} g^{\mu\nu} \right\}, \quad (6.90)$$

³²When comparing with the 4-component Feynman rule in ref. [48] note that $\mathcal{O}_{ij}^{\prime\prime L} = -\mathcal{O}_{ij}^{\prime\prime R*}$, c.f. eq. (I.20).

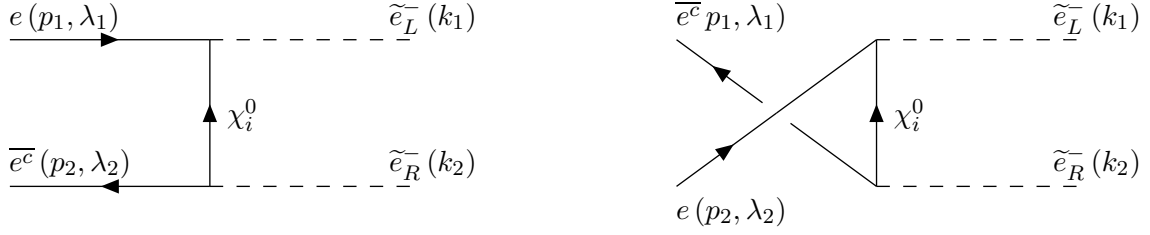


Figure 37: Feynman diagrams for $e^- e^- \rightarrow \tilde{e}_L^- \tilde{e}_R^-$.

where in the last equality we have applied eqs. (2.43)-(2.45). Now using

$$\sum_{\lambda_Z} \varepsilon^{\mu*} \varepsilon^\nu = -g^{\mu\nu} + k_Z^\mu k_Z^\nu / m_Z^2, \quad (6.91)$$

we obtain

$$\frac{1}{2} \sum_{\lambda_i, \lambda_j, \lambda_Z} |\mathcal{M}|^2 = \frac{2g^2}{c_W^2} \left\{ |\mathcal{O}_{ij}^{\prime\prime L}|^2 (-p_i \cdot k_j + 2p_i \cdot k_Z k_j \cdot k_Z / m_Z^2) + 3m_{\tilde{N}_i} m_{\tilde{N}_j} \text{Re}[(\mathcal{O}_{ij}^{\prime\prime L})^2] \right\} \quad (6.92)$$

and, noting that $2k_j \cdot k_Z = m_{\tilde{N}_i}^2 - m_{\tilde{N}_j}^2 - m_Z^2$, $2p_i \cdot k_j = m_{\tilde{N}_i}^2 + m_{\tilde{N}_j}^2 - m_Z^2$, and $2p_i \cdot k_Z = m_{\tilde{N}_i}^2 - m_{\tilde{N}_j}^2 + m_Z^2$, we get the total decay width

$$\Gamma(\tilde{N}_i \rightarrow Z^0 \tilde{N}_j) = \frac{1}{16\pi m_{\tilde{N}_i}^3} \lambda^{1/2}(m_{\tilde{N}_i}^2, m_Z^2, m_{\tilde{N}_j}^2) \left(\frac{1}{2} \sum_{\lambda_i, \lambda_j, \lambda_Z} |\mathcal{M}|^2 \right) \quad (6.93)$$

$$= \frac{g^2 m_{\tilde{N}_i}}{16\pi c_W^2} \lambda^{1/2}(1, r_Z, r_j) \left[|\mathcal{O}_{ij}^{\prime\prime L}|^2 (1 + r_j - 2r_Z + (1 - r_j)^2 / r_Z) + 6\text{Re}[(\mathcal{O}_{ij}^{\prime\prime L})^2] \sqrt{r_j} \right], \quad (6.94)$$

where

$$r_j \equiv m_{\tilde{N}_j}^2 / m_{\tilde{N}_i}^2, \quad \text{and} \quad r_Z \equiv m_Z^2 / m_{\tilde{N}_i}^2, \quad (6.95)$$

and the triangle kinematic function was defined in eq. (6.12). The result eq. (6.94) agrees with the original calculation in [81].

6.10 Selectron pair production in electron-electron collisions

6.10.1 $e^- e^- \rightarrow \tilde{e}_L^- \tilde{e}_R^-$

Here there are two Feynman graphs (neglecting the electron mass and Yukawa couplings), shown in Fig. 37. Note that these two graphs are related by interchange of the identical initial state electrons. Let the electrons have momenta p_1 and p_2 and the selectrons have momenta $k_{\tilde{e}_L}$ and $k_{\tilde{e}_R}$, so that $p_1^2 = p_2^2 = 0$; $k_1^2 = m_{\tilde{e}_L}^2$; $k_2^2 = m_{\tilde{e}_R}^2$; $s = (p_1 + p_2)^2 = (k_1 + k_2)^2$; $t = (k_1 - p_1)^2 = (k_2 - p_2)^2$; $u = (k_1 - p_2)^2 = (k_2 - p_1)^2$. The matrix element for the first graph, for each neutralino \tilde{N}_i exchanged in the t channel, is:

$$i\mathcal{M}_t = \left[i \frac{g}{\sqrt{2}} \left(N_{i2}^* + \frac{s_W}{c_W} N_{i1}^* \right) \right] \left[-i\sqrt{2}g \frac{s_W}{c_W} N_{i1} \right] x_1 \left[\frac{i(k_1 - p_1) \cdot \sigma}{(k_1 - p_1)^2 - m_{\tilde{N}_i}^2} \right] \bar{y}_2. \quad (6.96)$$

Here we have used the Feynman rules from Fig. 76. We employ the notation for the external wave functions $x_i = (\vec{p}_i, \lambda_i)$, $i = 1, 2$ and analogously for $y_i, \bar{x}_i, \bar{y}_i$. The matrix elements for the second (u -channel) graph are the same with the two incoming electrons exchanged, $e_1 \leftrightarrow e_2$:

$$i\mathcal{M}_u = (-1) \left[i \frac{g}{\sqrt{2}} \left(N_{i2}^* + \frac{s_W}{c_W} N_{i1}^* \right) \right] \left[-i\sqrt{2}g \frac{s_W}{c_W} N_{i1} \right] x_2 \left[\frac{i(k_1 - p_2) \cdot \sigma}{(k_1 - p_2)^2 - m_{\tilde{N}_i}^2} \right] \bar{y}_1. \quad (6.97)$$

Note that since we have written the fermion wave function spinors in the opposite order in \mathcal{M}_2 compared to \mathcal{M}_1 , there is a factor (-1) for Fermi-Dirac statistics. Alternatively, starting at the electron with momentum p_1 and using the Feynman rules as above, we can directly write:

$$i\mathcal{M}_u = \left[i \frac{g}{\sqrt{2}} \left(N_{i2}^* + \frac{s_W}{c_W} N_{i1}^* \right) \right] \left[-i\sqrt{2}g \frac{s_W}{c_W} N_{i1} \right] \bar{y}_1 \left[\frac{-i(k_1 - p_2) \cdot \bar{\sigma}}{(k_1 - p_2)^2 - m_{\tilde{N}_i}^2} \right] x_2. \quad (6.98)$$

This has no Fermi-Dirac factor (-1) because the wave function spinors are written in the same order as in \mathcal{M}_t . However, now the Feynman rule for the propagator has an extra minus sign, as can be seen in Fig. 3. We can also obtain eq. (6.98) from eq. (6.97) by using eq. (2.49). So we can write for the total amplitude:

$$\mathcal{M} = \mathcal{M}_t + \mathcal{M}_u = x_1 a \cdot \sigma \bar{y}_2 + \bar{y}_1 b \cdot \bar{\sigma} x_2, \quad (6.99)$$

where

$$a^\mu \equiv \frac{g^2 s_W}{c_W} (k_1^\mu - p_1^\mu) \sum_{i=1}^4 N_{i1} (N_{i2}^* + \frac{s_W}{c_W} N_{i1}^*) \frac{1}{t - m_{\tilde{N}_i}^2}, \quad (6.100)$$

$$b^\mu \equiv -\frac{g^2 s_W}{c_W} (k_1^\mu - p_2^\mu) \sum_{i=1}^4 N_{i1} (N_{i2}^* + \frac{s_W}{c_W} N_{i1}^*) \frac{1}{u - m_{\tilde{N}_i}^2}. \quad (6.101)$$

So, using eqs. (2.31) and (2.32):

$$|\mathcal{M}|^2 = (x_1 a \cdot \sigma \bar{y}_2) (y_2 a^* \cdot \sigma \bar{x}_1) + (\bar{y}_1 b \cdot \bar{\sigma} x_2) (\bar{x}_2 b^* \cdot \bar{\sigma} y_1) + (x_1 a \cdot \sigma \bar{y}_2) (\bar{x}_2 b^* \cdot \bar{\sigma} y_1) + (\bar{y}_1 b \cdot \bar{\sigma} x_2) (y_2 a^* \cdot \sigma \bar{x}_1). \quad (6.102)$$

Averaging over the initial state electron spins using eqs. (3.56)-(3.59), the a, b^* and a^*, b cross terms are proportional to m_e and can thus be neglected in our approximation. We get:

$$\frac{1}{4} \sum_{\lambda_1, \lambda_2} |\mathcal{M}|^2 = \frac{1}{4} \text{Tr}[a \cdot \sigma p_2 \cdot \bar{\sigma} a^* \cdot \sigma p_1 \cdot \bar{\sigma}] + \frac{1}{4} \text{Tr}[b \cdot \bar{\sigma} p_2 \cdot \sigma b^* \cdot \bar{\sigma} p_1 \cdot \sigma]. \quad (6.103)$$

These terms can be simplified using the identities:

$$\text{Tr}[(k_1 - p_1) \cdot \sigma p_2 \cdot \bar{\sigma} (k_1 - p_1) \cdot \sigma p_1 \cdot \bar{\sigma}] = \text{Tr}[(k_1 - p_2) \cdot \bar{\sigma} p_2 \cdot \sigma (k_1 - p_2) \cdot \bar{\sigma} p_1 \cdot \sigma] \quad (6.104)$$

$$= tu - m_{e_L}^2 m_{e_R}^2, \quad (6.105)$$

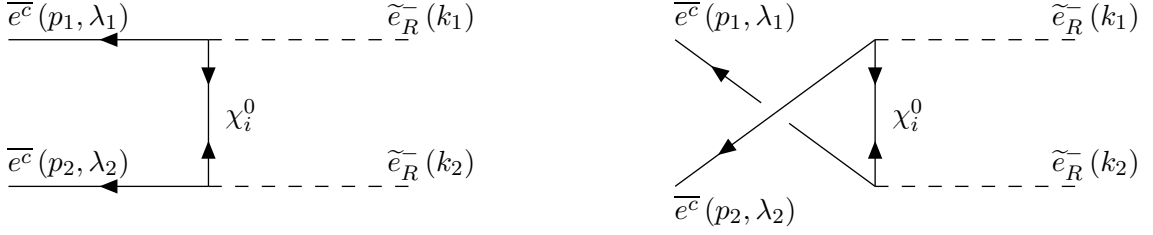


Figure 38: The two Feynman diagrams for $e^- e^- \rightarrow \tilde{e}_R^- \tilde{e}_R^-$ in the limit where $m_e \rightarrow 0$.

which follow from eq. (2.44) and (2.45), resulting in:

$$\frac{1}{4} \sum_{\lambda_1, \lambda_2} |\mathcal{M}|^2 = \frac{g^4 s_W^2}{4c_W^2} (tu - m_{\tilde{e}_L}^2 m_{\tilde{e}_R}^2) \sum_{i,j=1}^4 N_{j1} N_{i1}^* (N_{j2}^* + \frac{s_W}{c_W} N_{j1}^*) (N_{i2} + \frac{s_W}{c_W} N_{i1}) \left[\frac{1}{(t - m_{\tilde{N}_i}^2)(t - m_{\tilde{N}_j}^2)} + \frac{1}{(u - m_{\tilde{N}_i}^2)(u - m_{\tilde{N}_j}^2)} \right]. \quad (6.106)$$

To get the differential cross-section $d\sigma/dt$, multiply this by $1/(16\pi s^2)$:

$$\frac{d\sigma}{dt} = \frac{\pi \alpha^2}{4s_W^2 c_W^2} \left(\frac{tu - m_{\tilde{e}_L}^2 m_{\tilde{e}_R}^2}{s^2} \right) \sum_{i,j=1}^4 N_{j1} N_{i1}^* (N_{j2}^* + \frac{s_W}{c_W} N_{j1}^*) (N_{i2} + \frac{s_W}{c_W} N_{i1}) \left[\frac{1}{(t - m_{\tilde{N}_i}^2)(t - m_{\tilde{N}_j}^2)} + \frac{1}{(u - m_{\tilde{N}_i}^2)(u - m_{\tilde{N}_j}^2)} \right]. \quad (6.107)$$

To compare with the original calculation in [83] and with eq. E26, p. 244 in ref. [48], note that for a pure photino exchange, $N_{i1} \rightarrow c_W \delta_{i1}$ and $N_{i2} \rightarrow s_W \delta_{i1}$, so that

$$\frac{1}{4s_W^2 c_W^2} |N_{i1}|^2 |N_{i2} + \frac{s_W}{c_W} N_{i1}|^2 \rightarrow 1. \quad (6.108)$$

Also note that in [83] polarized electron beams are assumed. The result checks.

6.10.2 $e^- e^- \rightarrow \tilde{e}_R^- \tilde{e}_R^-$

For this process, there are again two Feynman graphs, which are related by the exchange of identical electrons in the initial state or equivalently by exchange of the identical selectrons in the final state, as shown in Fig. 38. (We again neglect the electron mass and thus the Higgsino coupling to the electron.) Let the electrons have momenta p_1 and p_2 and the selectrons have momenta k_1 and k_2 , so that $p_1^2 = p_2^2 = 0$; $k_1^2 = k_2^2 = m_{\tilde{e}_R}^2$; $s = (p_1 + p_2)^2$; $t = (k_1 - p_1)^2$; $u = (k_1 - p_2)^2$. Using the Feynman rules of Fig. 76, the amplitude for the first graph is:

$$i\mathcal{M}_t = \left(-i\sqrt{2}g \frac{s_W}{c_W} N_{i1} \right)^2 \left[\frac{i m_{\tilde{N}_i}}{(k_1 - p_1)^2 - m_{\tilde{N}_i}^2} \right] \bar{y}_1 \bar{y}_2 \quad (6.109)$$

for each exchanged neutralino. The amplitudes for the second graph are the same, but with the electrons interchanged:

$$i\mathcal{M}_u = \left(-i\sqrt{2}g\frac{s_W}{c_W}N_{i1}\right)^2 \left[\frac{i m_{\tilde{N}_i}}{(k_1 - p_2)^2 - m_{\tilde{N}_i}^2} \right] \bar{y}_1 \bar{y}_2. \quad (6.110)$$

Since we have chosen to write the external state wave function spinors in the same order in \mathcal{M}_t and \mathcal{M}_u , there is no factor of (-1) for Fermi-Dirac statistics. So, applying eq. (2.30), the total amplitude squared is:

$$|\mathcal{M}|^2 = \frac{4g^4 s_W^4}{c_W^4} (\bar{y}_1 \bar{y}_2)(y_2 y_1) \sum_{i,j=1}^4 (N_{i1})^2 (N_{j1}^*)^2 m_{\tilde{N}_i} m_{\tilde{N}_j} \left(\frac{1}{t - m_{\tilde{N}_i}^2} + \frac{1}{u - m_{\tilde{N}_i}^2} \right) \left(\frac{1}{t - m_{\tilde{N}_j}^2} + \frac{1}{u - m_{\tilde{N}_j}^2} \right) \quad (6.111)$$

The sum over the electron spins is obtained from

$$\sum_{\lambda_1, \lambda_2} (\bar{y}_1 \bar{y}_2)(y_2 y_1) = \text{Tr}[p_2 \cdot \bar{\sigma} p_1 \cdot \sigma] = 2p_2 \cdot p_1 = s. \quad (6.112)$$

So, using eq. (3.57), the spin-averaged differential cross-section is:

$$\frac{d\sigma}{dt} = \left(\frac{1}{2}\right) \frac{1}{16\pi s^2} \left(\frac{1}{4} \sum_{\lambda_1, \lambda_2} |\mathcal{M}|^2 \right) \quad (6.113)$$

$$= \frac{\pi \alpha^2}{2c_W^4} \sum_{i,j=1}^4 (N_{i1})^2 (N_{j1}^*)^2 \frac{m_{\tilde{N}_i} m_{\tilde{N}_j}}{s} \left(\frac{1}{t - m_{\tilde{N}_i}^2} + \frac{1}{u - m_{\tilde{N}_i}^2} \right) \left(\frac{1}{t - m_{\tilde{N}_j}^2} + \frac{1}{u - m_{\tilde{N}_j}^2} \right). \quad (6.114)$$

The first factor of $(1/2)$ in eq. (6.113) comes from the fact that there are identical sleptons in the final state and thus the phase space is degenerate.

To compare with [83] and also with eq. E27, p. 245 in ref. [48], note that for a pure photino exchange, $N_{i1} \rightarrow c_W \delta_{i1}$, so it checks.

6.10.3 $e^- e^- \rightarrow \tilde{e}_L^- \tilde{e}_L^-$

Again, in the limit of vanishing electron mass, there are two Feynman graphs, which are related by the exchange of identical electrons in the initial state or equivalently by exchange of the identical selectrons in the final state. As shown in Fig. 39, they are exactly like the previous example, but with all arrows reversed. Using the Feynman rules of Fig. 76, the amplitude for the first graph is:

$$\mathcal{M}_t = \left(i \frac{g}{\sqrt{2}} [N_{i2}^* + \frac{s_W}{c_W} N_{i1}^*] \right)^2 \left[\frac{i m_{\tilde{N}_i}}{(p_1 - k_1)^2 - m_{\tilde{N}_i}^2} \right] x_1 x_2 \quad (6.115)$$

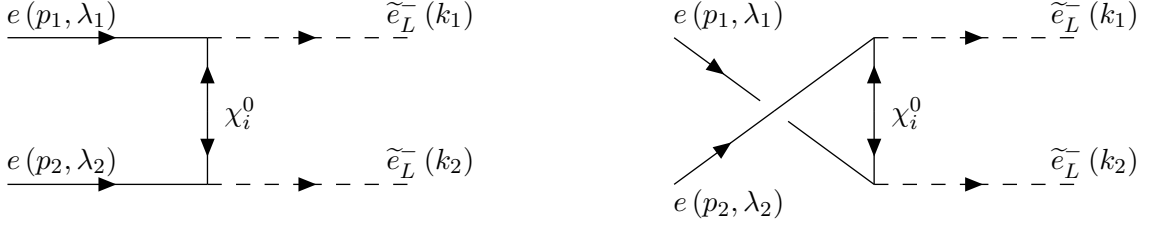


Figure 39: The two Feynman diagrams for $e^-e^- \rightarrow \tilde{e}_L^-\tilde{e}_L^-$ in the limit of vanishing electron mass.

for each exchanged neutralino. The amplitudes for the second graph are the same, but with $p_1 \leftrightarrow p_2$:

$$\mathcal{M}_u = \left(i \frac{g}{\sqrt{2}} [N_{i2}^* + \frac{s_W}{c_W} N_{i1}^*] \right)^2 \left[\frac{i m_{\tilde{N}_i}}{(p_2 - k_1)^2 - m_{\tilde{N}_i}^2} \right] x_1 x_2 \quad (6.116)$$

Since we have chosen to write the external state wave function spinors in the same order in \mathcal{M}_1 and \mathcal{M}_2 , there is no factor of (-1) for Fermi-Dirac statistics. The total amplitude squared is:

$$|\mathcal{M}|^2 = \frac{g^4}{4} (x_1 x_2) (\bar{x}_2 \bar{x}_1) \sum_{i,j=1}^4 (N_{i2}^* + \frac{s_W}{c_W} N_{i1}^*)^2 (N_{j2} + \frac{s_W}{c_W} N_{j1})^2 m_{\tilde{N}_i} m_{\tilde{N}_j} \left(\frac{1}{t - m_{\tilde{N}_i}^2} + \frac{1}{u - m_{\tilde{N}_i}^2} \right) \left(\frac{1}{t - m_{\tilde{N}_j}^2} + \frac{1}{u - m_{\tilde{N}_j}^2} \right). \quad (6.117)$$

The average over the electron spins follows from eq. (3.56):

$$\sum_{\lambda_1, \lambda_2} (x_1 x_2) (\bar{x}_2 \bar{x}_1) = \text{Tr}[p_2 \cdot \sigma p_1 \cdot \bar{\sigma}] = 2 p_2 \cdot p_1 = s. \quad (6.118)$$

So the spin-averaged differential cross-section is:

$$\frac{d\sigma}{dt} = \left(\frac{1}{2} \right) \frac{1}{16\pi s^2} \left(\frac{1}{4} \sum_{\lambda_1, \lambda_2} |\mathcal{M}|^2 \right) \quad (6.119)$$

$$= \frac{\pi \alpha^2}{32 s_W^4} \sum_{i,j=1}^4 (N_{i2}^* + \frac{s_W}{c_W} N_{i1}^*)^2 (N_{j2} + \frac{s_W}{c_W} N_{j1})^2 \frac{m_{\tilde{N}_i} m_{\tilde{N}_j}}{s} \left(\frac{1}{t - m_{\tilde{N}_i}^2} + \frac{1}{u - m_{\tilde{N}_i}^2} \right) \left(\frac{1}{t - m_{\tilde{N}_j}^2} + \frac{1}{u - m_{\tilde{N}_j}^2} \right) \quad (6.120)$$

where the first factor of $(1/2)$ in eq. (6.119) comes from the fact that there are identical sleptons in the final state. To compare with [83] and also with eq. (E27), p. 245 in ref. [48], note that for a pure photino exchange, $N_{i1} \rightarrow c_W \delta_{i1}$ and $N_{i2} \rightarrow s_W \delta_{i1}$, so it checks.

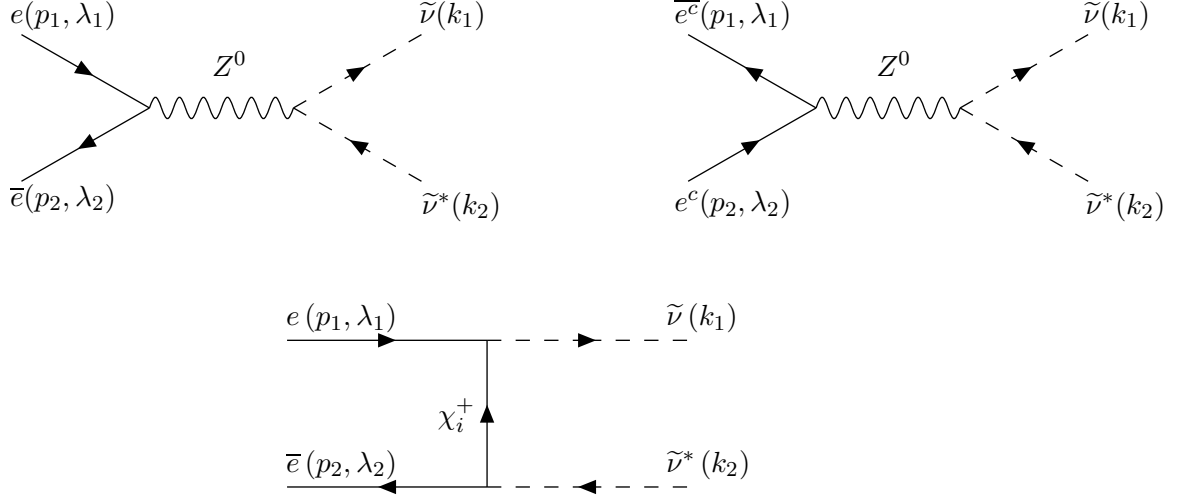


Figure 40: The Feynman diagrams for $e^-e^+ \rightarrow \tilde{\nu}\tilde{\nu}^*$.

6.11 $e^-e^+ \rightarrow \tilde{\nu}\tilde{\nu}^*$

Consider now the pair-production of sneutrinos in electron-positron collisions. There are two graphs featuring the s -channel exchange of the Z^0 . We will neglect the electron mass and Yukawa coupling, so there is only one graph involving the t -channel exchange of the charginos. These three Feynman diagrams are shown in in Fig. 40, where we have also defined the helicities and momenta of the particles. The Mandelstam variables can be expressed in terms of the external momenta and the sneutrino mass:

$$2p_1 \cdot p_2 = s; \quad 2k_1 \cdot k_2 = s - 2m_{\tilde{\nu}}^2; \quad (6.121)$$

$$2p_1 \cdot k_1 = 2p_2 \cdot k_2 = m_{\tilde{\nu}}^2 - t; \quad (6.122)$$

$$2p_1 \cdot k_2 = 2p_2 \cdot k_1 = m_{\tilde{\nu}}^2 - u. \quad (6.123)$$

Using the Feynman rules of Fig. 67, the amplitudes for the two s -channel Z boson exchange diagrams are:

$$i\mathcal{M}_1 = \left[-i \frac{g}{2c_W} (k_1 - k_2)_\mu \right] \left[\frac{-ig^{\mu\nu}}{(p_1 + p_2)^2 - m_Z^2 + i\Gamma_Z m_Z} \right] \left[i \frac{g}{c_W} (s_W^2 - 1/2) \right] x_1 \sigma_\nu \bar{y}_2 \quad (6.124)$$

$$i\mathcal{M}_2 = \left[-i \frac{g}{2c_W} (k_1 - k_2)_\mu \right] \left[\frac{-ig^{\mu\nu}}{(p_1 + p_2)^2 - m_Z^2 + i\Gamma_Z m_Z} \right] \left[i \frac{gs_W^2}{c_W} \right] \bar{y}_1 \bar{\sigma}_\nu x_2 \quad (6.125)$$

where the first factor in each case is the Feynman rule from the Z boson coupling to the sneutrinos (see Fig. 72c, ref. [48]). The t -channel diagram due to each chargino gives a contribution

$$i\mathcal{M}_3 = (-igV_{i1}^*) (-igV_{i1}) x_1 \left[\frac{i(k_1 - p_1) \cdot \sigma}{(k_1 - p_1)^2 - m_{\tilde{C}_i}^2} \right] \bar{y}_2, \quad (6.126)$$

using the rules of Fig. 75. Therefore, the total amplitude can be rewritten as:

$$\mathcal{M} = c_1 x_1(k_1 - k_2) \cdot \sigma \bar{y}_2 + c_2 \bar{y}_1(k_1 - k_2) \cdot \bar{\sigma} x_2 + c_3 x_1(k_1 - p_1) \cdot \sigma \bar{y}_2 \quad (6.127)$$

where

$$c_1 \equiv \frac{g^2(1 - 2s_W^2)}{4c_W^2 D_Z}, \quad c_2 \equiv -\frac{g^2 s_W^2}{2c_W^2 D_Z}, \quad c_3 \equiv g^2 \sum_{i=1}^2 |V_{i1}|^2 / (m_{\tilde{C}_j}^2 - t). \quad (6.128)$$

and $D_Z \equiv s - m_Z^2 + i\Gamma_Z m_Z$ is the denominator of the Z boson propagator.

We will now square the amplitude and sum over the electron and positron spins. In doing so, the interference terms involving c_2 will vanish for $m_e = 0$, because of eqs. (3.58) and (3.59).

Therefore, we have

$$\begin{aligned} \sum_{\lambda_1, \lambda_2} |\mathcal{M}|^2 &= \sum_{\lambda_1, \lambda_2} \left\{ |c_1|^2 x_1(k_1 - k_2) \cdot \sigma \bar{y}_2 y_2(k_1 - k_2) \cdot \sigma \bar{x}_1 \right. \\ &\quad + |c_2|^2 \bar{y}_1(k_1 - k_2) \cdot \bar{\sigma} x_2 \bar{x}_2(k_1 - k_2) \cdot \bar{\sigma} y_1 \\ &\quad + c_3^2 x_1(k_1 - p_1) \cdot \sigma \bar{y}_2 y_2(k_1 - p_1) \cdot \sigma \bar{x}_1 \\ &\quad \left. + 2\text{Re}[c_1 c_3 x_1(k_1 - k_2) \cdot \sigma \bar{y}_2 y_2(k_1 - p_1) \cdot \sigma \bar{x}_1] \right\} \quad (6.129) \end{aligned}$$

$$\begin{aligned} &= |c_1|^2 \text{Tr}[(k_1 - k_2) \cdot \sigma p_2 \cdot \bar{\sigma} (k_1 - k_2) \cdot \sigma p_1 \cdot \bar{\sigma}] \\ &\quad + |c_2|^2 \text{Tr}[(k_1 - k_2) \cdot \bar{\sigma} p_2 \cdot \sigma (k_1 - k_2) \cdot \bar{\sigma} p_1 \cdot \sigma] \\ &\quad + c_3^2 \text{Tr}[(k_1 - p_1) \cdot \sigma p_2 \cdot \bar{\sigma} (k_1 - p_1) \cdot \sigma p_1 \cdot \bar{\sigma}] \\ &\quad + 2\text{Re}[c_1] c_3 \text{Tr}[(k_1 - k_2) \cdot \sigma p_2 \cdot \bar{\sigma} (k_1 - p_1) \cdot \sigma p_1 \cdot \bar{\sigma}], \quad (6.130) \end{aligned}$$

where we have used eqs. (3.56) and (3.57) to do the spin sums to obtain the second equality. Now, applying the trace identities (2.44) and (2.45) and reducing the results using eqs. (6.121)-(6.123) and $u = 2m_\nu^2 - s - t$, we get

$$\sum_{\lambda_1, \lambda_2} |\mathcal{M}|^2 = -[st + (t - m_\nu^2)^2] (4|c_1|^2 + 4|c_2|^2 + c_3^2 + 4\text{Re}[c_1]c_3). \quad (6.131)$$

When $m_{\tilde{C}_1} = m_{\tilde{C}_2}$, this agrees with eqs. (E46)-(E48) of ref. [48]³³ and with [84]. The differential cross-section follows in the standard way by averaging over the initial-state spins:

$$\frac{d\sigma}{dt} = \frac{1}{16\pi s^2} \left(\frac{1}{4} \sum_{\lambda_1, \lambda_2} |\mathcal{M}|^2 \right). \quad (6.132)$$

Note that

$$t = m_\nu^2 - (1 - \beta \cos \theta)s/2; \quad \beta \equiv (1 - 4m_\nu^2/s)^{1/2}, \quad (6.133)$$

³³There is a typo in eq. (E48) of [48]; the right-hand side should be multiplied by $1/\cos^2 \theta_w$.

where θ is the angle between the initial-state electron and the final-state sneutrino in the center-of-momentum frame. The upper and lower limits t_+ and t_- are obtained by inserting $\cos\theta = \pm 1$ above, respectively.

Doing the integration over t to obtain the total cross-section, one obtains

$$\sigma = \int_{t_-}^{t_+} \frac{d\sigma}{dt} dt = \frac{g^4}{64\pi s} \left(S_Z + \sum_{i,j=1}^2 S_{ij} + \sum_{i=1}^2 S_{Zi} \right), \quad (6.134)$$

where

$$S_Z = \frac{\beta^3}{24c_W^4} (8s_W^4 - 4s_W^2 + 1) \frac{s^2}{|D_Z|^2}, \quad (6.135)$$

$$S_{ii} = |V_{i1}|^4 [(1 - 2\gamma_i)L_i - 2\beta], \quad (6.136)$$

$$S_{12} = S_{21} = |V_{11}V_{12}|^2 \left\{ [(m_{\tilde{C}_2}^2 + s\gamma_2^2)L_2 - (m_{\tilde{C}_1}^2 + s\gamma_1^2)L_1] / (m_{\tilde{C}_2}^2 - m_{\tilde{C}_1}^2) - \beta \right\}, \quad (6.137)$$

$$S_{Zi} = \frac{(2s_W^2 - 1)}{c_W^2} |V_{i1}|^2 \left[(m_{\tilde{C}_i}^2 + s\gamma_i^2)L_i + s\beta(\gamma_i - 1/2) \right] \frac{(s - m_Z^2)}{|D_Z|^2}, \quad (6.138)$$

with

$$\gamma_i \equiv (m_{\tilde{\nu}}^2 - m_{\tilde{C}_i}^2)/s, \quad L_i \equiv \ln \left(\frac{m_{\tilde{C}_i}^2 - t_-}{m_{\tilde{C}_i}^2 - t_+} \right). \quad (6.139)$$

This agrees with eqs. (E49)-(E52) of ref. [48] in the limit of degenerate charginos, or of a single wino chargino with $|V_{11}| = 1$ and $V_{12} = 0$ and with [84].

6.12 $e^-e^+ \rightarrow \tilde{N}_i\tilde{N}_j$

Next we consider the pair production of neutralinos via e^-e^+ annihilation. There are four Feynman graphs for s -channel Z^0 exchange, shown in Figure 41, and four for t -channel selectron exchange, shown in Figure 42. The momenta and polarizations are as labeled in the graphs. We denote the neutralino masses as $m_{\tilde{N}_i}, m_{\tilde{N}_j}$ and the selectron masses as $m_{\tilde{e}_L}$ and $m_{\tilde{e}_R}$. The electron mass will again be neglected. The kinematic variables are then given by

$$s = 2p_1 \cdot p_2 = m_{\tilde{N}_i}^2 + m_{\tilde{N}_j}^2 + 2k_i \cdot k_j, \quad (6.140)$$

$$t = m_{\tilde{N}_i}^2 - 2p_1 \cdot k_i = m_{\tilde{N}_j}^2 - 2p_2 \cdot k_j, \quad (6.141)$$

$$u = m_{\tilde{N}_i}^2 - 2p_2 \cdot k_i = m_{\tilde{N}_j}^2 - 2p_1 \cdot k_j. \quad (6.142)$$

By applying the Feynman rules of figs. 67 and 72, we obtain for the sum of the s -channel diagrams in Fig. 41,

$$i\mathcal{M}_Z = \frac{-ig^{\mu\nu}}{s - m_Z^2} \left[\frac{ig(s_W^2 - \frac{1}{2})}{c_W} x_1 \sigma_\mu \bar{y}_2 + \frac{igs_W^2}{c_W} \bar{y}_1 \bar{\sigma}_\mu x_2 \right] \left[\frac{ig}{c_W} O_{ij}''^L \bar{x}_i \bar{\sigma}_\nu y_j - \frac{ig}{c_W} O_{ji}''^L y_i \sigma_\nu \bar{x}_j \right], \quad (6.143)$$

where O_{ij}'' is given in eq. (I.20). The fermion spinors are denoted by $x_1 \equiv x(\vec{p}_1, \lambda_1)$, $\bar{y}_2 \equiv \bar{y}(\vec{p}_2, \lambda_2)$, $\bar{x}_i \equiv \bar{x}(\vec{k}_i, \lambda_i)$, $y_j \equiv y(\vec{k}_j, \lambda_j)$, etc. Note that we have combined the matrix elements

of the four diagrams by factorizing with respect to the common boson propagator. For the four t and u channel diagrams, we obtain, by applying the rules of Fig. 76:

$$i\mathcal{M}_{\tilde{e}_L}^{(t)} = (-1) \left[\frac{i}{t - m_{\tilde{e}_L}^2} \right] \left[\frac{ig}{\sqrt{2}} \left(N_{i2}^* + \frac{s_W}{c_W} N_{i1}^* \right) \right] \left[\frac{ig}{\sqrt{2}} \left(N_{j2} + \frac{s_W}{c_W} N_{j1} \right) \right] x_1 y_i \bar{y}_2 \bar{x}_j, \quad (6.144)$$

$$i\mathcal{M}_{\tilde{e}_L}^{(u)} = \left[\frac{i}{u - m_{\tilde{e}_L}^2} \right] \left[\frac{ig}{\sqrt{2}} \left(N_{j2}^* + \frac{s_W}{c_W} N_{j1}^* \right) \right] \left[\frac{ig}{\sqrt{2}} \left(N_{i2} + \frac{s_W}{c_W} N_{i1} \right) \right] x_1 y_j \bar{y}_2 \bar{x}_i, \quad (6.145)$$

$$i\mathcal{M}_{\tilde{e}_R}^{(t)} = (-1) \left[\frac{i}{t - m_{\tilde{e}_R}^2} \right] \left(-i\sqrt{2}g \frac{s_W}{c_W} N_{i1} \right) \left(-i\sqrt{2}g \frac{s_W}{c_W} N_{j1}^* \right) \bar{y}_1 \bar{x}_i x_2 y_j, \quad (6.146)$$

$$i\mathcal{M}_{\tilde{e}_R}^{(u)} = \left[\frac{i}{u - m_{\tilde{e}_R}^2} \right] \left(-i\sqrt{2}g \frac{s_W}{c_W} N_{j1} \right) \left(-i\sqrt{2}g \frac{s_W}{c_W} N_{i1}^* \right) \bar{y}_1 \bar{x}_j x_2 y_i. \quad (6.147)$$

The first factors of (-1) in each of eqs. (6.144) and (6.146) are present because the order of the spinors in each case is an odd permutation of the ordering $(1, 2, i, j)$ established by the s -channel contribution. The other contributions have spinors in an even permutation of that ordering.

The s -channel diagram contribution of eq. (6.143) can be profitably rearranged using the Fierz identities of eqs. (2.55)-(2.56). Then, combining the result with the t -channel and s -channel contributions, we have for the total:

$$\mathcal{M} = c_1 x_1 y_j \bar{y}_2 \bar{x}_i + c_2 x_1 y_i \bar{y}_2 \bar{x}_j + c_3 \bar{y}_1 \bar{x}_i x_2 y_j + c_4 \bar{y}_1 \bar{x}_j x_2 y_i, \quad (6.148)$$

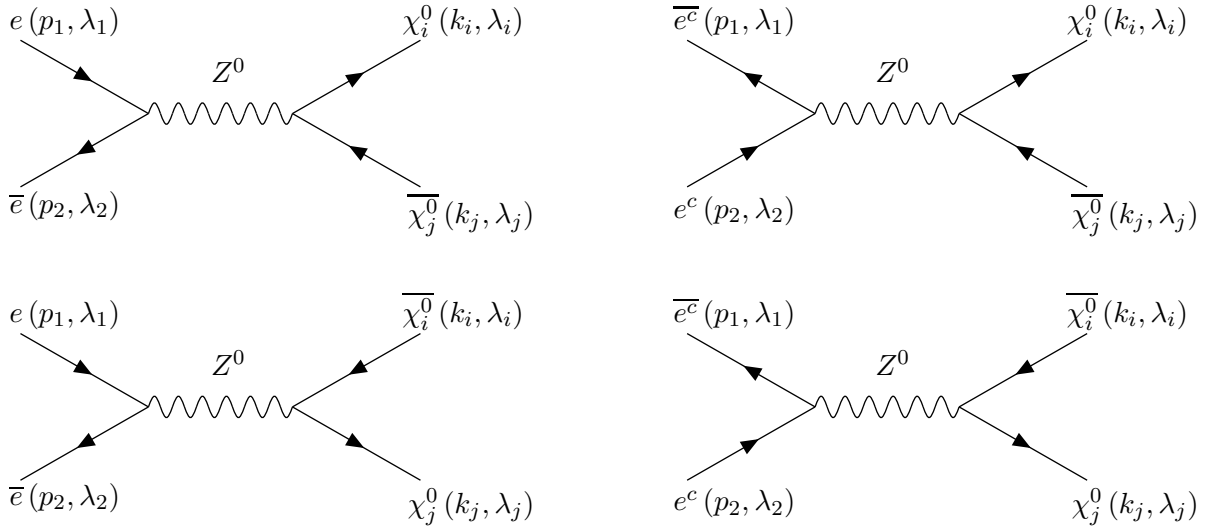


Figure 41: The four Feynman diagrams for $e^- e^+ \rightarrow \tilde{N}_i \tilde{N}_j$ via s -channel Z^0 exchange.

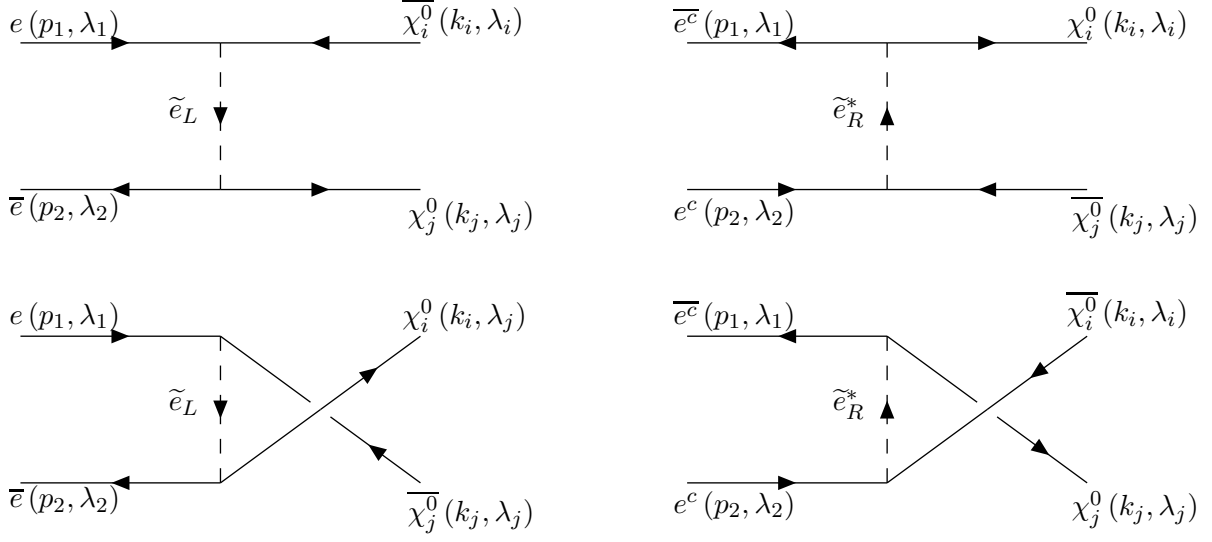


Figure 42: The four Feynman diagrams for $e^-e^+ \rightarrow \tilde{N}_i\tilde{N}_j$ via t -channel selectron exchange.

where

$$c_1 = \frac{g^2}{c_W^2} [(1 - 2s_W^2)O_{ij}^{\prime\prime L}/(s - m_Z^2) - (c_W N_{i2} + s_W N_{i1})(c_W N_{j2}^* + s_W N_{j1}^*)/2(u - m_{\tilde{e}_L}^2)], \quad (6.149)$$

$$c_2 = \frac{g^2}{c_W^2} [(2s_W^2 - 1)O_{ji}^{\prime\prime L}/(s - m_Z^2) + (c_W N_{i2}^* + s_W N_{i1}^*)(c_W N_{j2} + s_W N_{j1})/2(t - m_{\tilde{e}_L}^2)], \quad (6.150)$$

$$c_3 = \frac{2g^2 s_W^2}{c_W^2} [-O_{ij}^{\prime\prime L}/(s - m_Z^2) + N_{i1} N_{j1}^*/(t - m_{\tilde{e}_R}^2)], \quad (6.151)$$

$$c_4 = \frac{2g^2 s_W^2}{c_W^2} [O_{ji}^{\prime\prime L}/(s - m_Z^2) - N_{i1}^* N_{j1}/(u - m_{\tilde{e}_R}^2)]. \quad (6.152)$$

Now, when we square the amplitude and average over the initial-state fermion spins, the only terms that will survive in the massless electron limit are the ones that involve $x_1\bar{x}_1$ or $y_1\bar{y}_1$, and $x_2\bar{x}_2$ or $y_2\bar{y}_2$. This follows immediately from eqs. (3.58) and (3.59).

$$\begin{aligned} \sum_{\lambda_1, \lambda_2} |\mathcal{M}|^2 &= \sum_{\lambda_1, \lambda_2} \left(|c_1|^2 \bar{y}_j \bar{x}_1 x_1 y_j x_i y_2 \bar{y}_2 \bar{x}_i + |c_2|^2 \bar{y}_i \bar{x}_1 x_1 y_i x_j y_2 \bar{y}_2 \bar{x}_j \right. \\ &\quad + |c_3|^2 x_i y_1 \bar{y}_1 \bar{x}_i \bar{y}_j \bar{x}_2 x_2 y_j + |c_4|^2 x_j y_1 \bar{y}_1 \bar{x}_j \bar{y}_i \bar{x}_2 x_2 y_i \\ &\quad \left. + 2\text{Re}[c_1 c_2^* \bar{y}_i \bar{x}_1 x_1 y_j x_j y_2 \bar{y}_2 \bar{x}_i] + 2\text{Re}[c_3 c_4^* x_j y_1 \bar{y}_1 \bar{x}_i \bar{y}_i \bar{x}_2 x_2 y_j] \right) \end{aligned} \quad (6.153)$$

$$\begin{aligned} &= |c_1|^2 \bar{y}_j p_1 \cdot \bar{\sigma} y_j x_i p_2 \cdot \sigma \bar{x}_i + |c_2|^2 \bar{y}_i p_1 \cdot \bar{\sigma} y_i x_j p_2 \cdot \sigma \bar{x}_j \\ &\quad + |c_3|^2 x_i p_1 \cdot \sigma \bar{x}_i \bar{y}_j p_2 \cdot \bar{\sigma} y_j + |c_4|^2 x_j p_1 \cdot \sigma \bar{x}_j \bar{y}_i p_2 \cdot \bar{\sigma} y_i \\ &\quad + 2\text{Re}[c_1 c_2^* \bar{y}_i p_1 \cdot \bar{\sigma} y_j x_j p_2 \cdot \sigma \bar{x}_i] + 2\text{Re}[c_3 c_4^* x_j p_1 \cdot \sigma \bar{x}_i \bar{y}_i p_2 \cdot \bar{\sigma} y_j] \end{aligned} \quad (6.154)$$

where eqs. (3.56) and (3.57) have been used to do the spin sums to obtain the second equality.

Now we do the remaining spin sums using eqs. (3.56)-(3.59) again, obtaining:

$$\begin{aligned} \sum_{\lambda_1, \lambda_2, \lambda_i, \lambda_j} |\mathcal{M}|^2 &= |c_1|^2 \text{Tr}[p_1 \cdot \bar{\sigma} k_j \cdot \sigma] \text{Tr}[p_2 \cdot \sigma k_i \cdot \bar{\sigma}] + |c_2|^2 \text{Tr}[p_1 \cdot \bar{\sigma} k_i \cdot \sigma] \text{Tr}[p_2 \cdot \sigma k_j \cdot \bar{\sigma}] \\ &+ |c_3|^2 \text{Tr}[p_1 \cdot \sigma k_i \cdot \bar{\sigma}] \text{Tr}[p_2 \cdot \bar{\sigma} k_j \cdot \sigma] + |c_4|^2 \text{Tr}[p_1 \cdot \sigma k_j \cdot \bar{\sigma}] \text{Tr}[p_2 \cdot \bar{\sigma} k_i \cdot \sigma] \\ &+ 2\text{Re}[c_1 c_2^*] m_{\tilde{N}_i} m_{\tilde{N}_j} \text{Tr}[p_2 \cdot \sigma p_1 \cdot \bar{\sigma}] + 2\text{Re}[c_3 c_4^*] m_{\tilde{N}_i} m_{\tilde{N}_j} \text{Tr}[p_1 \cdot \sigma p_2 \cdot \bar{\sigma}]. \end{aligned} \quad (6.155)$$

Applying the trace identity of eq. (2.43) to this yields

$$\begin{aligned} \sum_{\text{spins}} |\mathcal{M}|^2 &= (|c_1|^2 + |c_4|^2) 4p_1 \cdot k_j p_2 \cdot k_i + (|c_2|^2 + |c_3|^2) 4p_1 \cdot k_i p_2 \cdot k_j \\ &+ 4\text{Re}[c_1 c_2^* + c_3 c_4^*] m_{\tilde{N}_i} m_{\tilde{N}_j} p_1 \cdot p_2 \end{aligned} \quad (6.156)$$

$$\begin{aligned} &= (|c_1|^2 + |c_4|^2) (u - m_{\tilde{N}_i}^2) (u - m_{\tilde{N}_j}^2) + (|c_2|^2 + |c_3|^2) (t - m_{\tilde{N}_i}^2) (t - m_{\tilde{N}_j}^2) \\ &+ 2\text{Re}[c_1 c_2^* + c_3 c_4^*] m_{\tilde{N}_i} m_{\tilde{N}_j} s. \end{aligned} \quad (6.157)$$

The differential cross-section then follows:

$$\frac{d\sigma}{dt} = \frac{1}{16\pi s^2} \left(\frac{1}{4} \sum_{\text{spins}} |\mathcal{M}|^2 \right). \quad (6.158)$$

This agrees with the first complete calculation presented in [85]. For the case of pure photino pair production, i.e. $N_{i1} \rightarrow c_W \delta_{i1}$ and $N_{i2} \rightarrow s_W \delta_{i1}$ and for degenerate selectron masses this also agrees with eq. (E9) of the erratum of [48]. Other earlier calculations with some simplifications are given in [86, 87].

Defining $\cos \theta = \hat{\mathbf{p}}_1 \cdot \hat{\mathbf{k}}_i$ (the cosine of the angle between the initial-state electron and one of the neutralinos in the center-of-momentum frame), the Mandelstam variables t, u can be written as

$$t = \frac{1}{2} \left[m_{\tilde{N}_i}^2 + m_{\tilde{N}_j}^2 - s + \lambda^{1/2}(s, m_{\tilde{N}_i}^2, m_{\tilde{N}_j}^2) \cos \theta \right], \quad (6.159)$$

$$u = \frac{1}{2} \left[m_{\tilde{N}_i}^2 + m_{\tilde{N}_j}^2 - s - \lambda^{1/2}(s, m_{\tilde{N}_i}^2, m_{\tilde{N}_j}^2) \cos \theta \right]. \quad (6.160)$$

Taking into account the identical fermions in the final state, the total cross section is

$$\sigma = \frac{1}{2} \int_{t_-}^{t_+} \frac{d\sigma}{dt} dt, \quad (6.161)$$

where t_- and t_+ are obtained by inserting $\cos \theta = \mp 1$ in eq. (6.159), respectively.

6.13 $e^- e^+ \rightarrow \tilde{C}_i^- \tilde{C}_j^+$

Next we consider the pair production of charginos in electron-positron collisions. The s -channel Feynman diagrams are shown in Fig. 43, where we have also introduced the notation for the

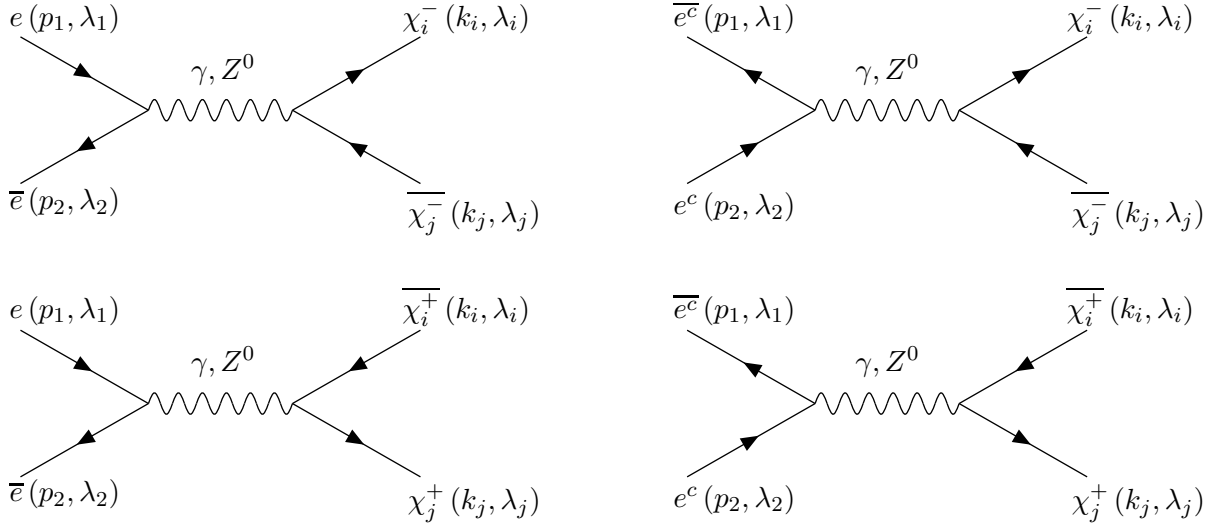


Figure 43: Feynman diagrams for $e^- e^+ \rightarrow \tilde{C}_i^- \tilde{C}_j^+$ via s -channel γ and Z^0 exchange.

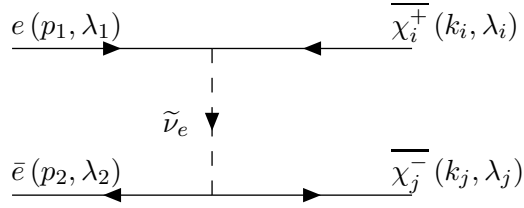


Figure 44: The Feynman diagram for $e^- e^+ \rightarrow \tilde{C}_i^- \tilde{C}_j^+$ via the t -channel exchange of a sneutrino.

fermion momenta and polarizations. The Mandelstam variables are given by

$$s = 2p_1 \cdot p_2 = m_{\tilde{C}_i}^2 + m_{\tilde{C}_j}^2 + 2k_i \cdot k_j, \quad (6.162)$$

$$t = m_{\tilde{C}_i}^2 - 2p_1 \cdot k_i = m_{\tilde{C}_j}^2 - 2p_2 \cdot k_j, \quad (6.163)$$

$$u = m_{\tilde{C}_i}^2 - 2p_2 \cdot k_i = m_{\tilde{C}_j}^2 - 2p_1 \cdot k_j. \quad (6.164)$$

Note that the negatively charged chargino carries momentum and polarization (k_i, λ_i) , while the positively charged one carries (k_j, λ_j) . Using the Feynman rules of Figs. 67 and 72, the sum of the photon-exchange diagrams is:

$$i\mathcal{M}_\gamma = \frac{-ig^{\mu\nu}}{s} (-ie x_1 \sigma_\mu \bar{y}_2 - ie \bar{y}_1 \bar{\sigma}_\mu x_2) (ie \delta_{ij} y_i \sigma_\nu \bar{x}_j + ie \delta_{ij} \bar{x}_i \bar{\sigma}_\nu y_j) \quad (6.165)$$

while the result from the Z -exchange diagrams is:

$$i\mathcal{M}_Z = \frac{-ig^{\mu\nu}}{s - m_Z^2} \left[\frac{ig}{c_W} (s_W^2 - \frac{1}{2}) x_1 \sigma_\mu \bar{y}_2 + \frac{igs_W^2}{c_W} \bar{y}_1 \bar{\sigma}_\mu x_2 \right] \left[-\frac{ig}{c_W} O_{ji}^L y_i \sigma_\nu \bar{x}_j - \frac{ig}{c_W} O_{ji}^R \bar{x}_i \bar{\sigma}_\nu y_j \right] \quad (6.166)$$

The t -channel Feynman diagram via sneutrino exchange is shown in Fig. 44. Applying the rules of Fig. 75, we find:

$$i\mathcal{M}_{\tilde{\nu}_e} = (-1) \frac{i}{t - m_{\tilde{\nu}_e}^2} (-igV_{i1}^* x_1 y_i) (-igV_{j1} \bar{y}_2 \bar{x}_j). \quad (6.167)$$

The Fermi-Dirac factor (-1) in this equation arises because the spinors appear an order which is an odd permutation of the order used in all of the s -channel diagram results.

One can now apply the Fierz transformation identities (2.55)-(2.57) to eqs. (6.165) and (6.166) to remove the σ and $\bar{\sigma}$ matrices. The result can be combined with the t -channel contribution to obtain a total matrix element \mathcal{M} with exactly the same form as eq. (6.148), but now with:

$$c_1 = 2e^2 \delta_{ij}/s - \frac{g^2}{c_W^2} (1 - 2s_W^2) O'_{ji}{}^R / (s - m_Z^2), \quad (6.168)$$

$$c_2 = 2e^2 \delta_{ij}/s - \frac{g^2}{c_W^2} (1 - 2s_W^2) O'_{ji}{}^L / (s - m_Z^2) + g^2 V_{i1}^* V_{j1} / (t - m_{\tilde{\nu}_e}^2), \quad (6.169)$$

$$c_3 = 2e^2 \delta_{ij}/s + \frac{2g^2 s_W^2}{c_W^2} O'_{ji}{}^R / (s - m_Z^2), \quad (6.170)$$

$$c_4 = 2e^2 \delta_{ij}/s + \frac{2g^2 s_W^2}{c_W^2} O'_{ji}{}^L / (s - m_Z^2). \quad (6.171)$$

The rest of this calculation is identical in form to eqs. (6.148)-(6.157), so that the result is:

$$\begin{aligned} \sum_{\text{spins}} |\mathcal{M}|^2 &= (|c_1|^2 + |c_4|^2)(u - m_{\tilde{C}_i}^2)(u - m_{\tilde{C}_j}^2) + (|c_2|^2 + |c_3|^2)(t - m_{\tilde{C}_i}^2)(t - m_{\tilde{C}_j}^2) \\ &\quad + 2\text{Re}[c_1 c_2^* + c_3 c_4^*] m_{\tilde{C}_i} m_{\tilde{C}_j} s. \end{aligned} \quad (6.172)$$

The differential cross-section then follows:

$$\frac{d\sigma}{dt} = \frac{1}{16\pi s^2} \left(\frac{1}{4} \sum_{\text{spins}} |\mathcal{M}|^2 \right). \quad (6.173)$$

Defining $\cos \theta = \hat{\mathbf{p}}_1 \cdot \hat{\mathbf{k}}_i$ (the cosine of the angle between the initial-state electron and \tilde{C}_i^- in the center-of-momentum frame), the Mandelstam variables t, u can be written as

$$t = \frac{1}{2} \left[m_{\tilde{C}_i}^2 + m_{\tilde{C}_j}^2 - s + \lambda^{1/2}(s, m_{\tilde{C}_i}^2, m_{\tilde{C}_j}^2) \cos \theta \right], \quad (6.174)$$

$$u = \frac{1}{2} \left[m_{\tilde{C}_i}^2 + m_{\tilde{C}_j}^2 - s - \lambda^{1/2}(s, m_{\tilde{C}_i}^2, m_{\tilde{C}_j}^2) \cos \theta \right]. \quad (6.175)$$

The total cross section can now be computed as

$$\sigma = \int_{t_-}^{t_+} \frac{d\sigma}{dt} dt \quad (6.176)$$

where t_- and t_+ are obtained with $\cos \theta = -1$ and $+1$ in eq. (6.174), respectively. Our results agree with the original first complete calculation in [88]. Earlier work with simplifying assumptions is given in [89]. An extended calculation for the production of polarized charginos is given in [90].

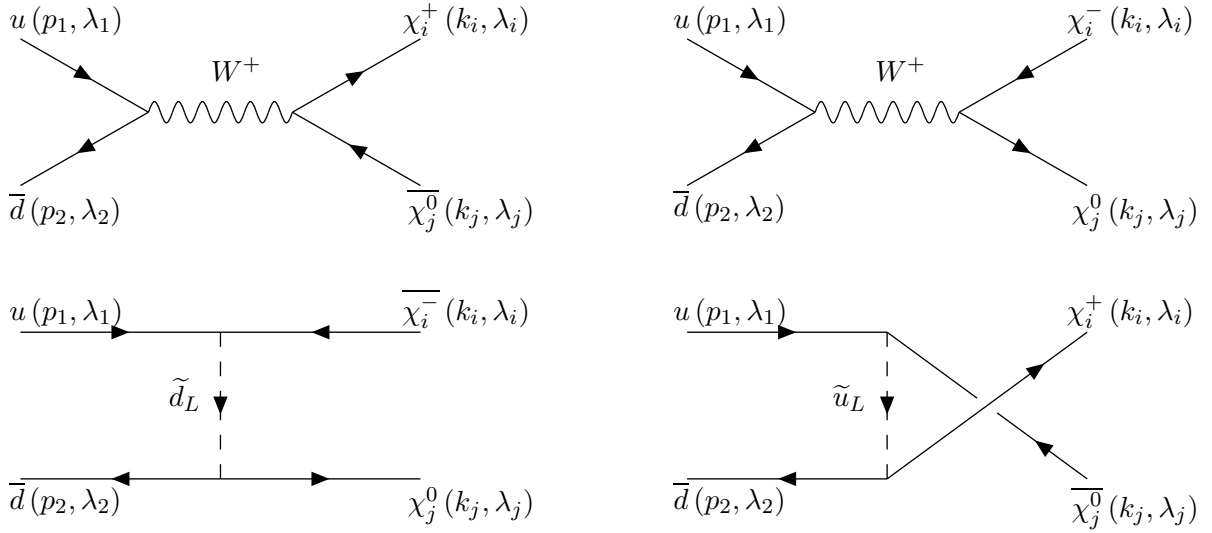


Figure 45: The four tree-level Feynman diagrams for $u\bar{d} \rightarrow \tilde{C}_i^+ \tilde{N}_j$.

6.14 $u\bar{d} \rightarrow \tilde{C}_i^+ \tilde{N}_j$

Next we consider the associated production of a chargino and a neutralino in quark, anti-quark collisions. The leading order Feynman diagrams are shown in Fig. 45, where we have also defined the momenta and the helicities. The corresponding Mandelstam variables are

$$s = 2p_1 \cdot p_2 = m_{\tilde{C}_i}^2 + m_{\tilde{N}_j}^2 + 2k_i \cdot k_j, \quad (6.177)$$

$$t = m_{\tilde{C}_i}^2 - 2p_1 \cdot k_i = m_{\tilde{N}_j}^2 - 2p_2 \cdot k_j, \quad (6.178)$$

$$u = m_{\tilde{C}_i}^2 - 2p_2 \cdot k_i = m_{\tilde{N}_j}^2 - 2p_1 \cdot k_j. \quad (6.179)$$

The matrix elements for the s -channel diagrams are obtained by applying the Feynman rules of figs. 67 and 73:

$$i\mathcal{M}_s = \frac{-ig^{\mu\nu}}{s - m_W^2} \left(\frac{ig}{\sqrt{2}} x_1 \sigma_\mu \bar{y}_2 \right) (igO_{ji}^{L*} \bar{x}_i \bar{\sigma}_\nu y_j + igO_{ji}^{R*} y_i \sigma_\nu \bar{x}_j). \quad (6.180)$$

The external spinors are denoted by $x_1 \equiv x(\vec{p}_1, \lambda_1)$, $\bar{y}_2 \equiv \bar{y}(\vec{p}_2, \lambda_2)$, $\bar{x}_i \equiv \bar{x}(\vec{k}_i, \lambda_i)$, $y_j \equiv y(\vec{k}_j, \lambda_j)$, etc. The matrix elements for the t and u channel graphs follow from the rules of figs. 75 and 76:

$$i\mathcal{M}_t = (-1) \frac{i}{t - m_{\tilde{d}_L}^2} (-igU_{i1}^*) \left(\frac{ig}{\sqrt{2}} [N_{j2} - \frac{s_W}{3c_W} N_{j1}] \right) x_1 y_i \bar{y}_2 \bar{x}_j \quad (6.181)$$

$$i\mathcal{M}_u = \frac{i}{u - m_{\tilde{u}_L}^2} (-igV_{i1}) \left(\frac{ig}{\sqrt{2}} [-N_{j2}^* - \frac{s_W}{3c_W} N_{j1}^*] \right) x_1 y_j \bar{y}_2 \bar{x}_i \quad (6.182)$$

The first factor of (-1) in eq. (6.181) is required because the order of the spinors $(1, i, 2, j)$ is in an odd permutation of the order $(1, 2, i, j)$ used in the s -channel and u -channel results.

Now we can use the Fierz relations eqs. (2.55) and (2.57) to rewrite the s -channel amplitude in a form without σ or $\bar{\sigma}$ matrices. Combining the result with the t -channel and u -channel contributions yields a total \mathcal{M} with exactly the same form as eq. (6.148), but now with

$$c_1 = -\sqrt{2}g^2 \left[O_{ji}^{L*}/(s - m_W^2) + V_{i1} \left(\frac{1}{2}N_{j2}^* + \frac{s_W}{6c_W}N_{j1}^* \right)/(u - m_{\tilde{u}_L}) \right], \quad (6.183)$$

$$c_2 = -\sqrt{2}g^2 \left[O_{ji}^{R*}/(s - m_W^2) + U_{i1}^* \left(\frac{1}{2}N_{j2}^* - \frac{s_W}{6c_W}N_{j1}^* \right)/(t - m_{\tilde{d}_L}) \right], \quad (6.184)$$

$$c_3 = c_4 = 0. \quad (6.185)$$

The rest of this calculation is identical in form to that of eqs. (6.148)-(6.157), leading to:

$$\sum_{\text{spins}} |\mathcal{M}|^2 = |c_1|^2 (u - m_{\tilde{C}_i}^2)(u - m_{\tilde{N}_j}^2) + |c_2|^2 (t - m_{\tilde{C}_i}^2)(t - m_{\tilde{N}_j}^2) + 2\text{Re}[c_1 c_2^*] m_{\tilde{C}_i} m_{\tilde{N}_j} s. \quad (6.186)$$

From this, one can obtain:

$$\frac{d\sigma}{dt} = \frac{1}{16\pi s^2} \left(\frac{1}{3 \cdot 4} \sum_{\text{spins}} |\mathcal{M}|^2 \right), \quad (6.187)$$

where we have included a factor of $1/3$ from the color average for the incoming quarks. Eq. (6.187) can be expressed in terms of the angle between the u quark and the chargino in the center-of-momentum frame, using

$$t = \frac{1}{2} \left[m_{\tilde{C}_i}^2 + m_{\tilde{N}_j}^2 - s + \lambda^{1/2}(s, m_{\tilde{C}_i}^2, m_{\tilde{N}_j}^2) \cos \theta \right], \quad (6.188)$$

$$u = \frac{1}{2} \left[m_{\tilde{C}_i}^2 + m_{\tilde{N}_j}^2 - s - \lambda^{1/2}(s, m_{\tilde{C}_i}^2, m_{\tilde{N}_j}^2) \cos \theta \right]. \quad (6.189)$$

This process occurs in proton-antiproton and proton-proton collisions, where \sqrt{s} is not fixed, and the angle θ is different than the lab frame angle. The usable cross-section depends crucially on experimental cuts. Our result in Eq. (6.187) agrees with the complete computation in [91]. Earlier calculations in special supersymmetric scenarios, *e.g.* with photino mass eigenstates are given in [87, 92]

6.15 $\tilde{N}_i \rightarrow \tilde{N}_j \tilde{N}_k \tilde{N}_\ell$

Next we consider the decay of a neutralino \tilde{N}_i to three lighter neutralinos: $\tilde{N}_j, \tilde{N}_k, \tilde{N}_\ell$. This decay is not likely to be phenomenologically relevant, because a variety of two-body decay modes will always be available. Furthermore, the calculation itself is quite complicated because of the large number of Feynman diagrams involved. Therefore, we consider this only as a matter-of-principle example of a process with four external-state Majorana fermions, and will restrict ourselves to writing down the contributing matrix element amplitudes.

At tree-level, the decay can proceed via a virtual Z^0 boson; the Feynman graphs are shown in Fig. 46. In addition, it can proceed via the exchange of any of the neutral scalar Higgs bosons

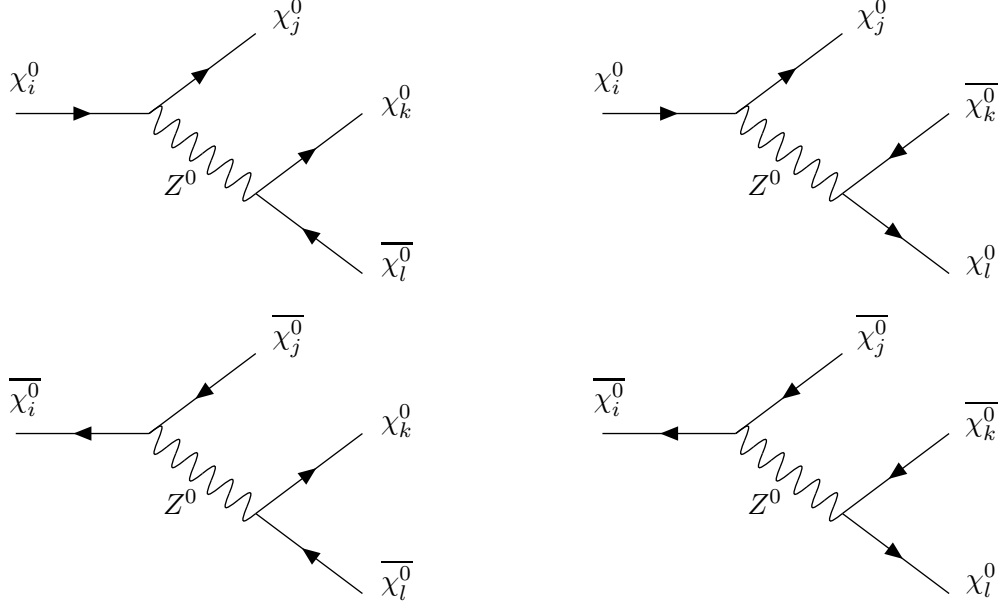


Figure 46: Four Feynman diagrams for $\tilde{N}_i \rightarrow \tilde{N}_j \tilde{N}_k \tilde{N}_\ell$ in the MSSM via Z^0 exchange. There are four more where $\tilde{N}_j \leftrightarrow \tilde{N}_k$ and another four where $\tilde{N}_j \leftrightarrow \tilde{N}_\ell$.

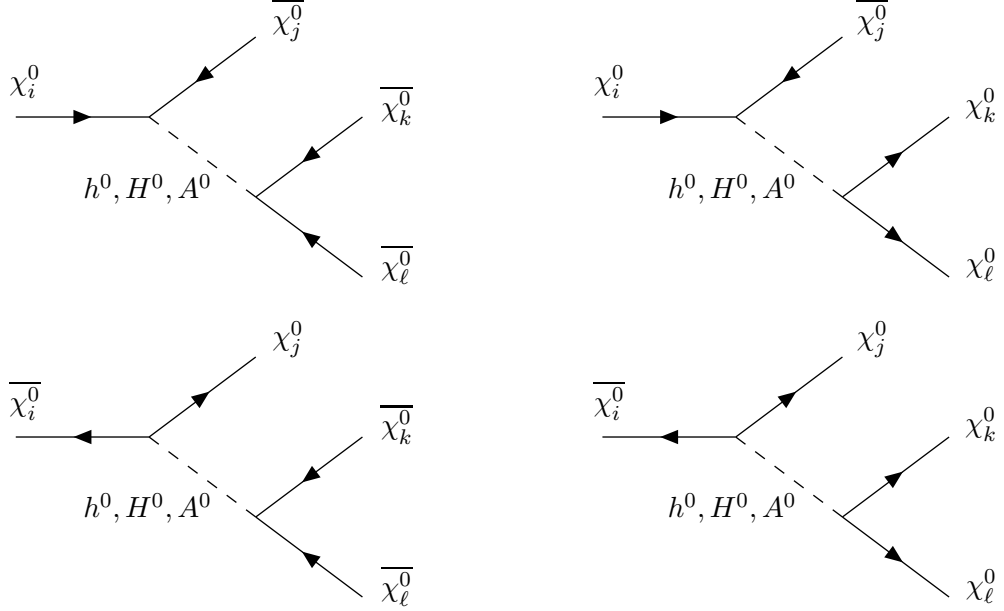


Figure 47: Four Feynman diagrams for $\tilde{N}_i \rightarrow \tilde{N}_j \tilde{N}_k \tilde{N}_\ell$ in the MSSM via $\phi^0 = h^0, H^0, A^0$ exchange. There are four more where $\tilde{N}_j \leftrightarrow \tilde{N}_k$ and another four where $\tilde{N}_j \leftrightarrow \tilde{N}_\ell$.

of the MSSM, $\phi^0 = h^0, H^0, A^0$, as shown in Fig. 47. Since any of the final state neutralinos can directly couple to the initial state neutralino there are two more diagrams for each one shown in Figs. 46 and 47, for a total of 48 tree-level diagrams (counting each intermediate Higgs boson state as distinct). In all cases, the four-momenta of the neutralinos $\tilde{N}_i, \tilde{N}_j, \tilde{N}_k, \tilde{N}_\ell$ are denoted p_i, k_j, k_k, k_ℓ respectively.

For the sum of the four diagrams in Fig. 46, we obtain by implementing the rules of Fig. 72, and using the Feynman gauge:

$$i\mathcal{M}_Z^{(1)} = \frac{-ig^2/c_W^2}{(p_i - k_j)^2 - m_Z^2} \left(O_{ji}^{\prime L} x_i \sigma_\mu \bar{x}_j - O_{ij}^{\prime L} \bar{y}_i \bar{\sigma}_\mu y_j \right) \left(O_{\ell k}^{\prime L} \bar{x}_k \bar{\sigma}^\mu y_\ell - O_{k\ell}^{\prime L} y_k \sigma^\mu \bar{x}_\ell \right), \quad (6.190)$$

[The external wave functions are $x_i \equiv x(\vec{p}_i, \lambda_i)$, $x_{j,k,\ell} \equiv x(\vec{k}_{j,k,\ell}, \lambda_{j,k,\ell})$, and analogously for $\bar{x}_{i,j,k,\ell}$, and $y_{i,j,k,\ell}$ and $\bar{y}_{i,j,k,\ell}$.] Note that we have factorized the sum of diagrams, taking advantage of the common virtual boson line propagator. The contributions from the diagrams related to these by permutations can now be obtained from the appropriate substitutions ($j \leftrightarrow k$) and ($j \leftrightarrow \ell$):

$$i\mathcal{M}_Z^{(2)} = (-1) \frac{-ig^2/c_W^2}{(p_i - k_k)^2 - m_Z^2} \left(O_{ki}^{\prime L} x_i \sigma_\mu \bar{x}_k - O_{ik}^{\prime L} \bar{y}_i \bar{\sigma}_\mu y_k \right) \left(O_{\ell j}^{\prime L} \bar{x}_j \bar{\sigma}^\mu y_\ell - O_{j\ell}^{\prime L} y_j \sigma^\mu \bar{x}_\ell \right), \quad (6.191)$$

$$i\mathcal{M}_Z^{(3)} = (-1) \frac{-ig^2/c_W^2}{(p_i - k_\ell)^2 - m_Z^2} \left(O_{\ell i}^{\prime L} x_i \sigma_\mu \bar{x}_\ell - O_{i\ell}^{\prime L} \bar{y}_i \bar{\sigma}_\mu y_\ell \right) \left(O_{jk}^{\prime L} \bar{x}_k \bar{\sigma}^\mu y_j - O_{kj}^{\prime L} y_k \sigma^\mu \bar{x}_j \right). \quad (6.192)$$

The first factors of (-1) in $i\mathcal{M}_Z^{(2)}$ and $i\mathcal{M}_Z^{(3)}$ are present because the order of the spinors in each case appear in an odd permutation of the canonical order set by $i\mathcal{M}_Z^{(1)}$. Note that if we were to proceed to a computation of the decay rate, the very first step would be to apply the Fierz relations of eqs. (2.55)-(2.57) to eliminate all of the σ and $\bar{\sigma}$ matrices in the above amplitudes.

The diagrams in Fig. (47) combine to give a contribution:

$$i\mathcal{M}_{\phi^0}^{(1)} = \frac{-i}{(p_i - k_j)^2 - m_{\phi^0}^2} (Y^{ij} x_i y_j + Y_{ij} \bar{y}_i \bar{x}_j) (Y^{k\ell} y_k y_\ell + Y_{k\ell} \bar{x}_k \bar{x}_\ell) \quad (6.193)$$

where we have adopted the shorthand notation $Y^{ij} = (Y_{ij})^* = Y^{\phi^0} \chi_i^0 \chi_j^0$. Again we have factored the amplitude using the common virtual boson propagator. As in the Z -exchange diagrams, the other contributions can be obtained by the appropriate substitutions:

$$i\mathcal{M}_{\phi^0}^{(2)} = (-1) \frac{-i}{(p_i - k_k)^2 - m_{\phi^0}^2} (Y^{ik} x_i y_k + Y_{ik} \bar{y}_i \bar{x}_k) (Y^{j\ell} y_j y_\ell + Y_{j\ell} \bar{x}_j \bar{x}_\ell) \quad (6.194)$$

$$i\mathcal{M}_{\phi^0}^{(3)} = (-1) \frac{-i}{(p_i - k_\ell)^2 - m_{\phi^0}^2} (Y^{i\ell} x_i y_\ell + Y_{i\ell} \bar{y}_i \bar{x}_\ell) (Y^{kj} y_k y_j + Y_{kj} \bar{x}_k \bar{x}_j) \quad (6.195)$$

The first factors of (-1) in $i\mathcal{M}_{\phi^0}^{(2)}$ and $i\mathcal{M}_{\phi^0}^{(3)}$ are needed because the spinors in each case are in an odd permutation of the canonical order established earlier.

Now the total matrix element is obtained by:

$$\mathcal{M} = \sum_{n=1}^3 \mathcal{M}_Z^{(n)} + \sum_{\phi^0} \sum_{n=1}^3 \mathcal{M}_{\phi^0}^{(n)} \quad (6.196)$$

as given above. When computing the total decay rate, additional attention must be paid to the case where two or more final state indices are equal, since the phase space is then reduced by the corresponding factor to avoid over-counting of identical final states. To the best of our knowledge this process has not been computed in the literature.

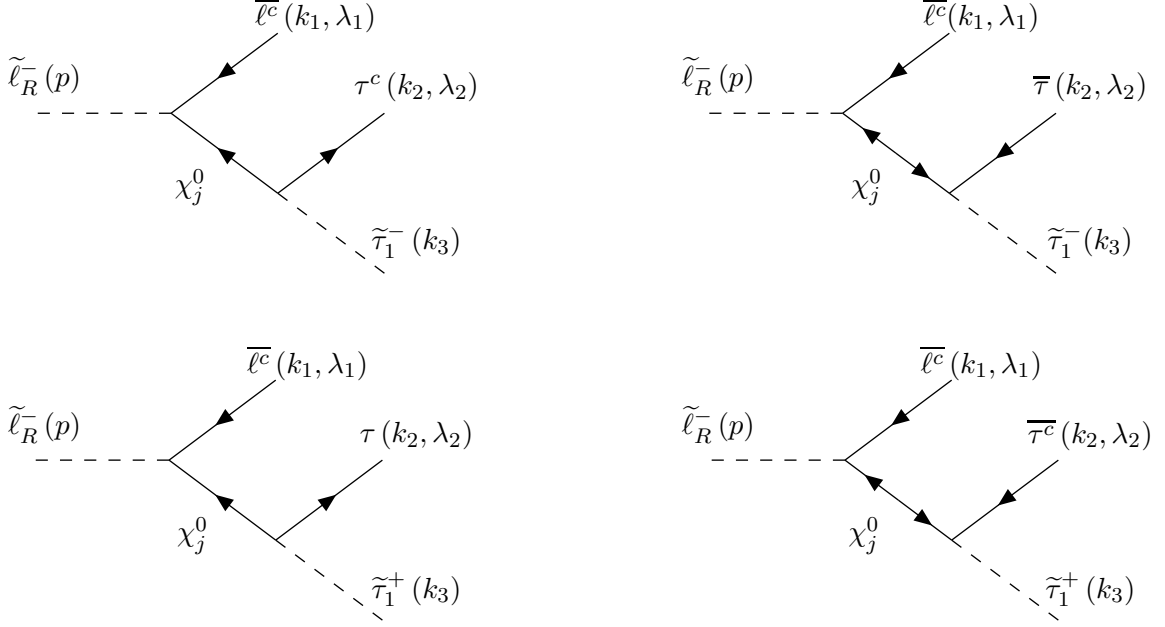


Figure 48: Feynman diagrams for the three-body slepton decays $\tilde{\ell}_R^- \rightarrow \ell^- \tau^+ \tilde{\tau}_1^-$ (top row) and $\tilde{\ell}_R^- \rightarrow \ell^- \tau^- \tilde{\tau}_1^+$ (bottom row) in the MSSM.

6.16 Three-body slepton decays $\tilde{\ell}_R^- \rightarrow \ell^- \tau^\pm \tilde{\tau}_1^\mp$ for $\ell = e, \mu$

In this subsection, we consider the three-body decays of sleptons through a virtual neutralino. The usual assumption in supersymmetric phenomenology is that these decays will have a very small branching fraction, because a two-body decay to a lighter neutralino and lepton is always open. However, in Gauge Mediated Supersymmetry Breaking models with a non-minimal messenger sector, the sleptons can be lighter than the lightest neutralino [93, 94]. In that case, the mostly right-handed smuon and selectron, $\tilde{\mu}_R$ and \tilde{e}_R , will decay by $\tilde{\ell}_R^- \rightarrow \ell^- \tau^\pm \tilde{\tau}_1^\mp$. The lightest stau mass eigenstate, $\tilde{\tau}_1^\pm$, is a mixture of the weak eigenstates $\tilde{\tau}_L^\pm$ and $\tilde{\tau}_R^\pm$, as described in Appendix I.4:

$$\tilde{\tau}_1^- = c_\tau^* \tilde{\tau}_R^- + s_\tau^* \tilde{\tau}_L^-, \quad (6.197)$$

and $\tilde{\tau}_1^+ = (\tilde{\tau}_1^-)^*$, while the $\tilde{\mu}_R$ and \tilde{e}_R are taken to be unmixed.

First consider the decay $\tilde{\ell}_R^- \rightarrow \ell^- \tau^+ \tilde{\tau}_1^-$, which proceed by the diagrams in the first row of Fig. 48. The momenta and polarizations of the particles are also indicated on the diagram. Using the Feynman rules of Fig. 78, we find that the amplitudes of these two diagrams, for each neutralino \tilde{N}_j exchanged, are:

$$i\mathcal{M}_1 = (-ia_j^{\tilde{\ell}})(-ia_j^{\tilde{\tau}^*}) y_1 \left[\frac{-i(p-k_1) \cdot \sigma}{(p-k_1)^2 - m_{\tilde{N}_j}^2} \right] \bar{x}_2, \quad (6.198)$$

$$i\mathcal{M}_2 = (-ia_j^{\tilde{\ell}})(-ib_j^{\tilde{\tau}}) y_1 \left[\frac{im_{\tilde{N}_j}}{(p-k_1)^2 - m_{\tilde{N}_j}^2} \right] y_2. \quad (6.199)$$

where

$$a_j^{\tilde{\ell}} = \sqrt{2}g'N_{j1}^*, \quad (6.200)$$

$$a_j^{\tilde{\tau}} = Y_\tau N_{j3}^* s_{\tilde{\tau}} + \sqrt{2}g'N_{j1}^* c_{\tilde{\tau}}, \quad (6.201)$$

$$b_j^{\tilde{\tau}} = Y_\tau N_{j3}^* c_{\tilde{\tau}}^* - \frac{1}{\sqrt{2}}(gN_{j2}^* + g'N_{j1}^*)s_{\tilde{\tau}}^*. \quad (6.202)$$

The spinor wavefunction factors are $y_1 = y(\vec{k}_1, \lambda_1)$, $y_2 = y(\vec{k}_2, \lambda_2)$, and $\bar{x}_2 = \bar{x}(\vec{k}_2, \lambda_2)$.

In the following, we will use the kinematic variables

$$z_\ell \equiv 2p \cdot k_1 / m_{\tilde{\ell}_R}^2 = 2E_\ell / m_{\tilde{\ell}_R}, \quad z_\tau \equiv 2p \cdot k_2 / m_{\tilde{\ell}_R}^2 = 2E_\tau / m_{\tilde{\ell}_R}, \quad (6.203)$$

$$r_{\tilde{N}_j} \equiv m_{\tilde{N}_j} / m_{\tilde{\ell}_R}, \quad r_{\tilde{\tau}} \equiv m_{\tilde{\tau}_1} / m_{\tilde{\ell}_R}, \quad (6.204)$$

$$r_\tau \equiv m_\tau / m_{\tilde{\ell}_R}, \quad r_\ell \equiv m_\ell / m_{\tilde{\ell}_R}. \quad (6.205)$$

The total amplitude then can be written as

$$\mathcal{M} = \sum_{j=1}^4 [c_j y_1(p - k_1) \cdot \sigma \bar{x}_2 + d_j y_1 y_2] \quad (6.206)$$

where

$$c_j = -a_j^{\tilde{\ell}} a_j^{\tilde{\tau}*} / [m_{\tilde{\ell}_R}^2 (r_{\tilde{N}_j}^2 - 1 + z_\ell)], \quad (6.207)$$

$$d_j = a_j^{\tilde{\ell}} b_j^{\tilde{\tau}} m_{\tilde{N}_j} / [m_{\tilde{\ell}_R}^2 (r_{\tilde{N}_j}^2 - 1 + z_\ell)]. \quad (6.208)$$

We consistently neglect the electron and muon Yukawa couplings (so $r_\ell = 0$) in the matrix elements, but not below in the kinematic integration over phase space, where the muon mass can be important.

Now using eqs. (2.30) and (2.31), we find

$$\begin{aligned} |\mathcal{M}|^2 = \sum_{j,k} \Big[& c_j c_k^* y_1(p - k_1) \cdot \sigma \bar{x}_2 x_2(p - k_1) \cdot \sigma \bar{y}_1 + d_j d_k^* y_1 y_2 \bar{y}_2 \bar{y}_1 \\ & + c_j d_k^* y_1(p - k_1) \cdot \sigma \bar{x}_2 \bar{y}_2 \bar{y}_1 + c_j^* d_k x_2(p - k_1) \cdot \sigma \bar{y}_1 y_1 y_2 \Big]. \end{aligned} \quad (6.209)$$

Now summing over the lepton spins using eqs. (3.56)-(3.59),

$$\begin{aligned} \sum_{\lambda_1, \lambda_2} |\mathcal{M}|^2 = \sum_{j,k} \Big[& c_j c_k^* \text{Tr}[(p - k_1) \cdot \sigma k_2 \cdot \vec{\sigma} (p - k_1) \cdot \sigma k_1 \cdot \vec{\sigma}] + d_j d_k^* \text{Tr}[k_2 \cdot \sigma k_1 \cdot \vec{\sigma}] \\ & - c_j d_k^* m_\tau \text{Tr}[(p - k_1) \cdot \sigma k_1 \cdot \vec{\sigma}] - c_j^* d_k m_\tau \text{Tr}[(p - k_1) \cdot \sigma k_1 \cdot \vec{\sigma}] \Big]. \end{aligned} \quad (6.210)$$

Taking the traces using eqs. (2.43) and (2.44) yields

$$\sum_{\text{spins}} |\mathcal{M}|^2 = \sum_{j,k} \left\{ c_j c_k^* [4k_1 \cdot (p - k_1) k_2 \cdot (p - k_1) - 2k_1 \cdot k_2 (p - k_1)^2] + 2d_j d_k^* k_1 \cdot k_2 - 4\text{Re}[c_j d_k^*] m_\tau k_1 \cdot (p - k_1) \right\} \quad (6.211)$$

$$= \sum_{j,k} \left\{ c_j c_k^* m_{\tilde{\ell}_R}^4 [(1 - z_\ell)(1 - z_\tau) - r_\tau^2 + r_\tau^2] + d_j d_k^* m_{\tilde{\ell}_R}^2 (z_\ell + z_\tau - 1 + r_\tau^2 - r_\tau^2) - 2\text{Re}[c_j d_k^*] m_\tau m_{\tilde{\ell}_R}^2 z_\ell \right\} \quad (6.212)$$

The differential decay rate for $\tilde{\ell}_R^- \rightarrow \ell^- \tau^+ \tilde{\tau}_1^-$ then follows:

$$\frac{d^2\Gamma}{dz_\ell dz_\tau} = \frac{m_{\tilde{\ell}_R}}{256\pi^3} \left(\sum_{\text{spins}} |\mathcal{M}|^2 \right) \quad (6.213)$$

The total decay rate in that channel can be found by integrating over z_ℓ, z_τ , with the limits (see for example ref. [75]):

$$2r_\ell < z_\ell < 1 + r_\ell^2 - (r_\tau + r_\tau)^2, \quad (6.214)$$

$$z_\tau \lesssim \frac{1}{2(1 - z_\ell + r_\ell^2)} \left[(2 - z_\ell)(1 + r_\ell^2 + r_\tau^2 - r_\tau^2 - z_\ell) \pm (z_\ell^2 - 4r_\ell^2)^{1/2} \lambda^{1/2} (1 + r_\ell^2 - z_\ell, r_\tau^2, r_\tau^2) \right]. \quad (6.215)$$

Now we turn to the competing decay $\tilde{\ell}_R^- \rightarrow \ell^- \tau^+ \tilde{\tau}_1^-$, with diagrams appearing in the second row of Fig. 48. By appealing again to the Feynman rules of Fig. 77, we find that the amplitude has exactly the same form as in eqs. (6.198) and (6.199), except now with $a_j^{\tilde{\tau}} \leftrightarrow b_j^{\tilde{\tau}}$. Therefore, the entire previous calculation goes through precisely as before, but now with

$$c_j = -a_j^{\tilde{\ell}} b_j^{\tilde{\tau}*} / [m_{\tilde{\ell}_R}^2 (r_{\tilde{N}_j}^2 - 1 + z_\ell)], \quad (6.216)$$

$$d_j = a_j^{\tilde{\ell}} a_j^{\tilde{\tau}} m_{\tilde{N}_j} / [m_{\tilde{\ell}_R}^2 (r_{\tilde{N}_j}^2 - 1 + z_\ell)]. \quad (6.217)$$

The differential decay widths found above can be integrated to find the total decay widths. The results agree with ref. [95], except that the signs of the coefficient $c_{ij}^{(3)}$ and $c_{ij}^{(4)}$ in that paper are incorrect and should be flipped. (Also, the notations for the sfermion mixing angle are different in that paper.) If $m_{\tilde{\ell}_R} - m_{\tilde{\tau}_1} - m_\tau$ is not too large, the resulting decays can have a macroscopic length in a detector, and the ratio of the two decay modes can provide an interesting probe of the supersymmetric Lagrangian.

6.17 Neutralino decay to photon and Goldstino: $\tilde{N}_i \rightarrow \gamma \tilde{G}$

The Goldstino \tilde{G} is a Weyl fermion that couples to the neutralino and photon fields according to the non-renormalizable Lagrangian term [96]:

$$\mathcal{L} = -\frac{a_i}{2} (\chi_i^0 \sigma_\mu \bar{\sigma}_\rho \sigma_\nu \partial^\mu \bar{\tilde{G}}) (\partial^\nu A^\rho - \partial^\rho A^\nu) + \text{c.c.} \quad (6.218)$$

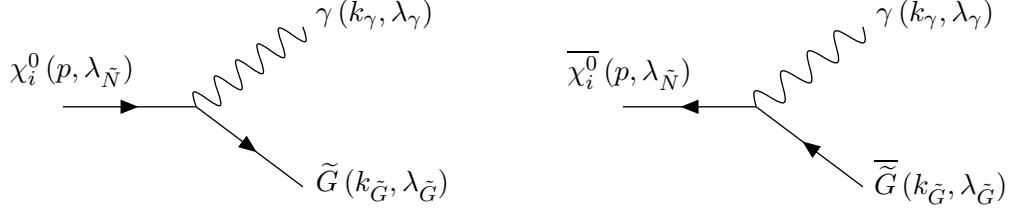


Figure 49: The two Feynman diagrams for $\tilde{N}_i \rightarrow \gamma \tilde{G}$ in supersymmetric models with a light Goldstino.

Here χ_i^0 is the left-handed two-component fermion field that corresponds to the neutralino \tilde{N}_i particle, \tilde{G} is the two-component fermion field corresponding to the (nearly) massless Goldstino, and the effective coupling is

$$a_i \equiv \frac{1}{\sqrt{2}\langle F \rangle} (N_{i1}^* \cos \theta_W + N_{i2}^* \sin \theta_W), \quad (6.219)$$

where N_{ij} the mixing matrix for the neutralinos [see eq. (I.23)], and $\langle F \rangle$ is the F -term expectation value associated with supersymmetry breaking. Therefore \tilde{N}_i can decay to γ plus \tilde{G} through the diagrams shown in Fig. 49, with amplitudes:

$$i\mathcal{M}_1 = i\frac{a_i}{2} x_{\tilde{N}} k_{\tilde{G}} \cdot \sigma (\varepsilon^* \cdot \bar{\sigma} k_\gamma \cdot \sigma - k_\gamma \cdot \bar{\sigma} \varepsilon^* \cdot \sigma) \bar{x}_{\tilde{G}}, \quad (6.220)$$

$$i\mathcal{M}_2 = -i\frac{a_i^*}{2} \bar{y}_{\tilde{N}} k_{\tilde{G}} \cdot \bar{\sigma} (\varepsilon^* \cdot \sigma k_\gamma \cdot \bar{\sigma} - k_\gamma \cdot \sigma \varepsilon^* \cdot \bar{\sigma}) y_{\tilde{G}}. \quad (6.221)$$

Here $x_{\tilde{N}} \equiv x(\vec{p}, \lambda_{\tilde{N}})$, $\bar{y}_{\tilde{N}} \equiv \bar{y}(\vec{p}, \lambda_{\tilde{N}})$, and $\bar{x}_{\tilde{G}} \equiv \bar{x}(\vec{k}_{\tilde{G}}, \lambda_{\tilde{G}})$, $y_{\tilde{G}} \equiv y(\vec{k}_{\tilde{G}}, \lambda_{\tilde{G}})$, and $\varepsilon^* = \varepsilon^*(\vec{k}_\gamma, \lambda_\gamma)$ are the external wavefunction factors for the neutralino, Goldstino, and photon, respectively. Using the on-shell condition $k_\gamma \cdot \varepsilon^* = 0$, we have $k_\gamma \cdot \sigma \varepsilon^* \cdot \bar{\sigma} = -\varepsilon^* \cdot \sigma k_\gamma \cdot \bar{\sigma}$ and $k_\gamma \cdot \bar{\sigma} \varepsilon^* \cdot \sigma = -\varepsilon^* \cdot \bar{\sigma} k_\gamma \cdot \sigma$ from eqs. (2.39) and (2.40). So we can rewrite the total amplitude as

$$\mathcal{M} = \mathcal{M}_1 + \mathcal{M}_2 = x_{\tilde{N}} A \bar{x}_{\tilde{G}} + \bar{y}_{\tilde{N}} B y_{\tilde{G}} \quad (6.222)$$

where

$$A = a_i k_{\tilde{G}} \cdot \sigma \varepsilon^* \cdot \bar{\sigma} k_\gamma \cdot \sigma, \quad (6.223)$$

$$B = -a_i^* k_{\tilde{G}} \cdot \bar{\sigma} \varepsilon^* \cdot \sigma k_\gamma \cdot \bar{\sigma}. \quad (6.224)$$

The complex square of the matrix element is therefore

$$|\mathcal{M}|^2 = x_{\tilde{N}} A \bar{x}_{\tilde{G}} x_{\tilde{G}} \hat{A} \bar{x}_{\tilde{N}} + \bar{y}_{\tilde{N}} B y_{\tilde{G}} \bar{y}_{\tilde{G}} \hat{B} y_{\tilde{N}} + x_{\tilde{N}} A \bar{x}_{\tilde{G}} \bar{y}_{\tilde{G}} \hat{B} y_{\tilde{N}} + \bar{y}_{\tilde{N}} B y_{\tilde{G}} x_{\tilde{G}} \hat{A} \bar{x}_{\tilde{N}}, \quad (6.225)$$

where \hat{A} and \hat{B} are obtained from A and B by reversing the order of the σ and $\bar{\sigma}$ matrices and taking the complex conjugates of a_i and ε . [See the discussion surrounding eqs. (4.23) and (4.24).]

Summing over the Goldstino spins using eqs. (3.56)-(3.59) now yields:

$$\sum_{\lambda_{\tilde{G}}} |\mathcal{M}|^2 = x_{\tilde{N}} A k_{\tilde{G}} \cdot \bar{\sigma} \hat{A} \bar{x}_{\tilde{N}} + \bar{y}_{\tilde{N}} B k_{\tilde{G}} \cdot \sigma \hat{B} y_{\tilde{N}}. \quad (6.226)$$

(The A, \hat{B} and \hat{A}, B cross terms vanish because of $m_{\tilde{G}} = 0$.) Now averaging over the neutralino spins using eqs. (3.56) and (3.57), we find

$$\frac{1}{2} \sum_{\lambda_{\tilde{N}}, \lambda_{\tilde{G}}} |\mathcal{M}|^2 = \frac{1}{2} \text{Tr}[A k_{\tilde{G}} \cdot \bar{\sigma} \hat{A} p \cdot \bar{\sigma}] + \frac{1}{2} \text{Tr}[B k_{\tilde{G}} \cdot \sigma \hat{B} p \cdot \sigma]. \quad (6.227)$$

$$= \frac{1}{2} |a_i|^2 \text{Tr}[\varepsilon^* \cdot \bar{\sigma} k_{\gamma} \cdot \sigma k_{\tilde{G}} \cdot \bar{\sigma} k_{\gamma} \cdot \sigma \varepsilon \cdot \bar{\sigma} k_{\tilde{G}} \cdot \sigma p \cdot \bar{\sigma} k_{\tilde{G}} \cdot \sigma] + (\sigma \leftrightarrow \bar{\sigma}). \quad (6.228)$$

Now use

$$k_{\gamma} \cdot \sigma k_{\tilde{G}} \cdot \bar{\sigma} k_{\gamma} \cdot \sigma = 2 k_{\tilde{G}} \cdot k_{\gamma} k_{\gamma} \cdot \sigma, \quad (6.229)$$

$$k_{\tilde{G}} \cdot \sigma p \cdot \bar{\sigma} k_{\tilde{G}} \cdot \sigma = 2 k_{\tilde{G}} \cdot p k_{\tilde{G}} \cdot \sigma, \quad (6.230)$$

which follow from eq. (2.41), and the corresponding identities with $\sigma \leftrightarrow \bar{\sigma}$, to obtain:

$$\frac{1}{2} \sum_{\lambda_{\tilde{N}}, \lambda_{\tilde{G}}} |\mathcal{M}|^2 = 2 |a_i|^2 (k_{\tilde{G}} \cdot k_{\gamma}) (k_{\tilde{G}} \cdot p) \text{Tr}[\varepsilon^* \cdot \bar{\sigma} k_{\gamma} \cdot \sigma \varepsilon \cdot \bar{\sigma} k_{\tilde{G}} \cdot \sigma] + (\sigma \leftrightarrow \bar{\sigma}). \quad (6.231)$$

Applying the photon spin sum identity

$$\sum_{\lambda_{\gamma}} \varepsilon^{\mu} \varepsilon^{\nu*} = -g^{\mu\nu} \quad (6.232)$$

and the trace identities eq. (2.44) and (2.45), we get

$$\frac{1}{2} \sum_{\lambda_{\gamma}, \lambda_{\tilde{N}}, \lambda_{\tilde{G}}} |\mathcal{M}|^2 = 16 |a_i|^2 (k_{\tilde{G}} \cdot k_{\gamma})^2 (k_{\tilde{G}} \cdot p) = 2 |a_i|^2 m_{\tilde{N}_i}^6. \quad (6.233)$$

So, the decay rate is [97]:

$$\Gamma(\tilde{N}_i \rightarrow \gamma \tilde{G}) = \frac{1}{16\pi m_{\tilde{N}_i}} \left(\frac{1}{2} \sum_{\lambda_{\gamma}, \lambda_{\tilde{N}}, \lambda_{\tilde{G}}} |\mathcal{M}|^2 \right) = |N_{i1} \cos \theta_W + N_{i2} \sin \theta_W|^2 \frac{m_{\tilde{N}_i}^5}{16\pi |\langle F \rangle|^2}. \quad (6.234)$$

6.18 Gluino pair production from gluon fusion: $gg \rightarrow \tilde{g}\tilde{g}$

In this subsection we will compute the cross-section for the process $gg \rightarrow \tilde{g}\tilde{g}$. The relevant Feynman diagrams are shown in Figure 50. The initial state gluons have $SU(3)_c$ adjoint representation indices a and b , with momenta p_1 and p_2 and polarization vectors $\varepsilon_1^{\mu} = \varepsilon^{\mu}(\vec{p}_1, \lambda_1)$ and $\varepsilon_2^{\mu} = \varepsilon^{\mu}(\vec{p}_2, \lambda_2)$ respectively. The final state gluinos carry adjoint representation indices c and d , with momenta k_1 and k_2 and wavefunction spinors $\bar{x}_1 = \bar{x}(\vec{k}_1, \lambda'_1)$ or $y_1 = y(\vec{k}_1, \lambda'_1)$ and $\bar{x}_2 = \bar{x}(\vec{k}_2, \lambda'_2)$ or $y_2 = y(\vec{k}_2, \lambda'_2)$, respectively.

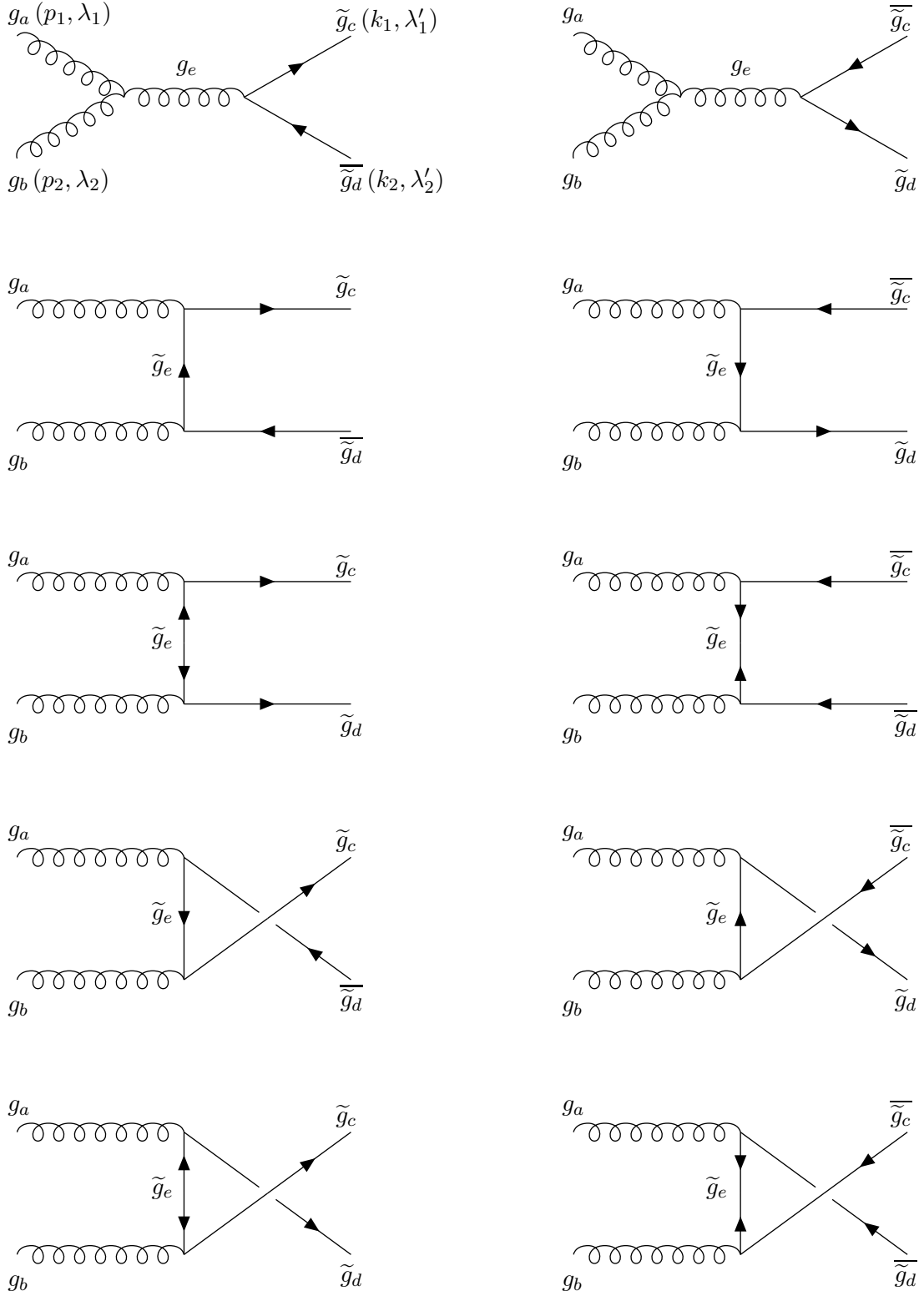


Figure 50: The ten Feynman diagrams for $gg \rightarrow \tilde{g}\tilde{g}$. The momentum and spin polarization assignments are indicated on the first diagram.

The Feynman rules for the gluino couplings in SUSYQCD are given in Fig. 79. For the two s -channel amplitudes, we obtain:

$$i\mathcal{M}_s = \left(-g_s f^{abe} [g_{\mu\nu}(p_1 - p_2)_\rho + g_{\nu\rho}(p_1 + 2p_2)_\mu - g_{\mu\rho}(2p_1 + p_2)_\nu] \right) \left(\frac{-ig^{\rho\kappa}}{s} \right) \varepsilon_1^\mu \varepsilon_2^\nu \left[(-g_s f^{cde}) \bar{x}_1 \bar{\sigma}_\kappa y_2 + (g_s f^{dce}) y_1 \sigma_\kappa \bar{x}_2 \right]. \quad (6.235)$$

The first factor is the Feynman rule for the three-gluon interaction of standard QCD, and the second factor is the gluon propagator. The next four (t -channel) diagrams have a total amplitude:

$$\begin{aligned} i\mathcal{M}_t = & (-g_s f^{cea} \varepsilon_1^\mu) (-g_s f^{edb} \varepsilon_2^\nu) \bar{x}_1 \bar{\sigma}_\mu \left[\frac{i(k_1 - p_1) \cdot \sigma}{(k_1 - p_1)^2 - m_{\tilde{g}}^2} \right] \bar{\sigma}_\nu y_2 \\ & + (g_s f^{eca} \varepsilon_1^\mu) (g_s f^{deb} \varepsilon_2^\nu) y_1 \sigma_\mu \left[\frac{i(k_1 - p_1) \cdot \bar{\sigma}}{(k_1 - p_1)^2 - m_{\tilde{g}}^2} \right] \sigma_\nu \bar{x}_2 \\ & + (-g_s f^{cea} \varepsilon_1^\mu) (g_s f^{deb} \varepsilon_2^\nu) \bar{x}_1 \bar{\sigma}_\mu \left[\frac{im_{\tilde{g}}}{(k_1 - p_1)^2 - m_{\tilde{g}}^2} \right] \sigma_\nu \bar{x}_2 \\ & + (g_s f^{eca} \varepsilon_1^\mu) (-g_s f^{edb} \varepsilon_2^\nu) y_1 \sigma_\mu \left[\frac{im_{\tilde{g}}}{(k_1 - p_1)^2 - m_{\tilde{g}}^2} \right] \bar{\sigma}_\nu y_2. \end{aligned} \quad (6.236)$$

Finally, the u -channel Feynman diagrams result in:

$$\begin{aligned} i\mathcal{M}_u = & (-g_s f^{eda} \varepsilon_1^\mu) (-g_s f^{ceb} \varepsilon_2^\nu) \bar{x}_1 \bar{\sigma}_\nu \left[\frac{i(k_1 - p_2) \cdot \sigma}{(k_1 - p_2)^2 - m_{\tilde{g}}^2} \right] \bar{\sigma}_\mu y_2 \\ & + (g_s f^{dea} \varepsilon_1^\mu) (g_s f^{ecb} \varepsilon_2^\nu) y_1 \sigma_\nu \left[\frac{i(k_1 - p_2) \cdot \bar{\sigma}}{(k_1 - p_2)^2 - m_{\tilde{g}}^2} \right] \sigma_\mu \bar{x}_2 \\ & + (g_s f^{dea} \varepsilon_1^\mu) (-g_s f^{ceb} \varepsilon_2^\nu) \bar{x}_1 \bar{\sigma}_\nu \left[\frac{im_{\tilde{g}}}{(k_1 - p_2)^2 - m_{\tilde{g}}^2} \right] \sigma_\mu \bar{x}_2 \\ & + (-g_s f^{eda} \varepsilon_1^\mu) (g_s f^{ecb} \varepsilon_2^\nu) y_1 \sigma_\nu \left[\frac{im_{\tilde{g}}}{(k_1 - p_2)^2 - m_{\tilde{g}}^2} \right] \bar{\sigma}_\mu y_2. \end{aligned} \quad (6.237)$$

We choose to work with *real* polarization vectors $\varepsilon_1, \varepsilon_2$. Since they must both be orthogonal to the initial-state collision axis in the center of momentum frame, we have:

$$\varepsilon_1 \cdot \varepsilon_1 = \varepsilon_2 \cdot \varepsilon_2 = -1 \quad (6.238)$$

$$\varepsilon_1 \cdot p_1 = \varepsilon_2 \cdot p_1 = \varepsilon_1 \cdot p_2 = \varepsilon_2 \cdot p_2 = 0, \quad (6.239)$$

$$\varepsilon_1 \cdot k_2 = -\varepsilon_1 \cdot k_1, \quad \varepsilon_2 \cdot k_2 = -\varepsilon_2 \cdot k_1, \quad (6.240)$$

and the sums over gluon polarizations will be accomplished by:

$$\sum_{\lambda_1} \varepsilon_1^\mu \varepsilon_1^\nu = \sum_{\lambda_2} \varepsilon_2^\mu \varepsilon_2^\nu = g^{\mu\nu} + 2(p_1^\mu p_2^\nu + p_2^\mu p_1^\nu) / s. \quad (6.241)$$

Before taking the complex square of the amplitude, it is convenient to rewrite the last two terms in each of eqs. (6.236) and (6.237) by using the identities [see eq. (3.12)]:

$$m_{\tilde{g}}\bar{x}_1 = y_1\bar{\sigma}\cdot k_1, \quad m_{\tilde{g}}y_1 = \bar{x}_1\sigma\cdot k_1. \quad (6.242)$$

Using eqs. (2.41) and (2.42), the resulting total matrix element is then reduced to a sum of terms that each contain exactly one σ or $\bar{\sigma}$ matrix. We define convenient factors:

$$G_s \equiv g_s^2 f^{abe} f^{cde} / s, \quad (6.243)$$

$$G_t \equiv g_s^2 f^{ace} f^{bde} / (t - m_{\tilde{g}}^2), \quad (6.244)$$

$$G_u \equiv g_s^2 f^{ade} f^{bce} / (u - m_{\tilde{g}}^2). \quad (6.245)$$

where the usual Mandelstam variables are:

$$s = (p_1 + p_2)^2 = (k_1 + k_2)^2, \quad (6.246)$$

$$t = (k_1 - p_1)^2 = (k_2 - p_2)^2, \quad (6.247)$$

$$u = (k_1 - p_2)^2 = (k_2 - p_1)^2. \quad (6.248)$$

Then the total amplitude is (noting that the gluon polarizations were chosen real):

$$\mathcal{M} = \mathcal{M}_s + \mathcal{M}_t + \mathcal{M}_u = \bar{x}_1 a \cdot \bar{\sigma} y_2 + y_1 a^* \cdot \sigma \bar{x}_2, \quad (6.249)$$

where

$$\begin{aligned} a^\mu \equiv & -(G_t + G_s)\varepsilon_1 \cdot \varepsilon_2 p_1^\mu - (G_u - G_s)\varepsilon_1 \cdot \varepsilon_2 p_2^\mu - 2G_t k_1 \cdot \varepsilon_1 \varepsilon_2^\mu - 2G_u k_1 \cdot \varepsilon_2 \varepsilon_1^\mu \\ & - i\epsilon^{\mu\nu\rho\kappa} \varepsilon_{1\nu} \varepsilon_{2\rho} (G_t p_1 - G_u p_2)_\kappa. \end{aligned} \quad (6.250)$$

Squaring the amplitude using eqs. (2.31) and (2.32), we get:

$$|\mathcal{M}|^2 = \bar{x}_1 a \cdot \bar{\sigma} y_2 \bar{y}_2 a^* \cdot \bar{\sigma} x_1 + y_1 a^* \cdot \sigma \bar{x}_2 x_2 a \cdot \sigma \bar{y}_1 + \bar{x}_1 a \cdot \bar{\sigma} y_2 x_2 a \cdot \sigma \bar{y}_1 + y_1 a^* \cdot \sigma \bar{x}_2 \bar{y}_2 a^* \cdot \bar{\sigma} x_1. \quad (6.251)$$

Now summing over the gluino spins using eqs. (3.56)-(3.59), we find:

$$\begin{aligned} \sum_{\lambda'_1, \lambda'_2} |\mathcal{M}|^2 = & \text{Tr}[a \cdot \bar{\sigma} k_2 \cdot \sigma a^* \cdot \bar{\sigma} k_1 \cdot \sigma] + \text{Tr}[a^* \cdot \sigma k_2 \cdot \bar{\sigma} a \cdot \sigma k_1 \cdot \bar{\sigma}] \\ & - m_{\tilde{g}}^2 \text{Tr}[a \cdot \bar{\sigma} a \cdot \sigma] - m_{\tilde{g}}^2 \text{Tr}[a^* \cdot \sigma a^* \cdot \bar{\sigma}]. \end{aligned} \quad (6.252)$$

Taking the traces with eqs. (2.43)-(2.45) yields:

$$\sum_{\lambda'_1, \lambda'_2} |\mathcal{M}|^2 = 8\text{Re}[a \cdot k_1 a^* \cdot k_2] - 4a \cdot a^* k_1 \cdot k_2 - 4i\epsilon^{\mu\nu\rho\kappa} k_{1\mu} k_{2\nu} a_\rho a_\kappa^* - 4m_{\tilde{g}}^2 \text{Re}[a^2]. \quad (6.253)$$

Now plugging in eqs. (6.250), we obtain:

$$\begin{aligned} \sum_{\lambda'_1, \lambda'_2} |\mathcal{M}|^2 = & 2(t - m_{\tilde{g}}^2)(u - m_{\tilde{g}}^2)[(G_t + G_u)^2 + 4(G_s + G_t)(G_s - G_u)(\varepsilon_1 \cdot \varepsilon_2)^2] \\ & + 16(G_t + G_u)[G_s(t - u) + G_t(t - m_{\tilde{g}}^2) + G_u(u - m_{\tilde{g}}^2)](\varepsilon_1 \cdot \varepsilon_2)(k_1 \cdot \varepsilon_1)(k_1 \cdot \varepsilon_2) \\ & - 32(G_t + G_u)^2(k_1 \cdot \varepsilon_1)^2(k_1 \cdot \varepsilon_2)^2. \end{aligned} \quad (6.254)$$

The sums over gluon polarizations can be done using eq. (6.241), which implies:

$$\sum_{\lambda_1, \lambda_2} 1 = 4, \quad \sum_{\lambda_1, \lambda_2} (\varepsilon_1 \cdot \varepsilon_2)^2 = 2, \quad (6.255)$$

$$\sum_{\lambda_1, \lambda_2} (\varepsilon_1 \cdot \varepsilon_2)(k_1 \cdot \varepsilon_1)(k_1 \cdot \varepsilon_2) = m_g^2 - (t - m_g^2)(u - m_g^2)/s \quad (6.256)$$

$$\sum_{\lambda_1, \lambda_2} (k_1 \cdot \varepsilon_1)^2 (k_1 \cdot \varepsilon_2)^2 = (m_g^2 - (t - m_g^2)(u - m_g^2)/s)^2. \quad (6.257)$$

Also, we can sum over colors using $f^{abe} f^{cde} f^{abe'} f^{cde'} = 2f^{abe} f^{cde} f^{ace'} f^{bde'} = N_c^2(N_c^2 - 1) = 72$, so:

$$\sum_{\text{colors}} G_s^2 = \frac{72g_s^4}{s^2}, \quad \sum_{\text{colors}} G_t^2 = \frac{72g_s^4}{(t - m_g^2)^2}, \quad (6.258)$$

$$\sum_{\text{colors}} G_u^2 = \frac{72g_s^4}{(u - m_g^2)^2}, \quad \sum_{\text{colors}} G_s G_t = \frac{36g_s^4}{s(t - m_g^2)}, \quad (6.259)$$

$$\sum_{\text{colors}} G_s G_u = -\frac{36g_s^4}{s(u - m_g^2)}, \quad \sum_{\text{colors}} G_t G_u = \frac{36g_s^4}{(t - m_g^2)(u - m_g^2)}. \quad (6.260)$$

Putting the factors together, and averaging over the initial state colors and spins, we have:

$$\frac{d\sigma}{dt} = \frac{1}{16\pi s^2} \left(\frac{1}{64} \sum_{\text{colors}} \frac{1}{4} \sum_{\text{spins}} |\mathcal{M}|^2 \right) \quad (6.261)$$

$$= \frac{9\pi\alpha_s^2}{4s^4} \left[2(t - m_g^2)(u - m_g^2) - 3s^2 - 4m_g^2 s + \frac{s^2(s + 2m_g^2)^2}{(t - m_g^2)(u - m_g^2)} - \frac{4m_g^4 s^4}{(t - m_g^2)^2(u - m_g^2)^2} \right], \quad (6.262)$$

which agrees with the result of [87, 98] (after some rearrangement). Note that in the center-of-momentum frame, the Mandelstam variable t is related to the scattering angle θ between an initial-state gluon and a final-state gluino by:

$$t = m_g^2 + \left(\cos \theta \sqrt{1 - 4m_g^2/s} - 1 \right) s/2. \quad (6.263)$$

Since the final state has identical particles, the total cross-section can now be obtained by:

$$\sigma = \frac{1}{2} \int_{t_-}^{t_+} \frac{d\sigma}{dt} dt \quad (6.264)$$

where t_{\pm} are obtained by inserting $\cos \theta = \pm 1$ into eq. (6.263)..

6.19 R-parity violating stau decay: $\tilde{\tau}_R^+ \rightarrow e^+ \bar{\nu}_\mu$

Next we consider the decay of a right-handed scalar tau via an R-parity violating $LL\bar{E}$ coupling. This is particularly relevant for a scalar tau LSP [99, 100] and resonant slepton production [101].

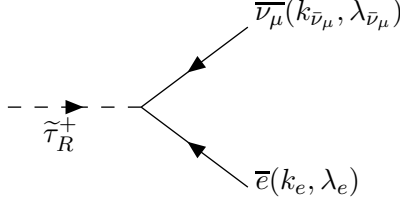


Figure 51: Feynman diagram for the R-parity violating decay $\tilde{\tau}_R^+ \rightarrow e^+ \bar{\nu}_\mu$

The Feynman diagram is shown in Fig. 6.19, where we have also defined the momenta and the helicities of the fermions. The amplitude is given by

$$i\mathcal{M} = -i\lambda y_e y_{\bar{\nu}_\mu}, \quad (6.265)$$

where we have denoted the external wave functions as $y_e \equiv y(\vec{k}_e, \lambda_e)$, and $y_{\bar{\nu}_\mu} \equiv y(\vec{k}_{\bar{\nu}_\mu}, \lambda_{\bar{\nu}_\mu})$, respectively. We have also written the R-parity-violating Yukawa coupling as $\lambda \equiv \lambda_{123}$ (see Appendix J). Using eq. (2.30), the amplitude squared is

$$|\mathcal{M}|^2 = |\lambda|^2 y_e y_{\bar{\nu}_\mu} \bar{y}_{\bar{\nu}_\mu} \bar{y}_e. \quad (6.266)$$

Summing over the fermion spins using eqs. (3.57) gives:

$$\sum_{\lambda_e, \lambda_{\bar{\nu}_\mu}} |\mathcal{M}|^2 = |\lambda|^2 \text{Tr}[k_e \cdot \sigma k_{\bar{\nu}_\mu} \cdot \bar{\sigma}] = |\lambda|^2 m_{\tilde{\tau}_R}^2, \quad (6.267)$$

where in the last step we have used the trace formula eq. (2.43), and neglected the mass of the electron and the neutrino. The total decay rate is then given by

$$\Gamma = \frac{1}{16\pi m_{\tilde{\tau}_R}} \left(\sum_{\lambda_e, \lambda_{\bar{\nu}_\mu}} |\mathcal{M}|^2 \right) = \frac{|\lambda|^2}{16\pi} m_{\tilde{\tau}_R}, \quad (6.268)$$

which agrees with the computation in [102–104]. Completely analogously we can obtain the total rate for the decays $\tilde{\nu}_\mu \rightarrow \tau^- e^+$ and $\tilde{e}_L \rightarrow \tau^- \bar{\nu}_\mu$, which proceed via the same operator, by replacing $m_{\tilde{\tau}_R} \rightarrow (m_{\tilde{e}_L}, m_{\tilde{\nu}_\mu})$, respectively.

In general the two-body decay rate of a sfermion \tilde{f} via the $LQ\bar{D}$ or $\bar{U}\bar{D}\bar{D}$ interaction is given by

$$\Gamma(\tilde{f} \rightarrow f_1 f_2) = \frac{C|\lambda|^2}{16\pi} m_{\tilde{f}}, \quad (6.269)$$

where we have neglected the masses $m_{1,2}$ of the final state fermions. The factor C denotes the color factor. For the slepton decays via $LQ\bar{D}$ which are summed over the final-state quark colors, $C = N_c = 3$. For the squark decays via $LQ\bar{D}$ where the initial state color is averaged over and the final-state color is summed, $C = 1$. For the squark decays via $\bar{U}\bar{D}\bar{D}$, $C = (N_c - 1)! = 2$. In realistic cases, one must also include the effects of mixing for the third-family sfermions, which we have omitted here for simplicity.

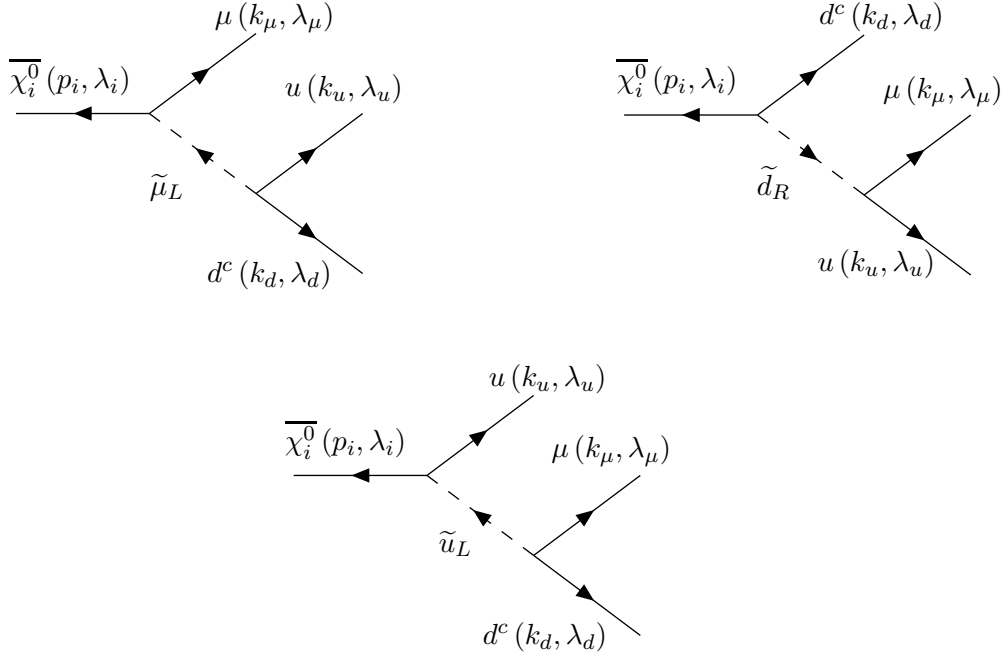


Figure 52: Feynman diagrams for the R-parity violating decay $\tilde{N}_i \rightarrow \mu^- u \bar{d}$.

6.20 R-parity violating neutralino decay: $\tilde{N}_i \rightarrow \mu^- u \bar{d}$

Next we consider the R-parity violating three-body decay of a neutralino $\tilde{N}_i \rightarrow \mu^- u \bar{d}$, which arises via the superpotential term $\lambda'_{211} L_\mu Q_1 \bar{D}_1$. This is of particular interest when the neutralino is the LSP, since it determines the final-state signatures [105, 106]. The three Feynman diagrams are shown in Fig. 52, including the definitions of the momenta and helicities. We have neglected sfermion mixing, i.e. we assume $\tilde{\mu}_L$, \tilde{u}_L , and \tilde{d}_R are mass eigenstates. Using the Feynman rules given in Figs. 76 (or 78) and 83, we obtain the amplitudes

$$i\mathcal{M}_1 = (i\lambda'^*) \left[\frac{i}{\sqrt{2}} (gN_{i2} + g'N_{i1}) \right] \left[\frac{i}{(p_i - k_\mu)^2 - m_{\tilde{\mu}_L}^2} \right] \bar{y}_i \bar{x}_\mu \bar{x}_u \bar{x}_d \quad (6.270)$$

$$i\mathcal{M}_2 = (i\lambda'^*) \left[-\frac{i\sqrt{2}}{3} g'N_{i1} \right] \left[\frac{i}{(p_i - k_d)^2 - m_{\tilde{d}_R}^2} \right] \bar{y}_i \bar{x}_d \bar{x}_\mu \bar{x}_u \quad (6.271)$$

$$i\mathcal{M}_3 = (i\lambda'^*) \left[-\frac{i}{\sqrt{2}} (gN_{i2} + g'N_{i1}/3) \right] \left[\frac{i}{(p_i - k_u)^2 - m_{\tilde{u}_L}^2} \right] \bar{y}_i \bar{x}_u \bar{x}_d \bar{x}_\mu \quad (6.272)$$

Here we have denoted the external wave functions as $\bar{y}_i \equiv \bar{y}(\vec{p}_i, \lambda_i)$, $\bar{x}_\mu \equiv \bar{x}(\vec{k}_\mu, \lambda_\mu)$, $\bar{x}_u \equiv \bar{x}(\vec{k}_u, \lambda_u)$, $\bar{x}_d \equiv \bar{x}(\vec{k}_d, \lambda_d)$, and written $\lambda' \equiv \lambda'_{211}$. In the following, we will neglect all of the

final-state fermion masses. The results will be expressed in terms of the kinematic variables

$$z_\mu \equiv 2p_i \cdot k_\mu / m_{\tilde{N}_i}^2 = 2E_\mu / m_{\tilde{N}_i}, \quad (6.273)$$

$$z_d \equiv 2p_i \cdot k_d / m_{\tilde{N}_i}^2 = 2E_d / m_{\tilde{N}_i}, \quad (6.274)$$

$$z_u \equiv 2p_i \cdot k_u / m_{\tilde{N}_i}^2 = 2E_u / m_{\tilde{N}_i} \quad (6.275)$$

which satisfy $z_\mu + z_d + z_u = 2$. Then we can rewrite the total matrix element as:

$$\mathcal{M} = c_1 \bar{y}_i \bar{x}_\mu \bar{x}_u \bar{x}_d + c_2 \bar{y}_i \bar{x}_d \bar{x}_\mu \bar{x}_u + c_3 \bar{y}_i \bar{x}_u \bar{x}_d \bar{x}_\mu \quad (6.276)$$

where

$$c_1 \equiv \frac{1}{\sqrt{2}} \lambda'^* (g N_{i2} + g' N_{i1}) / [m_{\tilde{\mu}_L}^2 - m_{\tilde{N}_i}^2 (1 - z_\mu)], \quad (6.277)$$

$$c_2 \equiv -\frac{\sqrt{2}}{3} \lambda'^* g' N_{i1} / [m_{\tilde{d}_R}^2 - m_{\tilde{N}_i}^2 (1 - z_d)], \quad (6.278)$$

$$c_3 \equiv -\frac{1}{\sqrt{2}} \lambda'^* (g N_{i2} + g' N_{i1} / 3) / [m_{\tilde{u}_L}^2 - m_{\tilde{N}_i}^2 (1 - z_u)]. \quad (6.279)$$

Before squaring the amplitude, it is convenient to use the Fierz identity (2.54) to reduce the number of terms:

$$\mathcal{M} = (c_1 - c_3) \bar{y}_i \bar{x}_\mu \bar{x}_u \bar{x}_d + (c_2 - c_3) \bar{y}_i \bar{x}_d \bar{x}_\mu \bar{x}_u. \quad (6.280)$$

Now, using eq. (2.30), we obtain

$$|\mathcal{M}|^2 = |c_1 - c_3|^2 \bar{y}_i \bar{x}_\mu x_\mu y_i \bar{x}_u \bar{x}_d x_d x_u + |c_2 - c_3|^2 \bar{y}_i \bar{x}_d x_d y_i \bar{x}_\mu \bar{x}_u x_u x_\mu \\ - 2\text{Re}[(c_1 - c_3)(c_2^* - c_3^*) \bar{y}_i \bar{x}_\mu x_\mu x_u \bar{x}_u \bar{x}_d x_d y_i], \quad (6.281)$$

where eq. (2.47) was used on the last term. Now summing over the fermion spins using eqs. (3.56)-(3.59), we obtain:

$$\sum_{\text{spins}} |\mathcal{M}|^2 = |c_1 - c_3|^2 \text{Tr}[k_\mu \cdot \bar{\sigma} p_i \cdot \sigma] \text{Tr}[k_d \cdot \bar{\sigma} k_u \cdot \sigma] + |c_2 - c_3|^2 \text{Tr}[k_d \cdot \bar{\sigma} p_i \cdot \sigma] \text{Tr}[k_u \cdot \bar{\sigma} k_\mu \cdot \sigma] \\ - 2\text{Re}[(c_1 - c_3)(c_2^* - c_3^*) \text{Tr}[k_\mu \cdot \bar{\sigma} k_u \cdot \sigma k_d \cdot \bar{\sigma} p_i \cdot \sigma]]. \quad (6.282)$$

Applying the trace formulas (2.43) and (2.45), we obtain

$$\sum_{\text{spins}} |\mathcal{M}|^2 = 4|c_1 - c_3|^2 p_i \cdot k_\mu k_d \cdot k_u + 4|c_2 - c_3|^2 p_i \cdot k_d k_\mu \cdot k_u \\ - 4\text{Re}[(c_1 - c_3)(c_2^* - c_3^*)] (k_\mu \cdot k_u p_i \cdot k_d + p_i \cdot k_\mu k_d \cdot k_u - k_\mu \cdot k_d p_i \cdot k_u) \quad (6.283) \\ = m_{\tilde{N}_i}^4 \left[|c_1|^2 z_\mu (1 - z_\mu) + |c_2|^2 z_d (1 - z_d) + |c_3|^2 z_u (1 - z_u) \right. \\ \left. - 2\text{Re}[c_1 c_2^*] (1 - z_\mu) (1 - z_d) - 2\text{Re}[c_1 c_3^*] (1 - z_\mu) (1 - z_u) \right. \\ \left. - 2\text{Re}[c_2 c_3^*] (1 - z_d) (1 - z_u) \right] \quad (6.284)$$

where in the last equality we have used eqs. (6.273)-(6.275) and

$$2k_\mu \cdot k_d = (1 - z_u)m_{\tilde{N}_i}^2, \quad 2k_\mu \cdot k_u = (1 - z_d)m_{\tilde{N}_i}^2, \quad 2k_d \cdot k_u = (1 - z_\mu)m_{\tilde{N}_i}^2. \quad (6.285)$$

The differential decay rate follows:

$$\frac{d^2\Gamma}{dz_\mu dz_d} = \frac{N_c m_{\tilde{N}_i}}{256\pi^3} \left(\frac{1}{2} \sum_{\text{spins}} |\mathcal{M}|^2 \right), \quad (6.286)$$

where a factor of $N_c = 3$ has been included for the sum over colors, a factor of $1/2$ to average over the neutralino spin, and the kinematic limits are

$$0 < z_\mu < 1, \quad (6.287)$$

$$1 - z_\mu < z_d < 1. \quad (6.288)$$

In the limit of heavy sfermions, the integrations over z_d and then z_μ are simple, with the result for the total decay width:

$$\Gamma = \frac{N_c m_{\tilde{N}_i}^5}{6144\pi^3} (|c'_1|^2 + |c'_2|^2 + |c'_3|^2 - \text{Re}[c'_1 c'^*_2 + c'_1 c'^*_3 + c'_2 c'^*_3]), \quad (6.289)$$

where the c'_i are obtained from c_i of eqs. (6.277)-(6.279) by neglecting $m_{\tilde{N}_i}^2$ in the denominators. Our results agree with the complete computation given in [103,104,107], where also the complete mixing was included. Earlier calculations with some simplifications are given in [106,108].

6.21 Top-quark condensation from a Nambu-Jona-Lasinio model gap equation

The previous examples have involved renormalizable field theories. However, there are cases in which it is preferable to use effective four-fermion interactions. The obvious historical example is the use of the four-fermion Fermi theory of weak decays. This has been superseded by a more complete and accurate theory of the weak interactions, but is still useful for leading-order calculations of low-energy processes. Another case of some interest is the use of strong coupling four-fermion interactions to drive symmetry breaking via a Nambu-Jona-Lasinio model [109], as in the top-quark condensate approach [110]- [113] to electroweak symmetry breaking.

Consider an effective four-fermion Lagrangian involving the top quark [111], written in two-component fermion form as:

$$\mathcal{L} = i\bar{t}\bar{\sigma}^\mu \partial_\mu t + i\bar{t}^c \bar{\sigma}^\mu \partial_\mu t^c + \frac{G}{\Lambda^2} (tt^c)(\bar{t}\bar{t}^c). \quad (6.290)$$

Here the Standard Model gauge interactions have been suppressed; the quantities within parentheses are color singlets. Note also that there is no top quark Yukawa coupling to a Higgs scalar boson, nor a top quark mass term, which would normally appear in the form $-m_t(tt^c + \bar{t}\bar{t}^c)$.

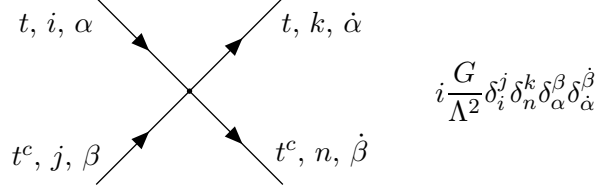


Figure 53: Feynman rule for the four-fermion interaction in the top-quark condensate model. The indices $i, j, k, n = 1, 2, 3$ are for color in the fundamental representation of $SU(3)$, and the indices $\alpha, \beta, \bar{\alpha}, \bar{\beta}$ are two-component spinor indices.

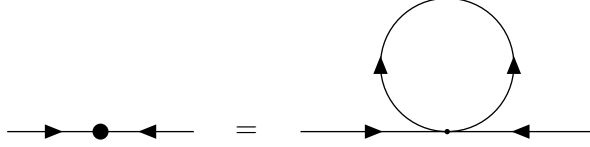


Figure 54: The Nambu-Jona-Lasinio gap equation for a possible dynamically generated top-quark mass m_t .

Instead, the effective top quark mass is supposed to be driven by a non-perturbatively large and positive dimensionless coupling G , with Λ the cutoff scale at which G arises from some more fundamental physics such as topcolor [113].

The Feynman rule for the four-fermion interaction can be derived from the mode expansion results of section 3, and is given in Fig. 53. The resulting gap equation for the dynamically generated top quark mass is shown in Fig. 54. Evaluating this using the Feynman rules of figs. 4 and 5, one finds:

$$-im_t \delta_i^j \delta_\alpha^\beta = (-1) \int^\Lambda \frac{d^4 k}{(2\pi)^4} \left(i \frac{G}{\Lambda^2} \delta_i^j \delta_n^k \delta_\alpha^\beta \delta_{\bar{\alpha}}^{\bar{\beta}} \right) \left(\delta_k^n \delta_{\bar{\beta}}^{\bar{\alpha}} \frac{im_t}{k^2 - m_t^2 + i\epsilon} \right). \quad (6.291)$$

Here i, j, k, n are color indices of the fundamental representation of $SU(3)$, and $\alpha, \beta, \bar{\alpha}, \bar{\beta}$ are two-component spinor indices. The factor of (-1) on the right-hand side is due to the presence of a fermion loop.

Euclideanizing the loop integration over k^μ by $k^2 \rightarrow -k_E^2$ and $\int d^4 k \rightarrow i \int d^4 k_E$, and then rewriting the integration in terms of $x = k_E^2$, this amounts to [111]:

$$m_t = \frac{2N_c G m_t}{16\pi^2 \Lambda^2} \int_0^{\Lambda^2} dx / (1 + m_t^2/x) \quad (6.292)$$

$$= \frac{3G m_t}{8\pi^2} [1 - (m_t^2/\Lambda^2) \ln(\Lambda^2/m_t^2) + \dots], \quad (6.293)$$

where $N_c = 3$ is the number of colors, and a factor of two arose from the sum over dotted spinor indices of $\delta_{\bar{\alpha}}^{\bar{\beta}} \delta_{\bar{\beta}}^{\bar{\alpha}}$.

For small or negative G , only the trivial solution $m_t = 0$ is possible. However, for $G \geq G_{\text{critical}} = 8\pi^2/3 \approx 26$, there is always a positive solution for m_t^2/Λ^2 [111]. It is now known

that this minimal version of the model cannot explain the top quark mass and the observed features of electroweak symmetry breaking, but extensions of it may be viable [114].

6.22 Electroweak vector boson self-energies from fermion loops

In this subsection, we consider the contributions to the self-energy functions of the Standard Model electroweak vector bosons coming from quark and lepton loops. (For a derivation of equivalent results in the four-component fermion formalism, see for example section 21.3 of [76].) The independent self-energies are given by $\Pi_{\mu\nu}^{WW}$, $\Pi_{\mu\nu}^{ZZ}$, $\Pi_{\mu\nu}^{Z\gamma} = \Pi_{\mu\nu}^{\gamma Z}$, and $\Pi_{\mu\nu}^{\gamma\gamma}$, as shown in figs. 55 and 56. In each case, $i\Pi_{\mu\nu}$ is equal to the sum of Feynman diagrams for two-point functions with amputated external legs, and is implicitly a function of the external momentum p^μ .

First consider the self-energy function for the W boson, shown in Fig. 55. The W boson only couples to left-handed fermions, so there is only one Feynman diagram for each Standard model weak isodoublet. Taking the external momentum flowing from left to right to be p , and the loop momentum flowing counterclockwise in the upper fermion line (f) to be k , we have from the Feynman rules of Fig. 67:

$$i\Pi_{\mu\nu}^{WW} = (-1)\mu^{2\epsilon} \int \frac{d^d k}{(2\pi)^d} \sum_{(f,f')} N_c^f \text{Tr} \left[\left(-i \frac{g}{\sqrt{2}} \bar{\sigma}_\mu \right) \left(\frac{ik \cdot \sigma}{k^2 - m_f^2} \right) \left(-i \frac{g}{\sqrt{2}} \bar{\sigma}_\nu \right) \left(\frac{i(k+p) \cdot \sigma}{(k+p)^2 - m_{f'}^2} \right) \right]. \quad (6.294)$$

Here μ is a regularization scale for dimensional regularization in $d \equiv 4 - 2\epsilon$ dimensions. The sum in eq. (6.294) is over the six isodoublet pairs $(f, f') = (e, \nu_e), (\mu, \nu_\mu), (\tau, \nu_\tau), (d, u), (s, c), (b, t)$.

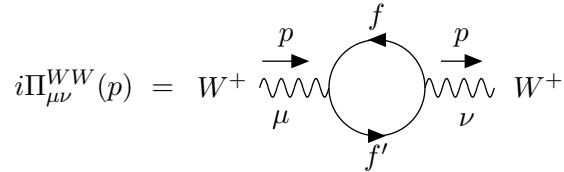


Figure 55: Contributions to the self-energy function for the W boson in the Standard Model, from loops involving the left-handed quark and lepton pairs $(f, f') = (e, \nu_e), (\mu, \nu_\mu), (\tau, \nu_\tau), (d, u), (s, c),$ and (b, t) . The momentum of the positively charged W^+ flows from left to right.

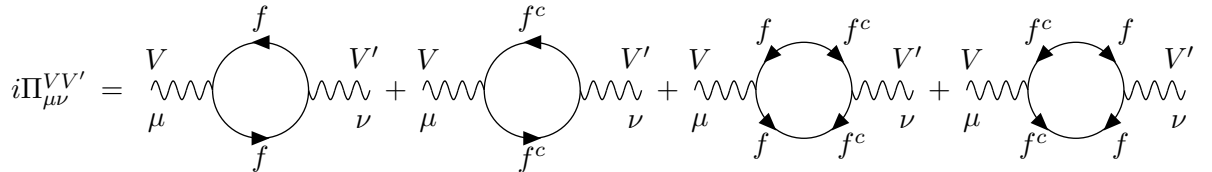


Figure 56: Contributions to the diagonal and off-diagonal self-energy functions for the neutral vector bosons $V, V' = \gamma, Z$ in the Standard Model, from loops involving the three generations of leptons and quarks: $f = e, \nu_e, \mu, \nu_\mu, \tau, \nu_\tau, d, u, s, c, b, t$.

and (b, t) with CKM mixing neglected, and

$$N_c^f = \begin{cases} 3, & f = \text{quarks}, \\ 1, & f = \text{leptons}. \end{cases} \quad (6.295)$$

The first factor of (-1) in eq. (6.294) is due to the presence of a closed fermion loop. The trace is taken over the two-component dotted spinor indices. Using eq. (A.25), it follows that

$$\Pi_{\mu\nu}^{WW} = \frac{g^2}{32\pi^2} \sum_f N_c^f I_{\mu\nu}(m_f^2, m_{f'}^2), \quad (6.296)$$

where we have defined

$$I_{\mu\nu}(x, y) = i(16\pi^2) \mu^{2\epsilon} \int \frac{d^d k}{(2\pi)^d} \frac{4k_\mu k_\nu + 2k_\mu p_\nu + 2k_\nu p_\mu - 2k \cdot (k + p) g_{\mu\nu}}{(k^2 - x)[(k + p)^2 - y]}. \quad (6.297)$$

This integral can be evaluated by the standard dimensional regularization methods [76, 115], with the result:

$$I_{\mu\nu}(x, y) = (p^2 g_{\mu\nu} - p_\mu p_\nu) I_1(p^2; x, y) + g_{\mu\nu} I_2(p^2; x, y), \quad (6.298)$$

where, after neglecting terms that vanish as $\epsilon \rightarrow 0$,

$$I_1(s; x, y) = -\frac{2}{3\epsilon} + \frac{2}{3s^2} \left\{ (2x - 2y - s)A(x) + (2y - 2x - s)A(y) \right. \\ \left. + [2(x - y)^2 - s(x + y) - s^2]B(s; x, y) - s(x + y) + s^2/3 \right\}, \quad (6.299)$$

$$I_2(s; x, y) = \frac{x + y}{\epsilon} - \frac{1}{s} \left\{ (x - y)[A(x) - A(y)] + [(x - y)^2 - s(x + y)]B(s; x, y) \right\}. \quad (6.300)$$

The functions

$$A(x) \equiv x \ln(x/Q^2) - x, \quad (6.301)$$

$$B(s; x, y) \equiv - \int_0^1 dt \ln \left(\frac{tx + (1 - t)y - t(1 - t)s - i\epsilon}{Q^2} \right), \quad (6.302)$$

are the finite parts of one-loop Passarino-Veltman functions, with the renormalization scale Q related to the regularization scale μ by the modified minimal subtraction relation

$$\mu^2 = Q^2 e^\gamma / 4\pi, \quad (6.303)$$

where $\gamma = 0.577216 \dots$ is Euler's constant.

The photon and Z boson have mixed self-energy functions, defined in Fig. 56. Applying

the pertinent Feynman rules from Fig. 67, we obtain:

$$\begin{aligned}
i\Pi_{\mu\nu}^{VV'} = (-1)\mu^{2\epsilon} \int \frac{d^d k}{(2\pi)^d} \sum_f N_c^f \text{Tr} \Bigg\{ & (-iG_V^f \bar{\sigma}_\mu) \left(\frac{ik \cdot \sigma}{k^2 - m_f^2} \right) (-iG_{V'}^f \bar{\sigma}_\nu) \left(\frac{i(k+p) \cdot \sigma}{(k+p)^2 - m_f^2} \right) \\
& + (-iG_V^{fc} \bar{\sigma}_\mu) \left(\frac{ik \cdot \sigma}{k^2 - m_f^2} \right) (-iG_{V'}^{fc} \bar{\sigma}_\nu) \left(\frac{i(k+p) \cdot \sigma}{(k+p)^2 - m_f^2} \right) \\
& + (-iG_V^f \bar{\sigma}_\mu) \left(\frac{im_f}{k^2 - m_f^2} \right) (iG_{V'}^{fc} \sigma_\nu) \left(\frac{im_f}{(k+p)^2 - m_f^2} \right) \\
& + (-iG_V^{fc} \bar{\sigma}_\mu) \left(\frac{im_f}{k^2 - m_f^2} \right) (iG_{V'}^f \sigma_\nu) \left(\frac{im_f}{(k+p)^2 - m_f^2} \right) \Bigg\}, \quad (6.304)
\end{aligned}$$

where V and V' can each be either γ or Z , and \sum_f is taken over the 12 Standard Model fermions. The corresponding Vff and $Vf^c f^c$ couplings are:³⁴

$$G_\gamma^f = -G_\gamma^{fc} = eQ_f, \quad (6.305)$$

$$G_Z^f = \frac{g}{c_W}(T_3^f - s_W^2 Q_f), \quad G_Z^{fc} = \frac{g}{c_W}s_W^2 Q_f. \quad (6.306)$$

The four terms in eq. (6.304) correspond to the four diagrams in Fig. 56, in the same order.

The first two terms in eq. (6.304) are computed exactly as for $\Pi_{\mu\nu}^{WW}$, while in the last two terms we use eq. (A.3) to compute the trace. It follows that the neutral electroweak vector boson self-energy function matrix, after dropping terms that vanish as $\epsilon \rightarrow 0$, is given by

$$\begin{aligned}
\Pi_{\mu\nu}^{VV'} = \frac{1}{16\pi^2} \sum_f N_c^f \Big[& (G_V^f G_{V'}^f + G_V^{fc} G_{V'}^{fc}) I_{\mu\nu}(m_f^2, m_f^2) \\
& + g_{\mu\nu} (G_V^f G_{V'}^{fc} + G_V^{fc} G_{V'}^f) m_f^2 I_3(m_f^2, m_f^2) \Big], \quad (6.307)
\end{aligned}$$

where $I_{\mu\nu}(x, y)$ was defined in eqs. (6.298)-(6.300), and we have defined the function

$$I_3(x, y) = -i(16\pi^2) \mu^{2\epsilon} \int \frac{d^d k}{(2\pi)^d} \frac{2}{(k^2 - x)[(k+p)^2 - y]} = \frac{2}{\epsilon} + 2B(p^2; x, y). \quad (6.308)$$

The photon self-energy function is a simple special case of eq. (6.307):

$$\Pi_{\mu\nu}^{\gamma\gamma} = \frac{1}{16\pi^2} \sum_f 2N_c^f (eQ_f)^2 [I_{\mu\nu}(m_f^2, m_f^2) - g_{\mu\nu} m_f^2 I_3(m_f^2, m_f^2)] \quad (6.309)$$

$$\begin{aligned}
& = \frac{\alpha}{3\pi} \sum_f N_c^f Q_f^2 (p^2 g_{\mu\nu} - p_\mu p_\nu) \left\{ -\frac{1}{\epsilon} + \frac{1}{3} - \frac{2}{p^2} [A(m_f^2) + m_f^2] \right. \\
& \quad \left. - \left(1 + \frac{2m_f^2}{p^2} \right) B(p^2; m_f^2, m_f^2) \right\}, \quad (6.310)
\end{aligned}$$

in agreement with the result given in, for example, eq. (7.90) of [76]. This formula satisfies $p^\mu \Pi_{\mu\nu}^{\gamma\gamma} = p^\nu \Pi_{\mu\nu}^{\gamma\gamma} = 0$ as required by the Ward identity of QED, and is regular in the limit $p^2 \rightarrow 0$.

³⁴Note that there is no contribution from ν_e^c , ν_μ^c , ν_τ^c , which do not exist in the Standard Model.

In each of eqs. (6.296), (6.307), and (6.310), there are $1/\epsilon$ poles, contained in the loop integral functions. In the $\overline{\text{MS}}$ renormalization scheme, these poles are simply removed by counterterms, which have no other effect.

In eqs. (6.294) and (6.304), we chose to write a $\bar{\sigma}_\mu$ for the left vertex in the Feynman diagram in each case. This is an arbitrary choice; we could also have chosen to use instead $-\sigma_\mu$ for the left vertex in any given diagram, as mentioned in the caption for Fig. 67. This would have dictated the replacements $\bar{\sigma} \leftrightarrow -\sigma$ throughout the expression for the diagram, including for the fermion propagators, as was indicated in Fig. 5. It is not hard to check that the result after computing the spinor index traces is unaffected. Note that the contribution proportional to $\epsilon_{\mu\nu\rho\kappa}$ from eq. (A.24) or eq. (A.25) vanishes; this is clear because the self-energy function is symmetric under interchange of vector indices, and there is only one independent momentum in the problem.

6.23 Self-energy and pole mass of the top quark

We next consider the one-loop calculation of the self-energy and the pole mass of the top quark in the Standard Model, including the effects of the gauge interactions and the top and bottom quark Yukawa couplings. As in Section 6.1, we treat this as a one-generation problem, neglecting CKM mixing. Consequently, the corresponding Yukawa couplings Y_t and Y_b are real and positive (by a suitable phase redefinition of the Higgs field³⁵). Using the formalism of subsection 4.6 for Dirac fermions, the independent 1PI self-energy functions are given by³⁶ Σ_{Lt} , Σ_{Rt} and Σ_{Dt} (defined in Fig. 22) as shown in Fig. 57. Note that in these diagrams, the physical top quark moves from right to left, carrying momentum p^μ . Then according to the general formula obtained in eq. (4.71), the top-quark pole squared mass will be given by:

$$M_t^2 - i\Gamma_t M_t = \frac{(m_t + \Sigma_{Dt})^2}{(1 - \Sigma_{LT})(1 - \Sigma_{Rt})}, \quad (6.311)$$

where m_t is the tree-level mass. Working consistently to one-loop order, this yields

$$M_t^2 - i\Gamma_t M_t = [m_t^2(1 + \Sigma_{LT} + \Sigma_{Rt}) + 2m_t \Sigma_{Dt}] \Big|_{s=m_t^2+i\epsilon}. \quad (6.312)$$

(It would be just as valid to substitute in $s = M_t^2 + i\epsilon$ here, as two-loop order effects are neglected.)

It remains to calculate the self-energy functions Σ_{Lt} , Σ_{Rt} and Σ_{Dt} . Two regularization procedures will be used simultaneously—the $\overline{\text{MS}}$ scheme based on dimensional regularization [116]

³⁵As shown in Section 3.2, after the fermion-mass matrix diagonalization procedure, the tree-level fermion masses are real and non-negative. If CKM mixing is neglected, it follows from eq. (H.13) that the corresponding diagonal Yukawa couplings are real and positive if the phase of the Higgs field is chosen such that the neutral Higgs vacuum expectation value $v > 0$.

³⁶Since the Yukawa couplings can be chosen real (in the one-generation model), $\bar{\Sigma}_{Lt} = \Sigma_{Lt}$. Note that after suppressing the color degrees of freedom, Σ_{Lt} , Σ_{Rt} and Σ_{Dt} are one-dimensional matrices, so we do not employ boldface letters in this case.

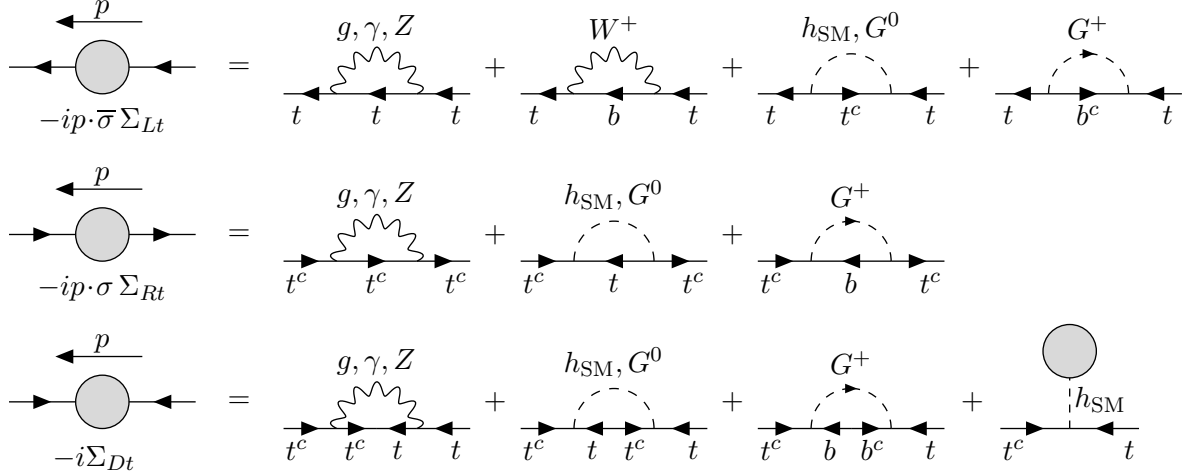


Figure 57: One-loop contributions to the 1PI self-energy functions for the top quark in the Standard Model. The external momentum of the physical top quark, p^μ , flows from the right to the left. The loop momentum k^μ in the text is taken to flow clockwise. Spinor and color indices are suppressed. The external legs are amputated. The last diagram contains one-loop tadpole contributions.

and the $\overline{\text{DR}}$ scheme based on dimensional reduction [117]. This is accomplished by integrating over the loop momentum in

$$d \equiv 4 - 2\epsilon \quad (6.313)$$

dimensions, but with the vector bosons possessing

$$D \equiv 4 - 2\epsilon\delta_{\overline{\text{MS}}} \quad (6.314)$$

components, where

$$\delta_{\overline{\text{MS}}} \equiv \begin{cases} 1 & \text{for } \overline{\text{MS}} \\ 0 & \text{for } \overline{\text{DR}}. \end{cases} \quad (6.315)$$

In other words, the metric $g^{\mu\nu}$ appearing explicitly in the vector propagator is treated as four-dimensional in $\overline{\text{DR}}$, but as d -dimensional in $\overline{\text{MS}}$. The renormalization scale Q is related to the regularization scale μ in both cases by the modified minimal subtraction relation of eq. (6.303).

The calculation of the non-tadpole contributions to the self-energy functions will be performed below in a general R_ξ gauge, with a vector boson propagator as in fig. 6. There are different ways to treat the tadpole contributions, corresponding to different choices for the Higgs VEV around which the tree-level Lagrangian is expanded. If one chooses to expand around the minimum of the tree-level Higgs potential, then there are no tree-level tadpoles, but there will be non-zero contributions from the last diagram shown in fig. 57. (This corresponds to the treatment given, for example, in ref. [118].) Alternatively, one can choose to expand around the

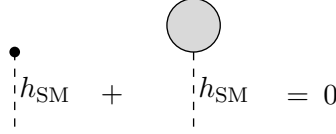


Figure 58: The tree-level Higgs tadpole cancels against the one-loop Higgs tadpole, provided that one expands around a Higgs VEV that minimizes the one-loop effective potential (rather than the tree-level Higgs potential, which would yield no tree-level tadpole).

Higgs VEV v that minimizes the one-loop Landau gauge³⁷ effective potential. In that case, the one-loop tadpole contribution is precisely cancelled by the tree-level Higgs tadpole, as shown in fig. 58. Here, we have in mind the latter prescription; the calculation for the pole mass is therefore complete without tadpole contributions provided that the tree-level top-quark mass is taken to be

$$m_t = Y_t v, \quad (6.316)$$

where Y_t is the $\overline{\text{MS}}$ or $\overline{\text{DR}}$ Yukawa coupling, and v is the Higgs VEV at the minimum of the one-loop effective potential in Landau gauge. To be consistent with this choice, $\xi = 0$ should be taken in all formulas below that involve electroweak gauge bosons or Goldstone bosons. (The gluon contribution is naturally independent of ξ because the gauge symmetry is unbroken, providing a check of gauge-fixing invariance.) Nevertheless, for the sake of generality we will keep the dependence on ξ in the computation of the individual non-tadpole self-energy diagrams below.

Consider the one-loop calculation of the self-energy Σ_{Lt} , which is the sum of individual diagram contributions $\Sigma_{Lt} = [\Sigma_{Lt}]_g + [\Sigma_{Lt}]_\gamma + [\Sigma_{Lt}]_Z + [\Sigma_{Lt}]_W + [\Sigma_{Lt}]_{h_{\text{SM}}} + [\Sigma_{Lt}]_{G^0} + [\Sigma_{Lt}]_{G^\pm}$. First, consider the diagrams involving exchanges of the scalars $\phi = h_{\text{SM}}, G^0, G^\pm$. These contributions all have the same form

$$-ip \cdot \bar{\sigma} [\Sigma_{Lt}]_\phi = \mu^{2\epsilon} \int \frac{d^d k}{(2\pi)^d} (-iY^*) \left(\frac{i(k+p) \cdot \bar{\sigma}}{(k+p)^2 - m_f^2} \right) (-iY) \left(\frac{i}{k^2 - m_\phi^2} \right), \quad (6.317)$$

where the loop momentum k^μ flows clockwise, and the couplings and propagator masses are, using the Feynman rules of figs. 68 and 69,

$$\text{for } \phi = h_{\text{SM}} : \quad Y = Y_t/\sqrt{2}; \quad m_f = m_t; \quad m_\phi^2 = m_{h_{\text{SM}}}^2, \quad (6.318)$$

$$\text{for } \phi = G^0 : \quad Y = iY_t/\sqrt{2}; \quad m_f = m_t; \quad m_\phi^2 = \xi m_Z^2, \quad (6.319)$$

$$\text{for } \phi = G^\pm : \quad Y = Y_b; \quad m_f = m_b; \quad m_\phi^2 = \xi m_W^2. \quad (6.320)$$

³⁷This procedure is considerably more involved outside of Landau gauge, because the propagators mix the longitudinal components of the vector boson with the Nambu-Goldstone bosons for $\xi \neq 0$ if one expands around a Higgs VEV that does not minimize the tree-level potential. This is the same reason the effective potential is traditionally calculated specifically in Landau gauge.

Multiplying both sides by $p \cdot \sigma$ and taking the trace over spinor indices using eq. (A.3), one finds

$$[\Sigma_{Lt}]_\phi = i|Y|^2 \frac{\mu^{2\epsilon}}{p^2} \int \frac{d^d k}{(2\pi)^d} \frac{p \cdot (k+p)}{[(k+p)^2 - m_f^2][k^2 - m_\phi^2]}. \quad (6.321)$$

Performing the loop momentum integration in the standard way [76, 115], and expanding in ϵ up to constant terms, one finds that in each case

$$[\Sigma_{Lt}]_\phi = -\frac{1}{16\pi^2} |Y|^2 I_{FS}(s; m_f^2, m_\phi^2). \quad (6.322)$$

Here we have introduced some notation for the loop integral:

$$I_{FS}(s; x, y) \equiv \frac{1}{2\epsilon} + [(s+x-y)B(s; x, y) + A(x) - A(y)]/2s, \quad (6.323)$$

where the Passarino-Veltman functions $A(x)$ and $B(s; x, y)$ were defined in eqs. (6.301) and (6.302). These functions depend on the renormalization scale Q , which is related to μ via eq. (6.303). It can be checked that $I_{FS}(s; x, y)$ has a smooth limit as $s \rightarrow 0$.

Next, let us consider the contributions to Σ_{Lt} involving the vector bosons $V = g, \gamma, Z, W$. These have the common form:

$$\begin{aligned} -ip \cdot \bar{\sigma} [\Sigma_{Lt}]_V &= \mu^{2\epsilon} \int \frac{d^d k}{(2\pi)^d} (-iG \bar{\sigma}_\mu) \left(\frac{i(k+p) \cdot \sigma}{(k+p)^2 - m_f^2} \right) (-iG \bar{\sigma}_\nu) \\ &\quad \left(\frac{-i}{k^2 - m_V^2} \right) \left(g^{\mu\nu} + \frac{(\xi-1)k^\mu k^\nu}{k^2 - \xi m_V^2} \right), \end{aligned} \quad (6.324)$$

where again the loop momentum k flows clockwise, and, using the rules of figs. 67 and 79:

$$\text{for } V = g : \quad G = g_s T^a; \quad m_f = m_t, \quad (6.325)$$

$$\text{for } V = \gamma : \quad G = e Q_t; \quad m_f = m_t, \quad (6.326)$$

$$\text{for } V = Z : \quad G = g(T_3^t - s_W^2 Q_t)/c_W; \quad m_f = m_t, \quad (6.327)$$

$$\text{for } V = W : \quad G = g/\sqrt{2}; \quad m_f = m_b. \quad (6.328)$$

In the case of gluon exchange ($V = g$), the T^a are the $SU(3)_C$ generators (with color indices suppressed). The adjoint representation index a is summed over, producing a factor of the Casimir invariant $(T^a T^a)_{ij} = C_F \delta_{ij} = \frac{4}{3} \delta_{ij}$. We now use $\bar{\sigma}_\mu \sigma_\rho \bar{\sigma}_\nu g^{\mu\nu} = (2-D) \bar{\sigma}_\rho$ [see eq. (A.11)]; note that this introduces a difference between the $\overline{\text{MS}}$ and $\overline{\text{DR}}$ schemes. Also, we use $k \cdot \bar{\sigma} (k+p) \cdot \sigma k \cdot \bar{\sigma} = (k^2 + 2k \cdot p) k \cdot \bar{\sigma} - k^2 p \cdot \bar{\sigma}$, which follows from eq. (2.42). One therefore obtains, after multiplying by $p \cdot \sigma$ and taking the trace over spinor indices:

$$\begin{aligned} [\Sigma_{Lt}]_V &= -i G^2 \frac{\mu^{2\epsilon}}{p^2} \int \frac{d^d k}{(2\pi)^d} \frac{1}{[(k+p)^2 - m_f^2][k^2 - m_V^2]} \left[(2-D) p \cdot (k+p) \right. \\ &\quad \left. + (k^2 k \cdot p + 2(k \cdot p)^2 - k^2 p^2) \frac{(\xi-1)}{k^2 - \xi m_V^2} \right]. \end{aligned} \quad (6.329)$$

Performing the loop momentum integration, one finds in each case that

$$[\Sigma_{Lt}]_V = -\frac{1}{16\pi^2} G^2 I_{FV}(s; m_f^2, m_V^2), \quad (6.330)$$

where we have introduced the notation

$$\begin{aligned} I_{FV}(s; x, y) = & \frac{\xi}{\epsilon} + [(s+x-y)B(s; x, y) + A(x) - A(y)]/s - \delta_{\overline{\text{MS}}} + \{(s-x)[A(y) - A(\xi y)] \\ & + [(s-x)^2 - y(s+x)]B(s; x, y) - [(s-x)^2 - \xi y(s+x)]B(s; x, \xi y)\}/2ys, \end{aligned} \quad (6.331)$$

after dropping terms that vanish as $\epsilon \rightarrow 0$. Combining the results of eqs. (6.322) and (6.330):

$$\begin{aligned} \Sigma_{Lt} = & -\frac{1}{16\pi^2} \left[(g_s^2 C_F + e^2 Q_t^2) I_{FV}(m_t^2; m_t^2, 0) + [g(T_3^t - s_W^2 Q_t)/c_W]^2 I_{FV}(m_t^2; m_t^2, m_Z^2) \right. \\ & + \frac{1}{2} g^2 I_{FV}(m_t^2; m_b^2, m_W^2) + \frac{1}{2} Y_t^2 I_{FS}(m_t^2; m_t^2, m_{h_{\text{SM}}}^2) \\ & \left. + \frac{1}{2} Y_t^2 I_{FS}(m_t^2; m_t^2, \xi m_Z^2) + Y_b^2 I_{FS}(m_t^2; m_b^2, \xi m_W^2) \right], \end{aligned} \quad (6.332)$$

where we have now substituted $s = m_t^2$. It is useful to note that for massless gauge bosons,

$$I_{FV}(x; x, 0) = \xi \left[\frac{1}{\epsilon} - \ln(x/Q^2) + 2 \right] + 1 - \delta_{\overline{\text{MS}}}. \quad (6.333)$$

The contributions to $\Sigma_{Rt} = [\Sigma_{Rt}]_g + [\Sigma_{Rt}]_\gamma + [\Sigma_{Rt}]_Z + [\Sigma_{Rt}]_{h_{\text{SM}}} + [\Sigma_{Rt}]_{G^0} + [\Sigma_{Rt}]_{G^\pm}$ are obtained similarly. [Note that there is no W boson contribution, since the right-handed top quark is an $SU(2)_L$ singlet.] For the scalar exchange diagrams with $\phi = h_{\text{SM}}, G^0, G^\pm$, the general form is:

$$-ip \cdot \sigma [\Sigma_{Rt}]_\phi = \mu^{2\epsilon} \int \frac{d^d k}{(2\pi)^d} (-iY) \left(\frac{i(k+p) \cdot \sigma}{(k+p)^2 - m_f^2} \right) (-iY^*) \left(\frac{i}{k^2 - m_\phi^2} \right). \quad (6.334)$$

and so

$$[\Sigma_{Rt}]_\phi = -\frac{1}{16\pi^2} |Y|^2 I_{FS}(s; m_f^2, m_\phi^2). \quad (6.335)$$

Here the couplings and propagator masses for h_{SM} and G^0 are the same as in eqs. (6.318), (6.319), but now, instead of eq. (6.320),

$$\text{for } \phi = G^\pm : \quad Y = -Y_t; \quad m_f = m_b; \quad m_\phi^2 = \xi m_W^2 \quad (6.336)$$

from fig. 69. For the contributions due to exchanges of vectors $v = g, \gamma, Z$, the general form is

$$\begin{aligned} -ip \cdot \sigma [\Sigma_{Rt}]_V = & \mu^{2\epsilon} \int \frac{d^d k}{(2\pi)^d} (iG \sigma_\mu) \left(\frac{i(k+p) \cdot \bar{\sigma}}{(k+p)^2 - m_f^2} \right) (iG \sigma_\nu) \\ & \left(\frac{-i}{k^2 - m_V^2} \right) \left(g^{\mu\nu} + \frac{(\xi-1)k^\mu k^\nu}{k^2 - \xi m_V^2} \right), \end{aligned} \quad (6.337)$$

where, using the rules of figs. 67 and 79:

$$\text{for } V = g : \quad G = -g_s T^a; \quad (6.338)$$

$$\text{for } V = \gamma : \quad G = -e Q_t; \quad (6.339)$$

$$\text{for } V = Z : \quad G = g s_W^2 Q_t / c_W, \quad (6.340)$$

with $m_f = m_t$ in each case. Using $\sigma_\mu \bar{\sigma}_\rho \sigma_\nu g^{\mu\nu} = (2 - D) \sigma_\rho$ [see eq. (A.10)] and $k \cdot \sigma (k + p) \cdot \bar{\sigma} k \cdot \sigma = (k^2 + 2k \cdot p) k \cdot \sigma - k^2 p \cdot \sigma$ [from eq. (2.41)], then multiplying by $p \cdot \bar{\sigma}$ and taking the trace over spinor indices [using eq. (A.3)], we obtain

$$[\Sigma_{Rt}]_V = -\frac{1}{16\pi^2} G^2 I_{FV}(s; m_t^2, m_V^2) \quad (6.341)$$

in terms of the same function appearing in eqs. (6.331) and (6.333). Adding up these contributions and taking $s = m_t^2$ yields

$$\begin{aligned} \Sigma_{Rt} = & -\frac{1}{16\pi^2} \left[(g_s^2 C_F + e^2 Q_t^2) I_{FV}(m_t^2; m_t^2, 0) + (g^2 Q_t^2 s_W^4 / c_W^2) I_{FV}(m_t^2; m_t^2, m_Z^2) \right. \\ & \left. + \frac{1}{2} Y_t^2 I_{FS}(m_t^2; m_t^2, m_{h_{\text{SM}}}^2) + \frac{1}{2} Y_t^2 I_{FS}(m_t^2; m_t^2, \xi m_Z^2) + Y_t^2 I_{FS}(m_t^2; m_b^2, \xi m_W^2) \right]. \end{aligned} \quad (6.342)$$

Next, consider the contributions to $\Sigma_{Dt} = [\Sigma_{Dt}]_g + [\Sigma_{Dt}]_\gamma + [\Sigma_{Dt}]_Z + [\Sigma_{Dt}]_{h_{\text{SM}}} + [\Sigma_{Dt}]_{G^0} + [\Sigma_{Dt}]_{G^\pm}$, ignoring the tadpole contribution for now. The diagrams involving the exchange of scalars $\phi = h_{\text{SM}}, G^0, G^\pm$ have the form:

$$-i[\Sigma_{Dt}]_\phi = \mu^{2\epsilon} \int \frac{d^d k}{(2\pi)^d} (-iY_1) \left(\frac{im_f}{(k+p)^2 - m_f^2} \right) (-iY_2) \left(\frac{i}{k^2 - m_\phi^2} \right), \quad (6.343)$$

so that

$$[\Sigma_{Dt}]_\phi = im_f Y_1 Y_2 \mu^{2\epsilon} \int \frac{d^d k}{(2\pi)^d} \frac{1}{[(k+p)^2 - m_f^2][k^2 - m_\phi^2]} \quad (6.344)$$

$$= \frac{1}{16\pi^2} m_f Y_1 Y_2 I_{\overline{FS}}(s; m_f^2, m_\phi^2) \quad (6.345)$$

where we have introduced the notation:

$$I_{\overline{FS}}(s; x, y) \equiv -\frac{1}{\epsilon} - B(s; x, y), \quad (6.346)$$

after dropping terms that vanish as $\epsilon \rightarrow 0$. The relevant couplings and masses are, from figs. 68 and 69:

$$\text{for } \phi = h_{\text{SM}} : \quad Y_1 = Y_2 = Y_t / \sqrt{2}; \quad m_f = m_t; \quad m_\phi^2 = m_{h_{\text{SM}}}^2, \quad (6.347)$$

$$\text{for } \phi = G^0 : \quad Y_1 = Y_2 = iY_t / \sqrt{2}; \quad m_f = m_t; \quad m_\phi^2 = \xi m_Z^2, \quad (6.348)$$

$$\text{for } \phi = G^\pm : \quad Y_1 = Y_b; \quad Y_2 = -Y_t; \quad m_f = m_b; \quad m_\phi^2 = \xi m_W^2. \quad (6.349)$$

The contributions from vector boson exchanges are of the form

$$-i[\Sigma_{Dt}]_V = \mu^{2\epsilon} \int \frac{d^d k}{(2\pi)^d} (iG_1 \sigma_\mu) \left(\frac{im_f}{(k+p)^2 - m_f^2} \right) (-iG_2 \bar{\sigma}_\nu) \left(\frac{-i}{k^2 - m_V^2} \right) \left(g^{\mu\nu} + \frac{(\xi-1)k^\mu k^\nu}{k^2 - \xi m_V^2} \right), \quad (6.350)$$

Using $\sigma_\mu \bar{\sigma}_\nu g^{\mu\nu} = D$ [see eq. (A.8)] and $k \cdot \sigma k \cdot \bar{\sigma} = k^2$ [from eq. (2.39)] yields

$$[\Sigma_{Dt}]_V = im_f G_1 G_2 \mu^{2\epsilon} \int \frac{d^d k}{(2\pi)^d} \frac{1}{[(k+p)^2 - m_f^2][k^2 - m_V^2]} \left[D + \frac{(\xi-1)k^2}{k^2 - \xi m_V^2} \right] \quad (6.351)$$

$$= \frac{1}{16\pi^2} m_f G_1 G_2 I_{\overline{F}V}(s; m_f^2, m_V^2) \quad (6.352)$$

where

$$I_{\overline{F}V}(s; x, y) \equiv -\frac{3+\xi}{\epsilon} - 3B(s; x, y) - \xi B(s; x, \xi y) + 2\delta_{\overline{\text{MS}}}, \quad (6.353)$$

after dropping terms that vanish as $\epsilon \rightarrow 0$. It is useful to note that for massless gauge bosons

$$I_{\overline{F}V}(x; x, 0) \equiv -\frac{3+\xi}{\epsilon} + (3+\xi)[\ln(x/Q^2) - 2] + 2\delta_{\overline{\text{MS}}}. \quad (6.354)$$

The relevant couplings are obtained from the rules of figs. 67 and 79:

$$\text{for } V = g : \quad G_1 = -G_2 = g_s T^a; \quad (6.355)$$

$$\text{for } V = \gamma : \quad G_1 = -G_2 = e Q_t; \quad (6.356)$$

$$\text{for } V = Z : \quad G_1 = g(T_3^t - s_W^2 Q_t)/c_W; \quad G_2 = g s_W^2 Q_t/c_W; \quad (6.357)$$

and $m_f = m_t$ in each case. Adding up these contributions and taking $s = m_t^2$, we have:

$$\begin{aligned} \Sigma_{Dt} = \frac{m_t}{16\pi^2} & \left\{ g^2 [(T_3^t - s_W^2 Q_t) s_W^2 Q_t / c_W^2] I_{\overline{F}V}(m_t^2; m_t^2, m_Z^2) - (g_s^2 C_F + e^2 Q_t^2) I_{\overline{F}V}(m_t^2; m_t^2, 0) \right. \\ & \left. + \frac{1}{2} Y_t^2 I_{\overline{F}S}(m_t^2; m_t^2, m_{h_{\text{SM}}}^2) - \frac{1}{2} Y_t^2 I_{\overline{F}S}(m_t^2; m_t^2, \xi m_Z^2) - Y_b^2 I_{\overline{F}S}(m_t^2; m_b^2, \xi m_W^2) \right\}. \quad (6.358) \end{aligned}$$

In each of the self-energy functions above, there are poles in $1/\epsilon$, contained within the functions I_{FV} , I_{FS} , $I_{\overline{F}V}$ and $I_{\overline{F}S}$. In the $\overline{\text{MS}}$ or $\overline{\text{DR}}$ schemes, these poles are simply canceled by counterterms, which have no other effect at one-loop order. The one-loop top-quark pole mass can now be obtained by plugging eqs. (6.332), (6.342), and (6.358) into eq. (6.312) with $\xi = 0$, as discussed earlier. It is not hard to check that the terms from the vector exchange diagrams that depend on ξm_W^2 and ξm_Z^2 then just cancel against contributions from massless Nambu-Goldstone bosons.

As a simple example, consider the one-loop pole mass with only QCD effects included. Then the result of eq. (6.312) has no imaginary part. Taking the square root (and dropping a

two-loop order part) yields the well-known result [119]:

$$M_{t,\text{pole}} = m_t(1 + \frac{1}{2}\Sigma_{Lt} + \frac{1}{2}\Sigma_{Rt}) + \Sigma_{Dt} \quad (6.359)$$

$$= m_t \left(1 - \frac{C_F g_s^2}{16\pi^2} \left[I_{FV}(m_t^2; m_t^2, 0) + I_{\overline{FV}}(m_t^2; m_t^2, 0) \right] \right) \quad (6.360)$$

$$= m_t \left(1 + \frac{\alpha_s}{4\pi} C_F \left[5 - \delta_{\overline{\text{MS}}} - 3 \ln(m_t^2/Q^2) \right] \right). \quad (6.361)$$

As another check, consider the imaginary part of the pole squared mass. Equation (6.312) implies, at leading order:

$$\Gamma_t = -\text{Im}[m_t(\Sigma_{Lt} + \Sigma_{Rt}) + 2\Sigma_{Dt}] \quad (6.362)$$

$$= \frac{m_t}{16\pi^2} \text{Im} \left[\frac{g^2}{2} I_{FV}(m_t^2; m_b^2, m_W^2) + (Y_t^2 + Y_b^2) I_{FS}(m_t^2; m_b^2, \xi m_W^2) \right. \\ \left. + 2Y_b^2 I_{\overline{FS}}(m_t^2; m_b^2, \xi m_W^2) \right]. \quad (6.363)$$

$$= \frac{1}{32\pi^2 m_t} \{ (g^2 + Y_t^2 + Y_b^2)(m_t^2 + m_b^2 - m_W^2) - 4Y_b^2 m_t^2 \} \text{Im}[B(m_t^2; m_b^2, m_W^2)]. \quad (6.364)$$

The fact that the ξ dependence cancelled here is a successful check of gauge-fixing invariance, since the tadpole diagram in fig. 57 does not contribute to the absorptive part of the self-energy. Now, using

$$\text{Im}[B(s; x, y)] = \begin{cases} 0 & \text{for } s \leq (\sqrt{x} + \sqrt{y})^2, \\ \pi \lambda^{1/2}(s, x, y)/s & \text{for } s > (\sqrt{x} + \sqrt{y})^2. \end{cases} \quad (6.365)$$

in eq. (6.364) reproduces the result of eq. (6.11) for the top-quark width at leading order.

6.24 Self-energy and pole mass of the gluino

The Feynman diagrams for the gluino self-energy are shown in Fig. 59. Since the gluino is a Majorana fermion, we can use the general formalism of subsection 4.6. We will compute the self-energy functions $\Xi_{\tilde{g}} \equiv \Xi_{\tilde{g}}^{\tilde{g}}$ and $\Omega_{\tilde{g}} \equiv \Omega_{\tilde{g}}^{\tilde{g}\tilde{g}}$ defined in Fig. 20, and infer $\overline{\Omega}_{\tilde{g}} \equiv \overline{\Omega}_{\tilde{g}\tilde{g}}$ from the latter by replacing all Lagrangian parameters by their complex conjugates.³⁸ From the general result of eq. (4.63), it follows that the gluino complex pole squared mass is related to the tree-level mass $m_{\tilde{g}}$ by

$$M_{\tilde{g}}^2 - iM_{\tilde{g}}\Gamma_{\tilde{g}} = [m_{\tilde{g}}^2(1 + 2\Xi_{\tilde{g}}) + m_{\tilde{g}}(\Omega_{\tilde{g}} + \overline{\Omega}_{\tilde{g}})] \Big|_{s=m_{\tilde{g}}^2+i\varepsilon} \quad (6.366)$$

at one-loop order.

It is convenient to split the self-energy functions into gluon/gluino loop and squark/gluino loop contributions, as

$$\Xi_{\tilde{g}} = [\Xi_{\tilde{g}}]_g + \sum_q \sum_{x=1,2} [\Xi_{\tilde{g}}]_{\tilde{q}_x}, \quad \text{and} \quad \Omega_{\tilde{g}} = [\Omega_{\tilde{g}}]_g + \sum_q \sum_{x=1,2} [\Omega_{\tilde{g}}]_{\tilde{q}_x}, \quad (6.367)$$

³⁸Suppressing the color degrees of freedom, Ξ , Ω and $\overline{\Omega}$ are one-dimensional matrices, so we do not employ boldface letters in this case.

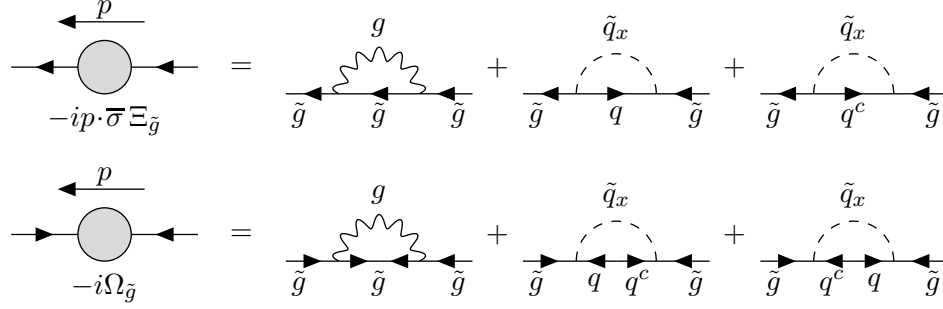


Figure 59: Self-energy functions for the gluino in supersymmetry. The external momentum p^μ flows from the right to the left. The loop momentum k^μ in the text is taken to flow clockwise. Spinor and color indices are suppressed. The index $x = 1, 2$ labels the two squark mass eigenstates of a given flavor $q = u, d, s, c, b, t$. Both x and q must be summed over. The external legs are amputated.

where the sum over q runs over the six squark flavors u, d, s, c, b, t , and $x = 1, 2$ corresponds to the two squark mass eigenstates [i.e., the two appropriate linear combinations (for fixed squark flavor) of \tilde{q}_L and \tilde{q}_R]. The gluon exchange contributions, following from the Feynman rules of Fig. 79, are:

$$-ip \cdot \bar{\sigma} [\Xi_{\tilde{g}}]_g \delta^{ab} = \mu^{2\epsilon} \int \frac{d^d k}{(2\pi)^d} (-g_s f^{aec} \bar{\sigma}_\mu) \left(\frac{i(k+p) \cdot \sigma}{(k+p)^2 - m_{\tilde{g}}^2} \right) \left(-g_s f^{ebc} \bar{\sigma}_\nu \right) \left(\frac{-i}{k^2} \right) \left(g^{\mu\nu} + (\xi - 1) \frac{k^\mu k^\nu}{k^2} \right), \quad (6.368)$$

$$-i [\Omega_{\tilde{g}}]_g \delta^{ab} = \mu^{2\epsilon} \int \frac{d^d k}{(2\pi)^d} (g_s f^{eac} \sigma_\mu) \left(\frac{im_{\tilde{g}}}{(k+p)^2 - m_{\tilde{g}}^2} \right) \left(-g_s f^{ebc} \bar{\sigma}_\nu \right) \left(\frac{-i}{k^2} \right) \left(g^{\mu\nu} + (\xi - 1) \frac{k^\mu k^\nu}{k^2} \right). \quad (6.369)$$

The internal gluon and gluino lines carry $SU(3)_c$ adjoint representation index indices c and e respectively, while the external gluinos on the left and right carry indices a and b respectively. The gluino external momentum p^μ flows from right to left, and the loop momentum k^μ flows clockwise. Comparing with the derivations of eqs. (6.330) and (6.352) in the previous subsection, and using $-f^{aec} f^{ebc} = f^{eac} f^{ebc} = \delta^{ab} C_A$ [with $C_A = 3$ for $SU(3)_c$], we can immediately conclude that

$$[\Xi_{\tilde{g}}]_g = -\frac{\alpha_s}{4\pi} C_A I_{FV}(s; m_{\tilde{g}}^2, 0), \quad (6.370)$$

$$[\Omega_{\tilde{g}}]_g = -\frac{\alpha_s}{4\pi} C_A m_{\tilde{g}} I_{\bar{F}V}(s; m_{\tilde{g}}^2, 0), \quad (6.371)$$

where the loop integral functions I_{FV} and $I_{\bar{F}V}$ were defined in eqs. (6.331) and (6.353).

Next consider the virtual squark-exchange diagrams contributing to $\Xi_{\tilde{g}}$. Labeling the quark

and squark with color indices j, k respectively, we have for each squark mass eigenstate:

$$\begin{aligned}
-i p \cdot \bar{\sigma} [\Xi_{\tilde{g}}]_{\tilde{q}_x} \delta^{ab} &= \mu^{2\epsilon} \int \frac{d^d k}{(2\pi)^d} (-i\sqrt{2} g_s T_j^{ak} L_{\tilde{q}_x}) \left(\frac{i(k+p) \cdot \bar{\sigma}}{(k+p)^2 - m_q^2} \right) (-i\sqrt{2} g_s T_k^{bj} L_{\tilde{q}_x}^*) \left(\frac{i}{k^2 - m_{\tilde{q}_x}^2} \right) \\
&+ \mu^{2\epsilon} \int \frac{d^d k}{(2\pi)^d} (i\sqrt{2} g_s T_k^{aj} R_{\tilde{q}_x}^*) \left(\frac{i(k+p) \cdot \bar{\sigma}}{(k+p)^2 - m_q^2} \right) (i\sqrt{2} g_s T_j^{bk} R_{\tilde{q}_x}) \left(\frac{i}{k^2 - m_{\tilde{q}_x}^2} \right). \quad (6.372)
\end{aligned}$$

This uses the Feynman rules shown in fig. 81, given in terms of the squark mixing parameters $L_{\tilde{q}_x}$ and $R_{\tilde{q}_x}$ defined in eqs. (I.29) and (I.30). Using $\text{Tr}[T^a T^b] = \frac{1}{2} \delta^{ab}$ and $|L_{\tilde{q}_x}|^2 + |R_{\tilde{q}_x}|^2 = 1$, and comparing to the derivation of eq. (6.322) of the previous subsection, we obtain:

$$[\Xi_{\tilde{g}}]_{\tilde{q}_x} = -\frac{\alpha_s}{4\pi} I_{FS}(s; m_q^2, m_{\tilde{q}_x}^2). \quad (6.373)$$

Similarly, for the last two diagrams of Fig. 59, we obtain:

$$\begin{aligned}
-i[\Omega_{\tilde{g}}]_{\tilde{q}_x} \delta^{ab} &= \mu^{2\epsilon} \int \frac{d^d k}{(2\pi)^d} (-i\sqrt{2} g_s T_k^{aj} L_{\tilde{q}_x}^*) \left(\frac{i m_q}{(k+p)^2 - m_q^2} \right) (i\sqrt{2} g_s T_j^{bk} R_{\tilde{q}_x}) \left(\frac{i}{k^2 - m_{\tilde{q}_x}^2} \right) \\
&+ \mu^{2\epsilon} \int \frac{d^d k}{(2\pi)^d} (i\sqrt{2} g_s T_j^{ak} R_{\tilde{q}_x}) \left(\frac{i m_q}{(k+p)^2 - m_q^2} \right) (-i\sqrt{2} g_s T_k^{bj} L_{\tilde{q}_x}^*) \left(\frac{i}{k^2 - m_{\tilde{q}_x}^2} \right), \quad (6.374)
\end{aligned}$$

again using the Feynman rules shown in fig. 81. As before, j and k are the color indices for the quark and the squark, respectively. Comparing to the derivation of eq. (6.345) of the previous subsection, we obtain:

$$[\Omega_{\tilde{g}}]_{\tilde{q}_x} = -\frac{\alpha_s}{2\pi} L_{\tilde{q}_x}^* R_{\tilde{q}_x} m_q I_{FS}(s; m_q^2, m_{\tilde{q}_x}^2). \quad (6.375)$$

Summing up the results obtained above, and taking $s = m_{\tilde{g}}^2$, we have:

$$\Xi_{\tilde{g}} = -\frac{\alpha_s}{4\pi} \left[C_A I_{FV}(m_{\tilde{g}}^2; m_{\tilde{g}}^2, 0) + \sum_q \sum_{x=1,2} I_{FS}(m_{\tilde{g}}^2; m_q^2, m_{\tilde{q}_x}^2) \right], \quad (6.376)$$

$$\Omega_{\tilde{g}} = -\frac{\alpha_s}{4\pi} \left[C_A m_{\tilde{g}} I_{FV}(m_{\tilde{g}}^2; m_{\tilde{g}}^2, 0) + 2 \sum_q \sum_{x=1,2} L_{\tilde{q}_x}^* R_{\tilde{q}_x} m_q I_{FS}(m_{\tilde{g}}^2; m_q^2, m_{\tilde{q}_x}^2) \right]. \quad (6.377)$$

As previously noted, we can now write down $\bar{\Omega}_{\tilde{g}}$ by replacing the Lagrangian parameters of eq. (6.377) by their complex conjugates:

$$\bar{\Omega}_{\tilde{g}} = -\frac{\alpha_s}{4\pi} \left[C_A m_{\tilde{g}} I_{FV}(m_{\tilde{g}}^2; m_{\tilde{g}}^2, 0) + 2 \sum_q \sum_{x=1,2} L_{\tilde{q}_x} R_{\tilde{q}_x}^* m_q I_{FS}(m_{\tilde{g}}^2; m_q^2, m_{\tilde{q}_x}^2) \right]. \quad (6.378)$$

Inserting the results of eqs. (6.376)–(6.378) into eq. (6.366), one obtains the result [120, 121]:

$$\begin{aligned}
M_{\tilde{g}}^2 - i M_{\tilde{g}} \Gamma_{\tilde{g}} &= m_{\tilde{g}}^2 \left[1 + \frac{\alpha_s}{2\pi} \left\{ C_A [5 - \delta_{\overline{\text{MS}}} - 3 \ln(m_{\tilde{g}}^2/Q^2)] \right. \right. \\
&\quad \left. \left. - \sum_q \sum_{x=1,2} \left[I_{FS}(m_{\tilde{g}}^2; m_q^2, m_{\tilde{q}_x}^2) + 2 \text{Re}[L_{\tilde{q}_x}^* R_{\tilde{q}_x}] \frac{m_q}{m_{\tilde{g}}} I_{FS}(m_{\tilde{g}}^2; m_q^2, m_{\tilde{q}_x}^2) \right] \right\} \right], \quad (6.379)
\end{aligned}$$

with $\delta_{\overline{\text{MS}}}$ defined in eq. (6.315).

6.25 Triangle anomaly from chiral fermion loops

As our final example, we consider the anomaly in chiral symmetries for fermions, arising from the triangle diagram involving three currents carrying vector indices.³⁹ Since the anomaly is independent of the fermion masses, we simplify the computation by setting all fermion masses to zero. In four-component notation, the treatment of the anomaly requires care because of the difficulty in defining a consistent and unambiguous γ_5 and the epsilon tensor in dimensional regularization. The same subtleties arise in two-component language, of course, but in a slightly different form since γ_5 does not appear explicitly.

We shall assemble all the $(\frac{1}{2}, 0)$ [left-handed] two-component fermion fields of the theory into a (generally reducible) multiplet ψ_j . For example, the fermions of the Standard Model are: $\psi_j = (\ell_k, \ell_k^c, \nu_k, q_{i\ell}, q_{i\ell}^c)$, where $k = 1, 2, 3$ and $i = 1, 2, \dots, 6$ are flavor labels and $\ell = 1, 2, 3$ are color labels [see Table 1]. The two-component spinor indices are suppressed here. Let the symmetry generators be given by Hermitian matrices T^a , so that the ψ_j transform as:

$$\delta\psi_j = i\theta^a (\mathbf{T}^a)_j{}^k \psi_k, \quad (6.380)$$

for infinitesimal parameters θ^a . The matrices \mathbf{T}^a form a reducible representation of a Lie algebra of the symmetry group. In particular, the \mathbf{T}^a have a block-diagonal structure, where each block separately transforms the corresponding field of ψ_j according to its symmetry transformation properties. Some or all of these symmetries may be gauged. The Feynman rule for the corresponding currents is the same as for external gauge bosons, (as in Fig. 8), and is shown in Fig. 60.

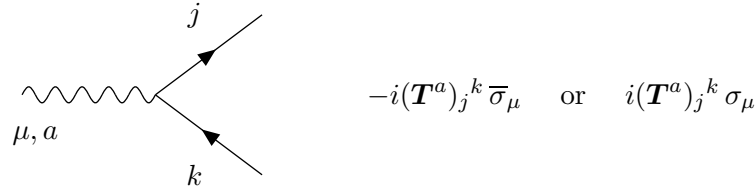


Figure 60: Feynman rule for the coupling of a current carrying vector index μ and corresponding to the symmetry generator \mathbf{T}^a acting on $(\frac{1}{2}, 0)$ [left-handed] fermions. Spinor indices are suppressed.

Figure 61 shows the two Feynman diagrams that contribute at one-loop to the three-point function of the symmetry currents. Applying the Feynman rules of Fig. 2 (with $m = 0$) for the propagators and Fig. 60 for the currents, the sum of these diagrams is given by:

³⁹The discussion here parallels that given in ref. [122], section 22.3.

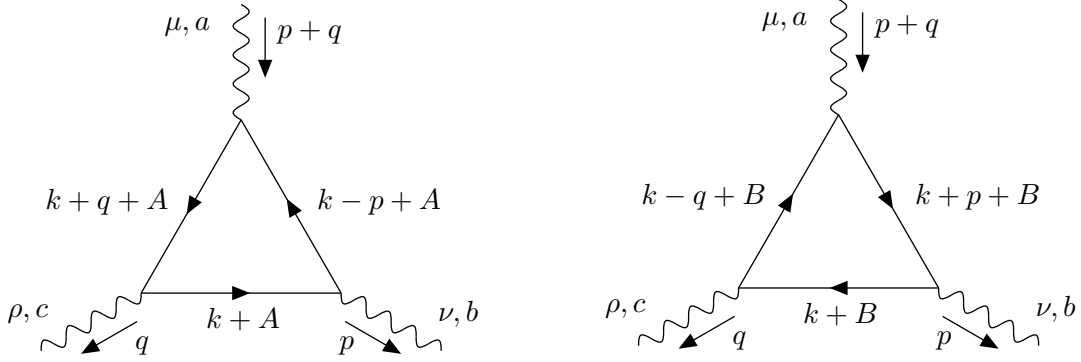


Figure 61: Triangle Feynman diagrams leading to the chiral fermion anomaly. Fermion spinor and flavor indices are suppressed. The fermion momenta as labeled flow in the arrow directions.

$$\begin{aligned}
i\Gamma_{\mu\nu\rho}^{abc} = & (-1) \int \frac{d^4k}{(2\pi)^4} \text{Tr} \left\{ (-i\bar{\sigma}_\mu \mathbf{T}^a) \frac{i(k-p+A) \cdot \sigma}{(k-p+A)^2} (-i\bar{\sigma}_\nu \mathbf{T}^b) \frac{i(k+A) \cdot \sigma}{(k+A)^2} (-i\bar{\sigma}_\rho \mathbf{T}^c) \frac{i(k+q+A) \cdot \sigma}{(k+q+A)^2} \right. \\
& \left. + (-i\bar{\sigma}_\mu \mathbf{T}^a) \frac{i(k-q+B) \cdot \sigma}{(k-q+B)^2} (-i\bar{\sigma}_\rho \mathbf{T}^c) \frac{i(k+B) \cdot \sigma}{(k+B)^2} (-i\bar{\sigma}_\nu \mathbf{T}^b) \frac{i(k+p+B) \cdot \sigma}{(k+p+B)^2} \right\}, \quad (6.381)
\end{aligned}$$

where the overall factor of (-1) is due to the presence of a closed fermion loop. The trace is taken over fermion flavor/group and spinor indices, both of which are suppressed. Writing

$$\text{Tr}(\{\mathbf{T}^a \mathbf{T}^b\} \mathbf{T}^c) = d^{abc} + \frac{i}{4} f^{abc}, \quad (6.382)$$

where *****

Although the symmetrized three-point function is ultraviolet finite, the individual loop momentum integrals are divergent, and must be defined with care. We do not regularize them by the usual procedure of continuing to $d = 4 - 2\epsilon$ dimensions, because the trace over sigma matrices crucially involves the antisymmetric tensor with four indices, brought in by eqs. (A.24) and (A.25), for which there is no consistent and unambiguous generalization outside of four dimensions. (This is related to the difficulty of defining γ_5 in the four-component spinor notation.) Because the individual integrals are linearly divergent, we must allow for arbitrary constant four-vectors A^μ and B^μ as offsets for the loop momentum when defining the loop integrations for the two diagrams [123]. The existence of these vectors corresponds to an ambiguity in the regulation procedure, which can be fixed to preserve some of the symmetries, as we will see below.

The persistence of the symmetry in the quantum theory for the currents labeled by μ, a and ν, b and ρ, c implies the conservation equations

$$(p+q)^\mu \Gamma_{\mu\nu\rho}^{abc} = 0, \quad -p^\nu \Gamma_{\mu\nu\rho}^{abc} = 0, \quad \text{and} \quad -q^\rho \Gamma_{\mu\nu\rho}^{abc} = 0, \quad (6.383)$$

respectively. Here we are interested in the potentially anomalous part obtained by symmetrizing over the indices a, b, c :

$$\mathcal{A}_{\mu\nu\rho}^{abc} = \frac{1}{6}i\Gamma_{\mu\nu\rho}^{abc} + [\text{five permutations of } a, b, c]. \quad (6.384)$$

Then the contribution of both diagrams involves the same group theory factor, the anomaly coefficient

$$d^{abc} = \frac{1}{2}\text{Tr}[\{T^a, T^b\}T^c]. \quad (6.385)$$

First, consider the result for $(p+q)^\mu \mathcal{A}_{\mu\nu\rho}^{abc}$. This can be simplified by rewriting

$$(p+q)^\mu = (k+q+A)^\mu - (k-p+A)^\mu, \quad (6.386)$$

$$(p+q)^\mu = (k+p+B)^\mu - (k-q+B)^\mu \quad (6.387)$$

in the first and second diagram terms, respectively, and then applying the formulas

$$v \cdot \sigma v \cdot \bar{\sigma} = v^2, \quad (6.388)$$

$$v \cdot \bar{\sigma} v \cdot \sigma = v^2, \quad (6.389)$$

which follow from eqs. (A.1), (A.2). After rearranging the terms using the cyclic property of the trace, we obtain:

$$(p+q)^\mu \mathcal{A}_{\mu\nu\rho}^{abc} = d^{abc} \text{Tr}[\sigma_\kappa \bar{\sigma}_\nu \sigma_\lambda \bar{\sigma}_\rho] X^{\kappa\lambda}, \quad (6.390)$$

where the integral is given by:

$$\begin{aligned} X^{\kappa\lambda} = \int \frac{d^4 k}{(2\pi)^4} & \left[\frac{(k-p+A)^\kappa (k+A)^\lambda}{(k-p+A)^2 (k+A)^2} - \frac{(k+q+A)^\kappa (k+A)^\lambda}{(k+q+A)^2 (k+A)^2} \right. \\ & \left. + \frac{(k+B)^\kappa (k-q+B)^\lambda}{(k+B)^2 (k-q+B)^2} - \frac{(k+B)^\kappa (k+p+B)^\lambda}{(k+B)^2 (k+p+B)^2} \right]. \end{aligned} \quad (6.391)$$

Naively, this integral appears to vanish, because the first term is equal to the negative of the fourth term after a momentum shift $k \rightarrow k-p+A-B$, and the second term is equal to the negative of the third term after $k \rightarrow k+q+A-B$. However, these momentum shifts are not valid for the individually divergent integrals. Instead, $X^{\kappa\lambda}$ can be evaluated by a Wick rotation to Euclidean space, followed by isolating the terms that contribute for large k^2 and are responsible for the integral not vanishing, and then use of the divergence theorem in four dimensions to rewrite the integral as one over a three-sphere with radius tending to infinity. The result is:

$$X^{\kappa\lambda} = \frac{i}{96\pi^2} \left[g^{\kappa\lambda} (p+q) \cdot (A+B) + (A-2B)^\kappa (p+q)^\lambda + (p+q)^\kappa (B-2A)^\lambda \right]. \quad (6.392)$$

Applying eq. (A.24), we get the result for the anomaly in the current labeled by μ, a :

$$(p+q)^\mu \mathcal{A}_{\mu\nu\rho}^{abc} = \frac{i}{48\pi^2} d^{abc} \left[(p+q)_\nu (A+B)_\rho + (A+B)_\nu (p+q)_\rho - g_{\nu\rho} (p+q) \cdot (A+B) \right. \\ \left. + 3i\epsilon_{\nu\rho\kappa\lambda} (p+q)^\kappa (A-B)^\lambda \right]. \quad (6.393)$$

Repeating all of the steps starting with eq. (6.386), we similarly obtain:

$$-p^\nu \mathcal{A}_{\mu\nu\rho}^{abc} = -\frac{i}{48\pi^2} d^{abc} \left[p_\rho (A+B)_\mu + p_\mu (A+B)_\rho - g_{\mu\rho} p \cdot (A+B) + 3i\epsilon_{\rho\mu\kappa\lambda} p^\kappa (A-B+2q)^\lambda \right], \quad (6.394)$$

$$-q^\rho \mathcal{A}_{\mu\nu\rho}^{abc} = -\frac{i}{48\pi^2} d^{abc} \left[q_\mu (A+B)_\nu + q_\nu (A+B)_\mu - g_{\mu\nu} q \cdot (A+B) + 3i\epsilon_{\mu\nu\kappa\lambda} q^\kappa (A-B-2p)^\lambda \right]. \quad (6.395)$$

[Alternatively, one can simply note that eq. (6.394) follows from eq. (6.393) by making the replacements $\mu \rightarrow \nu$, $\nu \rightarrow \rho$, $\rho \rightarrow \mu$, $A \rightarrow A+q$, $B \rightarrow B-q$, $p \rightarrow q$, and $q \rightarrow -p-q$, while eq. (6.395) follows from eq. (6.393) by making the replacements $\mu \rightarrow \rho$, $\nu \rightarrow \mu$, $\rho \rightarrow \nu$, $A \rightarrow A-p$, $B \rightarrow B+p$, $p \rightarrow -p-q$, and $q \rightarrow p$.]

From eqs. (6.393)–(6.395), it is clear that unless $A+B=0$, all three symmetries will definitely be anomalous unless $d^{abc}=0$. To avoid this, we choose $B=-A$, with the result:

$$(p+q)^\mu \mathcal{A}_{\mu\nu\rho}^{abc} = -\frac{1}{8\pi^2} d^{abc} \epsilon_{\nu\rho\kappa\lambda} (p+q)^\kappa A^\lambda, \quad (6.396)$$

$$-p^\nu \mathcal{A}_{\mu\nu\rho}^{abc} = \frac{1}{8\pi^2} d^{abc} \epsilon_{\rho\mu\kappa\lambda} p^\kappa (A+q)^\lambda, \quad (6.397)$$

$$-q^\rho \mathcal{A}_{\mu\nu\rho}^{abc} = \frac{1}{8\pi^2} d^{abc} \epsilon_{\mu\nu\kappa\lambda} q^\kappa (A-p)^\lambda. \quad (6.398)$$

It is still not possible to avoid an anomaly in all three symmetries if $d^{abc} \neq 0$. If one wants an anomaly to arise only in the current labeled by μ, a (for example, if the symmetries labeled by b, c are gauged), one must now choose $A=p-q$. The standard result follows:

$$(p+q)^\mu \mathcal{A}_{\mu\nu\rho}^{abc} = \frac{1}{4\pi^2} d^{abc} \epsilon_{\nu\rho\kappa\lambda} p^\kappa q^\lambda, \quad (6.399)$$

$$-p^\nu \mathcal{A}_{\mu\nu\rho}^{abc} = 0, \quad (6.400)$$

$$-q^\rho \mathcal{A}_{\mu\nu\rho}^{abc} = 0. \quad (6.401)$$

In particular, one cannot gauge all three symmetries a, b, c unless $d^{abc}=0$.

In writing down eq. (6.381), we chose to use the rules with $\bar{\sigma}$ matrices for the current vertices and σ matrices for the massless fermion propagators. If we had chosen the opposite prescription, the net effect would have been to obtain the same results as above, but with the opposite sign for all terms involving the epsilon tensor, due to the sign difference in eqs. (A.24) and (A.25). This leads to an overall sign ambiguity in the anomaly amplitude for the antisymmetric combination

of vector indices. Since the phase of the amplitude is not observable, this does not lead to a problem. However, when combining the two diagrams, or when including higher loop order diagrams, a consistent choice must be made. Note that the evaluation of the anomaly above relied on combining diagrams with a common spinor trace structure in eq. (6.390).

Appendix A: Two-component spinor identities in $d \neq 4$

When considering a theory regularized by dimensional continuation, one must be careful in treating cases with contracted spacetime vector indices μ, ν, ρ, \dots . Instead of taking on 4 possible values, these vector indices formally run over d values, where d is infinitesimally different from 4. This means that some identities that would hold in unregularized 4-dimensional theories are inconsistent and must not be used; other identities remain valid if d replaces 4 in the appropriate spots; and still other identities hold without modification.

Two important identities that do hold in $d \neq 4$ dimensions are:

$$[\sigma^\mu \bar{\sigma}^\nu + \sigma^\nu \bar{\sigma}^\mu]_\alpha{}^\beta = 2g^{\mu\nu} \delta_\alpha^\beta, \quad (\text{A.1})$$

$$[\bar{\sigma}^\mu \sigma^\nu + \bar{\sigma}^\nu \sigma^\mu]^{\dot{\alpha}}{}_{\dot{\beta}} = 2g^{\mu\nu} \delta_{\dot{\beta}}^{\dot{\alpha}}. \quad (\text{A.2})$$

The trace identities:

$$\text{Tr}[\sigma^\mu \bar{\sigma}^\nu] = \text{Tr}[\bar{\sigma}^\mu \sigma^\nu] = 2g^{\mu\nu} \quad (\text{A.3})$$

then follow. We also note that the spinor index trace identity

$$\text{Tr}[\mathbf{1}] = \delta_\alpha^\alpha = \delta_{\dot{\alpha}}^{\dot{\alpha}} = 2 \quad (\text{A.4})$$

continues to hold in dimensional continuation regularization methods.

In contrast, the Fierz identity (written here in three equivalent forms):

$$\sigma_{\alpha\dot{\alpha}}^\mu \bar{\sigma}_\mu^{\dot{\beta}\beta} = 2\delta_\alpha^\beta \delta_{\dot{\alpha}}^{\dot{\beta}} \quad (\text{A.5})$$

$$\sigma_{\alpha\dot{\alpha}}^\mu \sigma_{\mu\beta\dot{\beta}} = 2\epsilon_{\alpha\beta} \epsilon_{\dot{\alpha}\dot{\beta}} \quad (\text{A.6})$$

$$\bar{\sigma}^{\mu\dot{\alpha}\alpha} \bar{\sigma}_\mu^{\dot{\beta}\beta} = 2\epsilon^{\alpha\beta} \epsilon^{\dot{\alpha}\dot{\beta}} \quad (\text{A.7})$$

does not have a consistent, unambiguous meaning outside of 4 dimensions. (See for example refs. [124–126] and references therein.) However, the following identities that are implied by the

Fierz identity do consistently generalize to $d \neq 4$ spacetime dimensions:

$$[\sigma^\mu \bar{\sigma}_\mu]_\alpha{}^\beta = d \delta_\alpha^\beta \quad (\text{A.8})$$

$$[\bar{\sigma}^\mu \sigma_\mu]^{\dot{\alpha}}{}_{\dot{\beta}} = d \delta_{\dot{\beta}}^{\dot{\alpha}} \quad (\text{A.9})$$

$$[\sigma^\mu \bar{\sigma}^\nu \sigma_\mu]_{\alpha\dot{\beta}} = (2-d) \sigma_{\alpha\dot{\beta}}^\nu \quad (\text{A.10})$$

$$[\bar{\sigma}^\mu \sigma_\nu \bar{\sigma}_\mu]^{\dot{\alpha}\beta} = (2-d) \bar{\sigma}_{\dot{\nu}}^{\dot{\alpha}\beta} \quad (\text{A.11})$$

$$[\sigma^\mu \bar{\sigma}^\nu \sigma^\rho \bar{\sigma}_\mu]_\alpha{}^\beta = 4g^{\nu\rho} \delta_\alpha^\beta - (4-d) [\sigma^\nu \bar{\sigma}^\rho]_\alpha{}^\beta \quad (\text{A.12})$$

$$[\bar{\sigma}^\mu \sigma^\nu \bar{\sigma}^\rho \sigma_\mu]^{\dot{\alpha}}{}_{\dot{\beta}} = 4g^{\nu\rho} \delta_{\dot{\beta}}^{\dot{\alpha}} - (4-d) [\bar{\sigma}^\nu \sigma^\rho]^{\dot{\alpha}}{}_{\dot{\beta}}, \quad (\text{A.13})$$

$$[\sigma^\mu \bar{\sigma}^\nu \sigma^\rho \bar{\sigma}^\kappa \sigma_\mu]_{\alpha\dot{\beta}} = -2[\sigma^\kappa \bar{\sigma}^\rho \sigma^\nu]_{\alpha\dot{\beta}} + (4-d) [\sigma^\nu \bar{\sigma}^\rho \sigma^\kappa]_{\alpha\dot{\beta}} \quad (\text{A.14})$$

$$[\bar{\sigma}^\mu \sigma^\nu \bar{\sigma}^\rho \sigma^\kappa \bar{\sigma}_\mu]^{\dot{\alpha}\beta} = -2[\bar{\sigma}^\kappa \sigma^\rho \bar{\sigma}^\nu]^{\dot{\alpha}\beta} + (4-d) [\bar{\sigma}^\nu \sigma^\rho \bar{\sigma}^\kappa]^{\dot{\alpha}\beta}. \quad (\text{A.15})$$

Eq. (A.5) is the basis for other Fierz identities that hold in 4 dimensions, which are given in detail in Appendix A of ref. [38] as well as [37, 42, 43].

Identities that involve the (explicitly and inextricably 4-dimensional) $\epsilon^{\mu\nu\rho\kappa}$ symbol,

$$\bar{\sigma}^\mu \sigma^\nu \bar{\sigma}^\rho = g^{\mu\nu} \bar{\sigma}^\rho - g^{\mu\rho} \bar{\sigma}^\nu + g^{\nu\rho} \bar{\sigma}^\mu - i\epsilon^{\mu\nu\rho\kappa} \bar{\sigma}_\kappa, \quad (\text{A.16})$$

$$\sigma^\mu \bar{\sigma}^\nu \sigma^\rho = g^{\mu\nu} \sigma^\rho - g^{\mu\rho} \sigma^\nu + g^{\nu\rho} \sigma^\mu + i\epsilon^{\mu\nu\rho\kappa} \sigma_\kappa, \quad (\text{A.17})$$

$$\sigma^{\mu\nu} \sigma^\rho = \frac{i}{2} (g^{\nu\rho} \sigma^\mu - g^{\mu\rho} \sigma^\nu + i\epsilon^{\mu\nu\rho\kappa} \sigma_\kappa), \quad (\text{A.18})$$

$$\bar{\sigma}^{\mu\nu} \bar{\sigma}^\rho = \frac{i}{2} (g^{\nu\rho} \bar{\sigma}^\mu - g^{\mu\rho} \bar{\sigma}^\nu - i\epsilon^{\mu\nu\rho\kappa} \bar{\sigma}_\kappa), \quad (\text{A.19})$$

$$\bar{\sigma}^\mu \sigma^{\nu\rho} = \frac{i}{2} (g^{\mu\nu} \bar{\sigma}^\rho - g^{\mu\rho} \bar{\sigma}^\nu - i\epsilon^{\mu\nu\rho\kappa} \bar{\sigma}_\kappa), \quad (\text{A.20})$$

$$\sigma^\mu \bar{\sigma}^{\nu\rho} = \frac{i}{2} (g^{\mu\nu} \sigma^\rho - g^{\mu\rho} \sigma^\nu + i\epsilon^{\mu\nu\rho\kappa} \sigma_\kappa), \quad (\text{A.21})$$

$$\sigma^{\mu\nu} \sigma^{\rho\kappa} = -\frac{1}{4} (g^{\nu\rho} g^{\mu\kappa} - g^{\mu\rho} g^{\nu\kappa} + i\epsilon^{\mu\nu\rho\kappa}) \quad (\text{A.22})$$

$$\begin{aligned} & + \frac{i}{2} (g^{\nu\rho} \sigma^{\mu\kappa} + g^{\mu\kappa} \sigma^{\nu\rho} - g^{\mu\rho} \sigma^{\nu\kappa} - g^{\nu\kappa} \sigma^{\mu\rho}), \\ \bar{\sigma}^{\mu\nu} \bar{\sigma}^{\rho\kappa} & = -\frac{1}{4} (g^{\nu\rho} g^{\mu\kappa} - g^{\mu\rho} g^{\nu\kappa} - i\epsilon^{\mu\nu\rho\kappa}) \\ & + \frac{i}{2} (g^{\nu\rho} \bar{\sigma}^{\mu\kappa} + g^{\mu\kappa} \bar{\sigma}^{\nu\rho} - g^{\mu\rho} \bar{\sigma}^{\nu\kappa} - g^{\nu\kappa} \bar{\sigma}^{\mu\rho}). \end{aligned} \quad (\text{A.23})$$

are also only meaningful in exactly four dimensions. This applies as well to the trace identities which follow from them.⁴⁰ For example,

$$\text{Tr}[\sigma^\mu \bar{\sigma}^\nu \sigma^\rho \bar{\sigma}^\kappa] = 2 (g^{\mu\nu} g^{\rho\kappa} - g^{\mu\rho} g^{\nu\kappa} + g^{\mu\kappa} g^{\nu\rho} + i\epsilon^{\mu\nu\rho\kappa}), \quad (\text{A.24})$$

$$\text{Tr}[\bar{\sigma}^\mu \sigma^\nu \bar{\sigma}^\rho \sigma^\kappa] = 2 (g^{\mu\nu} g^{\rho\kappa} - g^{\mu\rho} g^{\nu\kappa} + g^{\mu\kappa} g^{\nu\rho} - i\epsilon^{\mu\nu\rho\kappa}). \quad (\text{A.25})$$

This could lead to ambiguities in loop computations where it is necessary to perform the computation in $d \neq 4$ dimensions (until the end of the calculation where the limit $d \rightarrow 4$ is taken).

⁴⁰This is analogous to the statement that $\text{Tr}(\gamma^5 \gamma^\mu \gamma^\nu \gamma^\rho \gamma^\kappa) = -4i\epsilon^{\mu\nu\rho\kappa}$ [in our convention where $\epsilon^{0123} = +1$] is only meaningful in $d = 4$ dimensions. In two-component notation, the equivalent result is $\text{Tr}[\sigma^\mu \bar{\sigma}^\nu \sigma^\rho \bar{\sigma}^\kappa - \bar{\sigma}^\mu \sigma^\nu \bar{\sigma}^\rho \sigma^\kappa] = 4i\epsilon^{\mu\nu\rho\kappa}$. In the literature various schemes have been proposed for defining the properties of γ^5 in $d \neq 4$ dimensions [126]. In two-component notation, this would translate into a procedure for dealing with general traces involving four or more σ and $\bar{\sigma}$ matrices.

However, in practice one typically finds that the above expressions appear multiplied by the metric and/or other external tensors (such as four-momenta appropriate to the problem at hand). In almost all such cases, two of the indices appearing in eqs. (A.24) and (A.25) are symmetrized which eliminates the $\epsilon^{\mu\nu\rho\kappa}$ term, rendering the resulting expressions unambiguous. Similarly, the sum of the above trace identities can be assigned an unambiguous meaning in $d \neq 4$ dimensions:

$$\text{Tr}[\sigma^\mu \bar{\sigma}^\nu \sigma^\rho \bar{\sigma}^\kappa] + \text{Tr}[\bar{\sigma}^\mu \sigma^\nu \bar{\sigma}^\rho \sigma^\kappa] = 4(g^{\mu\nu} g^{\rho\kappa} - g^{\mu\rho} g^{\nu\kappa} + g^{\mu\kappa} g^{\nu\rho}). \quad (\text{A.26})$$

By repeatedly applying the identities given in eqs. (A.1)–(A.3) to eqs. (A.24) and (A.25) in 4 dimensions and eq. (A.26) in d dimensions, and using the cyclic property of the trace, one can recursively derive trace formulas for products of 6 or more σ and $\bar{\sigma}$ matrices.

Appendix B: Explicit forms for the two-component spinor wave functions

In this Appendix, we construct the explicit forms for the eigenstates of the spin operator $\frac{1}{2}\vec{\sigma} \cdot \hat{\mathbf{s}}$, and we examine their properties.

Consider a spin-1/2 fermion in its rest frame and quantize the spin along a fixed axis specified by the unit vector

$$\hat{\mathbf{s}} \equiv (\sin \theta \cos \phi, \sin \theta \sin \phi, \cos \theta), \quad (\text{B.1})$$

with polar angle θ and azimuthal angle ϕ with respect to a fixed z -axis. The corresponding spin states will be called fixed-axis spin states. The relevant basis of two-component spinors χ_s are eigenstates of $\frac{1}{2}\vec{\sigma} \cdot \hat{\mathbf{s}}$, i.e.,

$$\frac{1}{2}\vec{\sigma} \cdot \hat{\mathbf{s}} \chi_s = s \chi_s, \quad s = \pm \frac{1}{2}. \quad (\text{B.2})$$

In order to construct the eigenstates of $\frac{1}{2}\vec{\sigma} \cdot \hat{\mathbf{s}}$, we first consider the case where $\hat{\mathbf{s}} = \hat{\mathbf{z}}$. In this case, we define the eigenstates of $\frac{1}{2}\sigma^3$ to be:

$$\chi_{1/2}(\hat{\mathbf{z}}) = \begin{pmatrix} 1 \\ 0 \end{pmatrix}, \quad \chi_{-1/2}(\hat{\mathbf{z}}) = \begin{pmatrix} 0 \\ 1 \end{pmatrix}. \quad (\text{B.3})$$

By convention, we have set an arbitrary overall multiplicative phase factor for each spinor of eq. (B.3) to unity. We then determine $\chi_s(\hat{\mathbf{s}})$ from $\chi_s(\hat{\mathbf{z}})$ by employing the spin-1/2 rotation operator that corresponds to a rotation from $\hat{\mathbf{z}}$ to $\hat{\mathbf{s}}$. However, this rotation operator is not unique. In the convention adopted here, we first perform a rotation by an angle ϕ about the z -axis [the corresponding rotation operator is denoted by $R(\hat{\mathbf{z}}, \phi)$]. This has no effect, of course, on the unit vector $\hat{\mathbf{z}}$. However, it does result in the modification of $\chi_s(\hat{\mathbf{z}})$ by an s -dependent phase factor. We then rotate by an angle θ about an axis $\hat{\mathbf{n}} = (-\sin \phi, \cos \phi, 0)$ [the corresponding

rotation operator is denoted by $R(\hat{\mathbf{n}}, \theta)$. As a result of the product of these two rotations [an explicit expression for R is given in eq. (B.19)], $\hat{\mathbf{z}}$ is rotated into $\hat{\mathbf{s}}$. Explicitly, $\hat{\mathbf{s}} = \mathcal{R}\hat{\mathbf{z}}$, where⁴¹

$$\mathcal{R} = R(\hat{\mathbf{n}}, \theta) R(\hat{\mathbf{z}}, \phi) = \begin{pmatrix} \cos \theta \cos \phi & -\sin \phi & \sin \theta \cos \phi \\ \cos \theta \sin \phi & \cos \phi & \sin \theta \sin \phi \\ -\sin \theta & 0 & \cos \theta \end{pmatrix}. \quad (\text{B.4})$$

Employing the spin-1/2 rotation operator corresponding to \mathcal{R} , we can compute $\chi_s(\hat{\mathbf{s}})$,

$$\chi_s(\hat{\mathbf{s}}) = \exp(-i\theta\hat{\mathbf{n}} \cdot \vec{\sigma}/2) \exp(-i\phi\sigma^3/2) \chi_s(\hat{\mathbf{z}}), \quad \hat{\mathbf{n}} = (-\sin \phi, \cos \phi, 0). \quad (\text{B.5})$$

Eq. (B.5) yields explicit forms⁴² for the eigenstates of $\frac{1}{2}\vec{\sigma} \cdot \hat{\mathbf{s}}$:

$$\chi_{1/2}(\hat{\mathbf{s}}) = \begin{pmatrix} e^{-i\phi/2} \cos \frac{\theta}{2} \\ e^{i\phi/2} \sin \frac{\theta}{2} \end{pmatrix}, \quad \chi_{-1/2}(\hat{\mathbf{s}}) = \begin{pmatrix} -e^{-i\phi/2} \sin \frac{\theta}{2} \\ e^{i\phi/2} \cos \frac{\theta}{2} \end{pmatrix}. \quad (\text{B.6})$$

These spinors are normalized such that

$$\chi_s^\dagger(\hat{\mathbf{s}}) \chi_{s'}(\hat{\mathbf{s}}) = \delta_{ss'}, \quad (\text{B.7})$$

and satisfy the following completeness relation:

$$\sum_s \chi_s(\hat{\mathbf{s}}) \chi_s^\dagger(\hat{\mathbf{s}}) = \begin{pmatrix} 1 & 0 \\ 0 & 1 \end{pmatrix}. \quad (\text{B.8})$$

The spinors $\chi_s(\hat{\mathbf{s}})$ and $\chi_{-s}(\hat{\mathbf{s}})$ are connected by the following relation:

$$\chi_{-s}(\hat{\mathbf{s}}) = -2s \begin{pmatrix} 0 & 1 \\ -1 & 0 \end{pmatrix} \chi_s^*(\hat{\mathbf{s}}). \quad (\text{B.9})$$

Consider a spin-1/2 fermion with four-momentum $p^\mu = (E, \vec{p})$, with $E = (|\vec{p}|^2 + m^2)^{1/2}$, and the direction of \vec{p} given by

$$\hat{\mathbf{p}} = (\sin \theta_p \cos \phi_p, \sin \theta_p \sin \phi_p, \cos \theta_p). \quad (\text{B.10})$$

Using eqs. (2.69), (2.70) and (B.6), one can employ eqs. (3.19)–(3.22) to obtain explicit expressions for the two-component spinor wave functions $x(\vec{p}, s)$, $y(\vec{p}, s)$, $\bar{x}(\vec{p}, s)$ and $\bar{y}(\vec{p}, s)$.

⁴¹In the more common convention in the literature, the factor of $R(\hat{\mathbf{z}}, \phi)$ is absent in the definition of \mathcal{R} . However, our choice for \mathcal{R} is motivated by the simplicity of the explicit form given in eq. (B.4).

⁴²Note that for $\phi \rightarrow \phi + 2\pi$, $\chi_s(\hat{\mathbf{s}}) \rightarrow -\chi_s(\hat{\mathbf{s}})$, which simply reflects that double-valueness of SU(2) transformations. However, as the overall phase of the spinor wave function is arbitrary, we shall restrict $0 \leq \phi < 2\pi$ and $0 \leq \theta \leq \pi$ in our definition of $\chi_s(\hat{\mathbf{s}})$.

Additional properties of the χ_s can be derived by introducing an orthonormal set of unit three-vectors $\hat{\mathbf{s}}^a$ that provide a basis for a right-handed coordinate system. Explicitly,

$$\hat{\mathbf{s}}^a \cdot \hat{\mathbf{s}}^b = \delta^{ab}, \quad (\text{B.11})$$

$$\hat{\mathbf{s}}^a \times \hat{\mathbf{s}}^b = \epsilon^{abc} \hat{\mathbf{s}}^c. \quad (\text{B.12})$$

We shall identify:

$$\hat{\mathbf{s}} = \hat{\mathbf{s}}^3 \quad (\text{B.13})$$

as the quantization axis $\hat{\mathbf{s}}$ used in defining the third component of the spin of the fermion in its rest frame. The unit vectors $\hat{\mathbf{s}}^1$ and $\hat{\mathbf{s}}^2$ are then chosen such that eqs. (B.11) and (B.12) are satisfied. To explicitly construct the $\hat{\mathbf{s}}^a$, we begin with the orthonormal set $\{\hat{\mathbf{x}}, \hat{\mathbf{y}}, \hat{\mathbf{z}}\}$, and rotate each unit vector with the rotation matrix \mathcal{R} given in eq. (B.4), so that $\hat{\mathbf{s}}^a = \mathcal{R}(\hat{\mathbf{x}}, \hat{\mathbf{y}}, \hat{\mathbf{z}})$. That is,

$$\begin{aligned} \mathbf{s}^{1\mu} &= (\cos \theta \cos \phi, \cos \theta \sin \phi, -\sin \theta), \\ \mathbf{s}^{2\mu} &= (-\sin \phi, \cos \phi, 0), \\ \mathbf{s}^{3\mu} &= (\sin \theta \cos \phi, \sin \theta \sin \phi, \cos \theta). \end{aligned} \quad (\text{B.14})$$

We can use the \mathbf{s}^a to extend the defining equation of χ_s [eq. (B.2)]:

$$\frac{1}{2} \vec{\sigma} \cdot \hat{\mathbf{s}}^a \chi_{s'} = \frac{1}{2} \tau_{ss'}^a \chi_s, \quad (\text{B.15})$$

where the $\tau_{ss'}^a$ are the matrix elements of the Pauli matrices.⁴³ That is, $\frac{1}{2} \vec{\sigma} \cdot (\mathbf{s}^1 \pm i \mathbf{s}^2)$ serve as ladder operators that connect the spinor wave functions $\chi_{1/2}$ and $\chi_{-1/2}$. Using eq. (B.7), it follows that eq. (B.15) is equivalent to:

$$\chi_s^\dagger \vec{\sigma} \cdot \hat{\mathbf{s}}^a \chi_{s'} = \tau_{ss'}^a. \quad (\text{B.16})$$

To prove eq. (B.16), we use eq. (B.5) to obtain:

$$\chi_s^\dagger(\hat{\mathbf{s}}) \vec{\sigma} \cdot \hat{\mathbf{s}}^a \chi_{s'}(\hat{\mathbf{s}}) = \chi_s^\dagger(\hat{\mathbf{z}}) e^{i\phi\sigma^3/2} e^{i\theta\hat{\mathbf{n}} \cdot \vec{\sigma}/2} \vec{\sigma} \cdot \hat{\mathbf{s}}^a e^{-i\theta\hat{\mathbf{n}} \cdot \vec{\sigma}/2} e^{-i\phi\sigma^3/2} \chi_{s'}(\hat{\mathbf{z}}). \quad (\text{B.17})$$

The above result can be simplified by using the following identity:

$$e^{-i\theta\hat{\mathbf{n}} \cdot \vec{\sigma}/2} \sigma^j e^{i\theta\hat{\mathbf{n}} \cdot \vec{\sigma}/2} = R^{ij}(\hat{\mathbf{n}}, \theta) \sigma^i, \quad (\text{B.18})$$

where

$$R^{ij}(\hat{\mathbf{n}}, \theta) = n^i n^j + (\delta^{ij} - n^i n^j) \cos \theta - \epsilon^{ijk} n^k \sin \theta. \quad (\text{B.19})$$

⁴³We use the symbol τ rather than σ to emphasize that the indices of the Pauli matrices τ^a are spin labels s, s' and *not* spinor indices $\alpha, \dot{\alpha}$. The first (second) row and column of the τ -matrices correspond to $s = 1/2$ ($-1/2$). For example, $\tau_{ss'}^3 = 2s\delta_{ss'}$ (no sum over s).

Thus,

$$\chi_s^\dagger(\hat{\mathbf{s}}) \vec{\sigma} \cdot \hat{\mathbf{s}}^a \chi_{s'}(\hat{\mathbf{s}}) = \chi_s^\dagger(\hat{\mathbf{z}}) \vec{\sigma} \cdot [R(\hat{\mathbf{z}}, -\phi) R(\hat{\mathbf{n}}, -\theta) \hat{\mathbf{s}}^a] \chi_{s'}(\hat{\mathbf{z}}). \quad (\text{B.20})$$

Since

$$\mathcal{R}^{-1} = R(\hat{\mathbf{z}}, -\phi) R(\hat{\mathbf{n}}, -\theta), \quad (\text{B.21})$$

where \mathcal{R} is the rotation matrix given in eq. (B.4), and $\mathcal{R}^{-1} \hat{\mathbf{s}}^a = (\hat{\mathbf{x}}, \hat{\mathbf{y}}, \hat{\mathbf{z}})$, it follows that

$$\vec{\sigma} \cdot [R(\hat{\mathbf{z}}, -\phi) R(\hat{\mathbf{n}}, -\theta) \hat{\mathbf{s}}^a] = \sigma^a. \quad (\text{B.22})$$

Consequently, we end up with

$$\chi_s^\dagger(\hat{\mathbf{s}}) \vec{\sigma} \cdot \hat{\mathbf{s}}^a \chi_{s'}(\hat{\mathbf{s}}) = \chi_s^\dagger(\hat{\mathbf{z}}) \sigma^a \chi_{s'}(\hat{\mathbf{z}}) \equiv \tau_{ss'}^a, \quad (\text{B.23})$$

which defines the matrix elements of the Pauli matrices, and our proof of eq. (B.16) is complete.

All the results of this Appendix also apply to the helicity spinors χ_λ , which are defined to be eigenstates of $\frac{1}{2} \vec{\sigma} \cdot \hat{\mathbf{p}}$, i.e.,

$$\frac{1}{2} \vec{\sigma} \cdot \hat{\mathbf{p}} \chi_\lambda(\hat{\mathbf{p}}) = \lambda \chi_\lambda(\hat{\mathbf{p}}), \quad \lambda = \pm \frac{1}{2}, \quad (\text{B.24})$$

where $\hat{\mathbf{p}}$ is given by eq. (B.10). Eqs. (B.3)–(B.9) also apply to the two-component helicity spinors after taking $\hat{\mathbf{s}} = \hat{\mathbf{p}}$ (i.e., identifying $\theta = \theta_p$ and $\phi = \phi_p$). In addition, in analogy with the $\hat{\mathbf{s}}^a$, we can introduce an orthonormal set of unit three-vectors $\hat{\mathbf{p}}^a$ such that

$$\begin{aligned} \mathbf{p}^{1\mu} &= (\cos \theta_p \cos \phi_p, \cos \theta_p \sin \phi_p, -\sin \theta_p), \\ \mathbf{p}^{2\mu} &= (-\sin \phi_p, \cos \phi_p, 0), \\ \mathbf{p}^{3\mu} &= \hat{\mathbf{p}}^\mu = (\sin \theta_p \cos \phi_p, \sin \theta_p \sin \phi_p, \cos \theta_p). \end{aligned} \quad (\text{B.25})$$

In particular, eqs. (B.11)–(B.16) apply as well to the two-component helicity spinors after taking $\hat{\mathbf{s}}^a = \hat{\mathbf{p}}^a$.

The overall phase of the helicity spinor wave function of a fermion is conventional. However, an ambiguity arises in the case of a pair of fermions in its two-particle rest frame, in which the corresponding fermion three-momenta are $\vec{\mathbf{p}}$ and $-\vec{\mathbf{p}}$, respectively. The helicity spinor wave function of the second fermion depends on the definition of $\chi_\lambda(-\hat{\mathbf{p}})$. In the convention of ref. [17], $\chi_\lambda(-\hat{\mathbf{p}})$ is obtained from $\chi_\lambda(\hat{\mathbf{z}})$ via a rotation by a polar angle $\pi - \theta_p$ and an azimuthal angle $\phi_p + \pi$ with respect to the $\hat{\mathbf{z}}$ -direction. Using this convention with our definition of the spinor wave function [eq. (B.5)] yields $\chi_\lambda(-\hat{\mathbf{p}}) = i \chi_{-\lambda}(\hat{\mathbf{p}})$. An alternative convention advocated by Jacob and Wick [127] is to define $\chi_\lambda(-\hat{\mathbf{p}})$ by starting with $\chi_{-\lambda}(\hat{\mathbf{z}})$ and then rotating the spinor by polar angle θ_p and azimuthal angle ϕ_p . In this case,

$$\chi_\lambda(-\hat{\mathbf{p}}) = \chi_{-\lambda}(\hat{\mathbf{p}}), \quad (\text{B.26})$$

and the extra phase factor is absent. We shall adopt the convention of eq. (B.26) in constructing helicity amplitudes of processes involving fermions.

Suppose that the two fermions considered above have equal mass. In the center-of-mass frame, if the four-momentum of one of the fermions is $p^\mu = (E, \vec{p})$, then the four-momentum of the other fermion is

$$\bar{p}^\mu \equiv (E, -\vec{p}). \quad (\text{B.27})$$

The following *numerical* identities are then satisfied: $\sigma \cdot \bar{p} = \bar{\sigma} \cdot p$ and $\bar{\sigma} \cdot \bar{p} = \sigma \cdot p$. However, in order to maintain covariance with respect to the undotted and dotted spinor indices, we shall write these identities as:

$$\sigma_{\alpha\dot{\beta}} \cdot \bar{p} = \sigma_{\alpha\dot{\alpha}}^0 (\bar{\sigma}^{\dot{\alpha}\beta} \cdot p) \sigma_{\beta\dot{\beta}}^0, \quad (\text{B.28})$$

$$\bar{\sigma}^{\dot{\alpha}\beta} \cdot \bar{p} = \bar{\sigma}^{0\dot{\alpha}\alpha} (\sigma_{\alpha\dot{\beta}} \cdot p) \bar{\sigma}^{0\dot{\beta}\beta}. \quad (\text{B.29})$$

Taking the matrix square root of both sides of eqs. (B.28) and (B.29) removes one of the factors of σ^0 and $\bar{\sigma}^0$, respectively. Hence,

$$x_\alpha(-\vec{p}, -\lambda) = \sqrt{\bar{p} \cdot \sigma} \chi_{-\lambda}(-\hat{p}) = \sigma^0 \sqrt{p \cdot \bar{\sigma}} \chi_\lambda(\vec{p}) = \sigma_{\alpha\dot{\beta}}^0 \bar{y}^{\dot{\beta}}(\vec{p}, \lambda), \quad (\text{B.30})$$

where we have used eqs. (3.19) and (B.26). In this way, we can derive the eight possible relations for the helicity spinor wave functions:

$$x_\alpha(-\vec{p}, -\lambda) = \sigma_{\alpha\dot{\beta}}^0 \bar{y}^{\dot{\beta}}(\vec{p}, \lambda), \quad x^\alpha(-\vec{p}, -\lambda) = \bar{y}_{\dot{\beta}}(\vec{p}, \lambda) \bar{\sigma}^{0\dot{\beta}\alpha}, \quad (\text{B.31})$$

$$y_\alpha(-\vec{p}, -\lambda) = \sigma_{\alpha\dot{\beta}}^0 \bar{x}^{\dot{\beta}}(\vec{p}, \lambda), \quad y^\alpha(-\vec{p}, -\lambda) = \bar{x}_{\dot{\beta}}(\vec{p}, \lambda) \bar{\sigma}^{0\dot{\beta}\alpha}, \quad (\text{B.32})$$

$$\bar{x}^{\dot{\alpha}}(-\vec{p}, -\lambda) = \bar{\sigma}^{0\dot{\alpha}\beta} y_\beta(\vec{p}, \lambda), \quad \bar{x}_{\dot{\alpha}}(-\vec{p}, -\lambda) = y^\beta(\vec{p}, \lambda) \sigma_{\beta\dot{\alpha}}^0, \quad (\text{B.33})$$

$$\bar{y}^{\dot{\alpha}}(-\vec{p}, -\lambda) = \bar{\sigma}^{0\dot{\alpha}\beta} x_\beta(\vec{p}, \lambda), \quad \bar{y}_{\dot{\alpha}}(-\vec{p}, -\lambda) = x^\beta(\vec{p}, \lambda) \sigma_{\beta\dot{\alpha}}^0. \quad (\text{B.34})$$

Appendix C: Path integral treatment of two-component fermion propagators

In Section 4.2 we derived the two-component fermion propagators in momentum space, which are the Fourier transforms of the free field expectation values of time-ordered products of two two-component fermion fields

$$\langle 0 | T \xi_\alpha(x) \bar{\xi}_{\dot{\beta}}(y) | 0 \rangle_{\text{FT}} \equiv \int d^4 w \langle 0 | T \xi_\alpha(x) \bar{\xi}_{\dot{\beta}}(y) | 0 \rangle e^{ip \cdot w}, \quad w \equiv x - y, \quad (\text{C.1})$$

where the (translationally invariant) expectation values $\langle 0 | T \xi_\alpha(x) \bar{\xi}_{\dot{\beta}}(y) | 0 \rangle$ are functions of the coordinate difference $w \equiv x - y$. In Section 4.2, the Fourier transforms of these quantities were computed by using the free-field expansion obtained from the canonical quantization procedure, and then evaluating the resulting spin sums. In this Appendix, we provide a derivation of the

same result by employing path integral techniques. We follow the analysis given in Appendix C of ref. [148] (with a few minor changes in notation). For a similar textbook treatment of two-component fermion propagators see for example ref. [115]. For the analogous treatment of the four-component fermion propagator, see for example ref. [76].

We first consider the action for a single massive neutral two-component fermion $\xi_\alpha(x)$, coupled to an anticommuting two-component fermionic source term $J_\alpha(x)$ [cf. eq. (3.1)]:

$$S = \int d^4x (\mathcal{L} + J\xi + \bar{\xi}\bar{J}) = \int d^4x \left\{ \frac{1}{2} [i\bar{\xi}\bar{\sigma}^\mu\partial_\mu\xi + i\xi\sigma^\mu\partial_\mu\bar{\xi} - m(\xi\xi + \bar{\xi}\bar{\xi})] + J\xi + \bar{\xi}\bar{J} \right\}, \quad (\text{C.2})$$

where we have split the kinetic energy term symmetrically into two terms. The generating functional is given by

$$W[J, \bar{J}] = N \int \mathcal{D}\xi \mathcal{D}\bar{\xi} e^{iS[\xi, \bar{\xi}, J, \bar{J}]}, \quad (\text{C.3})$$

where N is a normalization factor chosen such that $W[0, 0] = 1$ and $\mathcal{D}\xi \mathcal{D}\bar{\xi}$ is the integration measure. It is convenient to Fourier-transform the fields $\xi(x)$, $\bar{\xi}(x)$ and sources $J(x)$, $\bar{J}(x)$ in eq. (C.3), and rewrite the action in terms of the corresponding Fourier coefficients $\hat{\xi}(p)$, $\hat{\bar{\xi}}(p)$, $\hat{J}(p)$ and $\hat{\bar{J}}(p)$:

$$\xi_\alpha(x) = \int \frac{d^4p}{(2\pi)^4} e^{-ip \cdot x} \hat{\xi}_\alpha(p), \quad \bar{\xi}_{\dot{\alpha}}(x) = \int \frac{d^4p}{(2\pi)^4} e^{ip \cdot x} \hat{\bar{\xi}}_{\dot{\alpha}}(p), \quad (\text{C.4})$$

$$J_\alpha(x) = \int \frac{d^4p}{(2\pi)^4} e^{-ip \cdot x} \hat{J}_\alpha(p), \quad \bar{J}_{\dot{\alpha}}(x) = \int \frac{d^4p}{(2\pi)^4} e^{ip \cdot x} \hat{\bar{J}}_{\dot{\alpha}}(p). \quad (\text{C.5})$$

Furthermore, we introduce the integral representation of the delta function

$$\delta^{(4)}(x - x') = \int \frac{d^4p}{(2\pi)^4} e^{-ip \cdot (x - x')}. \quad (\text{C.6})$$

In order to rewrite eq. (C.3) in a more convenient matrix form, we introduce the following definitions:

$$\Omega(p) \equiv \begin{pmatrix} \hat{\bar{\xi}}^{\dot{\alpha}}(-p) \\ \hat{\xi}_\alpha(p) \end{pmatrix}, \quad X(p) \equiv \begin{pmatrix} \hat{J}_\alpha(p) \\ \hat{\bar{J}}^{\dot{\alpha}}(-p) \end{pmatrix}, \quad \mathcal{M}(p) \equiv \begin{pmatrix} p \cdot \sigma_{\alpha\dot{\beta}} & -m \delta_{\alpha}^{\dot{\beta}} \\ -m \delta^{\dot{\alpha}}_{\beta} & p \cdot \bar{\sigma}^{\dot{\alpha}\beta} \end{pmatrix}. \quad (\text{C.7})$$

Note that \mathcal{M} is a Hermitian matrix. We can then rewrite the action [eq. (C.2)] in the following matrix form [after using eqs. (2.47) and (2.48) to write the product of the spinor field and the source in a symmetrical fashion]:

$$S = \frac{1}{2} \int \frac{d^4p}{(2\pi)^4} \left(\Omega^\dagger \mathcal{M} \Omega + \Omega^\dagger X + X^\dagger \Omega \right). \quad (\text{C.8})$$

The linear term in the field Ω can be removed by a field redefinition

$$\Omega' = \Omega + \mathcal{M}^{-1} X. \quad (\text{C.9})$$

In terms of Ω' , the action now takes the convenient form:

$$S = \frac{1}{2} \int \frac{d^4 p}{(2\pi)^4} \left(\Omega'^{\dagger} \mathcal{M} \Omega' - X^{\dagger} \mathcal{M}^{-1} X \right), \quad (\text{C.10})$$

where the inverse of the matrix \mathcal{M} is given by

$$\mathcal{M}^{-1} = \frac{1}{p^2 - m^2} \begin{pmatrix} p \cdot \bar{\sigma}^{\dot{\alpha}\beta} & m \delta^{\dot{\alpha}\beta} \\ m \delta_{\alpha\dot{\beta}} & p \cdot \sigma_{\alpha\dot{\beta}} \end{pmatrix}. \quad (\text{C.11})$$

The Jacobian of the field transformation given in eq. (C.9) is unity. Hence, one can insert the new action, eq. (C.10), in the generating functional, eq. (C.3) to obtain (after dropping the primes on the two-component fermion fields):

$$W[\hat{J}, \hat{\bar{J}}] = N \int \mathcal{D}\xi \mathcal{D}\bar{\xi} \exp \left\{ \frac{i}{2} \int \frac{d^4 p}{(2\pi)^4} \left(\Omega^{\dagger} \mathcal{M} \Omega - X^{\dagger} \mathcal{M}^{-1} X \right) \right\} \quad (\text{C.12})$$

$$= N \left[\int \mathcal{D}\xi \mathcal{D}\bar{\xi} \exp \left\{ \frac{i}{2} \Omega^{\dagger} \mathcal{M} \Omega \right\} \right] \exp \left\{ -\frac{i}{2} \int \frac{d^4 p}{(2\pi)^4} X^{\dagger} \mathcal{M}^{-1} X \right\} \quad (\text{C.13})$$

$$= \exp \left\{ -\frac{i}{2} \int \frac{d^4 p}{(2\pi)^4} X^{\dagger} \mathcal{M}^{-1} X \right\}, \quad (\text{C.14})$$

where we have defined the normalization constant N such that $W[0, 0] = 1$. Inserting the explicit forms for X and \mathcal{M} into eq. (C.14), we obtain

$$\begin{aligned} W[\hat{J}, \hat{\bar{J}}] = \exp \left\{ -\frac{1}{2} \int \frac{d^4 p}{(2\pi)^4} \left(\hat{J}^{\alpha}(-p) \frac{ip \cdot \sigma_{\alpha\dot{\beta}}}{p^2 - m^2} \hat{\bar{J}}^{\dot{\beta}}(-p) + \hat{\bar{J}}_{\dot{\alpha}}(p) \frac{ip \cdot \bar{\sigma}^{\dot{\alpha}\beta}}{p^2 - m^2} \hat{J}_{\beta}(p) \right. \right. \\ \left. \left. + \hat{J}^{\alpha}(-p) \frac{im \delta_{\alpha\dot{\beta}}}{p^2 - m^2} \hat{J}_{\beta}(p) + \hat{\bar{J}}_{\dot{\alpha}}(p) \frac{im \delta^{\dot{\alpha}\beta}}{p^2 - m^2} \hat{\bar{J}}^{\dot{\beta}}(-p) \right) \right\}. \quad (\text{C.15}) \end{aligned}$$

Using eq. (2.49), it is convenient to rewrite the first two terms of the integrand on the right-hand side of eq. (C.15) in two different ways:

$$\begin{aligned} \frac{1}{2} \int \frac{d^4 p}{(2\pi)^4} \left[\hat{J}^{\alpha}(-p) \frac{ip \cdot \sigma_{\alpha\dot{\beta}}}{p^2 - m^2} \hat{\bar{J}}^{\dot{\beta}}(-p) + \hat{\bar{J}}_{\dot{\alpha}}(p) \frac{ip \cdot \bar{\sigma}^{\dot{\alpha}\beta}}{p^2 - m^2} \hat{J}_{\beta}(p) \right] \\ = \int \frac{d^4 p}{(2\pi)^4} \hat{J}^{\alpha}(-p) \frac{ip \cdot \sigma_{\alpha\dot{\beta}}}{p^2 - m^2} \hat{\bar{J}}^{\dot{\beta}}(-p) = \int \frac{d^4 p}{(2\pi)^4} \hat{\bar{J}}_{\dot{\alpha}}(p) \frac{ip \cdot \bar{\sigma}^{\dot{\alpha}\beta}}{p^2 - m^2} \hat{J}_{\beta}(p), \quad (\text{C.16}) \end{aligned}$$

where we have changed integration variables from $p \rightarrow -p$ in relating the two terms above. The vacuum expectation value of the time-ordered product of two spinor fields in configuration space is obtained by taking two functional derivatives of the generating functional with respect to the sources J and \bar{J} and then setting $J = \bar{J} = 0$ at the end of the computation (see, e.g., ref. [76]). For example,

$$\begin{aligned} \left(-i \frac{\vec{\delta}}{\delta J^{\alpha}(x_1)} \right) W[J, \bar{J}] \left(-i \frac{\overleftarrow{\delta}}{\delta \bar{J}^{\dot{\beta}}(x_2)} \right) \Big|_{J=\bar{J}=0} = N \int \mathcal{D}\xi \mathcal{D}\bar{\xi} \xi_{\alpha}(x_1) \bar{\xi}_{\dot{\beta}}(x_2) \exp i \int d^4 x \mathcal{L} \\ = \langle 0 | T \xi_{\alpha}(x_1) \bar{\xi}_{\dot{\beta}}(x_2) | 0 \rangle, \quad (\text{C.17}) \end{aligned}$$

where the functional derivatives act in the indicated direction (which ensures that no extra minus signs are generated due to the anticommutativity properties of the sources and their functional derivatives). To obtain the two-point functions involving the product of two spinor fields with different combinations of dotted and undotted spinors, it may be more convenient to write $J\xi = \xi J$ and/or $\bar{\xi} \bar{J} = \bar{J} \bar{\xi}$ in eq. (C.3). One can then easily verify the following expressions for the four possible two-point functions:

$$\langle 0|T\xi_\alpha(x_1)\bar{\xi}_{\dot{\beta}}(x_2)|0\rangle = \left(-i\frac{\vec{\delta}}{\delta J^\alpha(x_1)}\right)W[J,\bar{J}]\left(-i\frac{\overleftarrow{\delta}}{\delta \bar{J}^{\dot{\beta}}(x_2)}\right)\Big|_{J=\bar{J}=0}, \quad (\text{C.18})$$

$$\langle 0|T\xi^{\dot{\alpha}}(x_1)\xi^\beta(x_2)|0\rangle = \left(-i\frac{\vec{\delta}}{\delta \bar{J}_{\dot{\alpha}}(x_1)}\right)W[J,\bar{J}]\left(-i\frac{\overleftarrow{\delta}}{\delta J_\beta(x_2)}\right)\Big|_{J=\bar{J}=0}, \quad (\text{C.19})$$

$$\langle 0|T\xi^{\dot{\alpha}}(x_1)\bar{\xi}_{\dot{\beta}}(x_2)|0\rangle = \left(-i\frac{\vec{\delta}}{\delta \bar{J}_{\dot{\alpha}}(x_1)}\right)W[J,\bar{J}]\left(-i\frac{\overleftarrow{\delta}}{\delta \bar{J}^{\dot{\beta}}(x_2)}\right)\Big|_{J=\bar{J}=0}, \quad (\text{C.20})$$

$$\langle 0|T\xi_\alpha(x_1)\xi^\beta(x_2)|0\rangle = \left(-i\frac{\vec{\delta}}{\delta J^\alpha(x_1)}\right)W[J,\bar{J}]\left(-i\frac{\overleftarrow{\delta}}{\delta J_\beta(x_2)}\right)\Big|_{J=\bar{J}=0}. \quad (\text{C.21})$$

As an example, we provide details for the evaluation of eq. (C.18). Using eqs. (C.15) and (C.16), we obtain:

$$\langle 0|T\xi_\alpha(x_1)\bar{\xi}_{\dot{\beta}}(x_2)|0\rangle = \frac{\vec{\delta}}{\delta J^\alpha(x_1)}\left(\int\frac{d^4p}{(2\pi)^4}\hat{J}^\alpha(-p)\frac{ip\cdot\sigma_{\alpha\dot{\beta}}}{p^2-m^2}\hat{\bar{J}}^{\dot{\beta}}(-p)\right)\frac{\overleftarrow{\delta}}{\delta \bar{J}^{\dot{\beta}}(x_2)}. \quad (\text{C.22})$$

Using the chain rule for functional differentiation,

$$\frac{\delta}{\delta J^\alpha(x_1)} = \int d^4p_1 \frac{\delta \hat{J}^\beta(-p_1)}{\delta J^\alpha(x_1)} \frac{\delta}{\delta \hat{J}^\beta(-p_1)} = \int d^4p_1 e^{-ip_1\cdot x_1} \frac{\delta}{\delta \hat{J}^\alpha(-p_1)}, \quad (\text{C.23})$$

$$\frac{\delta}{\delta \bar{J}^{\dot{\beta}}(x_2)} = \int d^4p_2 \frac{\delta \hat{\bar{J}}^{\dot{\alpha}}(-p_2)}{\delta \bar{J}^{\dot{\beta}}(x_2)} \frac{\delta}{\delta \hat{\bar{J}}^{\dot{\alpha}}(-p_2)} = \int d^4p_2 e^{ip_2\cdot x_2} \frac{\delta}{\delta \hat{\bar{J}}^{\dot{\beta}}(-p_2)}, \quad (\text{C.24})$$

after using the inverse Fourier transform of eq. (C.5). Applying eqs. (C.23) and (C.24) to eq. (C.22), we obtain:

$$\langle 0|T\xi_\alpha(x_1)\bar{\xi}_{\dot{\beta}}(x_2)|0\rangle = \int \frac{d^4p}{(2\pi)^4} e^{-ip\cdot(x_1-x_2)} \frac{ip\cdot\sigma_{\alpha\dot{\beta}}}{p^2-m^2}, \quad (\text{C.25})$$

which is equivalent to eq. (4.1) of Section 4.2. With the same methods applied to eqs. (C.19)–(C.21), one can easily reproduce the results of eqs. (4.2)–(4.4).

We next consider the action for a single massive Dirac two-component fermion. We shall work in a basis of fields where the action, including external anticommuting sources, is given by

$$S[\chi, \bar{\chi}, \eta, \bar{\eta}, J_\chi, \bar{J}_\chi, J_\eta, \bar{J}_\eta] = \int d^4x \left[i\bar{\chi}\bar{\sigma}^\mu\partial_\mu\chi + i\bar{\eta}\bar{\sigma}^\mu\partial_\mu\eta - m(\chi\eta + \bar{\chi}\bar{\eta}) + J_\chi\chi + \bar{\chi}\bar{J}_\chi + J_\eta\eta + \bar{\eta}\bar{J}_\eta \right]. \quad (\text{C.26})$$

The techniques are similar to the ones used above. We introduce Fourier coefficients for all the fields and sources and define

$$\Omega_c(p) \equiv \begin{pmatrix} \hat{\eta}^{\dot{\alpha}}(-p) \\ \hat{\chi}_\alpha(p) \end{pmatrix}, \quad X_c(p) \equiv \begin{pmatrix} \hat{J}_{\eta\alpha}(p) \\ \hat{J}_\chi^{\dot{\alpha}}(-p) \end{pmatrix}. \quad (\text{C.27})$$

The action functional, eq. (C.26), can then be rewritten in matrix form as before (but with no overall factor of 1/2):

$$S = \int \frac{d^4p}{(2\pi)^4} \left(\Omega_c^\dagger \mathcal{M} \Omega_c + \Omega_c^\dagger X_c + X_c^\dagger \Omega_c \right), \quad (\text{C.28})$$

where \mathcal{M} is again given by eq. (C.7). The rest of the calculation goes through as before with few modifications, and yields the Dirac two-component fermion free-field propagators given in eqs. (4.5)–(4.8).

Appendix D: Matrix decompositions for mass matrix diagonalization

In scalar field theory, the diagonalization of the scalar squared-mass matrix M^2 is straightforward. For a theory of n complex scalar fields, M^2 is an hermitian $n \times n$ matrix that can be diagonalized by a unitary matrix W :

$$W^\dagger M^2 W = m^2 = \text{diag}(m_1^2, m_2^2, \dots, m_n^2). \quad (\text{D.1})$$

For a theory of n real scalar fields, M^2 is a real symmetric $n \times n$ matrix that can be diagonalized by an orthogonal matrix Q :

$$Q^T M^2 Q = m^2 = \text{diag}(m_1^2, m_2^2, \dots, m_n^2). \quad (\text{D.2})$$

In both cases, the eigenvalues, m_k^2 of M^2 are real. This is the standard matrix diagonalization problem that is treated in all elementary linear algebra textbooks.

In spin-1/2 fermion field theory, the diagonalization of the fermion mass matrix, which is treated in Section 3.2, does not take any of the above forms. In this appendix, we review the linear algebra theory relevant for the matrix decompositions associated with the charged and neutral spin-1/2 fermion mass matrix diagonalizations.

D.1 Singular Value Decomposition

The diagonalization of the charged (Dirac) fermion mass matrix requires the singular value decomposition of an arbitrary complex matrix M .

Theorem: For any complex $n \times n$ matrix M , unitary matrices L and R exist such that

$$L^T M R = M_D = \text{diag}(m_1, m_2, \dots, m_n), \quad (\text{D.3})$$

where the m_k are real and non-negative. This is called the singular value decomposition of the matrix M .

In general, the m_k are *not* the eigenvalues of M . Rather, the m_k are the *singular values* of the general complex matrix M , which are defined to be the non-negative square roots of the eigenvalues of $M^\dagger M$ (or equivalently of $M M^\dagger$). An equivalent definition of the singular values can be established as follows. Since $M^\dagger M$ is an hermitian non-negative matrix, its eigenvalues are real and non-negative and its eigenvectors, w_k , defined by $M^\dagger M w_k = m_k^2 w_k$, can be chosen to be orthonormal.⁴⁴ Consider first the eigenvectors corresponding to the positive eigenvalues of $M^\dagger M$. Then, we define the vectors v_k such that $M w_k = m_k v_k^*$. It follows that $m_k^2 w_k = M^\dagger M w_k = m_k M^\dagger v_k^*$, which yields: $M^\dagger v_k^* = m_k w_k$. Note that these equations also

⁴⁴We define the inner product of two vectors to be $\langle v|w \rangle \equiv v^\dagger w$. Then, v and w are orthonormal if $\langle v|w \rangle = 0$. The norm of a vector is defined by $\|v\| = \langle v|v \rangle^{1/2}$.

imply that $MM^\dagger v_k^* = m_k^2 v_k^*$. The orthonormality of the w_k implies the orthonormality of the v_k^* (and hence the v_k):

$$\delta_{jk} = \langle w_j | w_k \rangle = \frac{1}{m_j m_k} \langle M^\dagger v_j^* | M^\dagger v_k^* \rangle = \frac{1}{m_j m_k} \langle v_j^* | M M^\dagger v_k^* \rangle = \frac{m_k}{m_j} \langle v_j^* | v_k^* \rangle, \quad (\text{D.4})$$

which yields $\langle v_j^* | v_k^* \rangle = \delta_{jk}$.

If w_i is an eigenvector of $M^\dagger M$ with zero eigenvalue, then $0 = w_i^\dagger M^\dagger M w_i = \langle M w_i | M w_i \rangle$, which implies that $M w_i = 0$. Likewise, if v_i^* is an eigenvector of MM^\dagger with zero eigenvalue, then $0 = v_i^\dagger M M^\dagger v_i^* = \langle M^\dagger v_i^* | M^\dagger v_i^* \rangle^*$, which implies that $M^\dagger v_i^* = 0$. Because the eigenvectors of MM^\dagger [$M^\dagger M$] can be chosen orthonormal, the eigenvectors corresponding to the zero eigenvalues of M [M^\dagger] can be taken to be orthonormal.⁴⁵ Finally, these eigenvectors are also orthogonal to the eigenvectors corresponding to the non-zero eigenvalues of MM^\dagger [$M^\dagger M$]. That is,

$$\langle w_j | w_i \rangle = \frac{1}{m_j} \langle M^\dagger v_j^* | w_i \rangle = \frac{1}{m_j} \langle v_j^* | M w_i \rangle = 0, \quad (\text{D.5})$$

and similarly $\langle v_j | v_i \rangle = 0$, where the index i [j] runs over the eigenvectors corresponding to the zero [non-zero] eigenvalues.

Thus, we can define the singular values of a general complex matrix M to be the simultaneous solutions (with real non-negative m_k) of:⁴⁶

$$M w_k = m_k v_k^*, \quad v_k^\dagger M = m_k w_k^\dagger. \quad (\text{D.6})$$

The corresponding v_k (w_k), normalized to have unit norm, are called the left (right) singular vectors of M .

Proof of the singular value decomposition theorem: Eqs. (D.4) and (D.5) imply that the left [right] singular vectors can be chosen to be orthonormal. Consequently, the unitary matrix L [R] can be constructed such that its k th column is given by the left [right] singular vector v_k [w_k]. It then follows from eq. (D.6) that:

$$v_k^\dagger M w_\ell = m_k \delta_{k\ell}, \quad (\text{no sum over } k). \quad (\text{D.7})$$

In matrix form, eq. (D.7) coincides with eq. (D.3), and the singular value decomposition is established.

The singular values of a complex matrix M are unique (up to ordering), as they correspond to the eigenvalues of $M^\dagger M$ (or equivalently the eigenvalues of MM^\dagger). The unitary matrices L

⁴⁵In general, the multiplicity of zero eigenvalues of M [M^\dagger] is not equal to the multiplicity of zero eigenvalues of $M^\dagger M$ [MM^\dagger]. However the latter, which is equal to the number of linearly independent eigenvectors of $M^\dagger M$ [MM^\dagger] with zero eigenvalue, coincides with the number of linearly independent eigenvectors of M [M^\dagger] with zero eigenvalue. Moreover, the number of linearly independent w_i coincides with the number of linearly independent v_i .

⁴⁶One can always find a solution to eq. (D.6) such that the m_k are real and non-negative. Given a solution where m_k is complex, we simply write $m_k = |m_k| e^{i\theta}$ and redefine $v_k \rightarrow v_k e^{i\theta}$ to remove the phase θ .

and R are not unique. The matrix R can be determined directly from eq. (D.3) by computing $M_D^\dagger M_D = M_D^2$, which yields:

$$R^\dagger M^\dagger M R = M_D^2. \quad (\text{D.8})$$

That is, R is the unitary matrix that diagonalizes the non-negative definite matrix $M^\dagger M$. Since the eigenvectors, w_k of $M^\dagger M$ are orthonormal, each of the w_k corresponding to the non-degenerate eigenvalues of $M^\dagger M$ can be multiplied by an arbitrary phase $e^{i\theta_k}$. The w_k corresponding to a degenerate eigenvalue of $M^\dagger M$ can be replaced by any orthonormal linear combination of the corresponding w_k . It follows that within the subspace spanned by the eigenvectors of $M^\dagger M$ corresponding to non-degenerate eigenvalues, R is uniquely determined up to multiplication on the right by an arbitrary diagonal unitary matrix. Within the subspace spanned by the eigenvectors of $M^\dagger M$ corresponding to a given degenerate eigenvalue, R is determined up to multiplication on the right by an arbitrary unitary matrix.

Once R is fixed, L is determined by eq. (D.3):

$$L = (M^\top)^{-1} R^* M_D. \quad (\text{D.9})$$

However, if some of the diagonal elements of M_D are zero, then L is not uniquely defined. Writing M_D in 2×2 block form such that the upper left block is a diagonal matrix with positive diagonal elements and the other three blocks are equal to the zero matrix of the appropriate dimensions, it follows that, $M_D = M_D W$, where

$$W = \left(\begin{array}{c|c} \mathbb{1} & \mathbb{O} \\ \hline \mathbb{O} & W_0 \end{array} \right), \quad (\text{D.10})$$

W_0 is an arbitrary unitary matrix whose dimension is equal to the number of zeros that appear in the diagonal elements of M_D , and $\mathbb{1}$ and \mathbb{O} are respectively the identity matrix and zero matrix of the appropriate size. Hence, we can multiply both sides of eq. (D.9) on the right by W , which means that L is only determined up to multiplication on the right by an arbitrary unitary matrix whose form is given by eq. (D.10).⁴⁷

D.2 Takagi Diagonalization

The most general neutral spin-1/2 fermion mass matrix is complex and symmetric. To identify the physical eigenstates, this matrix must be diagonalized. However, the equation that governs

⁴⁷Of course, one can reverse the above procedure by first determining the unitary matrix L . Eq. (D.3) implies that $L^\top M M^\dagger L^* = M_D^2$, in which case L is determined up to multiplication on the right by an arbitrary [diagonal] unitary matrix within the subspace spanned by the eigenvectors corresponding to the degenerate [non-degenerate] eigenvalues of $M M^\dagger$. Having fixed L , one can obtain $R = M^{-1} L^* M_D$ from eq. (D.3). As above, R is only determined up to multiplication on the right by a unitary matrix whose form is given by eq. (D.10).

the identification of the physical fermion states is *not* the standard unitary similarity transformation. Instead it is a different diagonalization equation that was discovered by Takagi [69], and rediscovered many times since [70].⁴⁸

Theorem: For any complex symmetric $n \times n$ matrix M , there exists a unitary matrix Ω such that:

$$\Omega^\top M \Omega = M_D = \text{diag}(m_1, m_2, \dots, m_n), \quad (\text{D.11})$$

where the m_k are real and non-negative. This is the Takagi diagonalization⁴⁹ of the complex symmetric matrix M . **For a physics context see for example [67].**

In general, the m_k are *not* the eigenvalues of M . Rather, the m_k are the singular values of the symmetric matrix M . From eq. (D.11) it follows that:

$$\Omega^\dagger M^\dagger M \Omega = M_D^2 = \text{diag}(m_1^2, m_2^2, \dots, m_n^2). \quad (\text{D.12})$$

If all of the singular values m_k are non-degenerate, then one can determine Ω from eq. (D.12). This is no longer true if some of the singular values are degenerate. For example, if $M = \begin{pmatrix} 0 & 1 \\ 1 & 0 \end{pmatrix}$, then the singular value 1 is doubly-degenerate, but eq. (D.12) yields $\Omega^\dagger \Omega = \mathbb{1}_{2 \times 2}$, which does not specify Ω . That is, in the degenerate case, the physical fermion states *cannot* be determined by the diagonalization of $M^\dagger M$. Instead, one must make direct use of eq. (D.11). Below, we shall present a constructive method for determining Ω that is applicable in both the non-degenerate and the degenerate cases.

Eq. (D.11) can be rewritten as $M\Omega = \Omega^* M_D$, where the columns of Ω are orthonormal. If we denote the k th column of Ω by v_k , then,

$$M v_k = m_k v_k^*, \quad (\text{D.13})$$

where the m_k are the singular values and the vectors v_k are normalized to have unit norm. Following Ref. [138], the v_k are called the *Takagi vectors* of the complex symmetric $n \times n$ matrix M . The Takagi vectors corresponding to non-degenerate non-zero [zero] singular values are unique up to an overall sign [phase]. Any orthogonal [unitary] linear combination of Takagi vectors corresponding to a set of degenerate non-zero [zero] singular values is also a Takagi vector corresponding to the same singular value. Using these results, one can determine the degree of non-uniqueness of the matrix Ω . For definiteness, we fix an ordering of the diagonal elements of M_D .⁵⁰ If the singular values of M are distinct, then the matrix Ω is uniquely

⁴⁸Subsequently, it was recognized in Ref. [128] that the Takagi diagonalization was first established for nonsingular complex symmetric matrices by Autonne [129].

⁴⁹In Ref. [70], eq. (D.11) is called the Takagi factorization of a complex symmetric matrix. We choose to refer to this as Takagi *diagonalization* to emphasize and contrast this with the more standard diagonalization of normal matrices by a unitary similarity transformation. In particular, not all *complex* symmetric matrices are diagonalizable by a similarity transformation, whereas complex symmetric matrices are *always* Takagi-diagonalizable.

⁵⁰Permuting the order of the singular values is equivalent to permuting the order of the columns of Ω .

determined up to multiplication by a diagonal matrix whose entries are either ± 1 (i.e., a diagonal orthogonal matrix). If there are degeneracies corresponding to non-zero singular values, then within the degenerate subspace, Ω is unique up to multiplication on the right by an arbitrary orthogonal matrix. Finally, in the subspace corresponding to zero singular values, Ω is unique up to multiplication on the right by an arbitrary unitary matrix.

Proof of the Takagi diagonalization. To prove the existence of the Takagi diagonalization of a complex symmetric matrix, it is sufficient to provide an algorithm for constructing the orthonormal Takagi vectors v_k that make up the columns of Ω . This is achieved by rewriting the $n \times n$ complex matrix equation $Mv = mv^*$ [with m real and non-negative] as a $2n \times 2n$ real matrix equation [130, 131]:

$$M_R \begin{pmatrix} \operatorname{Re} v \\ \operatorname{Im} v \end{pmatrix} \equiv \begin{pmatrix} \operatorname{Re} M & -\operatorname{Im} M \\ -\operatorname{Im} M & -\operatorname{Re} M \end{pmatrix} \begin{pmatrix} \operatorname{Re} v \\ \operatorname{Im} v \end{pmatrix} = m \begin{pmatrix} \operatorname{Re} v \\ \operatorname{Im} v \end{pmatrix}, \quad \text{where } m \geq 0. \quad (\text{D.14})$$

Since $M = M^T$, the $2n \times 2n$ matrix $M_R \equiv \begin{pmatrix} \operatorname{Re} M & -\operatorname{Im} M \\ -\operatorname{Im} M & -\operatorname{Re} M \end{pmatrix}$ is a real symmetric matrix.⁵¹ In particular, M_R is diagonalizable by a real orthogonal similarity transformation, and its eigenvalues are real. Moreover, if m is an eigenvalue of M_R with eigenvector $(\operatorname{Re} v, \operatorname{Im} v)$, then $-m$ is an eigenvalue of M_R with (orthogonal) eigenvector $(-\operatorname{Im} v, \operatorname{Re} v)$. This observation implies that M_R has an equal number of positive and negative eigenvalues and an even number of zero eigenvalues.⁵² Thus, Eq. (D.13) has been converted into an ordinary eigenvalue problem for a real symmetric matrix. Since $m \geq 0$, we solve the eigenvalue problem $M_R u = mu$ for the eigenvectors corresponding to the non-negative eigenvalues.⁵³ It is straightforward to prove that the total number of linearly independent Takagi vectors is equal to n . Simply note that the orthogonality of $(\operatorname{Re} v_1, \operatorname{Im} v_1)$ and $(-\operatorname{Im} v_1, \operatorname{Re} v_1)$ with $(\operatorname{Re} v_2, \operatorname{Im} v_2)$ implies that $v_1^\dagger v_2 = 0$.

Thus, we have derived a constructive method for obtaining the Takagi vectors v_k . If there are degeneracies, one can always choose the v_k in the degenerate subspace to be orthonormal. The Takagi vectors then make up the columns of the matrix Ω in eq. (D.11). A numerical package for performing the Takagi diagonalization of a complex symmetric matrix has recently been presented in ref. [132] (see also refs. [138] and [139] for previous numerical approaches to Takagi diagonalization).

⁵¹The $2n \times 2n$ matrix M_R is a real representation of the $n \times n$ complex matrix M .

⁵²Note that $(-\operatorname{Im} v, \operatorname{Re} v)$ corresponds to replacing v_k in Eq. (D.13) by iv_k . However, for $m < 0$ these solutions are not relevant for Takagi diagonalization (where the m_k are by definition non-negative). The case of $m = 0$ is considered in footnote 53.

⁵³For $m = 0$, the corresponding vectors $(\operatorname{Re} v, \operatorname{Im} v)$ and $(-\operatorname{Im} v, \operatorname{Re} v)$ are two linearly independent eigenvectors of M_R ; but these yield only one independent Takagi vector v (since v and iv are linearly dependent).

D.3 Relation between Takagi diagonalization and the singular value decomposition

The Takagi diagonalization is a special case of the singular value decomposition. If the complex matrix M in eq. (D.3) is symmetric, then the Takagi diagonalization corresponds to $\Omega = L = R$. In this case, the left singular vectors and the right singular vectors coincide ($w_k = v_k$) and are identified with the Takagi vectors defined in eq. (D.13). Nevertheless, in contrast to the singular value decomposition, where R can be determined from eq. (D.8) modulo right multiplication by a [diagonal] unitary matrix in the [non]-degenerate subspace [and L is then determined by eq. (D.9) modulo multiplication on the right by eq. (D.10)], the matrix Ω cannot be determined from eq. (D.12) in cases where there is a degeneracy among the singular values, as previously noted. For example, one possible singular value decomposition of the matrix $M = \begin{pmatrix} 0 & 1 \\ 1 & 0 \end{pmatrix}$ can be obtained by choosing $R = I_2$ and $L = M$, in which case $M^\top M I_2 = I_2$. This, of course, is not a Takagi diagonalization. Since R is only defined modulo the multiplication on the right by an arbitrary 2×2 unitary matrix \mathcal{O} , then at least one singular value decomposition exists that is also a Takagi diagonalization. For the example under consideration, it is not difficult to deduce the Takagi diagonalization: $\Omega^\top M \Omega = I_2$, where

$$\Omega = \frac{1}{\sqrt{2}} \begin{pmatrix} 1 & i \\ 1 & -i \end{pmatrix} \mathcal{O}, \quad (\text{D.15})$$

and \mathcal{O} is any 2×2 orthogonal matrix.

Since the Takagi diagonalization is a special case of the singular value decomposition, it seems plausible that one can prove the former from the latter. This turns out to be correct; for completeness, we provide the proof below. Our second proof depends on the following lemma:

Lemma: For any symmetric unitary matrix V , there exists a unitary matrix U such that $V = U^\top U$.

Proof of the Lemma: For any $n \times n$ unitary matrix V , there exists a hermitian matrix H such that $V = \exp(iH)$ (this is the polar decomposition of V). If $V = V^\top$ then $H = H^\top = H^*$ (since H is hermitian). But, any real symmetric matrix can be diagonalized by an orthogonal transformation. It follows that V can also be diagonalized by an orthogonal transformation. That is, there exists a real orthogonal matrix Q such that⁵⁴ $Q^\top V Q = \text{diag}(e^{i\theta_1}, e^{i\theta_2}, \dots, e^{i\theta_n})$. Thus, the unitary matrix

$$U = \text{diag}(e^{i\theta_1/2}, e^{i\theta_2/2}, \dots, e^{i\theta_n/2}) Q^\top \quad (\text{D.16})$$

satisfies $V = U^\top U$ and the theorem is proven. Note that U is unique modulo multiplication on the left by an arbitrary real orthogonal matrix.

⁵⁴The eigenvalues of any unitary matrix are complex numbers of unit norm, i.e. pure phases.

Second Proof of the Takagi diagonalization. Starting from the singular value decomposition of M , there exist unitary matrices L and R such that $M = L^* M_D R^\dagger$, where M_D is the diagonal matrix of singular values. Since $M = M^\top = R^* M_D L^\dagger$, we have two different singular value decompositions for M . However, as noted below eq. (D.8), R is unique modulo multiplication on the right by an arbitrary [diagonal] unitary matrix within the [non-]degenerate subspace. Thus, it follows that a unitary matrix V exists of the latter form such that $L = RV$. Moreover, $V = V^\top$. This is manifestly true within the non-degenerate subspace where V is diagonal. Within the degenerate subspace, M_D is proportional to the identity matrix so that $L^* R^\dagger = R^* L^\dagger$. Inserting $L = RV$ then yields $V^\top = V$. Using the Lemma proved above, there exists a unitary matrix U such that $V = U^\top U$. Hence, in the singular value decomposition of a symmetric complex matrix, $M = L^* M_D R^\dagger$,

$$L = RU^\top U, \quad (\text{D.17})$$

for some unitary matrix U . Moreover, it is straightforward to show that:

$$M_D U^* = U^* M_D. \quad (\text{D.18})$$

Within the degenerate subspace, eq. (D.18) is trivially true since M_D is proportional to the identity matrix. Within the non-degenerate subspace V is diagonal; hence we may choose $U = U^\top = V^{1/2}$, so that eq. (D.18) is true since diagonal matrices commute. Using eqs. (D.17) and (D.18), we can write the singular value decomposition of M as follows

$$M = L^* M_D R^\dagger = L^* M_D = R^* U^\dagger U^* M_D R^\dagger = (RU^\top)^* M_D U^* R^\dagger = \Omega^* M_D \Omega^\dagger, \quad (\text{D.19})$$

where $\Omega \equiv RU^\top$ is a unitary matrix. Thus the existence of the Takagi diagonalization of an arbitrary complex symmetric matrix [eq. (D.11)] is once again proven.

Appendix E: Correspondence to four-component spinor notation

E.1 Dirac matrices and four-component spinors

Four-component spinor notation employs four-component Dirac spinor fields and the 4×4 Dirac gamma matrices, whose defining property is:

$$\{\gamma^\mu, \gamma^\nu\} = 2g^{\mu\nu}. \quad (\text{E.1})$$

The correspondence between the two-component notation of this paper and the four-component Dirac spinor notation is most easily exhibited in the basis in which γ_5 is diagonal (this is called the *chiral* representation). In 2×2 blocks, the gamma matrices are given by:

$$\gamma^\mu = \begin{pmatrix} 0 & \sigma^\mu_{\alpha\beta} \\ \bar{\sigma}^{\mu\dot{\alpha}\beta} & 0 \end{pmatrix}, \quad \gamma_5 \equiv i\gamma^0\gamma^1\gamma^2\gamma^3 = \begin{pmatrix} -\delta_{\alpha}^{\beta} & 0 \\ 0 & \delta^{\dot{\alpha}}_{\dot{\beta}} \end{pmatrix}. \quad (\text{E.2})$$

In addition, we introduce:⁵⁵

$$\frac{1}{2}\Sigma^{\mu\nu} \equiv \frac{i}{4}[\gamma^\mu, \gamma^\nu] = \begin{pmatrix} \sigma^{\mu\nu}{}_\alpha{}^\beta & 0 \\ 0 & \bar{\sigma}^{\mu\nu}{}_{\dot{\alpha}}{}^{\dot{\beta}} \end{pmatrix}. \quad (\text{E.3})$$

A four component Dirac spinor field, $\Psi(x)$, is made up of two mass-degenerate two-component spinor fields, $\chi_\alpha(x)$ and $\eta_\alpha(x)$ as follows:

$$\Psi(x) \equiv \begin{pmatrix} \chi_\alpha(x) \\ \bar{\eta}^{\dot{\alpha}}(x) \end{pmatrix}. \quad (\text{E.4})$$

We define chiral projections operators $P_L \equiv \frac{1}{2}(1 - \gamma_5)$ and $P_R \equiv \frac{1}{2}(1 + \gamma_5)$ so that

$$\Psi_L(x) \equiv P_L \Psi(x) = \begin{pmatrix} \chi_\alpha(x) \\ 0 \end{pmatrix}, \quad \Psi_R(x) \equiv P_R \Psi(x) = \begin{pmatrix} 0 \\ \bar{\eta}^{\dot{\alpha}}(x) \end{pmatrix}. \quad (\text{E.5})$$

The free fields can be expanded in a Fourier series; each mode is multiplied by a *commuting* spinor wave function as in eq. (3.66). The Dirac conjugate field $\bar{\Psi}$ and the charge conjugate field are respectively given by

$$\bar{\Psi}(x) \equiv \Psi^\dagger A = (\eta^\alpha(x), \bar{\chi}_{\dot{\alpha}}(x)), \quad (\text{E.6})$$

$$\Psi^c(x) \equiv C \bar{\Psi}^\top(x) = \begin{pmatrix} \eta_\alpha(x) \\ \bar{\chi}^{\dot{\alpha}}(x) \end{pmatrix}, \quad (\text{E.7})$$

where the Dirac conjugation matrix A and the charge conjugation matrix C satisfy [140, 141]:

$$A\gamma^\mu A^{-1} = \gamma^{\mu\dagger}, \quad C^{-1}\gamma^\mu C = -\gamma^{\mu\top}. \quad (\text{E.8})$$

It is conventional to impose two additional conditions:

$$\Psi = A^{-1}\bar{\Psi}^\dagger, \quad (\Psi^c)^c = \Psi. \quad (\text{E.9})$$

The first of these conditions together with eq. (E.6) is equivalent to the statement that $\bar{\Psi}\Psi$ is hermitian. The second condition corresponds to the statement that the charge conjugation operator applied twice is equal to the identity operator. Using eqs. (E.8) and (E.9) and the defining property of the gamma matrices [eq. (E.1)], one can show (independently of the gamma matrix representation) that the matrices A and C must satisfy:

$$A^\dagger = A, \quad C^\top = -C, \quad (AC)^{-1} = (AC)^*. \quad (\text{E.10})$$

⁵⁵In most textbooks, $\Sigma^{\mu\nu}$ is called $\sigma^{\mu\nu}$. Here, we use the former symbol so that there is no confusion with the two-component definition of $\sigma^{\mu\nu}$ given in eq. (2.58).

For completeness, we also introduce a matrix B that satisfies [140, 141]:

$$B\gamma^\mu B^{-1} = \gamma^{\mu\top}. \quad (\text{E.11})$$

The matrix B arises in the study of time reversal invariance of the Dirac equation. In the chiral representation, A , B and C are explicitly given by

$$A = \begin{pmatrix} 0 & \delta_{\dot{\alpha}\dot{\beta}} \\ \delta_{\alpha\beta} & 0 \end{pmatrix}, \quad B = \begin{pmatrix} \epsilon^{\alpha\beta} & 0 \\ 0 & -\epsilon_{\dot{\alpha}\dot{\beta}} \end{pmatrix}, \quad C = -\gamma_5 B^{-1} = \begin{pmatrix} \epsilon_{\alpha\beta} & 0 \\ 0 & \epsilon^{\dot{\alpha}\dot{\beta}} \end{pmatrix}. \quad (\text{E.12})$$

Note the numerical equalities, $A = \gamma^0$, $B = \gamma^1\gamma^3$ and $C = i\gamma^0\gamma^2$, although these identifications do not respect the structure of the undotted and dotted indices specified in eq. (E.12). In calculations that involve translations between two-component and four-component notation, the expressions given in eq. (E.12) should be used. In calculations involving only four-component notation, there is no harm in using the numerical values for the matrices noted above.

Using eqs. (E.8) and (E.11), the following results are easily derived:

$$A\Gamma A^{-1} = \eta_\Gamma^A \Gamma^\dagger, \quad \eta_\Gamma^A = \begin{cases} +1, & \text{for } \Gamma = \mathbb{1}, \gamma^\mu, \gamma^\mu\gamma_5, \Sigma^{\mu\nu}, \\ -1, & \text{for } \Gamma = \gamma_5, \Sigma^{\mu\nu}\gamma_5, \end{cases} \quad (\text{E.13})$$

$$B\Gamma B^{-1} = \eta_\Gamma^B \Gamma^\top, \quad \eta_\Gamma^B = \begin{cases} +1, & \text{for } \Gamma = \mathbb{1}, \gamma_5, \gamma^\mu, \\ -1, & \text{for } \Gamma = \gamma^\mu\gamma_5, \Sigma^{\mu\nu}, \Sigma^{\mu\nu}\gamma_5, \end{cases} \quad (\text{E.14})$$

$$C^{-1}\Gamma C = \eta_\Gamma^C \Gamma^\top, \quad \eta_\Gamma^C = \begin{cases} +1, & \text{for } \Gamma = \mathbb{1}, \gamma_5, \gamma^\mu\gamma_5, \\ -1, & \text{for } \Gamma = \gamma^\mu, \Sigma^{\mu\nu}, \Sigma^{\mu\nu}\gamma_5, \end{cases} \quad (\text{E.15})$$

where $\mathbb{1}$ is the 4×4 identity matrix.

The external two-component spinor momentum space wave functions are related to the traditional four-component spinors according to:

$$u(\vec{p}, s) = \begin{pmatrix} x_\alpha(\vec{p}, s) \\ \bar{y}^{\dot{\alpha}}(\vec{p}, s) \end{pmatrix}, \quad \bar{u}(\vec{p}, s) = (y^\alpha(\vec{p}, s), \bar{x}_{\dot{\alpha}}(\vec{p}, s)), \quad (\text{E.16})$$

$$v(\vec{p}, s) = \begin{pmatrix} y_\alpha(\vec{p}, s) \\ \bar{x}^{\dot{\alpha}}(\vec{p}, s) \end{pmatrix}, \quad \bar{v}(\vec{p}, s) = (x^\alpha(\vec{p}, s), \bar{y}_{\dot{\alpha}}(\vec{p}, s)), \quad (\text{E.17})$$

where $v(\vec{p}, s) = C\bar{u}(\vec{p}, s)^\top$. The spin quantum number takes on values $s = \pm\frac{1}{2}$, and refers either to the component of the spin as measured in the rest frame with respect to a fixed axis or to the helicity (as discussed in Section 3.1). One can check that u and v satisfy the Dirac equations⁵⁶

$$(\not{p} - m)u(\vec{p}, s) = (\not{p} + m)v(\vec{p}, s) = 0, \quad \bar{u}(\vec{p}, s)(\not{p} - m) = \bar{v}(\vec{p}, s)(\not{p} + m) = 0, \quad (\text{E.18})$$

⁵⁶We use the standard Feynman slash notation: $\not{p} \equiv \gamma_\mu p^\mu$ and $\not{S} \equiv \gamma_\mu S^\mu$.

corresponding to eqs. (3.9)–(3.12), and

$$(2s\gamma_5\mathcal{S} - 1)u(\vec{p}, s) = (2s\gamma_5\mathcal{S} - 1)v(\vec{p}, s) = 0, \quad \bar{u}(\vec{p}, s)(2s\gamma_5\mathcal{S} - 1) = \bar{v}(\vec{p}, s)(2s\gamma_5\mathcal{S} - 1) = 0, \quad (\text{E.19})$$

corresponding to eqs. (3.23)–(3.26), where the spin vector S^μ is defined in eq. (3.15). For massive fermions, eqs. (3.44)–(3.47) correspond to

$$u(\vec{p}, s)\bar{u}(\vec{p}, s) = \frac{1}{2}(1 + 2s\gamma_5\mathcal{S})(\not{p} + m), \quad (\text{E.20})$$

$$v(\vec{p}, s)\bar{v}(\vec{p}, s) = \frac{1}{2}(1 + 2s\gamma_5\mathcal{S})(\not{p} - m). \quad (\text{E.21})$$

To apply the above formulas to the massless case we must employ helicity states, where s is replaced by the helicity quantum number λ , and S^μ is defined by eq. (3.16). In particular, in the $m \rightarrow 0$ limit, $S^\mu = p^\mu/m + \mathcal{O}(m/E)$. Inserting this result in eqs. (E.18) and (E.19), it follows that the massless helicity spinors are eigenstates of γ_5

$$\gamma_5 u(\vec{p}, \lambda) = 2\lambda u(\vec{p}, \lambda), \quad \gamma_5 v(\vec{p}, \lambda) = -2\lambda v(\vec{p}, \lambda). \quad (\text{E.22})$$

Applying the same limiting procedure to eqs. (E.20) and (E.21) and using the mass-shell condition ($\not{p}\not{p} = p^2 = m^2$), one obtains the helicity projection operators for a massless spin-1/2 particle

$$u(\vec{p}, \lambda)\bar{u}(\vec{p}, \lambda) = \frac{1}{2}(1 + 2\lambda\gamma_5)\not{p}, \quad (\text{E.23})$$

$$v(\vec{p}, \lambda)\bar{v}(\vec{p}, \lambda) = \frac{1}{2}(1 - 2\lambda\gamma_5)\not{p}, \quad (\text{E.24})$$

which correspond to eqs. (3.52)–(3.55). Finally, the spin-sum identities

$$\sum_s u(\vec{p}, s)\bar{u}(\vec{p}, s) = \not{p} + m, \quad (\text{E.25})$$

$$\sum_s v(\vec{p}, s)\bar{v}(\vec{p}, s) = \not{p} - m, \quad (\text{E.26})$$

$$\sum_s u(\vec{p}, s)v^\top(\vec{p}, s) = (\not{p} + m)C^\top, \quad (\text{E.27})$$

$$\sum_s \bar{u}^\top(\vec{p}, s)\bar{v}(\vec{p}, s) = C^{-1}(\not{p} - m), \quad (\text{E.28})$$

$$\sum_s \bar{v}^\top(\vec{p}, s)\bar{u}(\vec{p}, s) = C^{-1}(\not{p} + m), \quad (\text{E.29})$$

$$\sum_s v(\vec{p}, s)u^\top(\vec{p}, s) = (\not{p} - m)C^\top, \quad (\text{E.30})$$

correspond to eqs. (3.56)–(3.59).

Bilinear covariants are quantities that are quadratic in the Dirac spinor field which transform irreducibly as Lorentz tensors. These are constructed from corresponding quantities that are

quadratic in the two-component fermion fields. To construct a translation table between the two-component form and the four-component forms for the bilinear covariants, we first introduce two Dirac spinor fields [*cf.* eq. (E.4)]:

$$\Psi_1(x) \equiv \begin{pmatrix} \chi_1(x) \\ \bar{\eta}_1(x) \end{pmatrix}, \quad \Psi_2(x) \equiv \begin{pmatrix} \chi_2(x) \\ \bar{\eta}_2(x) \end{pmatrix}, \quad (\text{E.31})$$

where spinor indices have been suppressed on the two-component fields $\chi_i(x)$ and $\bar{\eta}_i(x)$.⁵⁷ The following results are then obtained:⁵⁸

$$\bar{\Psi}_1 P_L \Psi_2 = \eta_1 \chi_2, \quad (\text{E.32})$$

$$\bar{\Psi}_1 P_R \Psi_2 = \bar{\chi}_1 \bar{\eta}_2, \quad (\text{E.33})$$

$$\bar{\Psi}_1 \gamma^\mu P_L \Psi_2 = \bar{\chi}_1 \bar{\sigma}^\mu \chi_2, \quad (\text{E.34})$$

$$\bar{\Psi}_1 \gamma^\mu P_R \Psi_2 = \eta_1 \sigma^\mu \bar{\eta}_2, \quad (\text{E.35})$$

$$\bar{\Psi}_1 \Sigma^{\mu\nu} P_L \Psi_2 = 2 \eta_1 \sigma^{\mu\nu} \chi_2, \quad (\text{E.36})$$

$$\bar{\Psi}_1 \Sigma^{\mu\nu} P_R \Psi_2 = 2 \bar{\chi}_1 \bar{\sigma}^{\mu\nu} \bar{\eta}_2. \quad (\text{E.37})$$

Note that eqs. (E.32)–(E.37) apply to both commuting and anti-commuting fermion fields. In particular, the above results imply that the following relations are satisfied by the (commuting) u and v spinors:

$$\bar{u}(\vec{p}_1, s_1) P_L v(\vec{p}_2, s_2) = -\bar{u}(\vec{p}_2, s_2) P_L v(\vec{p}_1, s_1), \quad (\text{E.38})$$

$$\bar{u}(\vec{p}_1, s_1) P_R v(\vec{p}_2, s_2) = -\bar{u}(\vec{p}_2, s_2) P_R v(\vec{p}_1, s_1), \quad (\text{E.39})$$

$$\bar{u}(\vec{p}_1, s_1) \gamma^\mu P_L v(\vec{p}_2, s_2) = \bar{u}(\vec{p}_2, s_2) \gamma^\mu P_R v(\vec{p}_1, s_1), \quad (\text{E.40})$$

$$\bar{u}(\vec{p}_1, s_1) \gamma^\mu P_R v(\vec{p}_2, s_2) = \bar{u}(\vec{p}_2, s_2) \gamma^\mu P_L v(\vec{p}_1, s_1). \quad (\text{E.41})$$

If a bilinear combination of the two-component spinors is given that does not conform to those listed in eqs. (E.32)–(E.37), then the corresponding four-component expression will necessarily involve a charge-conjugated four-component spinor. For example, $\bar{\Psi}_1^c P_L \Psi_2 = \chi_1 \chi_2$, *etc.* In general, if one replaces Ψ_j with Ψ_j^c ($j = 1$ and/or 2) in any of the above results, then in the corresponding two-component expression one simply interchanges $\chi_j \leftrightarrow \eta_j$ and $\bar{\chi}_j \leftrightarrow \bar{\eta}_j$.

⁵⁷Here i is a flavor index. In the convention of Section 3.2, the flavor index of an unbarred two-component field appears as a lowered index and the flavor index of a barred two-component fermion field appears as a raised index. If one wanted to introduce both raised and lowered indices for four-component fermion fields, one would demand that the flavor indices of $\Psi_L \equiv P_L \Psi$ and $\bar{\Psi}_R \equiv \bar{\Psi} P_L$ appear as lowered indices, whereas the flavor indices of $\Psi_R \equiv P_R \Psi$ and $\bar{\Psi}_L \equiv \bar{\Psi} P_R$ appear as raised indices. We shall follow this convention for chiral theories. However, such a convention is unwieldy for vector-like interactions. Hence when considering vector-like theories, we shall depart from this flavor index convention, and employ only lowered flavor indices for the fermion fields.

⁵⁸It is often useful to apply eq. (2.49) to eqs. (E.35), (E.44) and (E.45) and rewrite $\eta_1 \sigma^\mu \bar{\eta}_2 = -\bar{\eta}_2 \bar{\sigma}^\mu \eta_1$, where the minus sign has been employed for anticommuting spinors.

Using eqs. (E.32)–(E.37), it then follows that:

$$\bar{\Psi}_1 \Psi_2 = \eta_1 \chi_2 + \bar{\chi}_1 \bar{\eta}_2 \quad (\text{E.42})$$

$$\bar{\Psi}_1 \gamma_5 \Psi_2 = -\eta_1 \chi_2 + \bar{\chi}_1 \bar{\eta}_2 \quad (\text{E.43})$$

$$\bar{\Psi}_1 \gamma^\mu \Psi_2 = \bar{\chi}_1 \bar{\sigma}^\mu \chi_2 + \eta_1 \sigma^\mu \bar{\eta}_2 \quad (\text{E.44})$$

$$\bar{\Psi}_1 \gamma^\mu \gamma_5 \Psi_2 = -\bar{\chi}_1 \bar{\sigma}^\mu \chi_2 + \eta_1 \sigma^\mu \bar{\eta}_2 \quad (\text{E.45})$$

$$\bar{\Psi}_1 \Sigma^{\mu\nu} \Psi_2 = 2(\eta_1 \sigma^{\mu\nu} \chi_2 + \bar{\chi}_1 \bar{\sigma}^{\mu\nu} \bar{\eta}_2) \quad (\text{E.46})$$

$$\bar{\Psi}_1 \Sigma^{\mu\nu} \gamma_5 \Psi_2 = 2(-\eta_1 \sigma^{\mu\nu} \chi_2 + \bar{\chi}_1 \bar{\sigma}^{\mu\nu} \bar{\eta}_2). \quad (\text{E.47})$$

Note that eqs. (E.44) and (E.45) contain both σ^μ and $\bar{\sigma}^\mu$ [see footnote 58]. In addition, for anticommuting fermion fields, we may use $C^\top = -C$ to prove that

$$\bar{\Psi}_i^c \Gamma \Psi_j^c = \bar{\Psi}_j C \Gamma^\top C^{-1} \Psi_i = \eta_\Gamma^C \bar{\Psi}_j \Gamma \Psi_i, \quad (\text{E.48})$$

where the sign η_Γ^C is given in eq. (E.15).

The results derived above also apply to four-component Majorana fermions, Ψ_{Mi} , by setting $\eta_i = \chi_i$. However, the extra condition imposed by $\Psi_{Mi}^c = \Psi_{Mi}$ can yield further restrictions. For example, eqs. (E.44)–(E.47) imply [after employing eqs. (2.49)–(2.51)] that *anticommuting* Majorana four-component fermions satisfy:

$$\bar{\Psi}_{Mi} \gamma^\mu P_L \Psi_{Mj} = -\bar{\Psi}_{Mj} \gamma^\mu P_R \Psi_{Mi}, \quad (\text{E.49})$$

$$\bar{\Psi}_{Mi} \Sigma^{\mu\nu} \Psi_{Mj} = -\bar{\Psi}_{Mj} \Sigma^{\mu\nu} \Psi_{Mi}, \quad (\text{E.50})$$

$$\bar{\Psi}_{Mi} \Sigma^{\mu\nu} \gamma_5 \Psi_{Mj} = -\bar{\Psi}_{Mj} \Sigma^{\mu\nu} \gamma_5 \Psi_{Mi}. \quad (\text{E.51})$$

If we set $i = j$, we learn that $\bar{\Psi}_M \gamma^\mu \Psi_M = \bar{\Psi}_M \Sigma^{\mu\nu} \gamma \Psi_M = \bar{\Psi}_M \Sigma^{\mu\nu} \gamma_5 \Psi_M = 0$.

E.2 Feynman rules for four-component fermions

We now illustrate some basic applications of the the above formalism. First, we consider neutral and charged fermions interacting with a neutral scalar ϕ or neutral gauge boson A_a^μ .⁵⁹ To obtain the interactions of the four-component fermion fields, we first identify the neutral two-component fermion mass-eigenstate neutral fields ξ_i and the mass-degenerate charged pairs χ_j and η_j that combine to form the (mass eigenstate) Dirac fermions. Using eqs. (4.12), (4.17) and (4.20), we write out the following interaction Lagrangian in two-component form:

$$\begin{aligned} \mathcal{L}_{\text{int}} = & -\frac{1}{2}(\lambda^{ij} \xi_i \xi_j + \lambda_{ij} \bar{\xi}^i \bar{\xi}^j) \phi - (\kappa^{ij} \chi_i \eta_j + \kappa_{ij} \bar{\chi}^i \bar{\eta}^j) \phi \\ & - (G^a)_i{}^j \bar{\xi}^i \bar{\sigma}_\mu \xi_j A_a^\mu + [(G_R^a)_i{}^j \bar{\eta}^i \bar{\sigma}_\mu \eta_j - (G_L^a)_i{}^j \bar{\chi}^i \bar{\sigma}^\mu \chi_j] A_a^\mu, \end{aligned} \quad (\text{E.52})$$

⁵⁹Here, charged and neutral refer to some global or local U(1), which in general is orthogonal to the gauge group under which A_a^μ transforms.

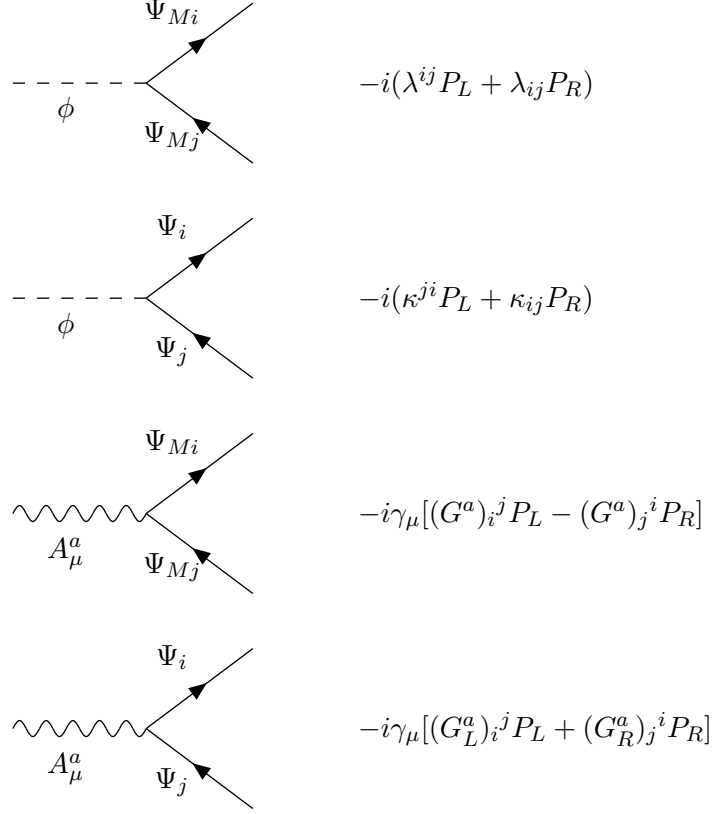


Figure 62: Feynman rules for four-component fermion interactions with neutral bosons

where G^a , G_L^a and G_R^a are hermitian matrices, λ is a complex symmetric matrix and κ is an arbitrary complex matrix, with $\lambda^{ij} \equiv \lambda_{ij}^*$ and $\kappa^{ij} \equiv \kappa_{ij}^*$. By assumption, χ and η have the opposite charges, while all other fields in eq. (E.52) are neutral. It is now simple to convert this result into four-component notation:

$$\begin{aligned} \mathcal{L}_{\text{int}} = & -\frac{1}{2}(\lambda^{ij} \bar{\Psi}_{Mi} P_L \Psi_{Mj} + \lambda_{ij} \bar{\Psi}_{Mi} P_R \Psi_{Mj}) \phi - (\kappa^{ji} \bar{\Psi}_i P_L \Psi_j + \kappa_{ij} \bar{\Psi}_i P_R \Psi_j) \phi \\ & - [(G^a)_i^j \bar{\Psi}_{Mi} \gamma_\mu P_L \Psi_{Mj} + (G_L^a)_i^j \bar{\Psi}_i \gamma_\mu P_L \Psi_j + (G_R^a)_j^i \bar{\Psi}_i \gamma_\mu P_R \Psi_j] A_\mu^a, \end{aligned} \quad (\text{E.53})$$

where Ψ_{Mj} [Ψ_j] are a set of Majorana [Dirac] four-component fermions. It is convenient to use eq. (E.50) to rewrite the term proportional to $(G^a)_i^j$ in eq. (E.53) as follows

$$(G^a)_i^j \bar{\Psi}_{Mi} \gamma^\mu P_L \Psi_{Mj} = \frac{1}{2} \bar{\Psi}_{Mi} \gamma^\mu [(G^a)_i^j P_L - (G_\xi)_j^i P_R] \Psi_{Mj}. \quad (\text{E.54})$$

Using standard four-component methods, the Feynman rules for the vertices are easily obtained and displayed in Fig. 62. Note that the arrows on the Dirac fermion lines depict the flow of the conserved charge. A Majorana fermion is neutral under all conserved charges (and thus equal to its own anti-particle). Thus an arrow on a Majorana fermion line simply reflects the structure of the interaction Lagrangian; i.e., $\bar{\Psi}_M$ [Ψ_M] is represented by an arrow pointing

out of [into] the vertex. The arrows are then used for determining the placement of the u and v spinors in an invariant amplitude.

We next treat the interaction of fermions with charged bosons. Here, we consider a set of neutral fermion mass-eigenstate fields ξ_i and a set of charged fermions denoted by pairs of oppositely charged mass-eigenstate fields χ_j and η_j . The charged scalar and vector bosons are complex fields denoted by Φ and W , respectively. We shall only consider the simplest case where the $U(1)$ charges of Φ , W and χ are assumed to be equal, with η having the opposite charge. The interaction Lagrangian in two-component form is

$$\begin{aligned} \mathcal{L}_{\text{int}} = & -\Phi^*[\kappa_1^{ij}\chi_i\xi_j + (\kappa_2)_{ij}\bar{\eta}^i\bar{\xi}^j] - \Phi[\kappa_2^{ij}\eta_i\xi_j + (\kappa_1)_{ij}\bar{\chi}^i\bar{\xi}^j] \\ & -W_\mu[(G_1)_i{}^j\bar{\chi}^i\bar{\sigma}^\mu\xi_j + (G_2)_i{}^j\bar{\xi}_i\bar{\sigma}^\mu\eta_j] - W_\mu^*[(G_1)_j{}^i\bar{\xi}^j\bar{\sigma}^\mu\chi_i + (G_2)_j{}^i\bar{\eta}^j\bar{\sigma}^\mu\xi_i], \end{aligned} \quad (\text{E.55})$$

where G_1 and G_2 are hermitian matrices and κ_1 and κ_2 are complex symmetric matrices, with $(\kappa_n)_{ij} \equiv (\kappa_n^{ij})^*$ [$n = 1, 2$]. We may then rewrite this in four-component notation:

$$\begin{aligned} \mathcal{L}_{\text{int}} = & -[(\kappa_2)^{ij}\bar{\Psi}_i P_L \Psi_{Mj} + (\kappa_1)_{ij}\bar{\Psi}_i P_R \Psi_{Mj}] \Phi \\ & -[(G_1)_i{}^j\bar{\Psi}_i \gamma^\mu P_L \Psi_{Mj} - (G_2)_j{}^i\bar{\Psi}_i \gamma^\mu P_R \Psi_{Mj}] W_\mu + \text{h.c.} \end{aligned} \quad (\text{E.56})$$

There is an equivalent form of the interaction given in eq. (E.56) where \mathcal{L} is written in terms of charge-conjugated fields [after using eq. (E.48)]. Noting that Majorana fermions are self-conjugate, the Feynman rules for the interactions of neutral and charged fermions with charged bosons can take two possible forms, as shown in Fig. 63. Here, the direction of an arrow on a Dirac fermion line is meaningful and indicates the direction of charge flow. However, we are free to choose either a Ψ or Ψ^c line to represent a Dirac fermion at any place in a given Feynman graph.⁶⁰ Moreover, the structure of the interactions above imply that the arrow directions on fermion lines flow continuously through the diagram. This requirement then determines the direction of the arrows on Majorana fermion lines.

Virtual Dirac fermion lines can either correspond to Ψ or Ψ^c . Here, there is no ambiguity in the propagator Feynman rule, since for free Dirac fermion fields,

$$\langle 0|T(\Psi_\alpha(x)\bar{\Psi}_\beta(y))|0\rangle = \langle 0|T(\Psi_\alpha^c(x)\bar{\Psi}_\beta^c(y))|0\rangle, \quad (\text{E.57})$$

so that the Feynman rule for the propagator of a Ψ and Ψ^c line, given in Fig. 64, are identical. Using eq. (E.2), the four-component fermion propagator Feynman rule can be expressed as a partitioned matrix of 2×2 blocks,

$$\begin{array}{c} \xleftarrow{p} \\ \alpha \quad \quad \quad \beta \end{array} = \left(\begin{array}{cc} \xleftarrow{\quad} & \xrightarrow{\quad} \\ \xrightarrow{\quad} & \xleftarrow{\quad} \end{array} \right) = \frac{i}{p^2 - m^2 + i\epsilon} \begin{pmatrix} m\delta_\alpha^\beta & p \cdot \sigma_{\alpha\dot{\beta}} \\ p \cdot \bar{\sigma}^{\dot{\alpha}\beta} & m\delta_{\dot{\alpha}\beta} \end{pmatrix}, \quad (\text{E.58})$$

⁶⁰Since the charge of Ψ^c is opposite to that of Ψ , the corresponding arrow direction of the two lines are also point in opposite directions.

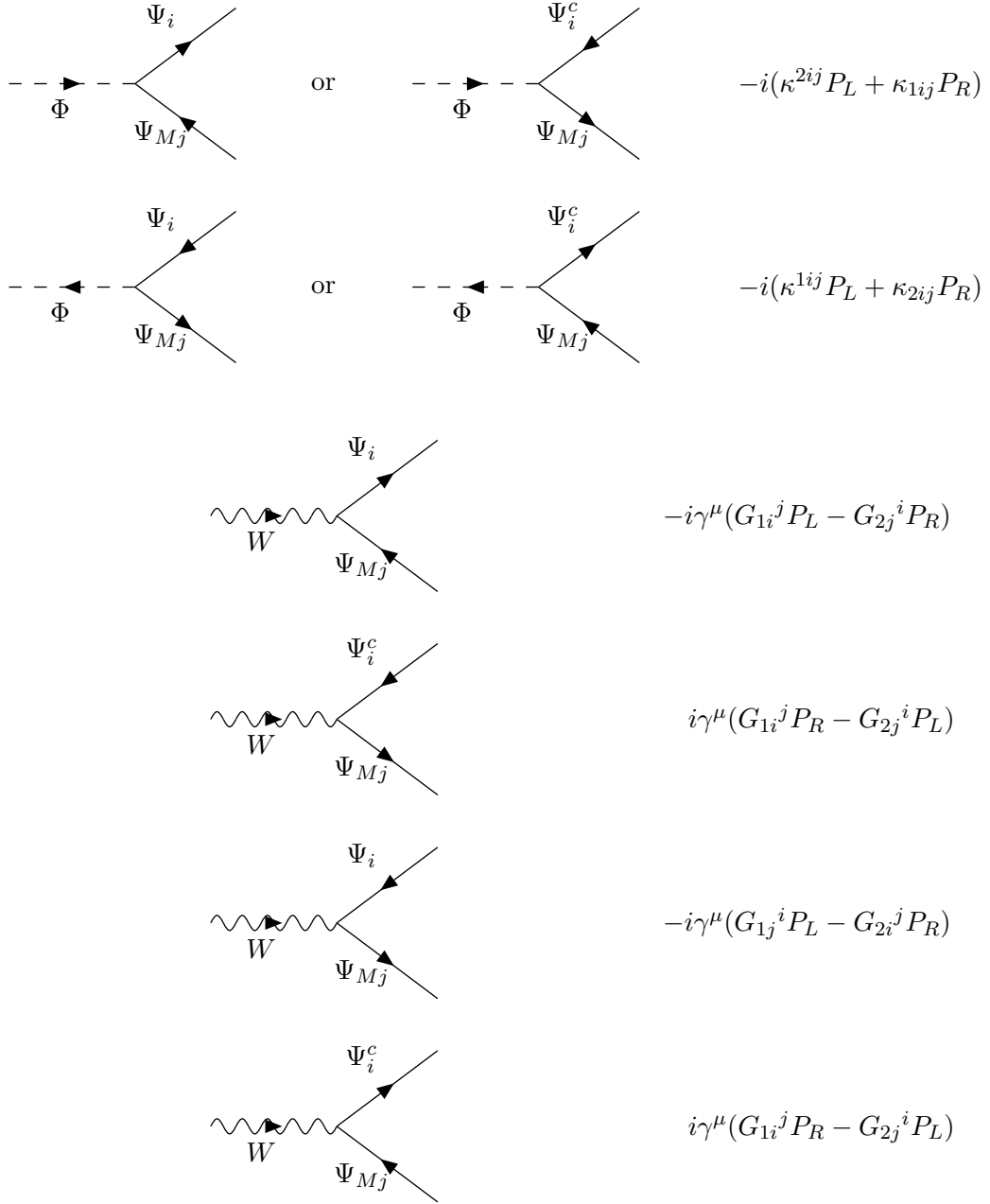


Figure 63: Feynman rules for four-component fermion interactions with charged bosons. The arrows on the boson and Dirac fermion lines indicate the direction of charge flow.



$$\frac{i(\not{p} + m)_{\alpha\beta}}{p^2 - m^2 + i\epsilon}$$

Figure 64: Feynman rule for propagator of a four-component fermion with mass m . This same rule applies to a Majorana, Dirac and charge-conjugated Dirac fermion. The four-component spinor labels are specified.

consisting of two-component fermion propagators defined in Fig. 2, with the undotted and dotted α [β] indices on the left [right] and with the momentum flowing from right to left.

The derivation of the four-component Dirac fermion propagator is treated in most modern textbooks of quantum field theory [see, e.g., ref. [76]]. Here, we briefly sketch the path-integral derivation of the four-component fermion propagator by exploiting the path integral treatment of the two-component fermion propagators outlined in Appendix C. Consider a single massive Dirac fermion $\Psi(x)$ coupled to an anticommuting four-component Dirac fermionic source term

$$J_\psi(x) \equiv \begin{pmatrix} J_{\eta\alpha}(x) \\ \bar{J}_\chi^\alpha(x) \end{pmatrix}. \quad (\text{E.59})$$

The corresponding action [eq. (C.2)] in four-component notation is given by

$$S = \int d^4x (\mathcal{L} + \bar{J}_\psi \Psi + \bar{\Psi} J_\psi) = \int d^4x [\bar{\Psi}(i\not{\partial} - m)\Psi + \bar{J}_\psi \Psi + \bar{\Psi} J_\psi]. \quad (\text{E.60})$$

Introducing the momentum space Fourier coefficients:

$$\Psi(x) = \int \frac{d^4p}{(2\pi)^4} e^{-ip \cdot x} \hat{\Psi}(p), \quad J_\psi(x) = \int \frac{d^4p}{(2\pi)^4} e^{-ip \cdot x} \hat{J}_\psi(p), \quad (\text{E.61})$$

we can identify the following four-component quantities with matrices of two-component quantities given in eqs. (C.7) and (C.27):

$$\hat{\Psi}(p) = A^{-1} \Omega_c(p), \quad \hat{J}_\psi(p) = X_c(p), \quad \not{p} - m = \mathcal{M}(p)A, \quad (\text{E.62})$$

where A is the Dirac conjugation matrix defined in eqs. (E.6) and (E.8). Using the results of Appendix C, one easily derives:

$$\langle 0 | T(\Psi(x_1) \bar{\Psi}(x_2)) | 0 \rangle = \left(-i \frac{\overrightarrow{\delta}}{\delta \bar{J}_\psi(x_1)} \right) W[J, \bar{J}] \left(-i \frac{\overleftarrow{\delta}}{\delta J_\psi(x_2)} \right) \Big|_{J_\psi = \bar{J}_\psi = 0}, \quad (\text{E.63})$$

where

$$W[J_\psi, \bar{J}_\psi] = \exp \left\{ -i \int \frac{d^4p}{(2\pi)^4} \hat{J}_\psi(p) \frac{\not{p} + m}{p^2 - m^2} \hat{J}_\psi(p) \right\}. \quad (\text{E.64})$$

Using the analogs of eqs. (C.23) and (C.24), we end up with the expected result

$$\langle 0 | T(\Psi(x_1) \bar{\Psi}(x_2)) | 0 \rangle = \int \frac{d^4p}{(2\pi)^4} e^{-ip \cdot (x_1 - x_2)} \frac{\not{p} - m}{p^2 - m^2}. \quad (\text{E.65})$$

In principle, the analogous computation can be carried out for a single four-component Majorana fermion field $\Psi_M(x)$ coupled to a Majorana fermionic source, $J_\xi(x)$. The corresponding action is similar to that of eq. (E.60), with an extra overall factor of $1/2$. However, in evaluating the functional derivative in eq. (E.64), one must take into account that the Majorana fermionic source $J_\xi(x)$ satisfies $J_\xi^\dagger \equiv C\bar{J}_\xi^\top = J_\xi$. Consequently, the functional derivative with respect to \bar{J}_ξ is related to the corresponding functional derivative with respect to J_ξ . As a result, the calculation of eq. (E.64) will yield two equal terms that will cancel the overall factor of $1/2$, and the end result will again be eq. (E.65). Nevertheless, this computation is somewhat awkward using four-component spinor notation, in contrast to the straightforward calculation of Appendix C.

E.3 Applications of four-component spinor Feynman rules

For a given process, there may be a number of distinct choices for the arrow directions on the Majorana fermion lines, which may depend on whether one represents a given Dirac fermion by Ψ or Ψ^c . However, different choices do *not* lead to independent Feynman diagrams.⁶¹ When computing an invariant amplitude, one first writes down the relevant Feynman diagrams with no arrows on any Majorana fermion line. The number of distinct graphs contributing to the process is then determined. Finally, one makes some choice for how to distribute the arrows on the Majorana fermion lines and how to label Dirac fermion lines (either as the field or its conjugate) in a manner consistent with the rules of Figs. 62 and 63. The end result for the invariant amplitude (apart from an overall unobservable phase) does not depend on the choices made for the direction of the fermion arrows.

Using the above procedure, the Feynman rules for the external fermion wave functions are the same for Dirac and Majorana fermions:

- $u(\vec{p}, s)$: incoming Ψ [or Ψ^c] with momentum \vec{p} parallel to the arrow direction,
- $\bar{u}(\vec{p}, s)$: outgoing Ψ [or Ψ^c] with momentum \vec{p} parallel to the arrow direction,
- $v(\vec{p}, s)$: outgoing Ψ [or Ψ^c] with momentum \vec{p} anti-parallel to the arrow direction,
- $\bar{v}(\vec{p}, s)$: incoming Ψ [or Ψ^c] with momentum \vec{p} anti-parallel to the arrow direction.

The proof that the above rules for external wave functions apply unambiguously to Majorana fermions is straightforward. Simply insert the plane wave expansion of the Majorana field:

$$\Psi_M(x) = \sum_s \int \frac{d^3\vec{p}}{(2\pi)^{3/2}(2E_p)^{1/2}} \left[u(\vec{p}, s) a(\vec{p}, s) e^{-ip \cdot x} + v(\vec{p}, s) a^\dagger(\vec{p}, s) e^{+ip \cdot x} \right] \quad (\text{E.66})$$

⁶¹In contrast, the two-component Feynman rules developed in Section 3 require that two vertices differing by the direction of the arrows on the two-component fermion lines must both be included in the calculation of the matrix element.

into eq. (E.53), and evaluate matrix elements for, *e.g.*, the decay of a scalar or vector particle into a pair of Majorana fermions.

We now reconsider the matrix elements for scalar and vector particle decays into fermion pairs and $2 \rightarrow 2$ elastic scattering of a fermion off a scalar and vector boson, respectively. We shall compute the matrix elements using the Feynman rules of Fig. 62, and check that the results agree with the ones obtained by two-component methods in Section 3.

The matrix element for the decay $\phi \rightarrow \Psi_M(\vec{p}_1, s_1)\Psi_M(\vec{p}_2, s_2)$ is given by

$$i\mathcal{M} = -i\bar{u}(\vec{p}_1, s_1)(\lambda P_L + \lambda^* P_R)v(\vec{p}_2, s_2). \quad (\text{E.67})$$

One can easily check that this result matches with eq. (4.26), which was derived using two-component techniques. Note that if one had chosen to switch the two final states (equivalent to switching the directions of the Majorana fermion arrows), then the resulting matrix element would simply exhibit an overall sign change [due to the results of eqs. (E.38) and (E.39)].⁶² Similarly, for $\phi \rightarrow \Psi_{Mi}\Psi_{Mj}$ ($i \neq j$) or for the decay into a pair of Dirac fermions, $\phi \rightarrow \bar{\Psi}\Psi$, one again obtains the invariant matrix element given in eq. (E.67).

For the decay $A_\mu \rightarrow \Psi_M(\vec{p}_1, s_1)\Psi_M(\vec{p}_2, s_2)$, one obtains:

$$i\mathcal{M} = iG_\xi \bar{u}(\vec{p}_1, s_1)\gamma^\mu \gamma_5 v(\vec{p}_2, s_2)\varepsilon_\mu. \quad (\text{E.68})$$

One can easily check that this result matches with eq. (4.29). For the decay into non-identical Majorana fermions, $A_\mu \rightarrow \Psi_{Mi}\Psi_{Mj}$ ($i \neq j$), we can use the Feynman rules of Fig. 62 to obtain:

$$i\mathcal{M} = -i\bar{u}(\vec{p}_i, s_i)\gamma^\mu [(G_\xi)_i^j P_L - (G_\xi)_j^i P_R] v(\vec{p}_j, s_j)\varepsilon_\mu, \quad (\text{E.69})$$

Again, we note that if one had chosen to switch the two final states (equivalent to switching the directions of the Majorana fermion arrows), then the resulting matrix element would simply exhibit an overall sign change [due to the results of eqs. (E.40) and (E.41)]. Finally, for the decay of the vector particle into a Dirac fermion-antifermion pair, $A_\mu \rightarrow \bar{\Psi}\Psi$, the matrix element is given by:

$$i\mathcal{M} = -i\bar{u}(\vec{p}_1, s_1)\gamma^\mu (G_L P_L - G_R P_R)v(\vec{p}_2, s_2)\varepsilon_\mu, \quad (\text{E.70})$$

which matches the result of eq. (4.33).

Turning to the elastic scattering of a neutral Majorana fermion and a neutral scalar, we shall examine two equivalent ways for computing the amplitude. Following the rules previously stated, there are two possible choices for the direction of arrows on the Majorana fermion lines. Thus, may evaluate either one of the following two diagrams:

⁶²The overall sign change is a consequence of the Fermi-Dirac statistics, and corresponds to changing which order one uses to construct the two particle final state.



plus a second diagram in each case (not shown) where the initial and final state scalars are crossed. Evaluating the first diagram above, the matrix element for $\phi\Psi_M \rightarrow \phi\Psi_M$ is given by:

$$\begin{aligned} i\mathcal{M} &= \frac{-i}{s-m^2} \bar{u}(\vec{p}_2, s_2) (\lambda P_L + \lambda^* P_R) (\not{p} + m) (\lambda P_L + \lambda^* P_R) u(\vec{p}_1, s_1) + (\text{crossed}) \\ &= \frac{-i}{s-m^2} \bar{u}(\vec{p}_2, s_2) [|\lambda|^2 \not{p} + (\lambda^2 P_L + (\lambda^*)^2 P_R) m] u(\vec{p}_1, s_1) + (\text{crossed}), \end{aligned} \quad (\text{E.71})$$

where m is the Majorana fermion mass, s is the center-of-mass energy squared. Using eqs. (E.2) and (E.16), one recovers the results of eq. (4.34). Had we chose to evaluate the second diagram instead, the resulting amplitude would have been given by:

$$i\mathcal{M} = \frac{-i}{s-m^2} \bar{v}(\vec{p}_1, s_1) [-|\lambda|^2 \not{p} + (\lambda^2 P_L + (\lambda^*)^2 P_R) m] v(\vec{p}_2, s_2) + (\text{crossed}). \quad (\text{E.72})$$

Using eqs. (E.16) and (E.17) and the results of eqs. (2.47)–(2.49) one can derive the following results:

$$\bar{v}(\vec{p}_1, s_1) v(\vec{p}_2, s_2) = -\bar{u}(\vec{p}_2, s_2) u(\vec{p}_1, s_1), \quad \bar{v}(\vec{p}_1, s_1) \gamma^\mu v(\vec{p}_2, s_2) = \bar{u}(\vec{p}_2, s_2) \gamma^\mu u(\vec{p}_1, s_1). \quad (\text{E.73})$$

Consequently, the amplitude computed in eq. (E.72) is just the negative of eq. (E.71). This is expected, since the order of spinor wave functions (12) in eq. (E.72) is an odd permutation (21) of the order of spinor wave functions in eq. (E.71). As in the two-component Feynman rules, the overall sign of the amplitude is arbitrary, but the relative signs of any pair of diagrams is not ambiguous. This relative sign is positive [negative] if the permutation of the order of spinor wave functions of one diagram relative to the other diagram is even [odd].

Next, we consider the elastic scattering of a charged fermion and a neutral scalar. Again, we examine two equivalent ways for computing the amplitude. Following the rules previously stated, there are two possible choices for the direction of arrows on the fermion lines, depending on whether we represent the fermion by Ψ or Ψ^c . Thus, we may evaluate either one of the following two diagrams:



plus a second diagram in each case (not shown) where the initial and final state scalars are crossed. Evaluating the first diagram above, the matrix element for $\phi\Psi \rightarrow \phi\Psi$ is given by

eq. (E.71), with λ replaced by κ . Had we chose to evaluate the second diagram instead, the resulting amplitude would have been given by eq. (E.72), with λ replaced by κ . Thus, the discussion above in the case of neutral fermion scattering processes also applies to charged fermion scattering processes.

In processes that only involve vertices with two Dirac fields, it is never necessary to use charge-conjugated Dirac fermion lines. In contrast, consider the following process that involves a vertex with one Dirac and one Majorana fermion. Specifically, we examine the scattering of a charged Dirac fermion and a charged scalar via the exchange of a neutral Majorana fermion, in which the charge of the outgoing fermion is opposite to that of the incoming fermion. If one attempts to draw the relevant Feynman diagram employing Dirac fermion lines but with no charge-conjugated Dirac fermion lines, one finds that there is no possible choice of arrow direction for the Majorana fermion that is consistent with the the vertex rules of Fig. 63. The resolution is simple: one can choose the incoming line to be Ψ and the outgoing line to be Ψ^c or vice versa. Thus, the two possible choices are given by:



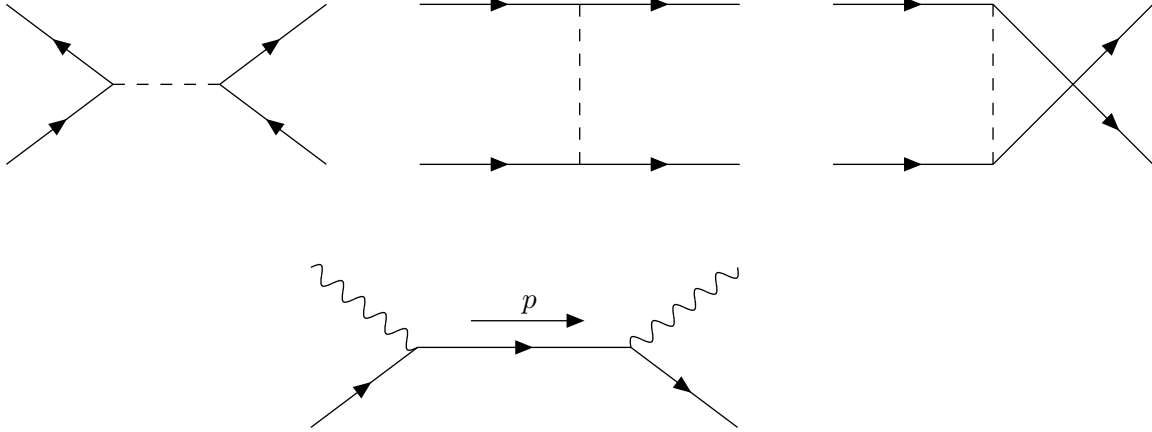
plus a second diagram in each case (not shown) in which the initial and final scalars are crossed. If we evaluate the first diagram, the resulting amplitude is given by:

$$\begin{aligned}
i\mathcal{M} &= \frac{-i}{s - m^2} \bar{u}(\vec{p}_2, s_2) (\kappa_1 P_L + \kappa_2^* P_R) (\not{p} + m) (\kappa_1 P_L + \kappa_2^* P_R) u(\vec{p}_1, s_1) + (\text{crossed}) \\
&= \frac{-i}{s - m^2} \bar{u}(\vec{p}_2, s_2) [\kappa_1 \kappa_2^* \not{p} + (\kappa_1^2 P_L + (\kappa_2^*)^2 P_R) m] u(\vec{p}_1, s_1) + (\text{crossed}), \quad (\text{E.74})
\end{aligned}$$

where m is the Majorana fermion mass. One can check that this is equivalent to eq. (4.38) obtained via the two-component methods. Had we evaluated the second diagram, then after using the relations given in eq. (E.73), one finds that the resulting amplitude is just the negative of eq. (E.74), as expected. As before, the relative sign between diagrams for the same process is not ambiguous.

In the literature, there are a number of alternative methods for dealing with scattering processes involving Majorana particles. For example, one can define a fermion-number violating propagator for four-component fermions (see, *e.g.*, [48]). These methods involve subtle choices of signs which often require first-principles computations to verify. The advantage of the method described above is that there is never any ambiguity in the choice of relative signs.

In the case of elastic scattering of a fermion and a neutral vector boson, the two contributing diagrams are



plus a second diagram (not shown) where the initial and final state vector bosons are crossed. Consider first the scattering of a neutral Majorana fermion of mass m . Using the Feynman rules of Fig. 62, we see that the Feynman rule for the $A_\mu \bar{\Psi}_M \Psi_M$ vertex is given by $iG_\xi \gamma^\mu \gamma_5$. Hence, the corresponding matrix element is given by

$$i\mathcal{M} = \frac{-iG_\xi^2}{s - m^2} \bar{u}(\vec{p}_2, s_2) \gamma \cdot \varepsilon_2^* (\not{p} - m) \gamma \cdot \varepsilon_1 u(\vec{p}_1, s_1) + (\text{crossed}), \quad (\text{E.75})$$

where we have used $\gamma^\nu \gamma_5 (\not{p} + m) \gamma^\mu \gamma_5 = \gamma^\nu (\not{p} - m) \gamma^\mu$. Using eqs. (E.2) and (E.16), one easily recovers the results of eq. (4.35).

Next, the invariant matrix element for the scattering of a Dirac fermion is given by

$$\begin{aligned} i\mathcal{M} &= \frac{-i}{s - m^2} \bar{u}(\vec{p}_2, s_2) \gamma \cdot \varepsilon_2^* (G_L P_L - G_R P_R) (\not{p} + m) \gamma \cdot \varepsilon_1 (G_L P_L - G_R P_R) u(\vec{p}_1, s_1) + (\text{crossed}) \\ &= \frac{-i}{s - m^2} \bar{u}(\vec{p}_2, s_2) \gamma \cdot \varepsilon_2^* [(G_L^2 P_L + G_R^2 P_R) \not{p} - G_L G_R m] \gamma \cdot \varepsilon_1 u(\vec{p}_1, s_1) + (\text{crossed}). \end{aligned} \quad (\text{E.76})$$

One can easily check that this result coincides with that of eq. (4.39).

Finally, we examine the elastic scattering of two identical Majorana fermions via scalar exchange. The three contributing diagrams are:

and the corresponding matrix element is given by

$$\begin{aligned} i\mathcal{M} &= \frac{-i}{s - m_\phi^2} [\bar{v}_1(\lambda P_L + \lambda^* P_R) u_2 \bar{u}_3(\lambda P_L + \lambda^* P_R) v_4] \\ &\quad + (-1) \frac{-i}{t - m_\phi^2} [\bar{u}_3(\lambda P_L + \lambda^* P_R) u_1 \bar{u}_4(\lambda P_L + \lambda^* P_R) u_2] \\ &\quad + \frac{-i}{u - m_\phi^2} [\bar{u}_4(\lambda P_L + \lambda^* P_R) u_1 \bar{u}_3(\lambda P_L + \lambda^* P_R) u_2], \end{aligned} \quad (\text{E.77})$$

where $u_i \equiv u(\vec{p}_i, s_i)$, $v_j \equiv u(\vec{p}_j, s_j)$ and m_ϕ is the exchanged scalar mass. The relative minus sign of the t -channel graph relative to the other two is obtained by noting that 3142 [4132] is an

odd [even] permutation of 1234. Using eqs. (E.2) and (E.16), one easily recovers the results of eq. (4.40).

subsection*E.4 Self-energy functions and pole masses for four-component fermions

In this section, we examine the self-energy functions and the pole masses for a set of four-component fermions. We first consider four-component Dirac fermion fields $\Psi_{\alpha i}$, where α is the four-component spinor index and i is the flavor index. The full, loop-corrected Feynman propagators with four-momentum p^μ are defined by the Fourier transforms [cf. footnote 13] of vacuum expectation values of time-ordered products of bilinears of the fully interacting four-component fermion fields:

$$\langle 0 | T \Psi_{\alpha i}(x) \bar{\Psi}_{\beta j}(y) | 0 \rangle_{\text{FT}} = i(\mathbf{S}_{\alpha\beta})_{ij}(p), \quad (\text{E.78})$$

with [149–159]

$$\mathbf{S}(p) \equiv \not{p} \left[P_L \mathbf{S}_L^\text{T}(p^2) + P_R \mathbf{S}_R(p^2) \right] + P_L \bar{\mathbf{S}}_D^\text{T}(p^2) + P_R \mathbf{S}_D(p^2), \quad (\text{E.79})$$

where the four-component spinor indices α and β and the flavor indices i and j have been suppressed. As in Section 4.6, we shall organize the computation of the full propagator in terms of the 1PI self-energy function [152]:⁶³

$$\Sigma(p) \equiv \not{p} \left[P_L \Sigma_L(p^2) + P_R \Sigma_R^\text{T}(p^2) \right] + P_L \Sigma_D(p^2) + P_R \bar{\Sigma}_D^\text{T}(p^2). \quad (\text{E.80})$$

Diagrammatically, $i\mathbf{S}$ and $-i\Sigma$ are shown in Fig. 65.



Figure 65: The full, loop-corrected propagator for four-component Dirac fermions, $i(\mathbf{S}_{\alpha\beta})_{ij}(p)$, is denoted by the shaded box, which represents the sum of all connected Feynman diagrams, with external legs included. The self-energy function for four-component Dirac fermions, $-i(\Sigma_{\alpha\beta})_{ij}(p)$, is denoted by the shaded circle, which represents the sum of all one-particle irreducible, connected Feynman diagrams with the external legs amputated. In both cases, The four-momentum p flows from right to left.

The hermiticity of the effective action implies that \mathbf{S} and Σ satisfy hermiticity conditions [142, 143]

$$[\mathbf{S}^\text{T}]^* = \mathbf{A} \mathbf{S} \mathbf{A}^{-1}, \quad [\Sigma^\text{T}]^* = \mathbf{A} \Sigma \mathbf{A}^{-1}, \quad (\text{E.81})$$

⁶³Our notation in eq. (E.80) differs from that of ref. [152], as we employ Σ_R^T instead of Σ_R . Our motivation for this choice is that in the case of Majorana fermions [cf. eq. (E.92)], we simply have $\Sigma_L = \Sigma_R$, without an extra transpose (or conjugation). We have also chosen to employ \mathbf{S}_L^T in eq. (E.79) for similar reasons.

where A is the Dirac conjugation matrix ($A = \gamma^0$ in all common representations) and the star symbol was defined in the paragraph below eq. (4.47). Applying eq. (E.81) to eqs. (E.79) and (E.80) then yields the following conditions for the complex matrix functions:

$$[S_L^T]^* = S_L, \quad [S_R^T]^* = S_R, \quad \bar{S}_D = S_D^*, \quad (\text{E.82})$$

$$[\Sigma_L^T]^* = \Sigma_L, \quad [\Sigma_R^T]^* = \Sigma_R, \quad \bar{\Sigma}_D = \Sigma_D^*. \quad (\text{E.83})$$

Starting at tree-level and comparing with Fig. 64, the full propagator function is given by:

$$S_{ij}(p) = (\not{p} + m)\delta_{ij}/(p^2 - m_i^2) + \dots, \quad (\text{E.84})$$

with no sum over i implied. The full loop-corrected propagator can be expressed diagrammatically in terms of the 1PI self-energy function:

$$\frac{\alpha}{i} \text{---} \square \text{---} \frac{\beta}{j} = \frac{\alpha}{i} \text{---} \frac{\beta}{j} + \frac{\alpha}{i} \text{---} \frac{\gamma}{k} \text{---} \bigcirc \text{---} \frac{\delta}{\ell} \text{---} \square \text{---} \frac{\beta}{j} \quad (\text{E.85})$$

As in Section 4.6, the algebraic representation of eq. (E.85) can be written as

$$S = T + T\Sigma S = (T^{-1} - \Sigma)^{-1}, \quad (\text{E.86})$$

where $T_{ij} \equiv (\not{p} + m)\delta_{ij}/(p^2 - m_i^2)$ is the tree-level contribution to S given in eq. (E.84). By writing the expressions for S and Σ given in eqs. (E.79) and (E.80) and T in block matrix form using eq. (E.2), one can verify that eq. (E.86) is equivalent to eq. (4.66). Consequently, the complex pole masses of the corresponding Dirac fermions are again determined from eq. (4.71).

In the special case of a parity-conserving vectorlike theory of Dirac fermions (such as QED or QCD), the pseudoscalar and pseudovector parts of $S(p)$ and $\Sigma(p)$ must be absent. Thus, the following relations must hold among the loop-corrected propagator functions and self-energy functions, respectively:

$$S_R = S_L^T, \quad S_D = [S_D^T]^*, \quad (\text{E.87})$$

$$\Sigma_L = \Sigma_R^T, \quad \Sigma_D = [\Sigma_D^T]^*, \quad (\text{E.88})$$

in agreement with eqs. (4.72) and (4.73).

In the case of a set of four-component Majorana fermion fields, we can still use the results of eqs. (E.79)–(E.86). However, one obtains additional constraints on the full propagator and self-energy matrix functions due to the Majorana condition $\Psi_{Mi} = C\bar{\Psi}_{Mi}^T$. Inserting this result into eq. (E.78), and making use of the anti-commutativity of the fermion fields, one easily derives:

$$\langle 0 | T \Psi_{M\alpha i}(x) \bar{\Psi}_{M\beta j}(y) | 0 \rangle_{\text{FT}} = C_{\alpha\gamma} \langle 0 | T \Psi_{M\delta i}(x) \bar{\Psi}_{M\gamma j}(y) | 0 \rangle_{\text{FT}} C_{\delta\beta}^{-1}. \quad (\text{E.89})$$

Consequently,

$$CS^{\mathsf{T}}C^{-1} = \mathbf{S}, \quad C\boldsymbol{\Sigma}^{\mathsf{T}}C^{-1} = \boldsymbol{\Sigma}. \quad (\text{E.90})$$

Inserting the expressions for \mathbf{S} and $\boldsymbol{\Sigma}$ [eqs. (E.79) and (E.80)] and using the result of eq. (E.48), it follows that:

$$\mathbf{S}_L = \mathbf{S}_R, \quad \mathbf{S}_D = \mathbf{S}_D^{\mathsf{T}}, \quad \overline{\mathbf{S}}_D = \overline{\mathbf{S}}_D^{\mathsf{T}}, \quad (\text{E.91})$$

$$\boldsymbol{\Sigma}_L = \boldsymbol{\Sigma}_R, \quad \boldsymbol{\Sigma}_D = \boldsymbol{\Sigma}_D^{\mathsf{T}}, \quad \overline{\boldsymbol{\Sigma}}_D = \overline{\boldsymbol{\Sigma}}_D^{\mathsf{T}}. \quad (\text{E.92})$$

As expected, with these constraints the form of eq. (4.66) matches precisely with the form of eq. (4.56), corresponding to the equation for the full propagator functions for a theory of generic two-component fermion fields. In the notation of Section 4.6, we can therefore identify: $C \equiv \mathbf{S}_L = \mathbf{S}_R$, $D \equiv \mathbf{S}_D$, $\Xi \equiv \boldsymbol{\Sigma}_L = \boldsymbol{\Sigma}_R$, and $\Omega \equiv \boldsymbol{\Sigma}_D$.

Appendix F: Covariant spin operators and the Bouchiat-Michel Formulae

Bouchiat and Michel derived a useful set of formulae [135] that generalize the spin-projection operators used in four-component spinor computations. In this Appendix, we establish the two-component analogues of the Bouchiat-Michel formulae, and demonstrate their equivalence to the corresponding four-component spinor formulae.

F.1 The covariant spin operators for a spin-1/2 fermion

Consider a massive spin-1/2 fermion of mass m and four-momentum p . We define a set of three four-vectors S_μ^a ($a = 1, 2, 3$) such that the S^a and p/m form an orthonormal set of four-vectors. In the rest frame of the fermion, where $p^\mu = (m; \vec{0})$, we can define

$$S^{a\mu} \equiv (0; \hat{\mathbf{s}}^a), \quad a = 1, 2, 3, \quad (\text{F.1})$$

where the unit vectors $\hat{\mathbf{s}}^a$ are a mutually orthonormal set of unit three-vectors that form a basis for a right-handed coordinate system. Explicit forms for the $\hat{\mathbf{s}}^a$ are given in eq. (B.14). Using eq. (2.71), the three four-vectors S_μ^a in a reference frame in which the four momentum of the fermion is $p^\mu = (E; \vec{p})$ is given by:

$$S^{a\mu} = \left(\frac{\vec{p} \cdot \hat{\mathbf{s}}^a}{m}; \hat{\mathbf{s}}^a + \frac{(\vec{p} \cdot \hat{\mathbf{s}}^a) \vec{p}}{m(E + m)} \right). \quad (\text{F.2})$$

As discussed in Appendix B, we identify $\hat{\mathbf{s}} = \hat{\mathbf{s}}^3$ as the quantization axis used in defining the third component of the spin of the fermion in its rest frame. It then follows that the spin four-vector, previously introduced in eq. (3.15) is given by $S^\mu = S^{3\mu}$.

The orthonormal set of four four-vectors p/m and the S^a satisfy the following Lorentz-covariant relations:

$$p \cdot S^a = 0, \quad (\text{F.3})$$

$$S^a \cdot S^b = -\delta^{ab}, \quad (\text{F.4})$$

$$\epsilon^{\mu\nu\lambda\sigma} p_\mu S_\nu^1 S_\lambda^2 S_\sigma^3 = -m, \quad (\text{F.5})$$

$$S_\mu^a S_\nu^b - S_\nu^a S_\mu^b = \epsilon^{abc} \epsilon_{\mu\nu\rho\sigma} (S^c)^\rho \frac{p^\sigma}{m}, \quad (\text{F.6})$$

$$S_\mu^a S_\nu^a = -g_{\mu\nu} + \frac{p_\mu p_\nu}{m^2}, \quad (\text{F.7})$$

where the sum over the repeated indices is implicitly assumed. It is convenient to define:

$$S_{ss'} \equiv S^a \tau_{ss'}^a, \quad s, s' = \pm \frac{1}{2}, \quad (\text{F.8})$$

where $\tau_{ss'}^a$ are the matrix elements of the Pauli matrices (see footnote 43). Then, we can rewrite eqs. (F.4) and (F.6) as:

$$g_{\mu\nu} S^\mu S^\nu = -3, \quad (\text{F.9})$$

$$S_\mu S_\nu - S_\nu S_\mu = \frac{i}{2m} \epsilon_{\mu\nu\rho\sigma} S^\rho p^\sigma. \quad (\text{F.10})$$

The S^μ serve as covariant spin operators for a spin-1/2 fermion. In particular, in the rest frame, the $\frac{1}{2} S^i$ satisfy the usual SU(2) commutation relations, with $\vec{S}^2 = \frac{3}{4}$ as expected for a spin-1/2 particle.

It is often desirable to work with helicity states. In this case, we choose:

$$\hat{s}^a = \hat{p}^a, \quad \text{i.e.,} \quad \theta = \theta_p \quad \text{and} \quad \phi = \phi_p, \quad (\text{F.11})$$

where the \hat{p}^a are defined in eq. (B.25) [with $\hat{p}^3 \equiv \hat{p}$], in which case eqs. (F.1)–(F.7) also apply to the two-component helicity spinors. Moreover, since $\hat{p}^a \cdot \hat{p} = 0$ for $a \neq 3$, it follows that $S^a = (0; \hat{p}^a)$ for $a = 1, 2$ in all reference frames obtained from the rest frame by a boost in the \hat{p} direction. Hence, in a reference frame where $p^\mu = (E; \vec{p})$, eqs. (B.14) and (F.2) provide explicit forms for the S^a ,

$$S^{1\mu} = (0; \cos \theta \cos \phi, \cos \theta \sin \phi, -\sin \theta), \quad (\text{F.12})$$

$$S^{2\mu} = (0; -\sin \phi, \cos \phi, 0), \quad (\text{F.13})$$

$$S^{3\mu} = \left(\frac{|\vec{p}|}{m}; \frac{E}{m} \hat{p} \right), \quad (\text{F.14})$$

in a coordinate system where $\hat{p} = (\sin \theta \cos \phi, \sin \theta \sin \phi, \cos \theta)$. As expected, $S^{3\mu}$ is the spin vector for helicity states obtained in eq. (3.16). In the high energy limit ($E \gg m$),

$$m S^{a\mu} = p^\mu \delta^{a3} + \mathcal{O}(m). \quad (\text{F.15})$$

F.2 Two-component spinor wave function relations

In Section 3.1, we wrote down explicit forms for the undotted spinor wave functions

$$x_\alpha(\vec{p}, s) = \sqrt{p \cdot \sigma} \chi_s, \quad x^\alpha(\vec{p}, s) = -2s \chi_{-s}^\dagger \sqrt{p \cdot \bar{\sigma}}, \quad (\text{F.16})$$

$$y_\alpha(\vec{p}, s) = 2s \sqrt{p \cdot \sigma} \chi_{-s}, \quad y^\alpha(\vec{p}, s) = \chi_s^\dagger \sqrt{p \cdot \bar{\sigma}}, \quad (\text{F.17})$$

and the dotted spinor wave functions

$$\bar{x}^{\dot{\alpha}}(\vec{p}, s) = -2s \sqrt{p \cdot \bar{\sigma}} \chi_{-s}, \quad \bar{x}_{\dot{\alpha}}(\vec{p}, s) = \chi_s^\dagger \sqrt{p \cdot \sigma}, \quad (\text{F.18})$$

$$\bar{y}^{\dot{\alpha}}(\vec{p}, s) = \sqrt{p \cdot \bar{\sigma}} \chi_s, \quad \bar{y}_{\dot{\alpha}}(\vec{p}, s) = 2s \chi_{-s}^\dagger \sqrt{p \cdot \sigma}, \quad (\text{F.19})$$

where $\sqrt{p \cdot \sigma}$ and $\sqrt{p \cdot \bar{\sigma}}$ are defined in eqs. (2.69) and (2.70). As shown in Appendix B, the two-component spinors χ_s satisfy:

$$\frac{1}{2} \vec{\sigma} \cdot \hat{s}^a \chi_{s'} = \frac{1}{2} \tau_{ss'}^a \chi_s, \quad \chi_s^\dagger(\hat{s}) \chi_{s'}(\hat{s}) = \delta_{ss'}, \quad s, s' = \pm \frac{1}{2}. \quad (\text{F.20})$$

Next, we use eqs. (2.72) and (2.73) to obtain:

$$\sqrt{p \cdot \sigma} S^a \cdot \bar{\sigma} \sqrt{p \cdot \sigma} = m \vec{\sigma} \cdot \hat{s}^a, \quad (\text{F.21})$$

$$\sqrt{p \cdot \bar{\sigma}} S^a \cdot \sigma \sqrt{p \cdot \bar{\sigma}} = -m \vec{\sigma} \cdot \hat{s}^a, \quad (\text{F.22})$$

which extends the results of eqs. (3.17) and (3.18). As a result, we obtain a generalization of eqs. (3.23)–(3.26):

$$(S^a \cdot \bar{\sigma})^{\dot{\alpha}\beta} x_\beta(\vec{p}, s') = \tau_{ss'}^a \bar{y}^{\dot{\alpha}}(\vec{p}, s), \quad (S^a \cdot \sigma)_{\alpha\dot{\beta}} \bar{y}^{\dot{\beta}}(\vec{p}, s') = -\tau_{ss'}^a x_\alpha(\vec{p}, s), \quad (\text{F.23})$$

$$(S^a \cdot \sigma)_{\alpha\dot{\beta}} \bar{x}^{\dot{\beta}}(\vec{p}, s') = -\tau_{s's}^a y_\alpha(\vec{p}, s), \quad (S^a \cdot \bar{\sigma})^{\dot{\alpha}\beta} y_\beta(\vec{p}, s') = \tau_{s's}^a \bar{x}^{\dot{\alpha}}(\vec{p}, s), \quad (\text{F.24})$$

$$x^\alpha(\vec{p}, s') (S^a \cdot \sigma)_{\alpha\dot{\beta}} = -\tau_{s's}^a \bar{y}_{\dot{\beta}}(\vec{p}, s), \quad \bar{y}_{\dot{\alpha}}(\vec{p}, s') (S^a \cdot \bar{\sigma})^{\dot{\alpha}\beta} = \tau_{s's}^a x^\beta(\vec{p}, s), \quad (\text{F.25})$$

$$\bar{x}_{\dot{\alpha}}(\vec{p}, s') (S^a \cdot \bar{\sigma})^{\dot{\alpha}\beta} = \tau_{ss'}^a y^\beta(\vec{p}, s), \quad y^\alpha(\vec{p}, s') (S^a \cdot \sigma)_{\alpha\dot{\beta}} = -\tau_{ss'}^a \bar{x}_{\dot{\beta}}(\vec{p}, s), \quad (\text{F.26})$$

where there is an implicit sum over the repeated label $s = \pm \frac{1}{2}$. As expected, the case of $a = 3$ simply reproduces the results of eqs. (3.23)–(3.26) obtained previously. The above equations also apply to helicity wave functions $x(\vec{p}, \lambda)$ and $y(\vec{p}, \lambda)$ by replacing s, s' with λ, λ' and defining the S^a by eqs. (F.12)–(F.14).

The derivation of eqs. (F.23)–(F.26) for arbitrary a closely follows the corresponding derivation for $a = 3$ previously given. For example, using eqs. (F.21) and (F.22) and the definitions for $x_\alpha(\vec{p}, s)$ and $\bar{y}^{\dot{\alpha}}(\vec{p}, s)$, we find (suppressing spinor indices),

$$\sqrt{p \cdot \sigma} S^a \cdot \bar{\sigma} x(\vec{p}, s') = \sqrt{p \cdot \sigma} S^a \cdot \bar{\sigma} \sqrt{p \cdot \sigma} \chi_{s'} = m \vec{\sigma} \cdot \hat{s}^a \chi_{s'} = m \tau_{ss'}^a \chi_s, \quad (\text{F.27})$$

after using eq. (F.20). Multiplying both sides of eq. (F.27) by $\sqrt{p \cdot \bar{\sigma}}$, we end up with

$$S \cdot \bar{\sigma} x(\vec{p}, s') = \tau_{ss'}^a \sqrt{p \cdot \bar{\sigma}} \chi_s = \tau_{ss'}^a \bar{y}(\vec{p}, s). \quad (\text{F.28})$$

Similarly,

$$S \cdot \sigma \bar{x}(\vec{p}, s') = 2s' \tau_{-s, -s'}^a \sqrt{p \cdot \sigma} \chi_{-s} = -\tau_{s' s}^a y(\vec{p}, s), \quad (\text{F.29})$$

where we have used:

$$4ss' \tau_{-s, -s'}^a = -\tau_{s' s}^a, \quad \text{for } s, s' = \pm 1/2. \quad (\text{F.30})$$

All the results of eqs. (F.23)–(F.26) can be derived in this manner.

F.3 Two-component Bouchiat-Michel formulae

To establish the Bouchiat-Michel formulae, we begin with the following identity:

$$\frac{1}{2}(\delta_{ss'} + \vec{\sigma} \cdot \hat{s}^a \tau_{ss'}^a) \sum_{t=\pm 1/2} \chi_t \chi_t^\dagger = \chi_{s'} \chi_s^\dagger. \quad (\text{F.31})$$

To verify eq. (F.31), we use eq. (F.20) to write $\vec{\sigma} \cdot \hat{s}^a \chi_t = \tau_{t't}^a \chi_{t'}$ and evaluated the product of two Pauli matrices:

$$\tau_{ss'}^a \tau_{t't}^a = 2 \delta_{st} \delta_{s't'} - \delta_{ss'} \delta_{tt'}. \quad (\text{F.32})$$

Using eq. (F.21) and the completeness relation given in eq. (B.8), we can rewrite eq. (F.31) as:

$$\chi_{s'} \chi_s^\dagger = \frac{1}{2} \left(\delta_{ss'} + \frac{1}{m} \sqrt{p \cdot \sigma} S_{ss'} \cdot \vec{\sigma} \sqrt{p \cdot \sigma} \right), \quad (\text{F.33})$$

where $S_{ss'}$ is defined in eq. (F.8). Hence, with both spinor indices in the lowered position,

$$\begin{aligned} x(\vec{p}, s') \bar{x}(\vec{p}, s) &= \sqrt{p \cdot \sigma} \chi_{s'} \chi_s^\dagger \sqrt{p \cdot \sigma} \\ &= \frac{1}{2} \sqrt{p \cdot \sigma} \left[\delta_{ss'} + \frac{1}{m} \sqrt{p \cdot \sigma} S_{ss'} \cdot \vec{\sigma} \sqrt{p \cdot \sigma} \right] \sqrt{p \cdot \sigma} \\ &= \frac{1}{2} \left[p \cdot \sigma \delta_{ss'} + \frac{1}{m} p \cdot \sigma S_{ss'} \cdot \vec{\sigma} p \cdot \sigma \right] \\ &= \frac{1}{2} [p \cdot \sigma \delta_{ss'} - m S_{ss'} \cdot \sigma]. \end{aligned} \quad (\text{F.34})$$

In the final step of eq. (F.34), we simplified the product of three dot-products by noting that $p \cdot S^a = 0$ implies that $S^a \cdot \vec{\sigma} p \cdot \sigma = -p \cdot \vec{\sigma} S^a \cdot \sigma$. Eq. (F.34) is the two-component version of one of the Bouchiat-Michel formulae. We list below a complete set of Bouchiat-Michel formulae, which can be derived by similar techniques:

$$x_\alpha(\vec{p}, s') \bar{x}_{\dot{\beta}}(\vec{p}, s) = \frac{1}{2} (p \delta_{ss'} - m S_{ss'}) \cdot \sigma_{\alpha \dot{\beta}}, \quad (\text{F.35})$$

$$\bar{y}^{\dot{\alpha}}(\vec{p}, s') y^\beta(\vec{p}, s) = \frac{1}{2} (p \delta_{ss'} + m S_{ss'}) \cdot \vec{\sigma}^{\dot{\alpha} \beta}, \quad (\text{F.36})$$

$$x_\alpha(\vec{p}, s') y^\beta(\vec{p}, s) = \frac{1}{2} \left(m \delta_{ss'} \delta_\alpha^\beta - [(\sigma \cdot S_{ss'}) (\vec{\sigma} \cdot p)]_\alpha^\beta \right), \quad (\text{F.37})$$

$$\bar{y}^{\dot{\alpha}}(\vec{p}, s') \bar{x}_{\dot{\beta}}(\vec{p}, s) = \frac{1}{2} \left(m \delta_{ss'} \delta_{\dot{\alpha}}^{\dot{\beta}} + [(\vec{\sigma} \cdot S_{ss'}) (\sigma \cdot p)]_{\dot{\beta}}^{\dot{\alpha}} \right). \quad (\text{F.38})$$

If we set $s = s'$, we recover eqs. (3.44)–(3.47) as expected.

An equivalent set of Bouchiat-Michel formulae can be obtained by raising and/or lowering the appropriate free spinor indices using eqs. (2.22) and (2.61):

$$\bar{x}^{\dot{\alpha}}(\vec{p}, s') x^{\beta}(\vec{p}, s) = \frac{1}{2}(p \delta_{s's} - m S_{s's}) \cdot \bar{\sigma}^{\dot{\alpha}\beta}, \quad (\text{F.39})$$

$$y_{\alpha}(\vec{p}, s') \bar{y}_{\dot{\beta}}(\vec{p}, s) = \frac{1}{2}(p \delta_{s's} + m S_{s's}) \cdot \sigma_{\alpha\dot{\beta}}, \quad (\text{F.40})$$

$$y_{\alpha}(\vec{p}, s') x^{\beta}(\vec{p}, s) = -\frac{1}{2} \left(m \delta_{s's} \delta_{\alpha}^{\beta} + [(\sigma \cdot S_{s's}) (\bar{\sigma} \cdot p)]_{\alpha}^{\beta} \right), \quad (\text{F.41})$$

$$\bar{x}^{\dot{\alpha}}(\vec{p}, s') \bar{y}_{\dot{\beta}}(\vec{p}, s) = -\frac{1}{2} \left(m \delta_{s's} \delta_{\dot{\alpha}}^{\dot{\beta}} - [(\bar{\sigma} \cdot S_{s's}) (\sigma \cdot p)]^{\dot{\alpha}}_{\dot{\beta}} \right). \quad (\text{F.42})$$

These latter set of formulae can also be verified directly by using the explicit forms for the two-component spinor wave functions. In this derivation, the spin labels in eqs. (F.39)–(F.42) are reversed relative to those in eqs. (F.35)–(F.38) due to eq. (F.30).

Other combinations of spinor bilinears are possible. However, eqs. (F.16)–(F.19) imply that the x and y spinors are related:

$$y(\vec{p}, s) = 2s x(\vec{p}, -s), \quad \bar{y}(\vec{p}, s) = 2s \bar{x}(\vec{p}, -s). \quad (\text{F.43})$$

Using eq. (F.43), all possible spinor bilinears can be obtained from eqs. (F.35)–(F.42).

Note that eqs. (F.35)–(F.43) also apply to helicity spinor wave functions $x(\vec{p}, \lambda)$ and $y(\vec{p}, \lambda)$ after replacing s, s' with λ, λ' and using the S^a as defined in eqs. (F.12)–(F.14). Strictly speaking, all results involving the spinor wave functions obtained up to this point apply in the case of a massive spin-1/2 fermion. If we take the massless limit, then the four-vector S^3 does not exist, as its definition depends on the existence of a rest frame. (In contrast, the four-vectors S^1 and S^2 do exist in the massless limit.) Nevertheless, massless helicity spinor wave functions are well-defined; explicit forms can be found in eqs. (3.35)–(3.38). Using these forms, one can derive the Bouchiat-Michel formulae for a massless spin-1/2 fermion:

$$x_{\alpha}(\vec{p}, \lambda') \bar{x}_{\dot{\beta}}(\vec{p}, \lambda) = \left(\frac{1}{2} - \lambda\right) \delta_{\lambda\lambda'} p \cdot \sigma_{\alpha\dot{\beta}}, \quad (\text{F.44})$$

$$\bar{y}^{\dot{\alpha}}(\vec{p}, \lambda') y^{\beta}(\vec{p}, \lambda) = \left(\frac{1}{2} + \lambda\right) \delta_{\lambda\lambda'} p \cdot \bar{\sigma}^{\dot{\alpha}\beta}, \quad (\text{F.45})$$

$$x_{\alpha}(\vec{p}, \lambda') y^{\beta}(\vec{p}, \lambda) = -\frac{1}{2} \left(\frac{1}{2} - \lambda'\right) \left(\frac{1}{2} + \lambda\right) [(\sigma \cdot S_{12}) (\bar{\sigma} \cdot p)]_{\alpha}^{\beta}, \quad (\text{F.46})$$

$$\bar{y}^{\dot{\alpha}}(\vec{p}, \lambda') \bar{x}_{\dot{\beta}}(\vec{p}, \lambda) = \frac{1}{2} \left(\frac{1}{2} + \lambda'\right) \left(\frac{1}{2} - \lambda\right) [(\bar{\sigma} \cdot S_{21}) (\sigma \cdot p)]^{\dot{\alpha}}_{\dot{\beta}}, \quad (\text{F.47})$$

where

$$S_{12} \equiv S_{\frac{1}{2}, -\frac{1}{2}} = S^1 - iS^2, \quad S_{21} \equiv S_{-\frac{1}{2}, \frac{1}{2}} = S^1 + iS^2. \quad (\text{F.48})$$

An explicit representation is given by:

$$\frac{1}{2} \sigma \cdot S_{12} = \begin{pmatrix} \sin \frac{\theta}{2} \cos \frac{\theta}{2} & e^{-i\phi} \sin^2 \frac{\theta}{2} \\ -e^{i\phi} \cos^2 \frac{\theta}{2} & -\sin \frac{\theta}{2} \cos \frac{\theta}{2} \end{pmatrix}, \quad \frac{1}{2} \bar{\sigma} \cdot S_{21} = \begin{pmatrix} \sin \frac{\theta}{2} \cos \frac{\theta}{2} & -e^{-i\phi} \cos^2 \frac{\theta}{2} \\ e^{i\phi} \sin^2 \frac{\theta}{2} & -\sin \frac{\theta}{2} \cos \frac{\theta}{2} \end{pmatrix}. \quad (\text{F.49})$$

The equivalent set of Bouchiat-Michel formulae, obtained by raising and/or lowering the appropriate free spinor indices, is given by:

$$\bar{x}^{\dot{\alpha}}(\vec{p}, \lambda') x^{\beta}(\vec{p}, \lambda) = (\tfrac{1}{2} - \lambda) \delta_{\lambda\lambda'} p \cdot \bar{\sigma}^{\dot{\alpha}\beta}, \quad (\text{F.50})$$

$$y_{\alpha}(\vec{p}, \lambda') \bar{y}_{\dot{\beta}}(\vec{p}, \lambda) = (\tfrac{1}{2} + \lambda) \delta_{\lambda\lambda'} p \cdot \sigma_{\alpha\dot{\beta}}, \quad (\text{F.51})$$

$$y_{\alpha}(\vec{p}, \lambda') x^{\beta}(\vec{p}, \lambda) = -\tfrac{1}{2}(\tfrac{1}{2} + \lambda')(\tfrac{1}{2} - \lambda) [(\sigma \cdot S_{12})(\bar{\sigma} \cdot p)]_{\alpha}{}^{\beta}, \quad (\text{F.52})$$

$$\bar{x}^{\dot{\alpha}}(\vec{p}, \lambda') \bar{y}_{\dot{\beta}}(\vec{p}, \lambda) = \tfrac{1}{2}(\tfrac{1}{2} - \lambda')(\tfrac{1}{2} + \lambda) [(\bar{\sigma} \cdot S_{21})(\sigma \cdot p)]^{\dot{\alpha}}{}_{\dot{\beta}}. \quad (\text{F.53})$$

As a check, one can verify that the above results follow from eqs. (F.35)–(F.42) by replacing s with λ , setting $mS^{a\mu} = p^{\mu} \delta^{a3}$, applying the mass-shell condition ($p^2 = m^2$), and taking the $m \rightarrow 0$ limit at the end of the computation.

We now demonstrate how to use the Bouchiat-Michel formulae to evaluate helicity amplitudes involving two equal-mass spin-1/2 fermions. A typical amplitude involving a fermion-antifermion pair, evaluated in the center-of-mass frame of the pair has the generic structure:

$$z(\vec{p}, \lambda) \Gamma z'(-\vec{p}, \lambda'), \quad (\text{F.54})$$

where z is one of the two-component spinor wave functions x , \bar{x} , y or \bar{y} , and Γ is a 2×2 matrix (in spinor space) made up of products of the identity matrix, σ and $\bar{\sigma}$. As an illustration, we evaluate:

$$\bar{x}_{\dot{\alpha}}(\vec{p}, \lambda) \Gamma^{\dot{\alpha}\beta} y_{\beta}(-\vec{p}, \lambda') = 2\lambda' \Gamma^{\dot{\alpha}\beta} x_{\beta}(-\vec{p}, -\lambda') \bar{x}_{\dot{\alpha}}(\vec{p}, \lambda) = 2\lambda' \Gamma^{\dot{\alpha}\beta} \sigma_{\beta\dot{\beta}}^0 \bar{y}^{\dot{\beta}}(\vec{p}, \lambda) \bar{x}_{\dot{\alpha}}(\vec{p}, \lambda), \quad (\text{F.55})$$

where we have used eqs. (B.31) and (F.43). We can now employ the Bouchiat-Michel formula to convert the above result into a trace. By a similar computation, all expressions of the form of eq. (F.54) can be expressed as a trace:

$$\bar{x}_{\dot{\alpha}}(\vec{p}, \lambda) \Gamma^{\dot{\alpha}\beta} y_{\beta}(-\vec{p}, \lambda') = \lambda' \text{Tr} [\Gamma \sigma^0 (m \delta_{\lambda\lambda'} + \bar{\sigma} \cdot S_{\lambda\lambda'} \sigma \cdot p)], \quad (\text{F.56})$$

$$y^{\alpha}(\vec{p}, \lambda) \Gamma_{\alpha\dot{\beta}} \bar{x}^{\dot{\beta}}(-\vec{p}, \lambda') = -\lambda' \text{Tr} [\Gamma \bar{\sigma}^0 (m \delta_{\lambda\lambda'} - \sigma \cdot S_{\lambda\lambda'} \bar{\sigma} \cdot p)], \quad (\text{F.57})$$

$$y^{\alpha}(\vec{p}, \lambda) \Gamma_{\alpha}{}^{\beta} y_{\beta}(-\vec{p}, \lambda') = \lambda' \text{Tr} [\Gamma \sigma^0 (\bar{\sigma} \cdot p \delta_{\lambda\lambda'} + m \bar{\sigma} \cdot S_{\lambda\lambda'})], \quad (\text{F.58})$$

$$\bar{x}_{\dot{\alpha}}(\vec{p}, \lambda) \Gamma^{\dot{\alpha}}{}_{\dot{\beta}} \bar{x}^{\dot{\beta}}(-\vec{p}, \lambda') = -\lambda' \text{Tr} [\Gamma \bar{\sigma}^0 (\sigma \cdot p \delta_{\lambda\lambda'} - m \sigma \cdot S_{\lambda\lambda'})], \quad (\text{F.59})$$

after making use of eqs. (F.35) and (F.38). Similarly, there are four additional results that make use of eqs. (F.39) and (F.42):

$$\bar{y}_{\dot{\alpha}}(\vec{p}, \lambda) \Gamma^{\dot{\alpha}\beta} x_{\beta}(-\vec{p}, \lambda') = \lambda' \text{Tr} [\Gamma \sigma^0 (m \delta_{\lambda'\lambda} - \bar{\sigma} \cdot S_{\lambda'\lambda} \sigma \cdot p)], \quad (\text{F.60})$$

$$x^{\alpha}(\vec{p}, \lambda) \Gamma_{\alpha\dot{\beta}} \bar{y}^{\dot{\beta}}(-\vec{p}, \lambda') = -\lambda' \text{Tr} [\Gamma \bar{\sigma}^0 (m \delta_{\lambda'\lambda} + \sigma \cdot S_{\lambda'\lambda} \bar{\sigma} \cdot p)], \quad (\text{F.61})$$

$$x^{\alpha}(\vec{p}, \lambda) \Gamma_{\alpha}{}^{\beta} x_{\beta}(-\vec{p}, \lambda') = -\lambda' \text{Tr} [\Gamma \sigma^0 (\bar{\sigma} \cdot p \delta_{\lambda'\lambda} - m \bar{\sigma} \cdot S_{\lambda'\lambda})], \quad (\text{F.62})$$

$$\bar{y}_{\dot{\alpha}}(\vec{p}, \lambda) \Gamma^{\dot{\alpha}}{}_{\dot{\beta}} \bar{y}^{\dot{\beta}}(-\vec{p}, \lambda') = \lambda' \text{Tr} [\Gamma \bar{\sigma}^0 (\sigma \cdot p \delta_{\lambda'\lambda} + m \sigma \cdot S_{\lambda'\lambda})]. \quad (\text{F.63})$$

For amplitudes involving equal mass fermions (or equal mass antifermions), other combinations of spinor bilinears appear in which one x -spinor above is replaced by a y -spinor or vice versa. These amplitudes can be reduced to one of the eight listed above by using eq. (F.43).

The traces are easily evaluated using the results of Appendix A. Here, we apply the above results to the amplitude for the decay $Z^0 \rightarrow f\bar{f}$ [see Section 6.2]. The corresponding center-of-mass frame helicity amplitude is a linear combination of eqs. (F.56) and (F.57) with $\Gamma = \bar{\sigma}$ and $\Gamma = \sigma$, respectively. Evaluating the corresponding terms, we find for $\Gamma = \bar{\sigma}$,

$$\bar{x}(\vec{p}, \lambda) \bar{\sigma}^\mu y(-\vec{p}, \lambda') = 2\lambda' [mg^{\mu 0} \delta_{\lambda\lambda'} + p^\mu S_{\lambda\lambda'}^0 - p^0 S_{\lambda\lambda'}^\mu - 2m(S^\mu S^0 - S^0 S^\mu)_{\lambda\lambda'}] , \quad (\text{F.64})$$

where we have used eq. (F.10) to replace the term with the Levi-Civita tensor. Similarly, we calculate for $\Gamma = \sigma$,

$$y(\vec{p}, \lambda) \sigma^\mu \bar{x}(-\vec{p}, \lambda') = 2\lambda' [-mg^{\mu 0} \delta_{\lambda\lambda'} + p^\mu S_{\lambda\lambda'}^0 - p^0 S_{\lambda\lambda'}^\mu + 2m(S^\mu S^0 - S^0 S^\mu)_{\lambda\lambda'}] . \quad (\text{F.65})$$

Eqs. (F.64) and (F.65) provide explicit forms for the $Z^0 \rightarrow f\bar{f}$ decay helicity amplitudes defined in eqs. (6.16) and (6.17).

The above method is not applicable if the two fermions have unequal mass. In order to compute the helicity amplitudes of the form given by eq. (F.54) for unequal masses, a generalization of the above techniques is required. Some methods for four-component spinor wave functions have been proposed in ref. [137]. We leave it as an exercise for the reader to translate these techniques so that they are applicable to helicity amplitudes expressed in terms of two-component spinor wave functions.

F.4 Four-component Bouchiat-Michel formulae

Using the results of Appendix E, the translation of the results of the previous section into four-component spinor notation is straightforward. First, we consider a massive spin-1/2 fermion. Eqs. (F.23)–(F.26) yield [141]:

$$\gamma_5 \not{s}^a u(\vec{p}, s') = \tau_{ss'}^a u(\vec{p}, s) , \quad \gamma_5 \not{s}^a v(\vec{p}, s') = \tau_{s's}^a v(\vec{p}, s) , \quad (\text{F.66})$$

$$\bar{u}(\vec{p}, s') \gamma_5 \not{s}^a = \tau_{ss'}^a \bar{u}(\vec{p}, s) , \quad \bar{v}(\vec{p}, s') \gamma_5 \not{s}^a = \tau_{s's}^a \bar{v}(\vec{p}, s) . \quad (\text{F.67})$$

In the case of $a = 3$, eqs. (F.66) and (F.67) reduce to those of eq. (E.19).

The four-component Bouchiat-Michel formulae [135–137] can be obtained from eqs. (F.35)–(F.42):

$$u(\vec{p}, s') \bar{u}(\vec{p}, s) = \frac{1}{2} [\delta_{ss'} + \gamma_5 \not{s}^3] (\not{p} + m) , \quad (\text{F.68})$$

$$v(\vec{p}, s') \bar{v}(\vec{p}, s) = \frac{1}{2} [\delta_{s's} + \gamma_5 \not{s}^3] (\not{p} - m) , \quad (\text{F.69})$$

where $S_{ss'} \equiv S^a \tau_{ss'}^a$. As expected, the above results for $s = s'$ correspond to the spin projection operators given in eqs. (E.20) and (E.21). Related formulae involving products of u and v -spinors

can be obtained by using

$$v(\vec{p}, s) = -2s\gamma_5 u(\vec{p}, -s), \quad u(\vec{p}, s) = 2s\gamma_5 v(\vec{p}, -s), \quad (\text{F.70})$$

which follow from eq. (F.43).

Eqs. (F.66)–(F.70) also apply to helicity u and v -spinors, after replacing s, s' with λ, λ' and using the S^a as defined in eq. (F.14). In the convention where the two-component spinor wave function satisfies eq. (B.26), the four-component versions of eqs. (B.31)–(B.34) yield:

$$u(-\vec{p}, -\lambda) = \gamma^0 u(\vec{p}, \lambda), \quad v(-\vec{p}, -\lambda) = \gamma^0 v(\vec{p}, \lambda), \quad (\text{F.71})$$

$$\bar{u}(-\vec{p}, -\lambda) = \bar{u}(\vec{p}, \lambda) \gamma^0, \quad \bar{v}(-\vec{p}, -\lambda) = \bar{v}(\vec{p}, \lambda) \gamma^0. \quad (\text{F.72})$$

In order to consider the massless limit, one must employ helicity spinors, as discussed in Appendix F.3. For $a = 1, 2$, eqs. (F.66) and (F.67) apply in the $m \rightarrow 0$ limit as written. The corresponding massless limit for the case of $a = 3$ is smooth and results in eq. (E.22). Similarly, the massless limit of the Bouchiat-Michel formulae for helicity spinors can be obtained by setting $mS^{a\mu} = p^\mu \delta^{a3}$, applying the mass-shell condition ($p^2 = m^2$), and taking the $m \rightarrow 0$ limit at the end of the computation. The end result is

$$u(p, \lambda') \bar{u}(p, \lambda) = \frac{1}{2}(1 + 2\lambda\gamma_5) \not{p} \delta_{\lambda\lambda'} + \frac{1}{2}\gamma_5 [\not{\mathcal{S}}^1 \tau_{\lambda\lambda'}^1 + \not{\mathcal{S}}^2 \tau_{\lambda\lambda'}^2] \not{p}, \quad (\text{F.73})$$

$$v(p, \lambda') \bar{v}(p, \lambda) = \frac{1}{2}(1 - 2\lambda\gamma_5) \not{p} \delta_{\lambda'\lambda} + \frac{1}{2}\gamma_5 [\not{\mathcal{S}}^1 \tau_{\lambda'\lambda}^1 + \not{\mathcal{S}}^2 \tau_{\lambda'\lambda}^2] \not{p}. \quad (\text{F.74})$$

As expected, when $\lambda = \lambda'$, we recover the helicity projection operators for massless spin-1/2 particles given in eqs. (E.23) and (E.24).

As before, we can use the Bouchiat-Michel formulae to evaluate helicity amplitudes involving two equal-mass spin-1/2 fermions. A typical amplitude involving a fermion-antifermion pair, evaluated in the center-of-mass frame of the pair, has the generic structure:

$$\bar{w}(\vec{p}, \lambda) \Gamma w'(-\vec{p}, \lambda'), \quad (\text{F.75})$$

where w is either a u or v spinor, w' is respectively either a v or u spinor, and Γ is a product of Dirac gamma matrices. For example,

$$\bar{u}(\vec{p}, \lambda) \Gamma v(-\vec{p}, \lambda') = -2\lambda' \bar{u}(\vec{p}, \lambda) \Gamma \gamma_5 u(-\vec{p}, -\lambda') = -2\lambda' \bar{u}(\vec{p}, \lambda) \Gamma \gamma_5 \gamma^0 u(\vec{p}, \lambda'), \quad (\text{F.76})$$

where we have used the results of eqs. (F.70) and (F.71). We can now employ the Bouchiat-Michel formula to convert the above result into a trace. By a similar computation, all expressions of the form of eq. (F.75) can be expressed as a trace:

$$\bar{u}(\vec{p}, \lambda) \Gamma v(-\vec{p}, \lambda') = -\lambda' \text{Tr} [\Gamma \gamma_5 \gamma^0 (\delta_{\lambda\lambda'} + \gamma_5 \not{\mathcal{S}}_{\lambda\lambda'}) (\not{p} + m)], \quad (\text{F.77})$$

$$\bar{v}(\vec{p}, \lambda) \Gamma u(-\vec{p}, \lambda') = \lambda' \text{Tr} [\Gamma \gamma_5 \gamma^0 (\delta_{\lambda'\lambda} + \gamma_5 \not{\mathcal{S}}_{\lambda'\lambda}) (\not{p} - m)]. \quad (\text{F.78})$$

These results are the four-component analogues of eqs. (F.56)–(F.59) and eqs. (F.60)–(F.63), respectively. For amplitudes that involve a pair of equal mass fermions [or equal mass antifermions], w and w' in eq. (F.75) are both u -spinors [or v -spinors]. Using eq. (F.70), these amplitudes can then be evaluated using the results of eqs. (F.77) and (F.78) above.

As an example, we consider once again the decay $Z^0 \rightarrow f\bar{f}$. The decay amplitude is equal to eq. (F.77), where Γ is a linear combination of $\frac{1}{2}\gamma^\mu(1 - \gamma_5)$ and $\frac{1}{2}\gamma^\mu(1 + \gamma_5)$. Evaluating the corresponding traces yields:

$$\bar{u}(\vec{p}, \lambda) \frac{1}{2}\gamma^\mu(1 - \gamma_5) v(-\vec{p}, \lambda') = 2\lambda' [mg^{\mu 0}\delta_{\lambda\lambda'} + p^\mu S_{\lambda\lambda'}^0 - p^0 S_{\lambda\lambda'}^\mu + i\epsilon^{0\mu\nu\rho}(S_{\lambda\lambda'})_\nu p_\rho] , \quad (\text{F.79})$$

$$\bar{u}(\vec{p}, \lambda) \frac{1}{2}\gamma^\mu(1 + \gamma_5) v(-\vec{p}, \lambda') = 2\lambda' [-mg^{\mu 0}\delta_{\lambda\lambda'} + p^\mu S_{\lambda\lambda'}^0 - p^0 S_{\lambda\lambda'}^\mu - i\epsilon^{0\mu\nu\rho}(S_{\lambda\lambda'})_\nu p_\rho] . \quad (\text{F.80})$$

Using eq. (F.10), we see that eqs. (F.79) and (F.80) reproduce exactly the results of eqs. (F.64) and (F.65), respectively.

Finally, we note that if the two fermions do not have the same mass, then the method presented above is not applicable. However, generalizations of the above method exist in the literature that can be employed to evaluate helicity amplitudes of the form of eq. (F.75) for unequal mass fermions; see, e.g., ref. [137].

Appendix G: The helicity amplitude technique

In this appendix, we discuss how to apply our formalism to the helicity amplitude technique. The latter is very useful when computing scattering cross sections for multi-particle final states, which is typically done numerically. We shall review the formalism of Hagiwara and Zeppenfeld (HZ) [63] and show how our formalism can be connected to theirs. In particular, we present a translation between the two in Table 2.

After factoring the propagators an arbitrary tree amplitude with external fermions can be expressed in terms of a “fermion string”

$$\bar{\psi}_1 P_{R,L} \phi_1 \phi_2 \dots \phi_n \psi_2 , \quad (\text{G.1})$$

where ψ_i denote the *four*-component spinor wave functions

$$\psi_i = u(p_i, \lambda_i) , \quad \text{or} \quad v(p_i, \lambda_i) , \quad (\text{G.2})$$

and $P_{R,L} = (1 \pm \gamma_5)/2$ are the standard projection operators [*cf.* eq. (E.5)] in the chiral representation. Furthermore, a_i stands for an arbitrary Lorentz four vector, which can be a four-momentum (p_i^μ), a vector boson wave-function ($\epsilon^\mu(p_i, \lambda_i)$) an axial vector ($\epsilon_{\nu\rho\kappa}^\mu p_i^\nu p_j^\rho p_k^\kappa$) or another fermion string with uncontracted Lorentz indices, *e.g.* $\bar{\psi}_3 \gamma^\mu \psi_4$.

Our Formalism	HZ Formalism
$x_\alpha(p, \lambda)$	$u(p, \lambda)_-$
$x^\alpha(p, \lambda)$	$-v^*(p, \lambda)_+$
$\bar{x}^{\dot{\alpha}}(p, \lambda)$	$-v(p, \lambda)_+$
$\bar{x}_{\dot{\alpha}}(p, \lambda)$	$u^*(p, \lambda)_-$
$y_\alpha(p, \lambda)$	$-v(p, \lambda)_-$
$y^\alpha(p, \lambda)$	$u^*(p, \lambda)_+$
$\bar{y}^{\dot{\alpha}}(p, \lambda)$	$u(p, \lambda)_+$
$\bar{y}_{\dot{\alpha}}(p, \lambda)$	$-v^*(p, \lambda)_-$
$p \cdot \sigma$	\not{p}_+
$p \cdot \bar{\sigma}$	\not{p}_-
σ^μ	σ_+^μ
$\bar{\sigma}^\mu$	σ_-^μ

Table 2: Translation between our notation and Hagiwara and Zeppenfeld (HZ) [63].

In order to rewrite the fermion string, eq. (G.1), in terms of two-component spinors, we need the HZ decomposition of the spinors (G.2)

$$\psi_i \equiv \begin{pmatrix} (\psi_i)_- \\ (\psi_i)_+ \end{pmatrix}, \quad u(p_i, \lambda_i) \equiv \begin{pmatrix} u(p_i, \lambda_i)_- \\ u(p_i, \lambda_i)_+ \end{pmatrix}, \quad v(p_i, \lambda_i) \equiv \begin{pmatrix} v(p_i, \lambda_i)_- \\ v(p_i, \lambda_i)_+ \end{pmatrix}. \quad (\text{G.3})$$

The corresponding expressions in our notation are given in Table 2. Note the additional sign for the v_\pm spinors. This is because HZ take $v(p, \lambda) = C \bar{u}^T(p, \lambda)$ with $C = i\gamma^2\gamma^0 = -i\gamma^0\gamma^2$, which differs by a sign from our convention. In deriving the correspondence between the notations it is helpful to note that

$$\sqrt{p \cdot \sigma} \chi_\lambda = \frac{E + m - 2\lambda|\vec{p}|}{\sqrt{2(E + m)}} \chi_\lambda = \omega_+(p) \chi_\lambda, \quad (\text{G.4})$$

$$\sqrt{p \cdot \bar{\sigma}} \chi_\lambda = \frac{E + m + 2\lambda|\vec{p}|}{\sqrt{2(E + m)}} \chi_\lambda = \omega_-(p) \chi_\lambda \quad (\text{G.5})$$

where we have used eq. (3.13) (labels) and, as in HZ, $\omega_\pm(p) \equiv \sqrt{E \pm |\vec{p}|}$. Note that we use our notation: $\lambda = \pm \frac{1}{2}$. In HZ $\lambda = \pm 1$.

After employing the Fierz identities given by eqs. (2.55)–(2.57) to get rid of Lorentz indices which are contracted between different fermion strings, the general fermion string can be

expressed as (in the notation of HZ)

$$\text{FS} = (\psi_1)_\alpha^\dagger [a_1, a_2, \dots, a_n]^\alpha (\psi_2)_{\delta_n \alpha}, \quad (\text{G.6})$$

with the 2-component spinor index $\alpha = \pm$, and $\delta_n = (-1)^{n+1}$. Furthermore

$$[a_1, a_2, \dots, a_n]^\alpha \equiv (\not{a}_1)_\alpha (\not{a}_2)_{-\alpha} \dots (\not{a}_n)_{\delta_n \alpha} \quad (\text{G.7})$$

where

$$(\not{a})_\pm = a_\mu \sigma_\pm^\mu. \quad (\text{G.8})$$

In our notation $\sigma_+^\mu = \sigma^\mu$ and $\sigma_-^\mu = \bar{\sigma}^\mu$, (*cf.* Table 2). Using the formalism developed in this paper and employing the Fierz identities given by eqs. (2.55)–(2.57), it is straightforward to express any tree amplitude involving external two component fermions in terms of fermion strings in the form (G.6). This is the immediate link between our work and HZ.

In order to see how to numerically compute amplitudes, we express FS in terms of the relevant momenta. In the following, we use our sign convention for the spinors v_\pm . We first rewrite FS as [63]

$$\text{FS} = C_i C_j \omega_{\alpha(2\lambda_i)}(p_i) \omega_{\alpha(2\lambda_j)}(p_j) S(p_i, a_1, a_2, \dots, a_n, p_j)_{\lambda_i \lambda_j}^\alpha, \quad (\text{G.9})$$

where

$$C_k = \begin{cases} 1 & \text{for } (\psi_k)_\tau = u(p_k, \lambda_k)_\tau, \\ (2\lambda_k)_\tau & \text{for } (\psi_k)_\tau = v(p_k, -\lambda_k)_\tau, \end{cases} \quad \tau = \pm 1, \quad \lambda = \pm \frac{1}{2} \quad (\text{G.10})$$

The function S can be expressed as

$$\begin{aligned} S(p_i, a_1, a_2, \dots, a_n, p_j)_{\lambda_i \lambda_j}^\alpha &= \left[\prod_{k=1}^n \sum_{\tau_k = \pm} (a_k)_{-\alpha \delta_k \tau_k} \right] T(p_i, a_1)_{(2\lambda_i) \tau_1} T(a_1, a_2)_{\tau_1 \tau_2} \\ &\quad \dots T(a_{n-1}, a_n)_{\tau_{n-1} \tau_n} T(a_n, p_j)_{\tau_n (2\lambda_j)} \end{aligned} \quad (\text{G.11})$$

where the functions T [58, 63] can be expressed entirely in terms of the relevant momenta.

$$T(a, b)_{++} = N_{ab}^{-1} \left[(|\vec{a}| + a_z)(|\vec{b}| + b_z) + (a_x - ia_y)(b_x + ib_y) \right] \quad (\text{G.12})$$

$$T(a, b)_{+-} = N_{ab}^{-1} \left[-(|\vec{a}| + a_z)(b_x - ib_y) + (a_x - ia_y)(|\vec{b}| + b_z) \right] \quad (\text{G.13})$$

$$T(a, b)_{-+} = -T(a, b)_{+-}^* \quad (\text{G.14})$$

$$T(a, b)_{--} = T(a, b)_{++}^* \quad (\text{G.15})$$

with the normalization factor given by

$$N_{ab} = \sqrt{|\vec{a}|(|\vec{a}| + a_z)|\vec{b}|(|\vec{b}| + b_z)}. \quad (\text{G.16})$$

Two-component fermion fields	SU(3)	SU(2) _L	Y	T ₃	Q = T ₃ + $\frac{1}{2}Y$
$\begin{pmatrix} u \\ d \end{pmatrix}$	triplet	doublet	$\frac{1}{6}$	$\frac{1}{2}$	$\frac{2}{3}$
	triplet		$\frac{1}{6}$	$-\frac{1}{2}$	$-\frac{1}{3}$
u^c	anti-triplet	singlet	$-\frac{2}{3}$	0	$-\frac{2}{3}$
d^c	anti-triplet	singlet	$\frac{1}{3}$	0	$\frac{1}{3}$
$\begin{pmatrix} \nu \\ e \end{pmatrix}$	singlet	doublet	$-\frac{1}{2}$	$\frac{1}{2}$	0
	singlet		$-\frac{1}{2}$	$-\frac{1}{2}$	-1
e^c	singlet	singlet	1	0	1

Table 3: Fermions of the Standard Model and their SU(3)×SU(2)_L×U(1)_Y quantum numbers.

Appendix H: Standard Model fermion interaction vertices

In the Standard Model, one generation of quarks and leptons is described by the two-component fermion fields listed in Table 3, where Y is the weak hypercharge, T_3 is the third component of the weak isospin, and $Q = T_3 + Y$ is the electric charge. After SU(2)_L×U(1)_Y breaking, the quark and lepton fields gain mass in such a way that the above two-component fields combine to make up four-component Dirac fermions:

$$U = \begin{pmatrix} u \\ \overline{u^c} \end{pmatrix}, \quad D = \begin{pmatrix} d \\ \overline{d^c} \end{pmatrix}, \quad E = \begin{pmatrix} e \\ \overline{e^c} \end{pmatrix}, \quad (\text{H.1})$$

while the neutrino remains massless. (The extension of the Standard Model to include neutrino mass will be treated elsewhere.)

Here, we follow the convention for particle symbols established in Table 1. Note that u and d are two-component fields, whereas the usual four-component quark and charged lepton fields are denoted by capital letters U , D and E . Consider a generic four-component field expressed in terms of the corresponding two-component fields:

$$F = \begin{pmatrix} f \\ \overline{f^c} \end{pmatrix}. \quad (\text{H.2})$$

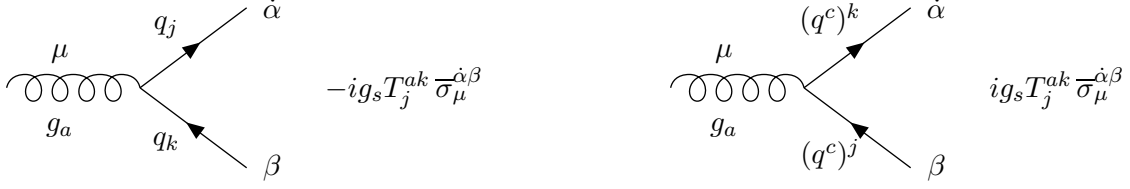


Figure 66: Fermionic Feynman rules for QCD that involve the gluon, with $q = u, d, c, s, t, b$. Lowered (raised) indices j, k correspond to the fundamental (anti-fundamental) representation of $SU(3)_c$. For each rule, a corresponding one with lowered spinor indices is obtained by $\bar{\sigma}_\mu^{\dot{\alpha}\beta} \rightarrow -\sigma_{\mu\beta\dot{\alpha}}$.

The electroweak quantum numbers of f are denoted by T_3^f , Y_f and Q_f , whereas the corresponding quantum numbers for f^c are $T_3^{f^c} = 0$ and $Q_{f^c} = Y_{f^c} = -Q_f$. Thus we have the correspondence to our general notation [eq. (E.4)]

$$f \longleftrightarrow \chi, \quad f^c \longleftrightarrow \eta. \quad (\text{H.3})$$

We can then immediately translate the couplings given in the general case in Fig. 9 to the Standard Model.

The QCD color interactions of the quarks are governed by the following interaction Lagrangian:

$$\mathcal{L}_{\text{int}} = -g_s A_a^\mu \bar{q}^{ji} \bar{\sigma}_\mu (\mathbf{T}^a)_j^k q_{ki}, \quad (\text{H.4})$$

summed over the generations i , where q is a (mass-eigenstate) quark field, j and k are $SU(3)$ color labels and \mathbf{T}^a are the color generators in the triplet representation of $SU(3)$. The corresponding Feynman rules are given in Fig. 66.

Next, we write out the Feynman rules for the electroweak interactions of quarks and leptons. Consider the charged current interactions of the quarks:

$$\mathcal{L}_{\text{int}} = -\frac{g}{\sqrt{2}} \left[\bar{\hat{u}}^i \bar{\sigma}^\mu \hat{d}_i W_\mu^+ + \bar{\hat{d}}^i \bar{\sigma}^\mu \hat{u}_i W_\mu^- \right], \quad (\text{H.5})$$

where the hatted symbols indicate interaction eigenstates and i labels the generations. Following the discussion of Appendix E, we convert to mass eigenstates for the quarks. That is, we introduce four unitary matrices, L_u , L_d , R_u and R_d , [cf. eq. (3.80)] such that

$$\hat{u}_i = (L_u)_i^j u_j, \quad \hat{d}_i = (L_d)_i^j d_j, \quad \hat{u}^{ci} = (R_u)^i_j u^{cj}, \quad \text{and} \quad \hat{d}^{ci} = (R_d)^i_j d^{cj}, \quad (\text{H.6})$$

where the unhatted fields u , d , u^c and d^c are the corresponding mass eigenstates. It then follows that $\bar{\hat{u}}^i \bar{\sigma}^\mu \hat{d}_i = \mathbf{K}_i^j \bar{u}^i \bar{\sigma}^\mu d_j$, where

$$\mathbf{K} = L_u^\dagger L_d \quad (\text{H.7})$$

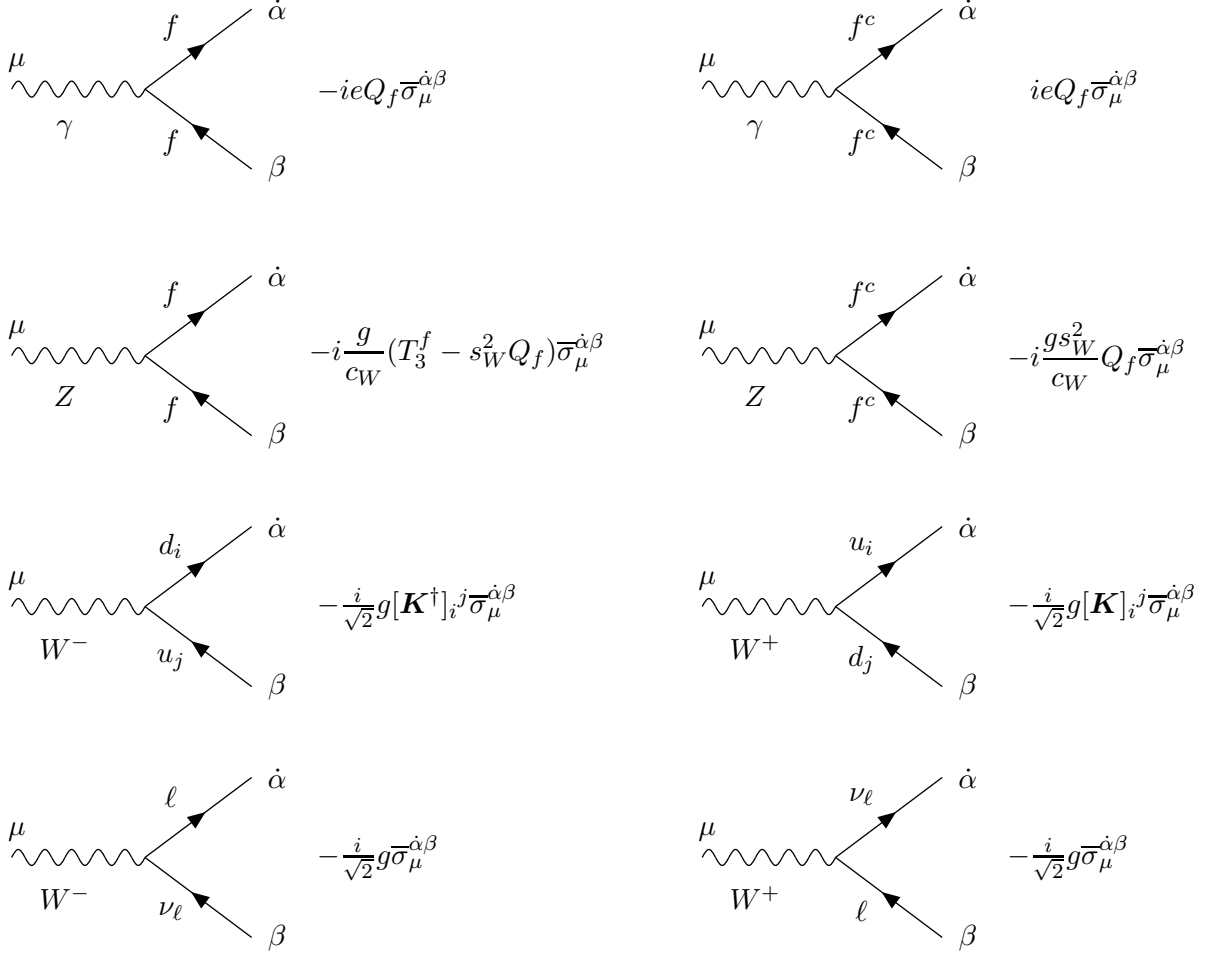


Figure 67: Feynman rules for the two-component fermion interactions with electroweak gauge bosons in the Standard Model. For the W bosons, the charge indicated is flowing into the vertex. The electric charge is denoted by Q_f , with $Q_e = -1$ for the electron, and T_3^f is $1/2$ for up-type quarks and neutrinos and is $-1/2$ for down-type quarks and charged leptons. The CKM mixing matrix is denoted \mathbf{K} , and $s_W \equiv \sin \theta_W$, $c_W \equiv \cos \theta_W$ and $e \equiv g \sin \theta_W$. For each rule, a corresponding one with lowered spinor indices is obtained by $\bar{\sigma}_\mu^{\dot{\alpha}\beta} \rightarrow -\sigma_{\mu\beta\dot{\alpha}}$.

is the unitary Cabibbo-Kobayashi-Maskawa (CKM) matrix.⁶⁴ The charged current interactions take the form

$$\mathcal{L}_{\text{int}} = -\frac{g}{\sqrt{2}} \left[\mathbf{K}_i^j \bar{u}^i \bar{\sigma}^\mu d_j W_\mu^+ + (\mathbf{K}^\dagger)_i^j \bar{d}^i \bar{\sigma}^\mu u_j W_\mu^- + \bar{\nu}^i \bar{\sigma}^\mu e_i W_\mu^+ + \bar{e}^i \bar{\sigma}^\mu \nu_i W_\mu^- \right], \quad (\text{H.8})$$

where

$$(\mathbf{K}^\dagger)_i^j \equiv \mathbf{K}_i^j \equiv (\mathbf{K}_j^i)^*. \quad (\text{H.9})$$

We have also included the leptons, which do not mix. (Note that the Standard Model does not have W^\pm interactions with u^c and d^c .) The corresponding Feynman rules are given in Fig. 67.

⁶⁴The CKM matrix elements V_{ij} as defined in ref. [144] are related by, for example, $V_{tb} = \mathbf{K}_3^3$ and $V_{us} = \mathbf{K}_1^2$.



Figure 68: Feynman rules for the Standard Model Higgs boson interactions with fermions.

The corresponding interaction of the fermions with the neutral gauge bosons are also given in Fig. 67. The neutral current interactions are flavor-conserving. For each of the rules of Fig. 67, we have chosen to employ $\bar{\sigma}_\mu^{\dot{\alpha}\beta}$. If the indices are lowered one should take $\bar{\sigma}_\mu^{\dot{\alpha}\beta} \rightarrow -\sigma_{\mu\beta\dot{\alpha}}$.

The Yukawa interactions of the fermions with the Higgs field are given by:

$$-\mathcal{L}_Y = (\mathbf{Y}_u)^i_j \left[\Phi^0 \hat{u}_i \hat{u}^{cj} - \Phi^+ \hat{d}_i \hat{u}^{cj} \right] + (\mathbf{Y}_d)^i_j \left[\Phi^- \hat{u}_i \hat{d}^{cj} + \Phi^{0*} \hat{d}_i \hat{d}^{cj} \right] + \text{c.c.} \quad (\text{H.10})$$

The Higgs fields can be written in terms of the physical Higgs scalar h_{SM} and Nambu-Goldstone bosons G^0, G^\pm as

$$\Phi^0 = v + \frac{1}{\sqrt{2}}(h_{\text{SM}} + iG^0) \quad (\text{H.11})$$

$$\Phi^+ = G^+ = (\Phi^-)^* = (G^-)^*. \quad (\text{H.12})$$

where $v = \sqrt{2}m_W/g \approx 175$ GeV. In the unitary gauge appropriate for tree-level calculations, the Nambu-Goldstone bosons become infinitely heavy and decouple. After diagonalization of the quark mass matrices,

$$(\mathbf{M}_u)^i_j = v(\mathbf{Y}_u)^i_j, \quad (\mathbf{M}_d)^i_j = v(\mathbf{Y}_d)^i_j, \quad (\text{H.13})$$

one obtains $L_u^\top \mathbf{M}_u R_u = \text{diag}(m_u, m_c, m_t)$ and $L_d^\top \mathbf{M}_d R_d = \text{diag}(m_d, m_s, m_b)$. The resulting Higgs-fermion interactions are diagonal as shown in Fig. 68. Here, the diagonalized Higgs-fermion Yukawa coupling matrices appear:

$$\text{diag}(Y_{u1}, Y_{u2}, Y_{u3}) \equiv \text{diag}(Y_u, Y_c, Y_t) = L_u^\top \mathbf{Y}_u R_u \quad (\text{H.14})$$

$$\text{diag}(Y_{d1}, Y_{d2}, Y_{d3}) \equiv \text{diag}(Y_d, Y_s, Y_b) = L_d^\top \mathbf{Y}_d R_d. \quad (\text{H.15})$$

Likewise, we define

$$Y_{e1} \equiv Y_e, \quad Y_{e2} \equiv Y_\mu, \quad Y_{e3} \equiv Y_\tau \quad (\text{H.16})$$

for the (unmixed) leptons. Note that bold-faced symbols are used for the non-diagonal Yukawa matrices, while non-bold-faced symbols are used for the diagonalized Yukawa couplings. The latter are related to the corresponding fermion masses by $Y_{fi} = m_{fi}/v$, where i labels the fermion generation. The corresponding interaction Lagrangian is

$$\mathcal{L}_{\text{int}} = \frac{1}{\sqrt{2}} h_{\text{SM}} \left[Y_{ui} u_i u^{ci} + Y_{di} d_i d^{ci} + Y_{ei} e_i e^{ci} \right] + \text{c.c.} \quad (\text{H.17})$$

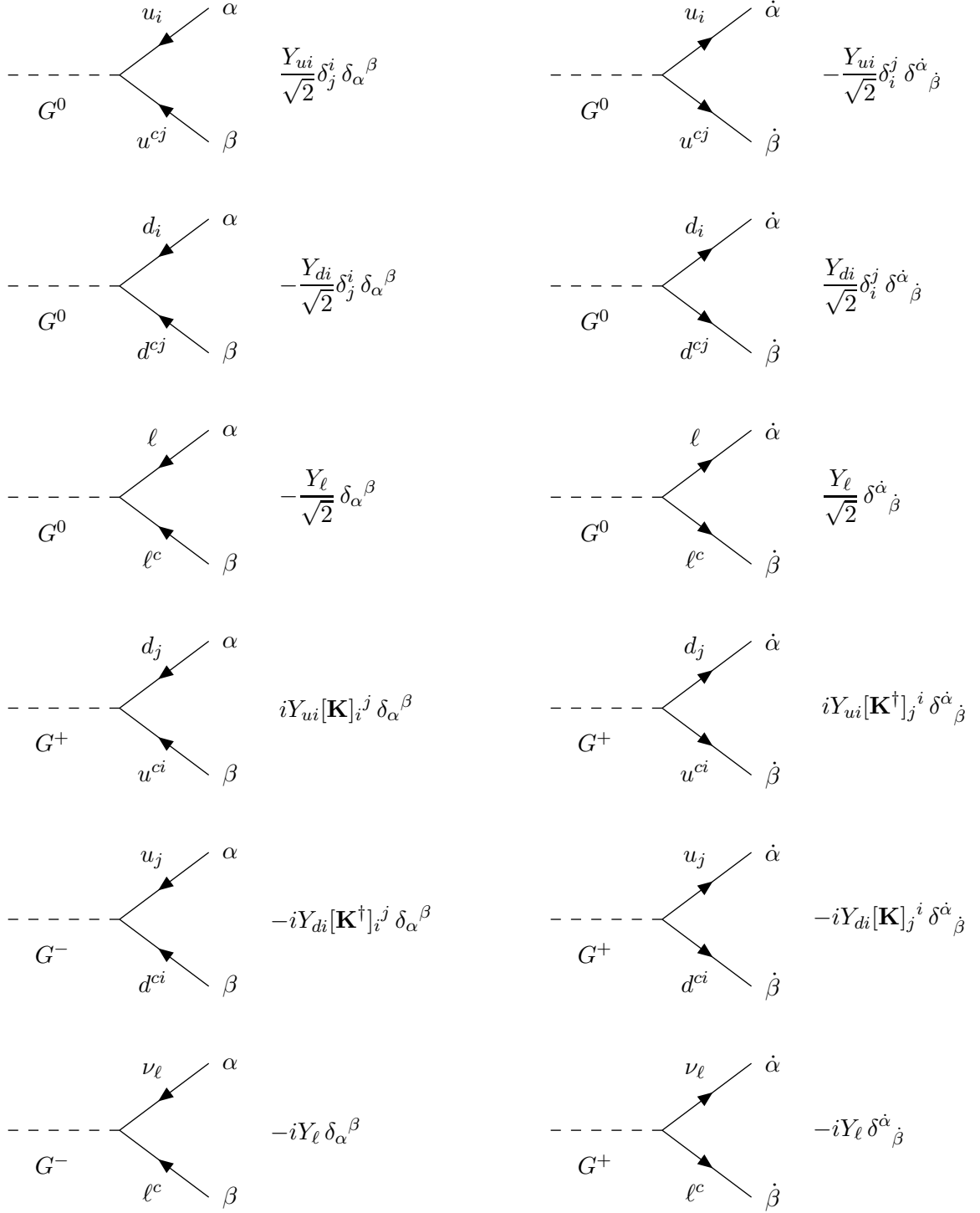


Figure 69: Feynman rules for the Standard Model Nambu-Goldstone boson interactions with quarks and leptons.

In the case of more general covariant gauge-fixing, including Feynman gauge or Landau gauge, the Goldstone bosons appear explicitly in internal lines of Feynman diagrams. The Feynman rules for G^0 -fermion interactions are flavor diagonal, whereas the corresponding rules for G^\pm have a flavor-changing component that depends on the CKM matrix elements. The relevant interaction Lagrangian for quarks follows from eqs. (H.10) and (H.15):

$$\mathcal{L}_{\text{int}} = \frac{i}{\sqrt{2}} [Y_{di}d_id^{ci} - Y_{ui}u_iu^{ci}] G^0 + Y_{ui}[\mathbf{K}]_i^j d_j u^{ci} G^+ - Y_{di}[\mathbf{K}^\dagger]_i^j u_j d^{ci} G^- + \text{c.c.} \quad (\text{H.18})$$

The resulting diagrammatic Feynman rules are shown in Fig. 69, together with the corresponding ones for the leptons.

Appendix I: MSSM Fermion Interaction Vertices

I.1 Higgs-fermion interaction vertices in the MSSM

The MSSM Higgs sector is a two-Higgs-doublet model containing eight real scalar degrees of freedom: one complex $Y = -1/2$ doublet, $H_d = (H_d^0, H_d^-)$ and one complex $Y = +1/2$ doublet, $H_u = (H_u^+, H_u^0)$. The notation reflects the form of the MSSM Higgs sector coupling to fermions: H_d^0 [H_u^0] couples exclusively to down-type [up-type] fermion pairs. In the supersymmetric model, both hypercharge $Y = -1/2$ and $Y = +1/2$ complex Higgs doublets are required in order that the theory (which now contains the corresponding higgsino superpartners) remain anomaly-free. The supersymmetric structure of the theory also requires (at least) these two Higgs doublets to generate mass for both “up”-type and “down”-type quarks and charged leptons.

To find the couplings of the Higgs fields, we expand them around vacuum expectation values v_d and v_u . Depending on the application, these may be chosen to be the minimum of the tree-level potential, or of the full loop-corrected effective potential, or just left arbitrary. The phases of the Higgs fields are chosen such that v_u and v_d are real and positive. That is, the tree-level MSSM Higgs sector conserves CP, which implies that the neutral Higgs mass eigenstates have definite CP quantum numbers. Spontaneous electroweak symmetry breaking results in three CP-odd Goldstone bosons G^\pm , G^0 , which are absorbed and become the longitudinal components of the W^\pm and Z . The remaining five physical Higgs particles consist of a charged Higgs pair H^\pm , one CP-odd scalar A^0 , and two CP-even scalars h^0 and H^0 . One can parameterize the mixing angles between Higgs gauge eigenstates and mass eigenstates by writing:

$$H_u^0 = v_u + \frac{1}{\sqrt{2}} \sum_{\phi^0} k_{u\phi^0} \phi_0, \quad (\text{I.1})$$

$$H_d^0 = v_d + \frac{1}{\sqrt{2}} \sum_{\phi^0} k_{d\phi^0} \phi_0, \quad (\text{I.2})$$

$$H_u^+ = \sum_{\phi^+} k_{u\phi^+} \phi_+, \quad (\text{I.3})$$

$$H_d^{-*} = \sum_{\phi^+} k_{d\phi^+} \phi_+, \quad (\text{I.4})$$

where, for $\phi^0 = (h^0, H^0, G^0, A^0)$,

$$k_{u\phi^0} = (\cos \alpha, \sin \alpha, i \sin \beta_0, i \cos \beta_0) \quad (\text{I.5})$$

$$k_{d\phi^0} = (-\sin \alpha, \cos \alpha, -i \cos \beta_0, i \sin \beta_0) \quad (\text{I.6})$$

and for $\phi^+ = (G^+, H^+)$,

$$k_{u\phi^+} = (\sin \beta_\pm, \cos \beta_\pm), \quad (\text{I.7})$$

$$k_{d\phi^+} = (-\cos \beta_\pm, \sin \beta_\pm). \quad (\text{I.8})$$

Here the normalization is such that, if one chooses v_u, v_d to be near the true minimum of the Higgs effective potential, then $v^2 \equiv v_d^2 + v_u^2 = 2m_W^2/g^2 \approx (175 \text{ GeV})^2$. Note that in the special case that v_u and v_d are the minimum of the *tree-level* potential, the mixing angles β_{\pm} in the charged Higgs sector and β_0 in the pseudo-scalar Higgs sectors coincide exactly with

$$\beta \equiv \arctan(v_u/v_d). \quad (\text{I.9})$$

However, if one expands around a more general choice of v_u, v_d , including for example the minimum of the full effective potential, then the tree-level mixing angles β_0 and β_{\pm} are distinct from each other and from β . (Depending on the choice of renormalization scale for a particular calculation, the tree-level potential in the MSSM may have a very different minimum from the true minimum of the full effective potential, or may not have a proper minimum at all.) Therefore, we do not assume anything specific about v_u and v_d except that they are real and positive.

The Higgs-quark Yukawa couplings in the gauge-interaction basis are given by:

$$-\mathcal{L} = (\mathbf{Y}_u)^i{}_j \left[\hat{u}_i \hat{u}^{cj} H_u^0 - \hat{d}_i \hat{u}^{cj} H_u^+ \right] + (\mathbf{Y}_d)^i{}_j \left[\hat{d}_i \hat{d}^{cj} H_d^0 - \hat{u}_i \hat{d}^{cj} H_d^- \right] + \text{c.c.} \quad (\text{I.10})$$

Let us change to the mass-eigenstate basis by using eq. (H.6) and (I.1)-(I.4). After diagonalization of the fermion mass matrices, $(\mathbf{M}_u)^i{}_j = v_u(\mathbf{Y}_u)^i{}_j$ and $(\mathbf{M}_d)^i{}_j = v_d(\mathbf{Y}_d)^i{}_j$ one obtains $L_u^\top \mathbf{M}_u R_u = \text{diag}(m_u, m_c, m_t)$ and $L_d^\top \mathbf{M}_d R_d = \text{diag}(m_d, m_s, m_b)$. The resulting neutral Higgs-fermion interactions are diagonal. Here, the diagonalized Higgs-fermion Yukawa coupling matrices appear:⁶⁵

$$\text{diag}(Y_{u1}, Y_{u2}, Y_{u3}) \equiv \text{diag}(Y_u, Y_c, Y_t) = L_u^\top \mathbf{Y}_u R_u, \quad (\text{I.11})$$

$$\text{diag}(Y_{d1}, Y_{d2}, Y_{d3}) \equiv \text{diag}(Y_d, Y_s, Y_b) = L_d^\top \mathbf{Y}_d R_d, \quad (\text{I.12})$$

and, for the leptons,

$$Y_{e1} = Y_e, \quad Y_{e2} = Y_\mu, \quad Y_{e3} = Y_\tau. \quad (\text{I.13})$$

The diagonalized Yukawa couplings are related to the corresponding fermion masses by

$$Y_{di} = m_{d_i}/v_d, \quad Y_{ei} = m_{e_i}/v_d, \quad Y_{ui} = m_{u_i}/v_u. \quad (\text{I.14})$$

The interactions of the neutral Higgs scalars $\phi^0 = (h^0, H^0, G^0, A^0)$ with Standard Model fermions are given in Fig. 70. Note that the last two rules involve $k_{d\phi^0}$ and $k_{u\phi^0}$, while the first

⁶⁵We have used the same symbol for the Yukawa couplings in the MSSM as we did for the Standard Model Yukawa couplings in Appendix H. However, it is important to note that they are normalized differently because of the presence of two Higgs VEVs. If we use a superscript SM to distinguish the Standard Model Yukawa couplings of Appendix H, then the MSSM Yukawa couplings defined here are related by $Y_{ui} = Y_{ui}^{\text{SM}}/\sin\beta$ and $Y_{di} = Y_{di}^{\text{SM}}/\cos\beta$ and $Y_{ei} = Y_{ei}^{\text{SM}}/\cos\beta$.

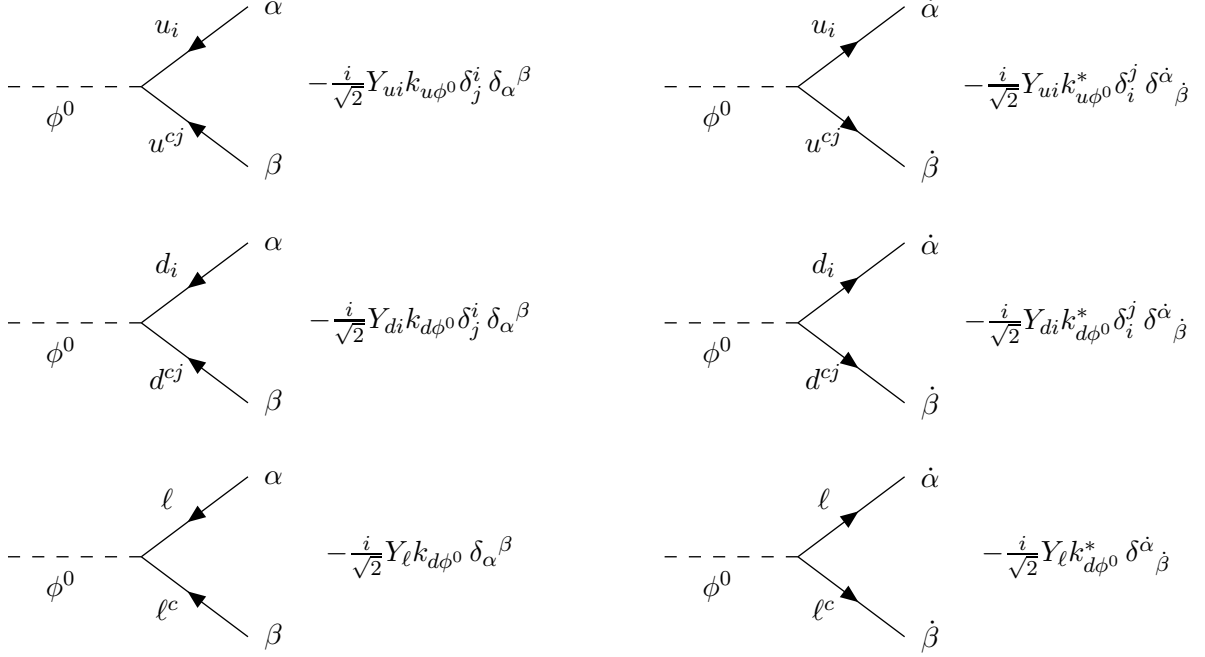


Figure 70: Feynman rules for the interactions of neutral Higgs bosons $\phi^0 = (h^0, H^0, G^0, A^0)$ with fermion-antifermion pairs in the MSSM. The repeated index j is not summed.

two rules involve their complex conjugates. This means that for h^0 and H^0 , starting with the rule with undotted fermion indices, one obtains the corresponding rule with dotted indices (with the direction of the arrows reversed) by taking $\delta_\alpha^\beta \rightarrow \delta_{\dot{\alpha}}^{\dot{\beta}}$. The situation for the pseudoscalar A^0 (and G^0) is different because k_{uA^0} and k_{dA^0} (and k_{uG^0} and k_{dG^0}) are purely imaginary. Starting with the rules for pseudoscalar interactions with fermions with undotted fermion indices, one obtains the corresponding rule with dotted indices (with the direction of the arrows reversed) by taking $\delta_\alpha^\beta \rightarrow -\delta_{\dot{\alpha}}^{\dot{\beta}}$. The minus sign in the last operation is a signal that A^0 and G^0 are CP-odd scalars.⁶⁶

The couplings of the charged Higgs boson to quark-antiquark pairs are not flavor diagonal and involve the CKM matrix \mathbf{K} . Starting with eq. (I.10), and changing to the mass-eigenstate basis as before, one obtains

$$\mathcal{L}_{\text{int}} = (L_d^\top \mathbf{Y}_u R_u)^i_j d_i u^{cj} H^+ \cos \beta + (L_u^\top \mathbf{Y}_d R_d)^i_j u_i d^{cj} H^- \sin \beta + \text{h.c.}, \quad (\text{I.15})$$

and the corresponding G^\pm interactions by taking $\sin \beta \rightarrow -\cos \beta$ and $\cos \beta \rightarrow \sin \beta$. Using eqs. (H.7) and (I.12), one obtains $(L_d^\top \mathbf{Y}_u R_u)^i_j = [\mathbf{K}]_j^i Y_{uj}$ and $(L_u^\top \mathbf{Y}_d R_d)^i_j = [\mathbf{K}^\dagger]_j^i Y_{dj}$, with no sum on repeated indices. The resulting charged-scalar Feynman rules are given in Fig. 71.

⁶⁶Because the Feynman rules for A^0 and G^0 arise from a term in \mathcal{L}_{int} proportional to $i \text{Im } H^0$, the latter i flips sign when the rule is conjugated resulting in the extra minus sign noted above. As an additional consequence, noting that the Feynman rules are obtained from $i\mathcal{L}_{\text{int}}$, the overall A^0 and G^0 rules are real.

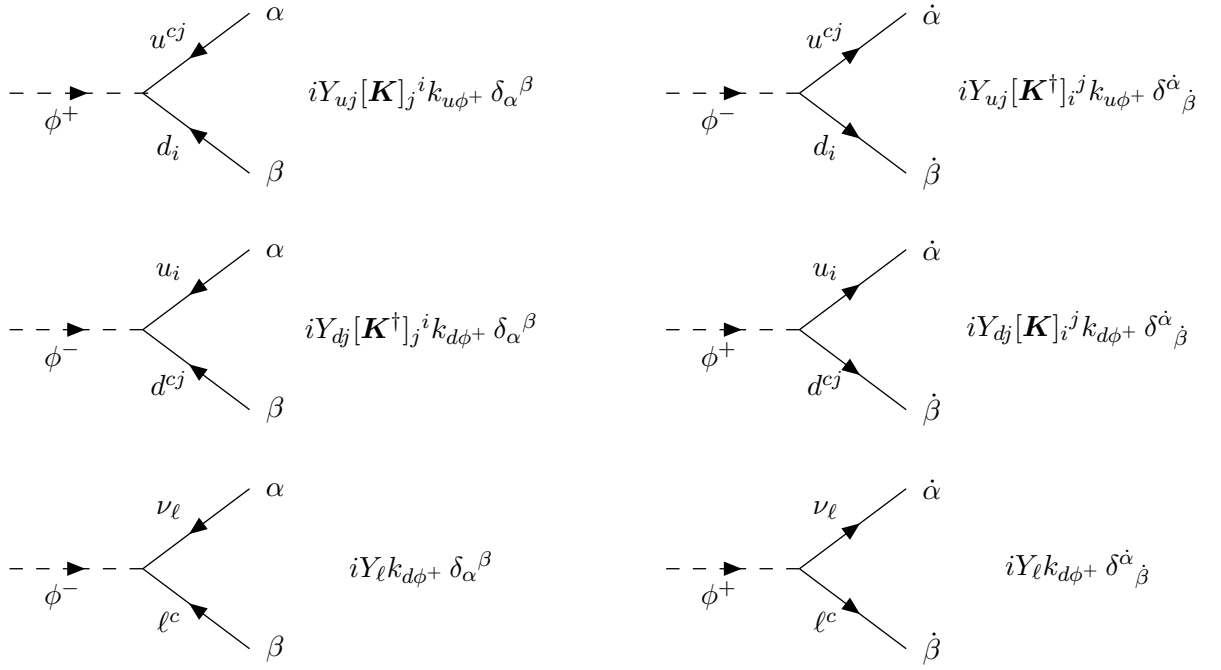


Figure 71: Feynman rules for the interactions of charged Higgs bosons $\phi^\pm = (G^\pm, H^\pm)$ with fermion-antifermion pairs in the MSSM.

I.2 Gauge interaction vertices for neutralinos and charginos

Following eqs. (C83) and (C88) of ref. [48], we define:

$$O_{ij}^L = -\frac{1}{\sqrt{2}}N_{i4}V_{j2}^* + N_{i2}V_{j1}^*, \quad (\text{I.16})$$

$$O_{ij}^R = \frac{1}{\sqrt{2}}N_{i3}^*U_{j2} + N_{i2}^*U_{j1}, \quad (\text{I.17})$$

$$O_{ij}'^L = -V_{i1}V_{j1}^* - \frac{1}{2}V_{i2}V_{j2}^* + \delta_{ij}s_W^2, \quad (\text{I.18})$$

$$O_{ij}'^R = -U_{i1}^*U_{j1} - \frac{1}{2}U_{i2}^*U_{j2} + \delta_{ij}s_W^2, \quad (\text{I.19})$$

$$O_{ij}''^L = -O_{ij}''^{R*} = \frac{1}{2}(N_{i4}N_{j4}^* - N_{i3}N_{j3}^*). \quad (\text{I.20})$$

Here U and V are the unitary matrices that diagonalize the chargino mass matrix:

$$U^*M_{\psi\pm}V^{-1} = \text{diag}(m_{\tilde{C}_1}, m_{\tilde{C}_2}), \quad (\text{I.21})$$

with

$$M_{\psi\pm} = \begin{pmatrix} M_2 & gv_u \\ gv_d & \mu \end{pmatrix}. \quad (\text{I.22})$$

Also, N is a unitary matrix that diagonalizes the neutralino mass matrix,

$$N^*M_{\psi 0}N^{-1} = \text{diag}(m_{\tilde{N}_1}, m_{\tilde{N}_2}, m_{\tilde{N}_3}, m_{\tilde{N}_4}), \quad (\text{I.23})$$

with

$$M_{\psi 0} = \begin{pmatrix} M_1 & 0 & -g'v_d/\sqrt{2} & g'v_u/\sqrt{2} \\ 0 & M_2 & gv_d/\sqrt{2} & -gv_u/\sqrt{2} \\ -g'v_d/\sqrt{2} & gv_d/\sqrt{2} & 0 & -\mu \\ g'v_u/\sqrt{2} & -gv_u/\sqrt{2} & -\mu & 0 \end{pmatrix}. \quad (\text{I.24})$$

We now list the gauge boson interactions with the neutralinos and charginos. The Feynman rules for Z and γ interactions with charginos and neutralinos are given in Fig. 72 and the corresponding rules for W^\pm interactions are given in Fig. 73. For each of these rules, one has a version with lowered spinor indices by replacing $\bar{\sigma}_\mu^{\dot{\alpha}\beta} \rightarrow -\sigma_{\mu\beta\dot{\alpha}}$. We label fermion lines with the symbols of the two-component fermion fields as given in Table 1. Note that the $Z\tilde{N}_i\tilde{N}_j$ interaction vertex also subsumes the $O_{ij}''^R$ interaction found in four-component Majorana Feynman rules as in ref. [48], due to the result of eq. (E.50) and the relation $O_{ij}''^R = -O_{ji}''^L$ of eq. (I.20).

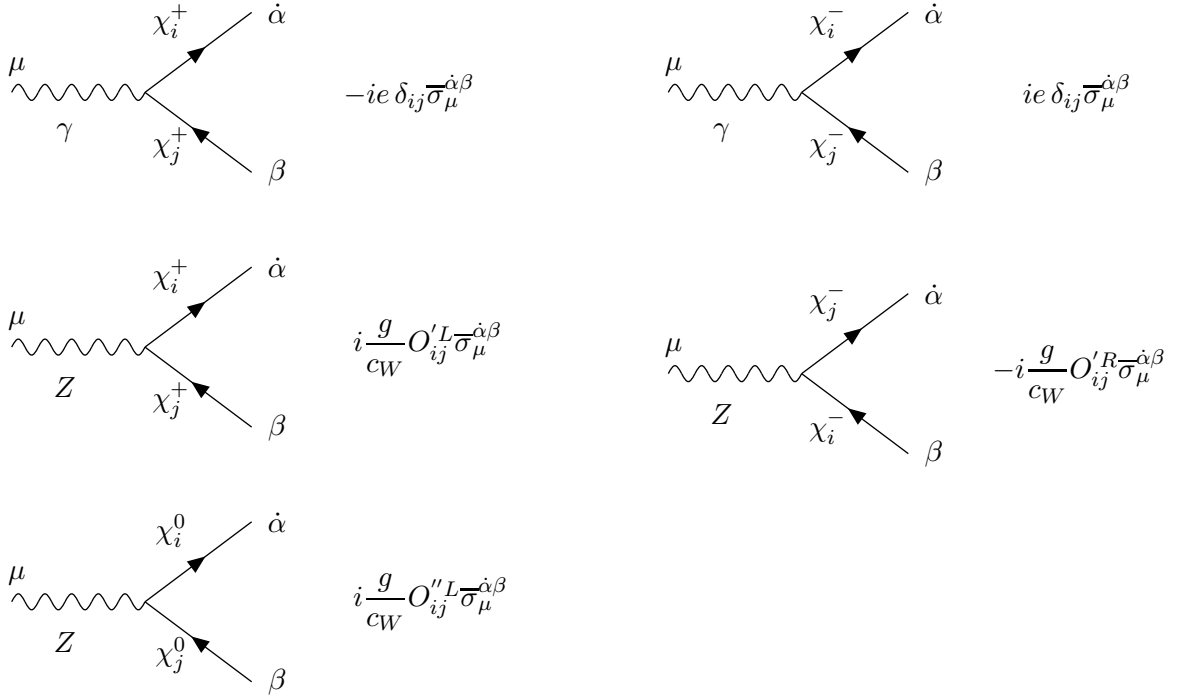


Figure 72: Feynman rules for the chargino and neutralino interactions with neutral gauge bosons. The coupling matrices are defined in eqs. (I.18)-(I.20). For each rule, a corresponding one with lowered spinor indices is obtained by $\bar{\sigma}_\mu^{\dot{\alpha}\beta} \rightarrow -\sigma_{\mu\beta\dot{\alpha}}$.

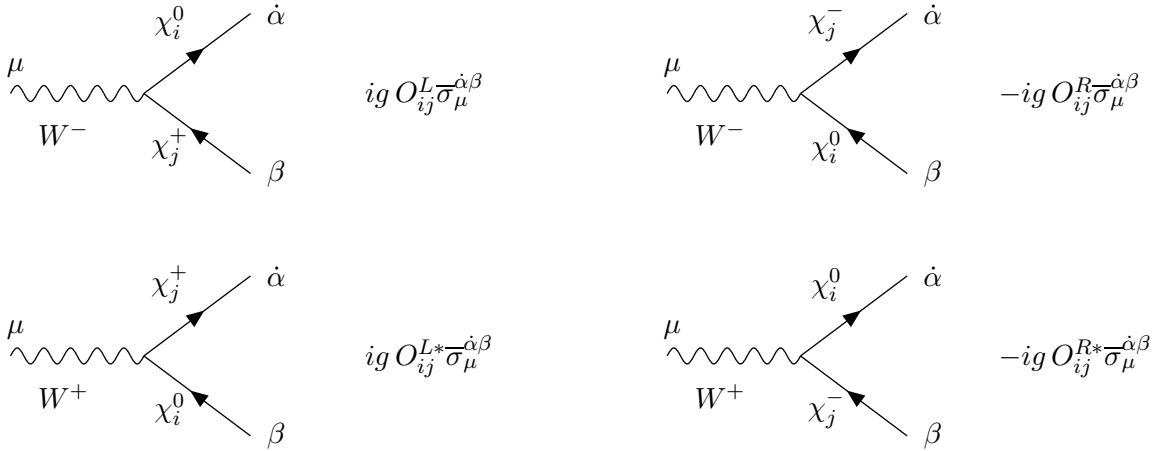


Figure 73: Feynman rules for the chargino and neutralino interactions with W^\pm gauge bosons. The charge indicated on the W boson is flowing into the vertex in each case. The coupling matrices are defined in eqs. (I.16) and (I.17). For each rule, a corresponding one with lowered spinor indices is obtained by $\bar{\sigma}_\mu^{\dot{\alpha}\beta} \rightarrow -\sigma_{\mu\beta\dot{\alpha}}$.

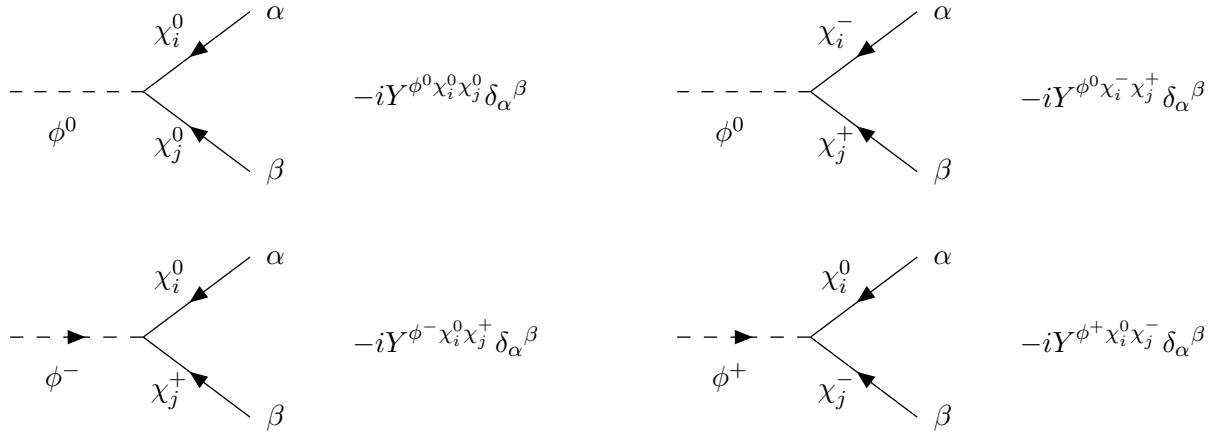


Figure 74: Feynman rules for the interactions of Higgs bosons $\phi^0 = (h^0, H^0, G^0, A^0)$ and $\phi^\pm = (G^\pm, H^\pm)$ with chargino-neutralino pairs. For each rule, there is a corresponding one with all arrows reversed, undotted indices changed to dotted indices with the opposite height, and the Y coupling (without the explicit i) replaced by its complex conjugate.

I.3 Higgs interactions with charginos and neutralinos

The couplings of chargino and neutralino mass eigenstates to the Higgs mass eigenstates can be written, in terms of the Higgs mixing parameters of eqs. (I.5) and (I.6) and the neutralino and chargino mixing matrices of the previous subsection, as:

$$Y^{\phi^0} \chi_i^0 \chi_j^0 = \frac{1}{2} (k_{d\phi^0}^* N_{i3}^* - k_{u\phi^0}^* N_{i4}^*) (g N_{j2}^* - g' N_{j1}^*) + (i \leftrightarrow j), \quad (\text{I.25})$$

$$Y^{\phi^0} \chi_i^+ \chi_j^- = \frac{g}{\sqrt{2}} (k_{u\phi^0}^* V_{i2}^* U_{j1}^* + k_{d\phi^0}^* V_{i1}^* U_{j2}^*) \quad (\text{I.26})$$

$$Y^{\phi^+} \chi_i^0 \chi_j^- = k_{d\phi^+} [g (N_{i3}^* U_{j1}^* - \frac{1}{\sqrt{2}} N_{i2}^* U_{j2}^*) - \frac{g'}{\sqrt{2}} N_{i1}^* U_{j2}^*] \quad (\text{I.27})$$

$$Y^{\phi^-} \chi_i^0 \chi_j^+ = k_{u\phi^-} [g (N_{i4}^* V_{j1}^* + \frac{1}{\sqrt{2}} N_{i2}^* V_{j2}^*) + \frac{g'}{\sqrt{2}} N_{i1}^* V_{j2}^*]. \quad (\text{I.28})$$

We list the Higgs boson interactions with the neutralinos and charginos in Fig. 74. For each of the Feynman rules in Fig. 74, one can reverse all arrows by taking $\delta_{\alpha}^{\beta} \rightarrow \delta_{\dot{\alpha}}^{\dot{\beta}}$ and complex conjugating the corresponding coupling (but not the overall factor of i).

I.4 Chargino and neutralino interactions with fermions and sfermions

In the MSSM, scalar partners of the two-component fields q and \bar{q}^c are the squarks, denoted by \tilde{q}_L and \tilde{q}_R , respectively. In our notation, \tilde{q}_L^* and \tilde{q}_R^* denote both the complex conjugate fields and the names of the corresponding anti-squarks. Thus u , \tilde{u}_L and \tilde{u}_R all have electric charges $+2/3$, whereas u^c , \tilde{u}_L^* and \tilde{u}_R^* all have electric charges $-2/3$. Likewise, the scalar partners of the two-component fields ℓ and $\bar{\ell}^c$ are the charged sleptons, denoted by $\tilde{\ell}_L$ and $\tilde{\ell}_R$, respectively, with $\ell = e, \mu, \tau$. The sneutrino, $\tilde{\nu}$ is the superpartner of the neutrino. There is no $\tilde{\nu}_R$, since there is no ν^c in the theory.

The Feynman rules for the chargino-quark-squark interactions are given in Fig. 75, and the rules for the neutralino-quark-squark interactions are given in Fig. 76. (Note that chargino interaction vertices involving $u^c \tilde{d}_R$ and $d^c \tilde{u}_R$ do not occur in the MSSM.) Here we have taken the quark and lepton two-component fields to be in a mass-eigenstate basis, and the squark and slepton field basis consists of the superpartners of these fields, as described above. Therefore, in practical applications, one must include unitary rotation matrix elements relating the the squarks and sleptons as given to the mass eigenstates, which can be different.

In principle, all sfermions with a given electric charge can mix with each other. However, there is a popular, and perhaps phenomenologically and theoretically favored, approximation in which only the sfermions of the third family have significant mixing. For $f = t, b, \tau$, one can then write the relationship between the gauge eigenstates \tilde{f}_L , \tilde{f}_R and the mass eigenstates \tilde{f}_1 , \tilde{f}_2 as

$$\begin{pmatrix} \tilde{f}_R \\ \tilde{f}_L \end{pmatrix} = X_{\tilde{f}} \begin{pmatrix} \tilde{f}_1 \\ \tilde{f}_2 \end{pmatrix} \quad (\text{I.29})$$

where

$$X_{\tilde{f}} = \begin{pmatrix} R_{\tilde{f}_1} & R_{\tilde{f}_2} \\ L_{\tilde{f}_1} & L_{\tilde{f}_2} \end{pmatrix} \quad (\text{I.30})$$

is a 2×2 unitary matrix. Then one can choose $R_{\tilde{f}_1} = L_{\tilde{f}_2}^* = c_{\tilde{f}}$, and $L_{\tilde{f}_1} = -R_{\tilde{f}_2}^* = s_{\tilde{f}}$ with

$$|c_{\tilde{f}}|^2 + |s_{\tilde{f}}|^2 = 1. \quad (\text{I.31})$$

If there is no CP violation, then $c_{\tilde{f}}$ and $s_{\tilde{f}}$ can be taken real, and they are the cosine and sine of a sfermion mixing angle.⁶⁷ For the other charged sfermions ($f = u, d, c, s, e, \mu$), one can use the same notation, and approximate $L_{\tilde{f}_2} = R_{\tilde{f}_1} = 1$ and $L_{\tilde{f}_1} = R_{\tilde{f}_2} = 0$. The resulting Feynman rules for squarks and sleptons that mix within each generation are shown in Figs. 77 and 78.

⁶⁷Our convention for the sfermion mixing has the property that for zero mixing angle, $\tilde{f}_1 = \tilde{f}_R$ and $\tilde{f}_2 = \tilde{f}_L$. The conventions most commonly found in the literature unfortunately do not have this nice property.

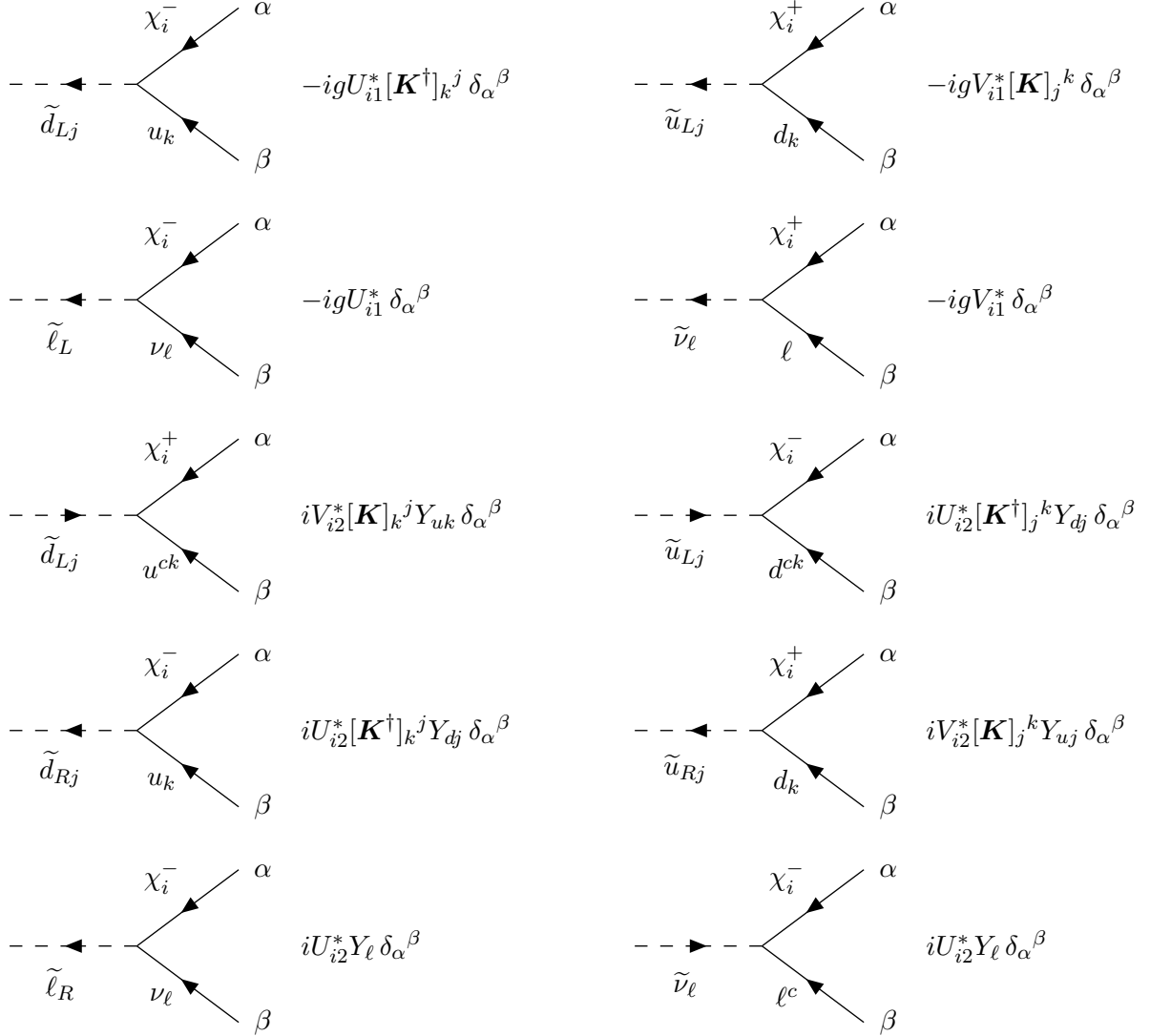


Figure 75: Feynman rules for the interactions of charginos with fermion/sfermion pairs in the MSSM. The fermions are taken to be in a mass-eigenstate basis, and the sfermions are in a basis whose elements are the supersymmetric partners of them. For each rule, there is a corresponding one with all arrows reversed, undotted indices changed to dotted indices with the opposite height, and the coupling (without the explicit i) replaced by its complex conjugate. An alternative version of these rules, for the case that mixing is allowed only among third-family sfermions, is given in Fig. 77.

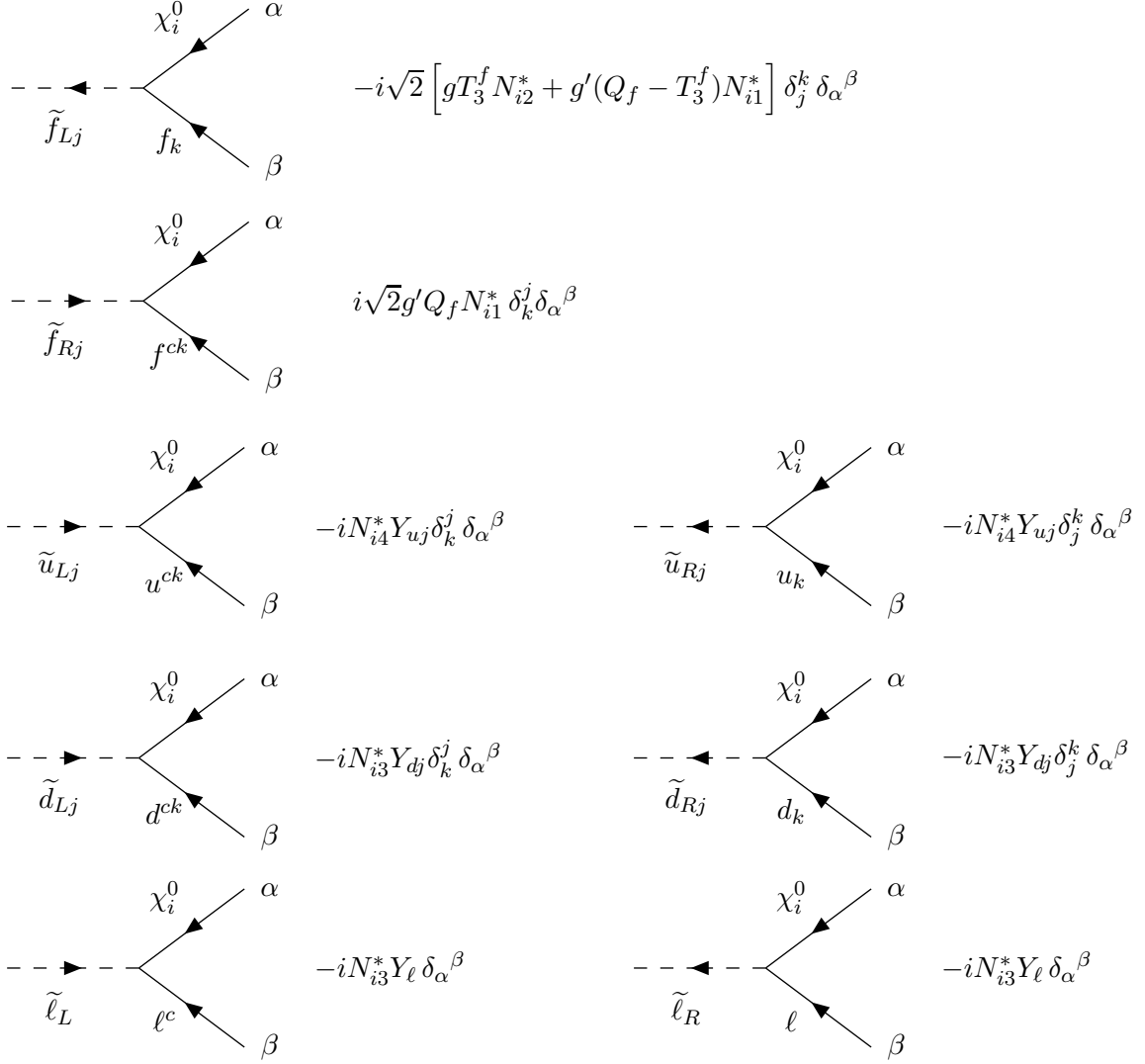


Figure 76: Feynman rules for the interactions of neutralinos with fermion/sfermion pairs in the MSSM. The fermions are taken to be in a mass-eigenstate basis, and the sfermions are in a basis whose elements are the supersymmetric partners of them. For each rule, there is a corresponding one with all arrows reversed, undotted indices changed to dotted indices with the opposite height, and the coupling (without the explicit i) replaced by its complex conjugate. An alternative version of these rules, for the case that mixing is allowed only among third-family sfermions, is given in Fig. 78.

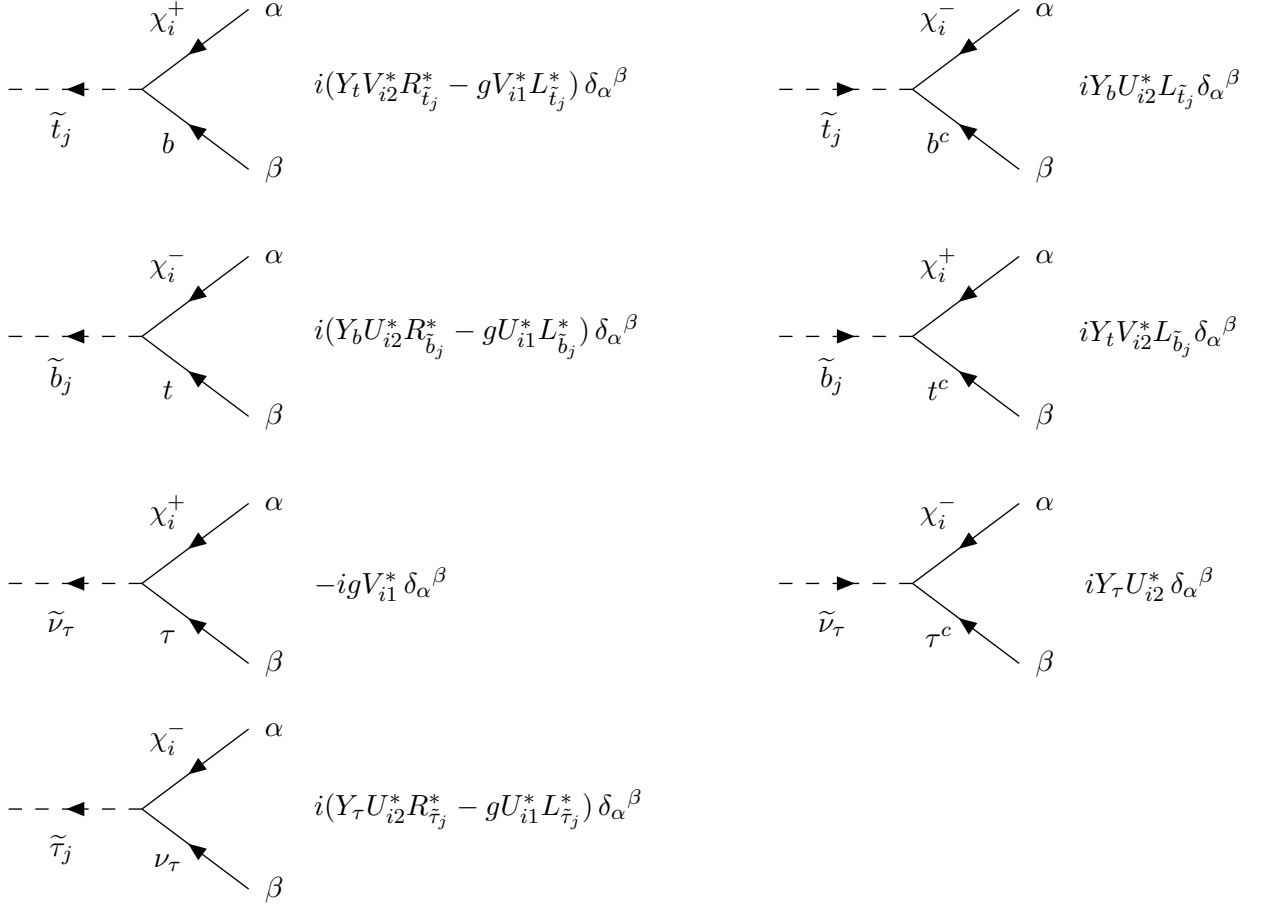


Figure 77: Feynman rules for the interactions of charginos with third-family fermion/sfermion pairs in the MSSM. The fermions are taken to be in a mass-eigenstate basis. CKM mixing is neglected, and the sfermions are assumed to only mix within the third family. The corresponding rules for the first and second families with the approximation of no mixing and vanishing fermion masses can be obtained from these by setting $Y_f = 0$ and $L_{\tilde{f}_2} = R_{\tilde{f}_1} = 1$ and $L_{\tilde{f}_1} = R_{\tilde{f}_2} = 0$ (so that $\tilde{f}_1 = \tilde{f}_R$ and $\tilde{f}_2 = \tilde{f}_L$). For each rule, there is a corresponding one with all arrows reversed, undotted indices changed to dotted indices with the opposite height, and the coupling (without the explicit i) replaced by its complex conjugate.

	$-i \left[Y_t N_{i4}^* R_{\tilde{t}_j}^* + \frac{1}{\sqrt{2}} (g N_{i2}^* + g' N_{i1}^*/3) L_{\tilde{t}_j}^* \right] \delta_\alpha^\beta$
	$-i \left[Y_t N_{i4}^* L_{\tilde{t}_j} - \frac{2\sqrt{2}}{3} g' N_{i1}^* R_{\tilde{t}_j} \right] \delta_\alpha^\beta$
	$-i \left[Y_b N_{i3}^* R_{\tilde{b}_j}^* + \frac{1}{\sqrt{2}} (-g N_{i2}^* + g' N_{i1}^*/3) L_{\tilde{b}_j}^* \right] \delta_\alpha^\beta$
	$-i \left[Y_b N_{i3}^* L_{\tilde{b}_j} + \frac{\sqrt{2}}{3} g' N_{i1}^* R_{\tilde{b}_j} \right] \delta_\alpha^\beta$
	$-\frac{i}{\sqrt{2}} (g N_{i2}^* - g' N_{i1}^*) \delta_\alpha^\beta$
	$-i \left[Y_\tau N_{i3}^* R_{\tilde{\tau}_j}^* - \frac{1}{\sqrt{2}} (g N_{i2}^* + g' N_{i1}^*) L_{\tilde{\tau}_j}^* \right] \delta_\alpha^\beta$
	$-i \left[Y_\tau N_{i3}^* L_{\tilde{\tau}_j} + \sqrt{2} g' N_{i1}^* R_{\tilde{\tau}_j} \right] \delta_\alpha^\beta$

Figure 78: Feynman rules for the interactions of neutralinos with third-family fermion/sfermion pairs in the MSSM. The same comments apply as for Fig. 77.

For each of the Feynman rules in figs. 75-78, one can reverse all arrows by taking $\delta_\alpha^\beta \rightarrow \delta_{\dot{\beta}}^{\dot{\alpha}}$ and taking the complex conjugate of the corresponding rule (but leaving the explicit factor of i intact).

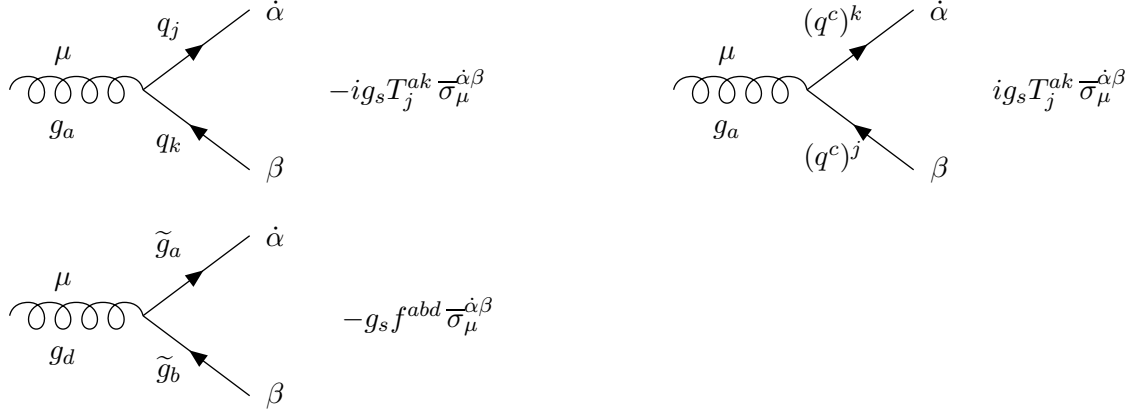


Figure 79: Fermionic Feynman rules for SUSY QCD that involve the gluon, with $q = u, d, c, s, t, b$. Lowered (raised) indices j, k correspond to the fundamental (anti-fundamental) representation of $SU(3)_c$. For each rule, a corresponding one with lowered spinor indices is obtained by $\bar{\sigma}_\mu^{\dot{\alpha}\beta} \rightarrow -\sigma_{\mu\beta\dot{\alpha}}$.

I.5 SUSY QCD Feynman Rules

In two component notation, the Lagrangian governing the gluon's interactions with fermions, which come from the covariant derivatives in the kinetic terms, is

$$\mathcal{L} = ig_s f^{abd} (\bar{\tilde{g}}_a \bar{\sigma}_\mu \tilde{g}_b) A_a^\mu - g_s T_j^{ak} \sum_q [\bar{q}^j \bar{\sigma}_\mu q_k - (\bar{q}^c)_k \bar{\sigma}_\mu (q^c)^j] A_a^\mu. \quad (\text{I.32})$$

Here g_s is the strong coupling constant, $a, b, d = 1, 2, \dots, 8$ are $SU(3)_c$ adjoint representation indices, and f^{abd} are the $SU(3)$ structure constants. Raised (lowered) indices $j, k = 1, 2, 3$ are color indices in the fundamental (anti-fundamental) representation. We have denoted the 2-component gluino field by \tilde{g}_a as in Table 1 and the gluon field by A_a^μ . The sum \sum_q is over the six flavors $q = u, d, s, c, b, t$ (in either the mass-eigenstate or electroweak gauge-eigenstate basis). The corresponding Feynman rules are shown in Fig. 79. The gluino-squark-quark Lagrangian is

$$\mathcal{L} = -\sqrt{2} g_s T_j^{ak} \sum_q \left[\tilde{g}_a q_k \tilde{q}_L^{*j} + \bar{\tilde{g}}_a \bar{q}^j \tilde{q}_{Lk} - \tilde{g}_a (q^c)^j \tilde{q}_{Rk} - \bar{\tilde{g}}_a (\bar{q}^c)_k \tilde{q}_R^{*j} \right], \quad (\text{I.33})$$

where the squark fields are taken to be in the same basis as the quarks. The Feynman rules resulting from these Lagrangian terms are shown in Fig. 80.

For practical applications, one typically takes the quark fields as the familiar mass eigenstates, and then does a unitary rotation on the squarks in the corresponding basis to obtain their mass eigenstate basis. In the approximation described above, in the paragraph containing eqs. (I.29)-(I.31), one obtains the Feynman rules of Fig. 81, as an alternative to those of Fig. 80.

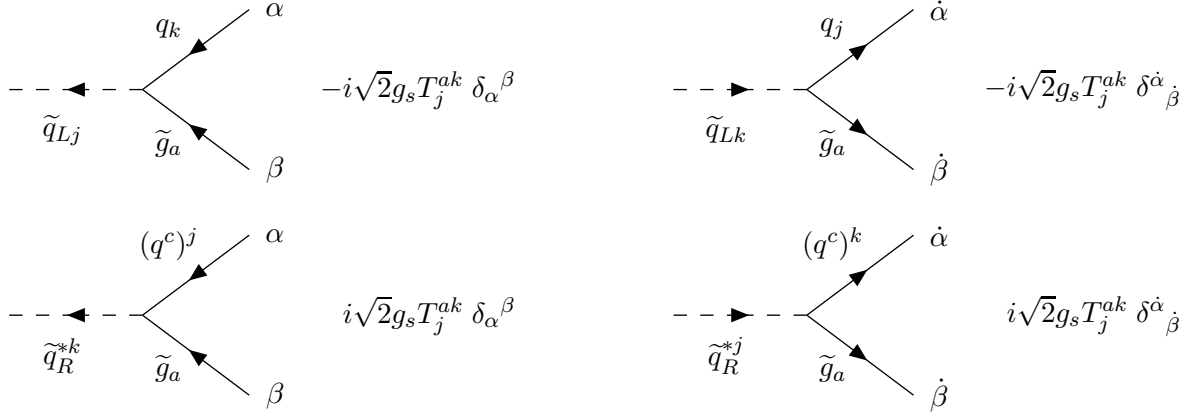


Figure 80: Fermionic Feynman rules for SUSY QCD that involve the squarks, in a basis corresponding to the quark mass eigenstates $q = u, d, c, s, t, b$. Lowered (raised) indices j, k correspond to the fundamental (anti-fundamental) representation of $SU(3)_c$, and the index a labels the adjoint representation carried by the gluino. The spinor index heights can be exchanged in each case, by replacing $\delta_\alpha^\beta \rightarrow \delta_\beta^\alpha$ or $\delta^{\dot{\alpha}}_{\dot{\beta}} \rightarrow \delta^{\dot{\beta}}_{\dot{\alpha}}$. For an alternative set of rules, incorporating LR mixing, see Fig. 81.

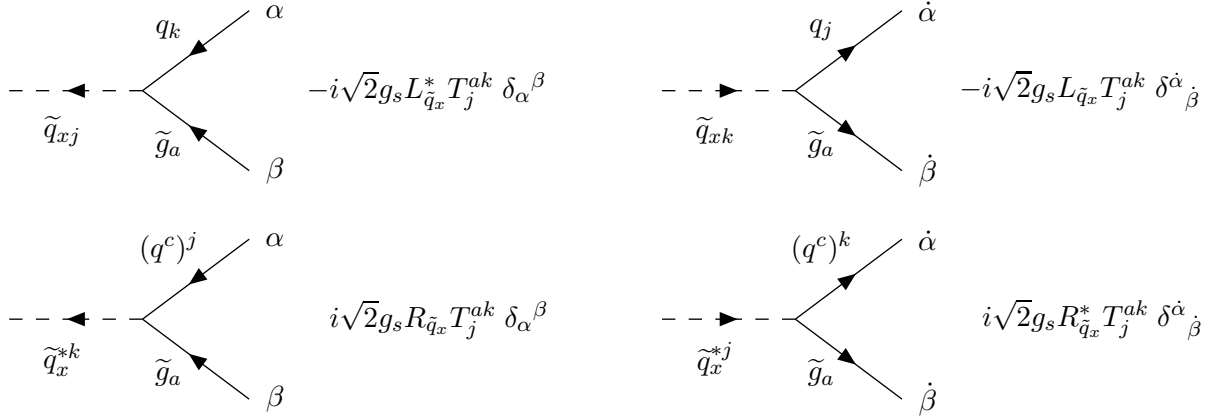


Figure 81: Fermionic Feynman rules for SUSY QCD that involve the squarks in the mass eigenstate basis labeled by $x = 1, 2$ and $q = u, d, c, s, t, b$, in the approximation that mixing is allowed only within a given flavor (typically, for the third family only), as in eq. (I.29). Lowered (raised) indices j, k correspond to the fundamental (anti-fundamental) representation of $SU(3)_c$, and the index a labels the adjoint representation carried by the gluino. The spinor index heights can be exchanged in each case, by replacing $\delta_\alpha^\beta \rightarrow \delta_\beta^\alpha$ or $\delta^{\dot{\alpha}}_{\dot{\beta}} \rightarrow \delta^{\dot{\beta}}_{\dot{\alpha}}$.

Appendix J: Trilinear R-Parity Violating Fermion Interaction Vertices

In the case of R-parity violation [145], the MSSM superpotential is extended by the following terms [146]:

$$W_{\mathcal{R}_p} = \frac{1}{2}\lambda_{ijk}\epsilon_{ab}L_i^a L_j^b \overline{E}_k + \lambda'_{ijk}\epsilon_{ab}L_i^a Q_j^b \overline{D}_k + \frac{1}{2}\lambda''_{ijk}\epsilon_{c_1 c_2 c_3} \overline{U}_i^{c_1} \overline{D}_j^{c_2} \overline{D}_k^{c_3} + \kappa_i \epsilon_{ab} L_i^a H_u^b. \quad (\text{J.1})$$

Here λ_{ijk} , λ'_{ijk} , λ''_{ijk} are dimensionless coupling constants and i, j, k are generation indices. $a, b = 1, 2$ and $c_1, c_2, c_3 = 1, 2, 3$ are $SU(2)$ and $SU(3)$ indices, respectively. L_i, Q_i are the lepton and quark $SU(2)$ -doublet left-chiral superfields. $\overline{E}_i, \overline{U}_i, \overline{D}_i$ are the charged lepton and quark $SU(2)$ -singlet left-chiral superfields. κ_i is a mass-dimension one parameter, which leads to mixing between the sleptons and Higgs fields, as well as between the leptons and Higgsinos. This modifies the Feynman rules of Appendix I through additional mixing matrices, which we do not include here [99]. Recently, the two-component fermion Feynman rules for the neutral fermions have been given in [147]. The intractions in eq. (J.1) can significantly alter the phenomenology at colliders (see for example [102, 105]), in particular, since the LSP is no longer stable. See the computations in Sects. 6.19, and 6.20.

The tri-linear terms in eq. (J.1) lead to additional Yukawa couplings as follows:

$$\mathcal{L}_{L\overline{L}\overline{E}} = -\frac{1}{2}\lambda_{ijk} \left[\tilde{\ell}_{Rk}^* \nu_i \ell_j + \tilde{\nu}_i \ell_j \ell_k^c + \tilde{\ell}_{Lj} \ell_k^c \nu_i - (i \leftrightarrow j) \right] + \text{c.c.}, \quad (\text{J.2})$$

$$\mathcal{L}_{LQ\overline{D}} = -\lambda'_{ijk} \left(\tilde{d}_{Rk}^* \nu_i d_j + \tilde{\nu}_i d_j d_k^c + \tilde{d}_{Lj} d_k^c \nu_i - \tilde{d}_{Rk}^* \ell_i u_j - \tilde{u}_{Lj} d_k^c \ell_i - \tilde{\ell}_{Li} u_j d_k^c \right) + \text{c.c.}, \quad (\text{J.3})$$

$$\mathcal{L}_{\overline{U}\overline{D}\overline{D}} = -\frac{1}{2}\lambda''_{ijk}\epsilon_{c_1 c_2 c_3} \left[\tilde{u}_{Ri}^{c_1*} d_j^{cc_2} d_k^{cc_3} + \tilde{d}_{Rj}^{c_2*} u_i^{cc_1} d_k^{cc_3} + \tilde{d}_{Rk}^{c_3*} u_i^{cc_1} d_j^{cc_2} \right] + \text{c.c.}, \quad (\text{J.4})$$

where repeated indices are summed over. The extra factors of $\frac{1}{2}$ are convenient due to the anti-symmetry in the corresponding couplings: $\lambda_{ijk} = -\lambda_{jik}$, $\lambda''_{ijk} = -\lambda''_{ikj}$. Using eq. (4.9), and Fig. 8 we can now directly determine the corresponding Feynman rules. These are given in Figs. 82, 83, and 84. The same Lagrangian for the Yukawa interactions is given in terms of 4-component fermions in [103, 104], for example.

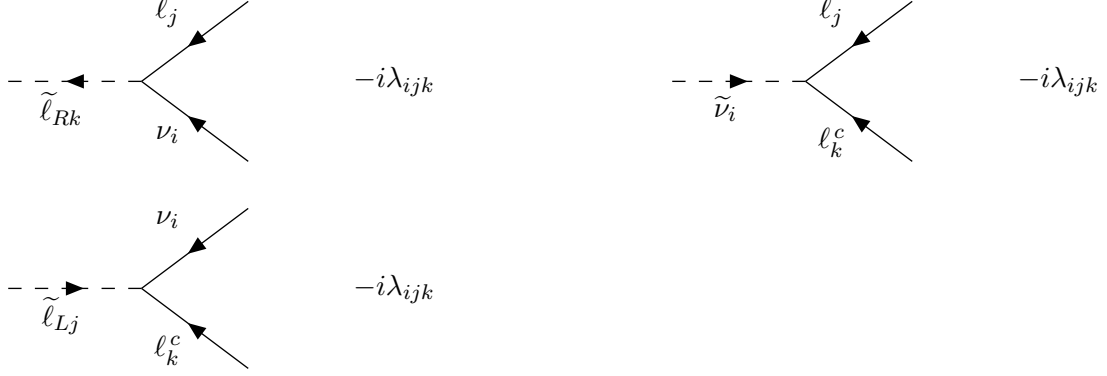


Figure 82: Feynman rules for the Yukawa couplings of two-component fermions due to the supersymmetric, R-parity violating superpotential terms $LL\bar{E}$. For each diagram, there is another with all arrows reversed and $\lambda_{ijk} \rightarrow \lambda_{ijk}^*$.

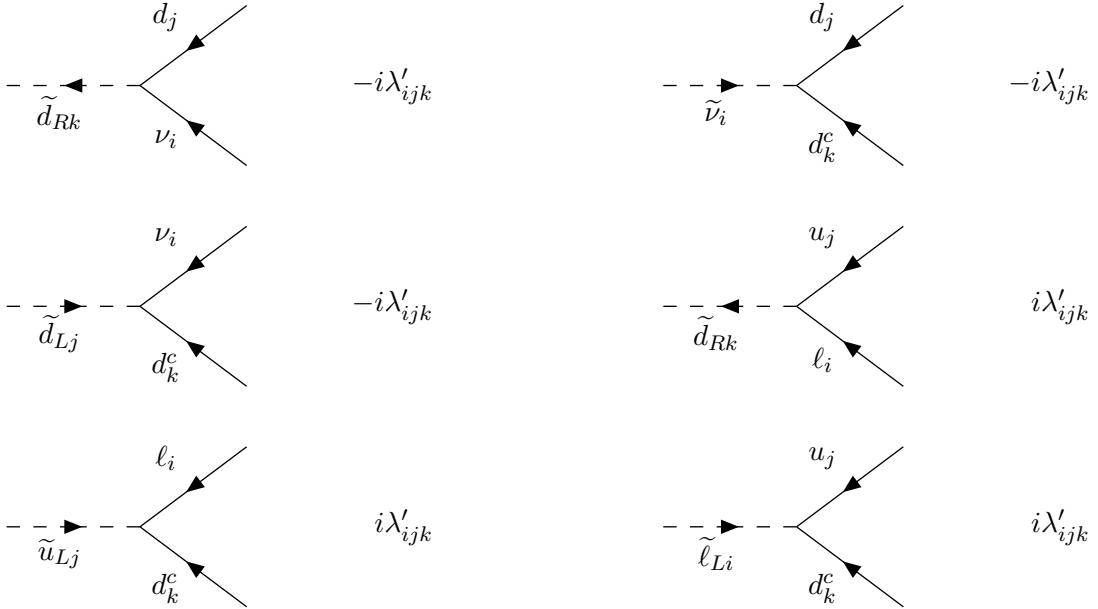


Figure 83: Feynman rules for the Yukawa couplings of two-component fermions for the supersymmetric, R-parity violating superpotential term $LQ\bar{D}$. For each diagram, there is another with all arrows reversed and $\lambda'_{ijk} \rightarrow \lambda_{ijk}^*$.

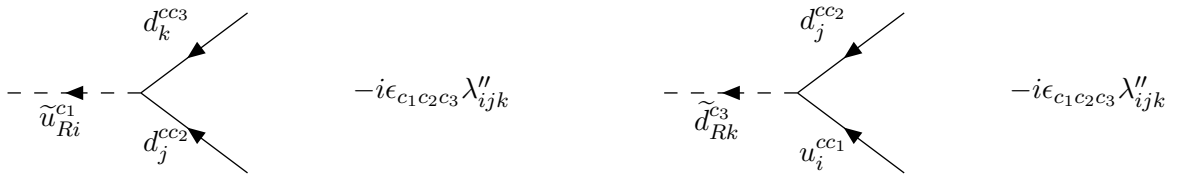


Figure 84: Feynman rules for the Yukawa couplings of two-component fermions due to the supersymmetric, R-parity violating superpotential terms $\bar{U}D\bar{D}$. For each diagram, there is another with all arrows reversed and $\lambda''_{ijk} \rightarrow \lambda_{ijk}^*$.

References

- [1] E. Cartan, Bull. Math. France 41 (1913) 53.
- [2] E. Cartan, Theory of Spinors, (Hermann, Paris, 1966). The first edition of this book appeared in 1937.
- [3] P. A. M. Dirac, Proc. Royal Soc. (A) 117 (1928) p.610, P. A. M. Dirac, Proc. Royal Soc. (A) 118 (1928) p.351.
- [4] H. Weyl, Gruppentheorie und Quantenmechanik, S. Hirzel Verlag, Leipzig, 1928. (English translation: The theory of groups and quantum mechanics, translated from the 2d. rev. German ed. by H. P. Robertson, Dover Publications, New York, 1949.)
- [5] B. L. van der Waerden, Nachrichten Akad. Wiss. Göttingen, Math.-physik. Kl., p. 100 (1929)
- [6] O. LaPorte, and G. E. Uhlenbeck, Phys. Rev. 37 (1931) 1380.
- [7] L. Infeld and B. L. van der Waerden, Sitzber. preuss. Akad. d. Wiss., Physik.-math. Kl. 380 (1933)
- [8] B. L. van der Waerden, Group Theory and Quantum Mechanics, Springer-Verlag, Heidelberg, 1974. The original version of this book was published in German in 1932.
- [9] J. A. Schouten, Journal of Math. and Phys. 10 (1931) p.239.
- [10] W. L. Bade and H. Jehle, Rev. Mod. Phys. 25 (1953) 714-728.
- [11] F. Cap, Fortschritte der Physik 2, (1954) p.207-231.
- [12] E.M. Corson, Introduction to Tensors, Spinors and Relativistic Wave Equations (Blackie and Son, London, 1953).
- [13] H. Umezawa, Quantum Field Theory (North-Holland Publishing Company, Amsterdam, 1956).
- [14] P. Roman, Theory of Elementary Particles (North-Holland Publishing Company, Amsterdam, 1960).
- [15] J. Rzewuski, Field Theory Volume 1: Classical Theory (PWN-Polish Scientific Publishers, Warsaw, 1958, published in Great Britain by Iliffe Books Ltd., London, 1967).
- [16] V.B. Berestetskii, E.M. Lifshitz and L.P. Pitaevskii, Relativistic Quantum Theory (Pergamon Press, Oxford, UK, 1971).

- [17] Peter A. Carruthers, J. Math. Phys., **9** (1968) 1835; *Spin and Isospin in Particle Physics* (Gordon and Breach Science Publishers, New York, 1971).
- [18] Yu. V. Novozhilov, Introduction to Elementary Particle Theory (Pergammon Press, Oxford, UK, 1975).
- [19] I. Bialynicki-Birula and Z. Bialynicki-Birula, Quantum Electrodynamics (Polish Scientific Publishers, Warsaw and Pergammon Press, Oxford, UK, 1975). In this book, the dotted/undotted indices make a brief appearance in Appendix I.
- [20] V.B. Berestetskii, E.M. Lifshitz and L.P. Pitaevskii, Quantum Electrodynamics (Pergammon Press, Oxford, UK, 1980).
- [21] F. Scheck, Electromagnetism and Strong Interactions: An Introduction to Theoretical Particle Physics (2nd edition) (Springer-Verlag, Berlin, 1983).
- [22] R. Penrose and W. Rindler, Spinors and Space-Time, volume 1: Two-Spinor Calculus and Relativistic Fields (Cambridge University Press, Cambridge, UK, 1984).
- [23] Roman U. Sexl and Helmuth K. Urbantke, Relativity, Groups, Particles: Special Relativity and Relativistic Symmetry in Field and Particle Physics (Springer-Verlag, Vienna, 1992).
- [24] R. Ticciati, Quantum Field Theory for Mathematicians (Cambridge University Press, Cambridge, UK, 1999).
- [25] W. Siegel, “Fields,” arXiv:hep-th/9912205.
- [26] A.I. Akhiezer and S.V. Peletminsky, Fields and Fundamental Interactions (Taylor & Francis, London, 2002).
- [27] Milutin Blagojević, Gravitation and Gauge Symmetries (Institute of Physics Publishing, Bristol, UK, 2002).
- [28] Heinrich Saller, Operational Quantum Theory II: Relativistic Structures (Springer-Verlag, New York, 2006).
- [29] Moshe Carmeli and Shimon Malin, Theory of Spinors: An Introduction (World Scientific, Singapore, 2000).
- [30] Jean Hladik, Spinors in Physics (Springer-Verlag, New York, 1999).
- [31] Mark Srednicki, Quantum Field Theory (Cambridge University Press, Cambridge, UK, 2007)

- [32] J. Wess and J. Bagger, *Supersymmetry and Supergravity* (Princeton University Press, Princeton, NJ, 1992).
- [33] S.J. Gates Jr., M.T. Grisaru, M. Roček and W. Siegel, *Superspace or One Thousand and One Lessons in Supersymmetry* (The Benjamin Cummins Publishing Company, Reading, MA, 1983).
- [34] G. Ross, *Grand Unified Theories* (Benjamin-Cummings Publishing Co., 1984)
- [35] Prem P. Srivastava, *Supersymmetry, Superfields and Supergravity: an introduction* (Adam Hilger, Bristol, UK, 1986).
- [36] P. West, *Introduction to Supersymmetry and Supergravity* (World Scientific, Singapore, 1986)
- [37] H.J.W. Müller-Kirsten and A. Wiedemann, *Supersymmetry: An Introduction with Conceptual and Calculational Details* (World Scientific, Singapore, 1987).
- [38] D. Bailin and A. Love, *Supersymmetric Gauge Field Theory and String Theory* (Institute of Physics Publishing, Bristol, UK, 1994).
- [39] Joseph L. Buchbinder and Sergei M. Kuzenko, *Ideas and Methods of Supersymmetry and Supergravity or a Walk through Superspace* (Institute of Physics Publishing, Bristol, UK, 1995).
- [40] S.K. Soni and S. Singh, *Supersymmetry: Basics and Concepts* (Narosa Publishing House, New Delhi, 2000).
- [41] A.S. Galperin, E.A. Ivanov, V.I. Ogievetsky and E.S. Sokatchev, *Harmonic Superspace* (Cambridge University Press, Cambridge, UK, 2001).
- [42] Manuel Drees, Rohini M. Godbole and Probir Roy, *Theory and Phenomenology of Sparticles* (World Scientific, Singapore, 2004).
- [43] J. Terning, *Modern Supersymmetry* (Oxford Science Publications, Oxford, UK, 2006).
- [44] Pierre Binétruy, *Supersymmetry: Theory, Experiment and Cosmology* (Oxford University Press, Oxford, UK, 2006).
- [45] I. J. R. Aitchison, *Supersymmetry in Particle Physics: An Elementary Introduction*, (Cambridge University Press, Cambridge, UK, 2007). An earlier version of this book is available at [arXiv:hep-ph/0505105](https://arxiv.org/abs/hep-ph/0505105).
- [46] K. M. Case, *Phys. Rev.* 107 (1957) p.307.

- [47] H. P. Nilles, Phys. Rept. **110** (1984) 1.
- [48] H. E. Haber and G. L. Kane, Phys. Rept. **117** (1985) 75.
- [49] S.P. Martin, “A Supersymmetry Primer,” [hep-ph/9709356].
- [50] W. Pauli, Annalen Phys. **18S5** (1933) 305; W. Pauli, Annalen Phys. **18S5** (1933) 337; V. Bargmann, Sitzber. preuss. Akad. Wiss., Physik.-math. Kl., 346 (1932); W. Kofink, Math. Z. 51 (1949) 702.
- [51] J. D. Bjorken and M. C. Chen, Phys. Rev. **154** (1966) 1335.
- [52] G. R. Henry, Phys. Rev. **154** (1967) 1534.
- [53] H. W. Fearing and R. R. Silbar, Phys. Rev. D **6** (1972) 471.
- [54] J. O. Eeg, J. Math. Phys. **21** (1980) 170.
- [55] G. Passarino, Phys. Rev. D **28** (1983) 2867.
- [56] G. Passarino, Nucl. Phys. B **237** (1984) 249.
- [57] R. Kleiss, Nucl. Phys. B **241** (1984) 61.
- [58] R. Kleiss and W. J. Stirling, Nucl. Phys. B **262** (1985) 235.
- [59] A. Ballestrero and E. Maina, Phys. Lett. B **350** (1995) 225 [arXiv:hep-ph/9403244].
- [60] G. Chalmers and W. Siegel, Phys. Rev. D **59** (1999) 045012 [arXiv:hep-ph/9708251]; G. Chalmers and W. Siegel, Phys. Rev. D **59** (1999) 045013 [arXiv:hep-ph/9801220].
- [61] G. R. Farrar and F. Neri, Phys. Lett. **130B** (1983) 109 [Addendum-ibid. **152B** (1985) 443].
- [62] A. Kersch and F. Scheck, Nucl. Phys. B **263** (1986) 475.
- [63] K. Hagiwara and D. Zeppenfeld, Nucl. Phys. B **274** (1986) 1.
- [64] F. A. Berends and W. Giele, Nucl. Phys. B **294** (1987) 700; . A. Berends, W. T. Giele and H. Kuijf, Nucl. Phys. B **321** (1989) 39.
- [65] S. Dittmaier, Phys. Rev. D **59** (1999) 016007 [arXiv:hep-ph/9805445].
- [66] S. Dittmaier, “Gauge boson production in electron - photon collisions”, Ph. D. thesis, RX-1526 (WÜRZBURG).
- [67] J. Schechter and J. W. F. Valle, Phys. Rev. D **22** (1980) 2227.

- [68] J. Schechter and J. W. F. Valle, Phys. Rev. D **24** (1981) 1883 [Erratum-ibid. D **25** (1982) 283].
- [69] T. Takagi, Japan J. Math. **1** (1925) 83.
- [70] R.A. Horn and C.R. Johnson, *Matrix Analysis* (Cambridge University Press, Cambridge, England, 1990).
- [71] D.S. Bernstein, *Matrix Mathematics: Theory, Facts, And Formulas With Application To Linear Systems Theory* (Princeton University Press, Princeton, NJ, 2005).
- [72] H. J. Bhabha, Proc. Roy. Soc (London) A 154 (1935) 195.
- [73] S. Weinberg, Phys. Rev. Lett. **19** (1967) 1264.
- [74] M. Kobayashi and T. Maskawa, Prog. Theor. Phys. **49** (1973) 652; N. Cabibbo, Phys. Rev. Lett. **10** (1963) 531.
- [75] V.D. Barger and R.J.N. Phillips, *Collider Physics*, Addison Wesley Longman, 1996.
- [76] M. Peskin and D. Schroeder, *Introduction to Quantum Field Theory* (Addison Wesley, Reading, MA, 1995).
- [77] L. B. Okun, *Leptons and Quarks*, North-Holland Publishing Company, Amsterdam, 1982
- [78] This was first calculated for electrons in: L. Resnick, M. K. Sundaresan and P. J. S. Watson, Phys. Rev. D **8** (1973) 172.
- [79] J.F. Gunion, H.E. Haber, G. Kane and S. Dawson, *The Higgs Hunter's Guide* (Perseus Publishing, Cambridge, MA, 2000).
- [80] D. A. Dicus, S. Nandi and X. Tata, Phys. Lett. B **129** (1983) 451 [Erratum-ibid. B **145** (1984) 448].
- [81] J. F. Gunion and H. E. Haber, Phys. Rev. D **37** (1988) 2515.
- [82] J. F. Gunion and H. E. Haber, Nucl. Phys. B **272** (1986) 1 [Erratum-ibid. B **402** (1993) 567].
- [83] W. Y. Keung and L. Littenberg, Phys. Rev. D **28** (1983) 1067.
- [84] R. M. Barnett, K. S. Lackner and H. E. Haber, Phys. Rev. Lett. **51** (1983) 176; Phys. Rev. D **29** (1984) 1381.
- [85] A. Bartl, H. Fraas and W. Majerotto, Nucl. Phys. B **278**, 1 (1986).

- [86] J. R. Ellis, J. M. Frere, J. S. Hagelin, G. L. Kane and S. T. Petcov, Phys. Lett. B **132** (1983) 436; E. Reya, Phys. Lett. B **133** (1983) 245; P. Chiappetta, J. Soffer, P. Taxil, F. M. Renard and P. Sorba, Nucl. Phys. B **262** (1985) 495 [Erratum-ibid. B **279** (1987) 824];
- [87] S. Dawson, E. Eichten and C. Quigg, Phys. Rev. D **31** (1985) 1581.
- [88] A. Bartl, H. Fraas and W. Majerotto, Z. Phys. C **30** (1986) 441.
- [89] D. A. Dicus, S. Nandi, W. W. Repko and X. Tata, Phys. Rev. Lett. **51** (1983) 1030 [Erratum-ibid. **51** (1983) 1813]; P. Chiappetta, J. Soffer, P. Taxil, F. M. Renard and P. Sorba, Nucl. Phys. B **262** (1985) 495 [Erratum-ibid. B **279** (1987) 824].
- [90] S. Y. Choi, A. Djouadi, H. K. Dreiner, J. Kalinowski and P. M. Zerwas, Eur. Phys. J. C **7** (1999) 123 [arXiv:hep-ph/9806279].
- [91] W. Beenakker, M. Klasen, M. Kramer, T. Plehn, M. Spira and P. M. Zerwas, Phys. Rev. Lett. **83** (1999) 3780 [arXiv:hep-ph/9906298].
- [92] H. Baer, K. Hagiwara and X. Tata, Phys. Rev. D **35** (1987) 1598.
- [93] S. Dimopoulos, M. Dine, S. Raby and S. D. Thomas, Phys. Rev. Lett. **76** (1996) 3494 [arXiv:hep-ph/9601367].
- [94] G. F. Giudice and R. Rattazzi, Phys. Rept. **322** (1999) 419 [arXiv:hep-ph/9801271].
- [95] S. Ambrosanio, G. D. Kribs and S. P. Martin, Nucl. Phys. B **516**, 55 (1998) [hep-ph/9710217].
- [96] P. Fayet, Phys. Lett. B **70**, 461 (1977); Phys. Lett. B **86**, 272 (1979). R. Casalbuoni et al., Phys. Lett. B **215**, 313 (1988); Phys. Rev. D **39**, 2281 (1989).
- [97] N. Cabibbo, G.R. Farrar and L. Maiani, Phys. Lett. B **105**, 155 (1981), D.R. Stump, M. Wiest and C.P. Yuan, Phys. Rev. D **54**, 1936 (1996) [hep-ph/9601362], S. Dimopoulos, M. Dine, S. Raby and S.D. Thomas, Phys. Rev. Lett. **76**, 3494 (1996) [hep-ph/9601367], S. Ambrosanio et al., Phys. Rev. Lett. **76**, 3498 (1996) [hep-ph/9602239], Phys. Rev. D **54**, 5395 (1996) [hep-ph/9605398].
- [98] P. R. Harrison and C. H. Llewellyn Smith, Nucl. Phys. B **213**, 223 (1983) [Erratum-ibid. B **223**, 542 (1983)],
- [99] B. C. Allanach, A. Dedes and H. K. Dreiner, Phys. Rev. D **69** (2004) 115002 [hep-ph/0309196].

- [100] B. C. Allanach, M. A. Bernhardt, H. K. Dreiner, C. H. Kom and P. Richardson, arXiv:hep-ph/0609263.
- [101] S. Dimopoulos and L. J. Hall, Phys. Lett. B **207** (1988) 210; J. Erler, J. L. Feng and N. Polonsky, Phys. Rev. Lett. **78** (1997) 3063 [arXiv:hep-ph/9612397]; H. K. Dreiner, P. Richardson and M. H. Seymour, Phys. Rev. D **63** (2001) 055008 [arXiv:hep-ph/0007228]; H. K. Dreiner, S. Grab, M. Kramer and M. K. Trenkel, arXiv:hep-ph/0611195.
- [102] S. Dimopoulos, R. Esmailzadeh, L. J. Hall and G. D. Starkman, Phys. Rev. D **41** (1990) 2099.
- [103] H. K. Dreiner, P. Richardson and M. H. Seymour, JHEP **0004** (2000) 008 [arXiv:hep-ph/9912407].
- [104] P. Richardson, [hep-ph/0101105].
- [105] H. K. Dreiner and G. G. Ross, Nucl. Phys. B **365** (1991) 597.
- [106] S. Dawson, Nucl. Phys. B **261** (1985) 297.
- [107] E. A. Baltz and P. Gondolo, Phys. Rev. D **57** (1998) 2969 [arXiv:hep-ph/9709445].
- [108] J. Butterworth and H. K. Dreiner, Nucl. Phys. B **397** (1993) 3 [arXiv:hep-ph/9211204]; H. K. Dreiner, M. Guchait and D. P. Roy, Phys. Rev. D **49** (1994) 3270 [arXiv:hep-ph/9310291]; H. K. Dreiner and P. Morawitz, Nucl. Phys. B **428**, 31 (1994) [Erratum-ibid. B **574**, 874 (2000)] [arXiv:hep-ph/9405253].
- [109] Y. Nambu and G. Jona-Lasinio, Phys. Rev. **122**, 345 (1961); Phys. Rev. **124**, 246 (1961).
- [110] Y. Nambu, EFI-88-62-CHICAGO, Proc. of 1988 Int. Workshop New Trends in Strong Coupling Gauge Theories, Nagoya, Japan, Aug 24-27, 1988; V.A. Miransky, M. Tanabashi and K. Yamawaki, Mod. Phys. Lett. A **4**, 1043 (1989); Phys. Lett. B **221**, 177 (1989); W.J. Marciano, Phys. Rev. Lett. **62**, 2793 (1989); Phys. Rev. D **41**, 219 (1990);
- [111] W.A. Bardeen, C.T. Hill and M. Lindner, Phys. Rev. D **41**, 1647 (1990).
- [112] D.E. Clague and G.G. Ross, Nucl. Phys. B **364** (1991) 43.
- [113] C.T. Hill, Phys. Lett. B **266**, 419 (1991).
- [114] C.T. Hill and E.H. Simmons, Phys. Rept. **381**, 235 (2003) [Erratum-ibid. **390**, 553 (2004)] [hep-ph/0203079].
- [115] P. Ramond, *Field theory: A modern primer* (Perseus Books, 2nd ed. 1994).

- [116] G. 't Hooft and M. J. G. Veltman, Nucl. Phys. B **44**, 189 (1972). W.A. Bardeen, A.J. Buras, D.W. Duke and T. Muta, Phys. Rev. D **18**, 3998 (1978).
- [117] W. Siegel, Phys. Lett. B **84**, 193 (1979); D. M. Capper, D. R. T. Jones and P. van Nieuwenhuizen, Nucl. Phys. B **167**, 479 (1980).
- [118] R. Hempfling and B.A. Kniehl, Phys. Rev. D **51**, 1386 (1995) [hep-ph/9408313].
- [119] R. Tarrach, Nucl. Phys. B **183**, 384 (1981).
- [120] S.P. Martin and M.T. Vaughn, Phys. Lett. B **318**, 331 (1993) [hep-ph/9308222].
- [121] D.M. Pierce and A. Papadopoulos, Nucl. Phys. B **430**, 278 (1994) [hep-ph/9403240], D.M. Pierce, J.A. Bagger, K.T. Matchev and R.j. Zhang, Nucl. Phys. B **491**, 3 (1997) [hep-ph/9606211].
- [122] S. Weinberg, “The Quantum Theory of Fields. Vol. 2: Modern Applications,”
- [123] R. Jackiw, in *Current Algebra and Anomalies*, by S.B. Trieman, R. Jackiw, B. Zumino and E. Witten (Princeton University Press, Princeton, NJ, 1985).
- [124] W. Siegel, Phys. Lett. B **94**, 37 (1980).
- [125] L. V. Avdeev and A. A. Vladimirov, Nucl. Phys. B **219**, 262 (1983).
- [126] See for example M. S. Chanowitz, M. Furman and I. Hinchliffe, Nucl. Phys. B **159**, 225 (1979), and references therein.
- [127] M. Jacob and G.C. Wick, Ann. Phys. (NY) **7** (1959) 404.
- [128] R.A. Horn and C.R. Johnson, *Topics in Matrix Analysis* (Cambridge University Press, Cambridge, England, 1991).
- [129] L. Autonne, *Sur les matrices hypohermitiennes et sur les matrices unitaire*, Annales de l’Université de Lyon, Nouvelle Série I, Fasc. **38** (1915) 1–77.
- [130] S.Y. Choi and M. Drees, unpublished. This proof was inspired by the diagonalization algorithm of hermitian matrices in W.H. Williams, B.P. Flannery, S.A. Teukolsky and W.T. Vetterling, *Numerical Recipes in Fortran 77* (Cambridge University Press, Cambridge, England, 1999), section 11.4. A similar method of proof is outlined in Ref. [70], section 4.4, problem 2 (on pp. 212–213) and section 4.6, problem 15 (on p. 254).
- [131] S.Y. Choi, H.E. Haber, J. Kalinowski and P.M. Zerwas, ****
- [132] T. Hahn, arXiv:physics/0607103.

- [133] T. Hahn, Nucl. Phys. Proc. Suppl. **116** (2003) 363 [arXiv:hep-ph/0210220].
- [134] T. Hahn, *In the Proceedings of 2005 International Linear Collider Workshop (LCWS 2005), Stanford, California, 18-22 Mar 2005, pp 0604* [arXiv:hep-ph/0506201].
- [135] C. Bouchiat and L. Michel, Nucl. Phys. **5** (1958) 416; L. Michel, Suppl. Nuovo Cim. **14** (1959) 95.
- [136] H.E. Haber, “Spin Formalism and Applications to New Physics Searches,” in the Proceedings of the 21st SLAC Summer Institute on Particle Physics: Spin Structure in High Energy Processes, SLAC, Stanford, CA 26 July–6 August 1993, pp. 231–272. [arXiv:hep-ph/9405376].
- [137] R. Vega and J. Wudka, Phys. Rev. **D53** (1996) 5286 [Erratum: **D56** (1997) 6037], [arXiv:hep-ph/9511318]
- [138] A. Bunse–Gerstner and W.B. Gragg, J. Comp. Appl. Math. **21** (1988) 41; W. Xu and S. Qiao, “A Divide–and–Conquer Method for the Takagi Factorization,” Technical Report No. CAS 05–01–SQ, (February 2005).
- [139] X. Wang and S. Qiao, in the Proceedings of the International Conference on Parallel and Distributed Processing Techniques and Applications, Vol. I, edited by H.R. Arabnia, pp. 206–212, Las Vegas, Nevada, USA, June 2002, pp. 206–212; F.T. Luk and S. Qiao, in *Advanced Signal Processing Algorithms, Architectures, and Implementations XI*, edited by F.T. Luk, Proc. SPIE **4474** (2001) 254.
- [140] J.M. Jauch and F. Rohrlich, *The Theory of Photons and Electrons*, second expanded edition (Springer-Verlag, New York, 1976), Appendix A2-2;
- [141] D. Bailin, *Weak Interactions*, second edition (Adam Hilger Ltd., Bristol, England, 1982), chapter 2.
- [142] K.I. Aoki, Z. Hioki, M. Konuma, R. Kawabe and T. Muta, Prog. Theor. Phys. Suppl. **73** (1982) 1; M. Bohm, H. Spiesberger and W. Hollik, Fortsch. Phys. **34** (1986) 687.
- [143] M. Bohm, A. Denner and H. Joos, *Gauge theories of the strong and electroweak interaction*, (Teubner, Stuttgart, Germany, 2001).
- [144] S. Eidelman *et al.* [Particle Data Group Collaboration], “Review of particle physics,” Phys. Lett. B **592** (2004) 1.
- [145] H.K. Dreiner, [hep-ph/9707435]; R. Barbier *et al.*, [hep-ph/0406039].

- [146] S. Weinberg, Phys. Rev. D **26** (1982) 287; N. Sakai and T. Yanagida, Nucl. Phys. B **197** (1982) 533.
- [147] A. Dedes, S. Rimmer, J. Rosiek and M. Schmidt-Sommerfeld, Phys. Lett. B **627**, 161 (2005) [arXiv:hep-ph/0506209]; A. Dedes, S. Rimmer and J. Rosiek, JHEP **0608**, 005 (2006) [arXiv:hep-ph/0603225].
- [148] A. Dedes, S. Rimmer and J. Rosiek, JHEP **0608** (2006) 005. [arXiv:hep-ph/0603225].
- [149] J.F. Donoghue, Phys. Rev. **D19** (1979) 2772.
- [150] M. Capdequi Peyranere and M. Talon, Nuovo Cim. **A75** (1983) 205.
- [151] A. Denner and T. Sack, Nucl. Phys. **B347** (1990) 203. A. Denner, Fortsch. Phys. **41** (1993) 307.
- [152] B.A. Kniehl and A. Pilaftsis, Nucl. Phys. **B474**, 286 (1996) [arXiv:hep-ph/9601390]. A. Pilaftsis, Phys. Rev. **D65** (2002) 115013 [arXiv:hep-ph/0203210].
- [153] S. Kiyoura, M. M. Nojiri, D.M. Pierce and Y. Yamada, Phys. Rev. **D58** (1998) 075002 [arXiv:hep-ph/9803210]; D.M. Pierce, in *Supersymmetry, Supergravity and Supercolliders*, Proceedings of the Theoretical Advanced Study Institute in Elementary Particle Physics (TASI 97), Bounler, CO, 1–27 Jun 1997, edited by J.A. Bagger (World Scientific, Singapore, 1999) pp. 343–389 [arXiv:hep-ph/9805497].
- [154] P. Gambino and P.A. Grassi, Phys. Rev. **D62** (2000) 076002 [arXiv:hep-ph/9907254].
- [155] A.O. Bouzas, Eur. Phys. J. **C20** (2001) 239 [Erratum: *ibid.* **C27** (2003) 623] [arXiv:hep-ph/0101101].
- [156] Y. Yamada, Phys. Rev. **D64** (2001) 036008 [arXiv:hep-ph/0103046].
- [157] D. Espriu, J. Manzano and P. Talavera, Phys. Rev. **D66** (2002) 076002 [arXiv:hep-ph/0204085].
- [158] Y. Zhou, J. Phys. **G29** (2003) 1031 [arXiv:hep-ph/0301090]; Mod. Phys. Lett. **A21** (2006) 2763 [arXiv:hep-ph/0502186].
- [159] Y. Liao, Phys. Rev. **D69** (2004) 016001 [arXiv:hep-ph/0309034].